TRANSIENT FLEXURAL WAVE PROPAGATION IN BEAMS WITH DISCONTINUITIES OF CROSS SECTION

MOHAMMED MOOSA MEHDI AL-MOUSAWI

Thesis submitted for the degree of

Doctor of Philosophy

Department of Mechanical Engineering

The City University

London, August 1982

TABLE OF CONTENTS

LIST OF TABLES

LIST OF ILLUSTRATIONS

ACKNOWLEDGEMENTS

The author is deeply indepted to his supervisor Dr.H.R.Harrison for the guidance and constant encouragement throughout the course of this work. Thanks are also due to Mr. A.L.Dods,technician supervisor , for the kind assistance in the instrumentation arrangement.

Deep gratitude is extended to the author's wife ,Basima,for continued support and encouragement .

DECLARATION

I grant powers of discretion to the University Librarian to allow this thesis to be copied in whole or in part without further reference to me. This permission covers only single copies made for study purpose, subject to normal conditions of acknowledgement .

Mohammed M. Mehdi Al-Mousawi

ABSTRACT

An investigation was carried out to determine the transient response of finite beams with discontinuities of cross section subjected to eccentric longitudinal impact. Experiments were performed on several stepped beams with increased and reduced cross section and with various end conditions.

The analysis was based on the Timoshenko beam theory which takes into account the effects of shear deformation and rotatory inertia. The governing equations were solved as a system of two second order hyperbolic partial differential equations .

The numerical solution was obtained by the method of characteristics and theoretical predictions were in excellent agreement with experimental observations at several monitoring positions along the various test beams.

The agreement between theoretical and experimental results verified the adequacy of the Timoshenko theory and its numerical solution for describing the flexural wave propagation in beams with discontinuities of cross section .

The effect of the discontinuity of beam cross section on the bending moment time distribution showed the importance of reflections in estimating the level of stresses and strains in structural elements when subjected to transient dynamic loading .

The computer program developed in this work can be used to obtain numerical solutions for a wide range of flexural wave propagation problems in beams with discontinuities of cross section with various end conditions and loading configurations .

NOMENCLATURE

A	cross sectional area
A_i	cross sectional area which contributes resistance to dynamic inertia
A_s	cross sectional area which contributes resistance to shearing
c_1	dilatational wave velocity in a beam ($\sqrt{E\ I_b/\rho\ I_i}$)
c_2	shear wave velocity in a beam ($\sqrt{A_s G/\rho\ A_i}$)
d_i	diameter
DR	diameter ratio R_2/R_1
E	modulus of elasticity
e	eccentricity of longitudinal impact
e_i	input voltage of Wheatstone bridge
e_o	output voltage of Wheatstone bridge
f	frequency
f_c	cutoff frequency
f_n	natural frequency of flexural vibration
GF	gauge factor ($\Delta R/R_g$)
G	modulus of rigidity ($E/2(1+\nu)$)
h_i	beam height for stepped beam of rectangular cross section
I_b	cross sectional moment of area which contributes resistance to bending
I_i	cross sectional area which contributes resistance to dynamic inertia
k^2	shear correction factor
L	length of beam
L_1	length of the discontinues beam in region 1
L_2	length of the discontinues beam in region 2
LR	length ratio L_1/L
M	bending moment
M_o	number of lines to be evaluated in the physical plane
$\bar{M}$	dimensionless bending moment (ML/EI)
$\bar{m}$	dimensionless bending moment (Md/EI)

n	number of modes
P	axial force due to eccentric impact
Q	shear force
$\bar{Q}$	dimensionless shear force ($QL^2/E\ I$)
r	cross sectional radius of gyration ($\sqrt{I\ /\ A}$)
R_1	radius of the discontinues cylindrical beam in region 1
R_2	radius of the discontinues cylindrical beam in region 2
R_{gi}	resistance of strain gauge
ΔR_{gi}	change of resistance in an active strain gauge
R_{sh}	shunt resistance
t	time
t_o	rise time of input bending moment
$\bar{t}$	dimensionless time ($c_1 t/L$)
$\bar{t}_o$	dimensionless rise time ($c_1 t_o/L$)
$\bar{T}$	dimensionless time ($c_1 t/d$)
u_i	generalised displacement variables
v	velocity
$\bar{v}$	dimensionless velocity (v/c_2)
w	width of stepped rectangular beam
x	coordinate along the beam
$\bar{x}$	dimensionless coordinate along the beam (x/L)
x_o	x coordinate at the boundary
Δx	mesh size
$\Delta\bar{x}$	dimensionless mesh size ($\Delta x/L$)
y	deflection due to bending moment
z	deflection due to shear
$\beta_n L$	roots of frequency equation
ε	strain
ε_{eq}	equivalent strain
ε_{net}	net strain of Wheatstone bridge

λ, μ	Lame's constant of elasticity
ν	Poisson's ratio
ρ	density of beam material
σ	stress (P/A)
τ	normalised time ($c_1 t$)
τ	normalised rise time ($c_1 t_o$)
τ_{rc}	total rise time of strain gauge
τ_{rg}	rise time of strain gauge
τ_{rw}	rise time of strain wave
ψ	rotation of cross section about neutral axis
ω	velocity of rotation of cross section
$\bar{\omega}$	dimensionless velocity of rotation ($\omega L/c_1$)

CHAPTER 1

INTRODUCTION

The behaviour of structural elements under impact loading is a subject of great interest in dynamical structural analysis. When forces are applied to an elastic body over a very short period, the response should be considered in terms of wave propagation theory.

Although beams are among the simplest engineering structures, the propagation of waves can be quite complicated especially if boundaries such as end surfaces and abrupt changes which cause reflections are present.

The study of transient waves has important implications and find many applications for structures used in land, sea, air and space when they are subjected to impact.

A revival of interest in the field of elastic wave propagation during the last three decades was made possible through the rapid development of computing facilities and the advance of experimental equipment.

The problems of flexural wave propagation in beams are not so extensively treated as, for example, are the problems of longitudinal wave propagation. This was due to complexities involved in the propagation of flexural waves and their dispersive character.

To the author's knowledge, there has been no previous solution to the problem of flexural waves in beams with discontinuity of cross-section subjected to eccentric impact, the problem investigated in this thesis.

The Euler-Bernoulli theory is found to be inadequate for the study of transient bending waves since it led to the physically

impossible conclusion that disturbances are propagated instantaneously and neglected the effects of shear deformation and rotatory inertia.

The exact theory based on the equations of the theory of elasticity goes back to Pochhammer and Chree who investigated the case of infinitely long beams of circular cross-section. Their equations cannot be applied to semi-infinite and finite bars with arbitrarily prescribed end conditions and the solutions involve such mathematical complications which makes them, from the engineering point of view, of limited practical use.

The Timoshenko theory provides the only approximate theory that contains the essential features of the exact theory in simplified form. With this theory a greater accuracy than the Euler-Bernoulli theory is achieved by including the effect of shear deformation and rotatory inertia in the governing equations.

The Timoshenko theory provides for only two modes of transmission and consequently two branches of the dispersion curve, while the exact theory provides an infinite number of modes and an infinite number of higher branches of the dispersion curve.

The Timoshenko equation gives excellent agreement with the exact theory so far as the lowest branch of the dispersion curve is concerned. The agreement of both theories in the next highest branch of the dispersion curve is not very good.

An extensive literature survey of previous theoretical and experimental research will demonstrate the importance of the Timoshenko beam theory in the field of flexural waves and boundaries.

Although the Timoshenko beam equations were formulated as

long ago as 1921, numerical solutions and applications appeared only in the last 25 years, when computer facilities became available.

After careful consideration of several solution methods, the method of characteristics is chosen for the numerical solution presented in this work and the method is shown to be inherently stable and convergent.

Several cases of flexural wave propagation problems are treated with the developed TMOTCU computer programs numerically, and solutions are obtained for semi-infinite, finite beams and finite beams with discontinuity of cross-section.

The experimental work is concentrated on the monitoring of antisymmetric strain components in finite stepped beams of circular and rectangular cross-section subjected to eccentric impact at low velocity.

Comparison of numerical predictions and experimental observations are presented with particular emphasis on the bending moment and bending strain-time distribution as opposed to the normal mode frequency analysis usually used for steady state vibration. The input bending moment is assumed in a trapezoidal shape with a finite rise time.

The experimental and theoretical results demonstrate the effect of abrupt change of cross-section on the reflected and transmitted bending waves where reflections have to be taken into consideration when estimating the level of antisymmetrical stresses and strains in finite beams with discontinuity of cross-section.

CHAPTER II

REVIEW OF THEORETICAL STUDIES

2.1. Historical background of elastic wave propagasion in bars

The theory of transverse waves in elastic solids had its beginning in the works of Leonard Euler (1744) and Daniel Bernoulli (1751) who derived the partial differential equation governing the flexural vibration of a bar by the variation of strain-energy function by which they had previously expressed the work done in bending.

The concept of transverse vibration transmitted through a medium was originally based on the developments of Fresnel's theory, 1816, which used the concept of transverse waves to explain the propagation of light, which was thought to be a disturbance propagating in an elastic aether.

Navier (1821) was the first to investigate the theory of transverse body waves and he formulated the general equations of equilibrium and vibration of elastic bodies. In his derivation, he considered forces acting between the individual molecules of a deformed elastic body.

In 1822, Cauchy discoveredmost aspects of the theory of elasticity including the dynamic equations of motion. He was the first to introduce the concept of strain and stress which simplified greatly the derivation of the equations. Cauchy obtained stress-strain relations for isotropic materials and used the following assumptions: (1) linear stress-strain relationship (2) the principal planes of stress are normal to the principal axis of strain.

Cauchy (1826) treated the problem of longitudinal impact of two rods of the same material and cross-section. He concluded, that the impulse terminates whenever the two bars have different velocities of impact, which is not true.

In 1829, Poisson discussed the three equations of equilibrium and

the three conditions at the boundary and proved that these equations were not only necessary but also sufficient to ensure the equilibrium of any portion of the body. He succeeded in integrating the equations of motion and showed that if a disturbance was produced in a small portion of a body, it resulted in two kinds of waves, the dilatational wave which was associated with the motion of the particle normal to the wave front and accompanied by a volume change, and a distortional wave, associated with the particle motion tangential to the wave front, where there was distortion without volume change. The first faster wave is also called the irrotational wave, and the other wave is also called the equivoluminal or transverse wave.

By that time, it was realised that the problem of wave propagation in an elastic solid needed to be investigated in a different manner than those concerned with the normal modes of vibration. Poisson (1831) and Ostrogradsky (1831) used a synthesis method of the simple harmonic solutions of the initial distribution of displacement and velocity to determine the displacement at any point and at any time.

In 1833, Poisson attempted to solve the same problem of longitudinal impact of two bars, previously treated by Cauchy, by a method of integrating trigonometrical series, by which it was extremely difficult to find a general solution. By an error in the analysis, Poisson arrived at the conclusion, that when the bars are of the same material and cross-section, they never separate unless they are equal in length.

Seebeck (1849) presented an equation for the transverse displacement of an elastic bar and showed that the difference between E values obtained by statical and vibrational methods was extremely small. He omitted in his solution the effect of angular rotation of the cross-section of the rod, as was pointed out by Todhunter and Pearson (1893).

Bareé de Saint-Venant made wide ranging contributions to the theory of longitudinal and transverse impact. In 1853, he considered the

problem of a central impact on a simply supported beam of uniform cross-section and based his solution on different modes of vibration. He calculated the deflection at the middle and his results coincided with those given by H. Cox (1849), when only the first, most important term of the series representing the maximum deflection was considered. However, Saint Venants solution for the problem of transverse impact was not complete, since the local deformation at the point where the impinging ball strikes the beam, was not considered. In addition, the assumption that the ball remained in contact with the beam until maximum deflection was reached, is not realistic. Furthermore, this solution was not applicable when the bar was very long and the striking ball had a small weight with a very great impact velocity.

Saint-Venant made important discoveries in the theory of elasticity. In 1856, he was the first to examine the assumptions of the elementary Euler-Bernoulli theory of bending, namely that cross-section of a beam remains plane during deformation and that the longitudinal fibers of a beam are in a state of simple tension or compression. Saint-Venant showed that these two assumptions are only fullfilled in uniform bending when the beam is subjected to two equal and opposite couples applied at the end and is not applicable to the case of transverse bending, where shearing stresses cause warping of the cross-section, which will not remain plane during bending. Saint-Venant was the first to point out the incorrectness of the Euler-Bernoulli theory for flexural vibration and suggested important corrections. He was interested not only in statical stress-analysis, but studied the dynamical action of loads moving along the beam and various types of impact problems producing lateral and longitudinal vibrations.

Saint-Venant (1856) formulated the principle which carries now his name. According to this principle, the effects produced by deviation from the assigned laws of loading are unimportant except

near the ends of the bent beam; and near the ends, they produce merely "local perturbation". The condition for the validity of the results in practice is that the length of the beam should be many times greater than the largest cross-sectional dimension.

M. Bresse (1859) discussed the problem of longitudinal and lateral vibration of rods and considered moment of inertia and shear distribution over the cross section, in connection with his works on arched structures. He was the first to suggest correction terms for both rotatory inertia and transverse shear. However, the equation presented by Bresse for transverse vibration of uniform simply supported beams, included a term which took into account the effect of rotatory inertia, but not the shear correction.

A Saint-Venant memoir, published in 1867, treated the collision of two rods of the same material and of equal cross-section, by means of the equation of vibration in term of arbitrary functions, for various impact velocities of bars with various length.

In this connection, Saint-Venant derived the most important relation for the duration of impact as $2l/c$, where l is the length of the shorter bar and c is the so called velocity of sound ($\sqrt{E/\rho}$).

A second problem discussed in the same paper was the problem of longitudinal impact of beams in the form of truncated cones. Solutions were obtained, as before, by trigonometrical series which were lengthy. Solutions for both problems were presented graphically for the values of velocity and displacement. These diagrams may be considered as the first x-t diagrams, constructed for impact problems.

Saint-Venant (1868) had given trigonometrical solutions for the problem of a prismatical bar fixed at one end and subjected to the influence of transient compressional wave due to a longitudinal impact at the other end. His solution was again based on the assumption that the striker becomes rigidly attached to the end. Summing the first few

terms of the trigonometric series, Saint-Venant was able to find the motion of the bar end. But in calculating stresses, the series did not converge rapidly enough to allow the computation of an accurate result. He pointed out the need to use some closed form expression for the solution instead of infinite series.

Solutions in term of finite discontinuous functions were obtained by Boussinesq (1882) and independently by Sébert and Hugoniot (1882) and Saint-Venant (1883) presented these solutions in his famous annotated translation of Clebsch's book and used them for graphical representation of the successive stages of the longitudinal impact of the bar for the whole duration of impact and for various ratio's of the mass of the bar to that of the striking mass.

Saint-Venant was the first to investigate the problem of wave propagation in bars and based his researches in part on the assumption that they made simultaneous contact over the entire area of the end, a condition which is extremely difficult to achieve. A modification of this theory was suggested by Hertz (1882), on the basis of an electrostatic analogy for the contact of two elastic bodies with curved contact surfaces under the action of a static compressive force as an approximation for the actual dynamic loading.

The Saint-Venant theory reflected with sufficient approximation the state of strains and stresses at positions of considerable distance from the point of loading and support.

The impact forces in the immediate vicinity of the impact point could be dtermined more successfully by the Hertzian theory.

Saint-Venant (1883) presented a detailed theory of the transverse impact of bars, which included the analytical and numerical solution of various problems of bars vibrating transversly with a load attached to it.

Boussinesq suggested in 1895 the general wave solution of the

equation of motion for longitudinal impact, in the form of forward and backward travelling waves.

Boussinesq (1885) investigated also the problem of transverse vibration of a uniform bar for various types of loading, in the form of discontinuous functions. The important contribution of Bresse was not mentioned in the investigations of transverse vibration problems by Saint-Venant and Boussinesq.

Lord Rayleigh (1885) discovered a third type of wave propagating parallel to the surface with a velocity slightly smaller than the velocity of a distortional wave. This wave, called Rayleigh surface wave, decays exponentially towards the interior of the body.

L. Pochhammer (1876) investigated, on the basis of the general theory of elasticity, the problem of longitudinal, torsional and flexural vibrations in an infinitely long beam of uniform circular cross-section. The displacements in the general trancendental frequency equations were given in terms of infinite harmonic wave train, as a product of sinusoidal and Bessel functions. For the lowest branch of the frequency equations, Pochhammer obtained first and second approximations for extensional (longitudinal) waves and a first approximation for flexural waves. Although it is extremely difficult to use these complex equations to study transient flexural wave propagation problems they have been guides in the use of approximate wave theories. The same equations were given by Chree (1889).

Wave propagation involving dispersion is important for investigations related to flexural wave problems.

Cauchy (1830) and Green (1839) discussed the propagation of plane waves through a crystalline medium and obtained equations for the velocity of propagation.

Hamilton (1839) investigated the velocity of propagation of a finite train of waves in a dispersive medium, in his work on the

theory of light. Kelvin's group method of approximating integral representations of dispersive waves was included in his work on water waves in 1887.

Lord Rayleigh (1894) discussed the problem of lateral vibration of rods and included in the derived equation of motion, a correction for the rotatory inertia. This correction is usually atributed to him, although it was originally given by Bresse, as early as 1859.

Lamb (1917) was concerned with the investigation of flexural waves in plates and he pointed out the inadequacy of the Euler-Bernoulli theory which predicts that the effect of a localised disturbance begin instantanously at all distances.

Timoshenko (1921, 1922) corrected the Euler-Bernoulli equation for flexural waves by including the effect of the shear deformation in addition the correction term for rotatory inertia.Although the shear correction term was originally suggested by Bresse, Timoshenko was the first to include it in the approximate theory dealing with flexural wave propagation in a rod. This theory forms the basis of the present investigation.

The brief history, presented in this section, of the work of the classical elastician, written during the 19th century and mostly in French, was based on books which include comprehensive survey of the history of the theory of elasticity, such as: Todhunter and Pearson (1886); Love (1892); and Timoshenko (1953).

2.2. The Timoshenko beam theory

2.2.1. Flexuralvibration of beams

The simplest theory governing the flexural vibration of beams is the Euler-Bernoulli theory, which assumes that the bar element deformation is in the form of transverse displacement only. This theory assumes, in addition to the assumptions of uniform homogeneous and constant cross section, that the deflection is small and that plane cross-sections remains plane and perpendicular to the neutral axis after deformation,which means neglecting shearing deformations. The Euler-Bernoulli equation for bending vibration neglects also the rotatory-inertia effect. However, at low frequencies, the theory gives satisfactorily the frequency spectrum and mode shape of beams in steady-state harmonic vibration.

The Pochhammer-Chree theory includes a set of equations for flexural vibrations and is only applicable to an infinite bar in which continuous sinusoidal waves are progagated in either direction. This three-dimensional theory of elasticity cannot be used to construct solutions for finite and semi-infinite bars. In addition, the complexity of the frequency equations makes it very difficult to use them for practical solutions.

When the Timoshenko beam theory is applied to the case of an infinite bar of circular cross-section although it is approximate and one-dimensional, it gives remarkable agreement with the exact theory of elasticity, especially in the first branch of the dispersion curve, which is the primary flexural mode, as was shown by Davies (1948).

The Timoshenko theory is more accurate than the Euler-Bernoulli theory in governing transverse and flexural free and forced vibrations of a beam where frequency equations, displacement curves and mode shapes are determined.

The Euler-Bernoulli equation can be obtained directly form the Timoshenko beam equations, when the terms that take into account the effects of rotatory inertia and shear deformation are omitted.

Although Bresse was the first to discuss, in 1859, the effect of non-uniform shear distribution over the cross-section and to include a term for the effect of rotatory inertia in his equation of motion for lateral vibration, it is justified to attribute the theory which takes these effects in to account to Timoshenko since he was the first to include both terms in the equation for flexural vibration of beams.

Timoshenko (1921) derived the equation for flexural vibration and obtained the frequency equation for a simply supported prismatic bar of length 1. He showed the importance of the correction for shear which is for some cases several times greater than the correction for rotatory inertia. In a second paper in 1922, Timoshenko obtained the solution for the case of a beam of rectangular section and approximate solutions were found for the cases of plane strain and of plane stress. The case of a bar of circular cross section was also investigated and values of shear correction factor for both cross-sections were suggested. His solution was not applicable to other boundary condition. Goens (1931) used the Timoshenko equations and obtained complex exact expressions for the case of a free-free beam. The roots of these expressions yield the frequencies of vibration by an approximate numerical evaluation for . bars of circular cross-section and various lengths. He used his results for the determination of Young's modulus.

Davies (1937) investigated the transverse vibration of a fixed-free bar under the effects of a shear force and bending moment. He used the Timoshenko beam equation and obtained a solution for the frequency equations which satisfied the boundary conditions. The solutions were approximations of the series expansions where terms of

higher orders were neglected. The fundamental modes were determined for several bars of different materials and dimensions. The importance of the effects of rotatory inertia and shear were emphasised.

Kruszewski (1949) gave general solutions for the Timoshenko beam equations and solved them for uniform cantilever and free-free beams. The frequencies of the first three modes were presented graphically. His results showed that the effect of shear increased in the higher modes and caused a significant decrease in the frequency value.

Sutherland and Goodman (1951) have found that shear distortion is particularly important at the higher frequencies. They gave a general solution for the lateral free vibration of a pin-ended beam and natural frequencies were obtained for a simply supported and for a cantilever beams.

Traill-Nash and Collar (1953) pointed out that a complete new spectrum of natural frequencies appeared when both shear flexibility and rotatory inertia were taken into account. The importance of higher frequencies in bending vibration were shown in connection with aircraft components, such as wings, fuselages and propellers. Various types of end conditions were investigated and the first five natural frequencies were calculated usinga matrixiteration process and the effect of shear flexibility was found to be considerable.

Anderson (1953) compared various solution methods for flexural vibrations, treated by the Timoshenko beam theory and pointed out certain advantages of power series expansions, according to the principles of superposition, over Laplace transformation solutions. The series solution presented in this paper was exactly the same as the one published previously by Sutherland and Goodman (1951) for the case of a simply supported beam. The slight numerical difference in the values of the graphs was due to a somewhat higher value used for the shear correction factor.

Dolph (1954) pointed out the existance of two sinusoidal modes of different frequencies corresponding to the same spatial factor in the solutions based on Timoshenko theory. He considered the separation of variables and the orthogonality relations as in a typical eigenvalue problem and presented a normal mode solution for a uniform hinged-hinged beam.

Howe and Howe (1955) demonstrated the usefulness of electronic differential analyser in determining solutions for the lateral vibration of beams according to the Timoshenko beam theory. They based their solution on a system of four simultaneous first order differential equations, previously given by Dolph and paid particular attention to the mode shapes. Half a dozen trials were necessary to find a satisfactory solution according to the normal mode method, applied to the case of a free-free beam.

Huang (1958, 1961) investigated in two papers the effects of rotatory inertia and shear on the flexural vibration of beams. A solution was obtained for the Timoshenko beam equation by the energy method of Ritz when applied to a simply supported beam. In his second paper, he presented frequency equations for a combination of various types of end conditions using normal mode solutions.

Since the middle of the sixties and through the seventies the finite element method has been applied to the bending vibration of beams treated by the Timoshenko theory. Several Timoshenko beam elements have been developed and only a brief account of the research papers published in this area will be given here.

Hurty and Rubenstein (1964) used an energy approach to develop generalized mass matrix and stiffness matrix including the effect of rotatory inertia and shear. These effects were illustrated in determining natural frequencies and corresponding mode shapes for a uniform simply supported beams.

Archer (1965) presented a consistent mass-matrix and a stiffness-matrix for the vibration analysis of a Timoshenko beam.

Kapur (1966) derived a finite element for theTimoshenko beam in which a cubic plynomial function was assumed for both bending and shear deformation, where no coupling between these two displacements was permitted and hence, the problem was overspecified.

Egle (1969) presented an approximate Timoshenko beam theory designed to eliminate coupling between shear deformation and rotatory inertia.

Nickel and Secor (1972) derived stiffness and mass matrices for what they called TIM 7, a matrix of order 7, which was reduced to TIM 4 using the constraint given by Egle.

Davis et.al (1972) used an element model similar to TIM 4 which had the limitation that natural boundary conditions at the free end or hinged end could not be applied.

Thomas et.al (1973) pointed out that some errors in the matrices of one of the elements given by Archer (1965) caused some confusion and led, when applied, to some unacceptable results. They proposed an element with three degrees of freedom at each of the two modes. This element was used to calculate the natural frequencies of a cantilever beam and the results were compared with the use of other elements.

Dong and Wolf (1973) used quadratic interpolations for the displacement variables of a finite element for the Timoshenko beam. Hamilton's principle was used to derive the equations of motion in discrete co-ordinates. Frequencies were obtained by the present element for a simply supported beam, two-bay frame and a hinged arch. Ramamurti and Mahrenholtz (1974) used simultaneous iteration method to determine eigen frequencies for the flexural vibration problem. The authors concluded, from the relatively high difference between theoretical and experimental frequency values, that the actual structure had to be modified to reduce the number of modal points to meet the available

storage of the computer.

J. Thomas and Abbas (1975) suggested a four nodal degrees of freedom for a two noded Timoshenko beam finite element which incorporated natural boundary conditons. The mass and stiffness matrices are based on cubic polynomial expansions for total deflection and bending slope are derived from energy expressions. In a discussion by D.L. Thomas (1976) it was noted that it is not possible to claim that any one element is the "best" model vibration analysis of Timoshenko beams. The choice of element must depend on the required accuracy, the nature of the structure, the relative importance of shear and rotatory inertia, and the number of degrees of freedom available.

Downs (1976) detected an additional mode due to shear oscillation when he re-examined the equations of Dolph, Huang and Howe, et.al This mode was identified in the frequency discretized analysis of an eight segment simply supported, uniform Timoshenko beam, as well as a finite element solution using consistent mass theory.

Rao et.al (1976) suggested a finite element model for vibration of non-uniform beams. Bishop and Price (1976) used the Timoshenko theory in the dynamical structural analysis of ship hulls as a non-conservative system.

2.2.2. Transient flexural wave propagation in beams

The Euler-Bernoulli theory is inadequate for the treatment of transient bending wave propagation problems, since it assumes that disturbances with infinitely short wave lenghts, which are associated with high frequency branches, will propogate with an infinite velocity. The transient input gives rise to higher frequencies, when the duration of impact is much smaller than the fundamental period of the vibration of the structure. Hence, according to the Euler-Bernoulli theory transient disturbances should be felt immediately at the far end of the

beam and this is physically impossible and contrary to the results of the Pochhammer-Chree theory which predicts finite values for the velocity of propagation of stress waves. Furthermore, the Euler-Bernoulli theory assumes that the displacement of the bar consists solely of translation.

As regarding the exact theory, the complexity of the displacement and frequency equations makes it impossible to use for practical problems of flexural wave propagation and, in addition, it cannot satisfy the end conditions, together withzero stresses at the lateral surfaces. However, the Pochhammer-Chree theory has been used to determine phase volocities and group velocities of sinusoidal waves in narrow beams and beams of circular cross-section.

Dispersion relations play an important role in the propagation of flexural waves in elastic bounded solids. A pulse can be seen as the Fourier integral of a number of sinusoidal components of different frequencies, which will travel with different velocities and dispersion is the cause for the distortion of the wave. It is necessary for dispersion analysis to determine the variation of the phase velocity c_p i.e. the velocity of propagation of surfaces of constant phase, with the wave length, as well as the group velocity c_g, i.e. the velocity of propagation of a wave packet of almost the same wave length. For flexural waves, the group velocity is more important since it is the velocity of the rate of transmission of energy.

The Timoshenko beam equation, which takes into account the effects of rotatory inertia and shear on the displacement of the beam, gives a high degree of accuracy over a wide range of wave lengths for flexural waves in bars. From the engineering point of view, the Timoshenko theory is the best known theory to deal with transient flexural wave propagation. The Timoshenko beam theory provides the dynamic equations of motion for transient waves in finite, semi-infinite and finite beams.The Timoshenko beam equations are applicable to flexural waves due to transverse impact

as well as flexural waves due to eccentric longitudinal impact.

Some research works compared the results obtained by theoretical models with experiments. This will be mentioned in this chapter briefly and dealtwith more extensively in chapter 6 which presents a review of experimental works.

Timoshenko (1913) investigated the transverse impact of a simply supported beam of square cross-section and used the theory of lateral vibration in connection with Hertz theory, to evaluate numerically the deflection of a short beam 15.35 cm long, 1x1 cm cross section, struck in the middle by a steel sphere of 1 cm radius. He used energy consideration, considering the transformation of the kinetic energy of the striking mass into potential energy of bending in the beam, with some estimate of energy loss due to impact. The integral equations were solved numerically by dividing the time into small increments during which the contact force between the striking mass and the beam could be considered constant.

The same problem of a central impact of a simply supported beam was investigated by Arnold (1937) who compared experimental results with theoretical calculations based on the previously mentioned Timoshenko analysis. A more detailed theoretical study of the same problem was given by Christopherson (1951) .

Lennertz (1937) calculated the fundamental period and the maximum deflection for the two simply supported beams originally discussed by Timoshenko (1913) and obtained comparable results. He considered the impact as a whole rather than as a succession of steps. Lennertz assumed that the duration of impact was small compared with the period of the fundamental mode of vibration, which was justified if only the fundamental mode was stimulated, which meant neglecting the effect of higher modes and therefore was not justified.

Lee (1940) used an improvement of the method used by Lennertz with

a modified Hertzian expression and obtained a solution for central impact of a uniform simply supported beam. His calculations compared well with the experiments of Arnold.

Bancroft (1941) was the first to solve the Pochhammer-Chree equations for the propagation of longitudinal waves and formulated the propagation velocity in term of two variables: the Poisson's ratio and the ratio of the diameter of the bar to the wave length. He discussed qualitatively the flexural mode and pointed out the complexity of the flexural modes. He obtained only the lowest root of the equation.

Prescott (1942) gave the frequency equation in determinantal form for the case of flexural vibration, but he did not evaluate the determinant derived from the exact theory of elasticity. He also derived the Timoshenko beam equations by energy considerations and found that the elementary theory of transverse vibration was inadequate for transient loadings. The velocity of flexural waves depends on their wave length and approaches that of Rayleigh surface waves when the wave length becomes small compared with the lateral dimensions of the bar. Prescott obtained numerical results for the velocity of flexural waves in a bar of circular cross-section.

Flügge (1942) observed the prediction of the Timoshenko theory that discontinuities are propagated at definite finite velocities, c_1 $(=\sqrt{E/\rho})$ and c_2 $(=\sqrt{k^2G/\rho})$. He pointed out that discontinuities of bending moment and angular velocity are propagated with c_1, whereas discontinuities of shear force or transverse velocity are propagated with c_2.

Hudson (1943) solved the determinant of the frequency equation, given by Prescott, for flexural vibration and dispersion curves were presented for various values of Poisson's ratio. Hudson overlooked the higher modes of the flexural waves and assumed wrongly that they

did not exist.

Cremer (1943) discussed the two distinct velocities appearing in the Timoshenko equation and pointed out that better agreement with the exact theory can be reached if the value of the shear correction factor is so adjusted as to produce a value for the shear velocity c_2 which corresponds to the asymptotic value of the lowest mode of the exact theory.

Davidson and Meier (1946) used the Timoshenko beam theory to study thepropagation of transverse waves in prismatical bars in connection with slender tools used in the percussion drilling of rock. Eccentric longitudinal impact was studied experimentally.

Pfeiffer (1947) was the first to use the method of characteristics for the general solution of the Timoshenko beam equation as a system of two second order partial differential equations. He discussed the propagation of discontinuities along the characteristic lines and described in detail all the steps needed to carry out the numerical calculation. However, Pfeiffer did not present a particular numerical example. The method of characteristics will be discussed in chapter three (section 3.2.4.).

Cooper (1947) discussed the dispersive nature of the longitudial and flexural waves on the basis of the exact theory and pointed out that it was difficult to get information other than that the maximum velocity propagation for any disturbance is the velocity of dilatational waves c_D.

Davies (1948) was the first to verify the Pochhammer-Chree theory experimentally and pointed out the differences between the elementary theory and this "exact" theory. For flexural waves, Davies constructed dispersion curves for phase velocity and group velocity for the first bending modes for a Poisson ratio $\gamma = 0.29$. The values for the flexural curve of the exact theory were interpolated from Hudson's data. The dispersion curves dervied from the Timoshenko theory were shown to agree

well over a wide range of a a/Λ with the values derived from the exact theory. Davies concluded that the Timoshenko theory prediction for the velocity of propagation of the leading edge of a flexural pulse, i.e. $c_2=\sqrt{k^2G/\rho}$, suffers only a small precentage of difference for almost any form of cross-section. However, one could expect flexural pulses to be progagated with higher velocities, if higher branches of the dispersion curves are considered. Davies paper included an extensive experimental part based on the modification of the Hopkinson pressure bar, which justified the assumption of the uniform distribution of the stresses over the cross-section and hence with the use of the one-dimensional theory.

Uflyand (1948) used the Timoshenko beam equation to solve the problem of an infinite beam subjected to a concentrated load of a step-function time history. He employed Laplace transformation method to obtain displacement solutions. He was the first to show that contour integration would give exact travelling wave solutions for the theory. He approached the problem by cutting the infinite beam at a station just to one side of the load and treated the unloaded, semi-infinite portion of the beam. His interpretation of the assumed boundary conditions was incorrect.

De Juhasz (1949) presented a graphical analysis of several longitudinal impact problems as a way to avoid difficulties involved in mathematical analysis. Tridimensional diagrams, so called "Stereograms" were constucted on the basis of x-t diagrams and v-p diagrams. Thegraphical analysis was based on two assumptions, namely that of constant velocity of propagation and that of linear relationship between the change of striking velocity v and the change of stress. Although no dispersion relations were involved, the stereograms were too complicated even for basic problems of longitudinal impact of bars. The method was based on the original graphical analysis, given by

Saint-Venant and on several previous works of the author, as well as the contributions of Bergeron, originally devised for water-hamer calculations.

Duwez (1950) studied the deformation of an infinitely long beam subjected to a concentrated transverse load of constant velocity. He investigated the influence of impact velocity and duration of impact on the deflection characteristics of the beam by a theory originally developed by Boussinesq. For steel, the plastic deformation was assumed to be localised at the point of impact. However, for soft materials such as annealed copper, plastic deformation had to be considered. The discrepencies between theoretical and experimental results were attributed to the effects of end supports and the dispersion characteristic of the transverse waves.

Approximate theories for transverse waves in plates and two dimensional compressional waves in bars werestimulated by the Timoshenko beam theory. Directly from the three-dimensional equations of motion, Mindlin (1951) deduced a two-dinensional theory for flexural motions of plates which takes into account the effects of rotatory inertia and shear, in the same manner as Timoshenko's theory. Mindlin's theory was similar to the one given by Uflyand (1948) and by Reissner (1945). Mindlin and Herman (1951) derived from the general theory of elasticity a one-diminsional theory of compressional waves in elastic rods. The obtained equations for radial and longitudinal motions of a bar were similar to the Timoshenko's equations for rotational and transverse motions of a beam and could be treated in a similar manner.

Dengler and Goland (1951) pointed out that the boundary conditions of Uflyand were incorrect and solved the same problem, avoiding the difficulties of boundary conditons by working with the original 4th order nonhomogeneous Timoshenko equation and a lateral impulsive load applied to the beam mid span in the form of a two Dirac function product in

terms of t and x. The results appeared in closed form solutions, which required the evaluation of complicated integrals. Another difficulty was that of defining proper boundary conditions in the "total deflection approach". The contour analysis included an error in connection with singularity problems, which was corrected in a later publication of the authors, in 1955.

Schirmer (1952) discussed the problem of flexural waves in Timoshenko beam and compared solutions based on a system of two second order partial differential equations in terms of transverse displacement y and angular rotation ψ and their derivatives. He used Laplace transformation for the dispersion analysis and used the method of characteristics for obtaining bending moment distribution along the beam at certain times after a bending moment input at on end.

Miklowitz (1953) pointed out the difficulties involved in the solution methods suggested by Uflyand and Dengler et.al and modified the Uflyand method and gave correct interpretation to his boundary conditions. He treated the lateral deflection components due to rotary inertia and shear separately in essentially the same way as used by Schirmer. This approach provided insight into the physical nature of the travelling wave character and possessed definite advantages in reducing the mathematical difficulties in establishing the boundary conditions and obtaining the transformation for the case of an infinite beam under the action of a concentrated transverse load, treated previously in the works of Uflyand and Dengler et.al. It is not always easy to obtain transform solutions for various end conditions and it is more difficult to evaluate them numerically. In 1960, Miklowitz applied the same method to yield travelling wave solution for flexural waves in plates.

Leonard and Budiansky (1953) used the method of characteristics to obtain numerical travelling wave solutions for Timoshenko beams of

various end conditions subjected to step velocity, step bending moment and ramp-platform bending moments. However, for mathemetical simplicity, the solutions were based on the equality of the two propagation velocities, which is physically unrealistic. The characteristic equation, derived by the authors, was based on the Timoshenko beam theory as a system of four first order partial differential equations. For some cases, the solutions were compared with closed form solutions and with modal solution.

Eringen (1953) applied the generalized-Galerkin method and collocation method to obtain the contact force and the displacement by the use of the Hertz's law, for transverse impact of beams and plates with various end conditions. Deflection curves were obtained by using Dirac δ-function, having the same impulse as the contact force F(t).

Newman (1955) obtained a solution of the Timoshenko equation for a half-period sine excitation applied at the root of a cantilever beam and the appropriate initial and end conditions were specified by means of the use of a variational principle. The relation between maximum dynamic strain and relative impact duration was plotted and Newman found that a thin slender bar (L/r=300) was subjected to 25.5% higher strain than a thick short bar (L/r=30) at the clamped end in short duration impact. Newman used Laplace transformation for his frequency based analysis.

Boley and Chao (1955) presented Laplace transformation solution of the Timoshenko beam equations for transverse impact of semi-infinite elastic beams. Laplace transformations were used for various types of sudden loadings and the obtained curves for bending moment and shear force for several positions were compared with elementary beam theory results.

In a second paper in 1955, Boley described the behaviour of beams under lateral impact by means of an approximate "travelling-wave"

approach, based on energy considerations. Numerical results were obtained for a very short portion of the beam near the point of impact of the order of the cross-section dimension, and for very short times. However, in a later paper of Boley and Chao (1958), these short-comings were removed from this method and solutions were obtained for semi-infinite beams under step-inputs of velocity and bending moment. Deflection curves for finite simply-supported beams were constructed by superposition of semi-infinite beam results according to the method of images, as given by Leonard and Budiansky (1953).

Jones (1955) obtained a solution for flexural stresses in an infinite beam loaded by a transverse point load. His solution was based on Timoshenko's theory of transverse vibration, solved by the use of Fourier transforms, from which asymptotic approximations were found by the method of stationary phase. The numerical evaluation for the variation of amplitude of bending moment and of wave length were presented.

Barnhart and Goldsmith (1957) developed a theory for the transverse impact of spheres on elastic beams which incorporated a dynamic plastic force-identation law and permitted the evaluation of the effect of an arbitrarily large number of beam bending modes. The theoretical stress-time histories based on this theory which took account of the higher modes were in a better agreement up to the peak value with the observed data than curves based on Hertz law whose shape during the initial loading increase did not agree too well with the experimental results. However, the peak value obtained by both theoretical methods was in fair agreement with the experiment at the point of impact.

Abramson (1957) pointed out the wrong statement of Hudson who calculated the first root of the frequency equation, and assumed therefore, that flexural waves are propagated in one mode only.

Abramson computated the three lowest modes of the determinant of flexural wave transmission, based on the Pochhammer-Chree theory. Dispersion curves were presented for ν=0.29 and used to study the rate of energy transmission in terms of group velocity. Hence, the author was able to obtain some additional insight into the physical phenomena involed in the flexural response of beams to impulsive loads.

In a second paper by Ripperger and Abramson (1957), the authors compared the predictions of the Pochhammer-Chree theory concerning the arrival time of flexural waves with experimental results and found that initial distrurbances were propagated at the dilatational wave velocity and the bending wave pulse was propagated by a continuous series of arrivals. The authors were able to establish the adequacy of the Timoshenko beam theory in predicting quite accurately the arrival times for all but the very sharpest impact. Furthermore the amplitude response is predicted very well by the Timoshenko theory. So, it was concluded that, for all practical purposes, the Timoshenko theory provided an adequate representation of the propagational characteristics of bending waves.

Plass (1958) extended the use of the method of characteristics to the general case of different propagation velocities. He studied various types of end conditions for Timoshenko beams under half-sine form of end impacts of moment, shear, angular velocity and transverse velocity. For comparison purposes, the case of a simply supported semi-infinite beam under the action of a sinusoidal end moment, was solved by Laplace transforms in addition to its solution by the method of characteristics. Comparison with experimental data, due to Ripperger (1955) showed good agreement, except where the pulses were extremely short.

Flugge and Zajac (1959) investigated several solution methods other than the method of characteristics, none of which could yield

a complete solution at all points of the beam. However, a combination of them could give an almost complete solution for a semi-infinite, simply supported beam under the action of a step-function end bending moment. The numerical results in the neighborhood of the end were obtained using the Laplace transformation together with term-by-term inversion. For long times the integral, obtained from the contour integration near the point of impact, was evaluated to obtain asymptotic solutions using the stationary phase method of Kelvin. The method was a complicated combination of several not so easily obtainable functions such as Bessel function, Laplace transforms and Fourier transforms.

Kuo presented in two papers, in 1959 and 1961, the results of a theoretical and experimental study of bending waves in a semi-infinite Timoshenko free-free beam subjected to a dynamically applied end moment. He used the method of characteristics, in the same manner as Leonard and Budiansky , and in order to simplify the numerical analysis, k^2G/E is taken equal to unity which is the same as two equal characteristic velocities, which is physically incorrect. The effects of slenderness ratio and the change of rise-time were studied and the results were compared with a second theoretical treatment, based on Euler-Bernoulli theory by the normal mode method. The comparison of the Timoshenko beam theory results and observed data was limited to the initial stress build up and the discrepancy was most marked in the phase shifting.

Jones (1964) used the exact two-dimensional theory of plane-strain transverse waves in a beam by the application of a transverse force having a step function time variation. The bar width was great in comparision with its depth i.e. the bar was in the form of a plate. The solution was used for the assessment of the validity of Timoshenko's theory and its advantage over elementary theory.

Chou and Mortimer (1966) pointed out the advantages of the method of characteristics, when compared with the mode super-position method

and the Laplace transform method, in solving transient response problems. They treated several elastic wave propagation problems including the Timoshenko beam equation as a system of second-order hyperbolic partial differential equations, using the mothod of characteristics . The governing equations for the propagation of discontinuities along the characteristic lines were obtained. Various types of input loadings were used for integration along the characteristic lines to evaluate time-histories of stresses. The method presented an improvement on the numerical method given by Chou and Konig in 1965, regarding the propagation of discontinuities.

Chou and Koenig (1966) compared their results for the method of characteristics, with the results of other methods, where such solutions existed and found excellent agreement.

David and Koenig (1967) used a so-called "direct finite element analysis" to solve dynamic flexural travelling wave problem in infinte beams and plates. They obtained numerical results for a very short cantilever beam with a step velocity input applied at the free end, according to the Timoshenko beam theory. The effect of reflection on the evaluated bending moment and shear force was included.

Bejda (1967) investigated the problem of the propagation and reflection of stress waves in elastic-visco plastic beams, using the method of characteristics for both regions. Numerical results were obtained for a cantilever beam under suddenly applied bending moment and shear force to the free end.

Edge (1970) investigated the response of aircraft arresting hook units to impact with obstacles in connection with aircraft landing, using two numerical wave propagation methods, namely the method of characteristics and the direct finite element analysis. He obtained a solution based on the Timoshenko beam theory for naval and land-based aircraft hook units and pointed out the advantage of the method of

characteristics for obtaining bounce dimensions in land based cases.

Garrelick (1969) considered the response of a link spring supported beam subjected to a uniform velocity input by the Timoshenko theory represented as a conservative second order hyperbolic system and solved by means of a dual eigen function expansion, where the system consisted of real and positive eigen values and orthogonal eigen functions. The results for the moment at midspan and the shear at the support were compared with the results of the Euler-Bernoulli theory and the discrepancies were mostly pronounced in the vicinity of higher oscillations representing reflected wave fronts. The results may be applicable to sonic boom problems and other problems such as packaging.

Ranganath (1971) employed the Timoshenko theory to solve the problem of transverse impact of an infinite elastic beam by a semi-infinite elastic rod. The system of the hyperbolic equation were solved by Laplace transformation and compared with experimental data, as well as with a second theoretical solution obtained by a finite difference technique. Both theoretical results correlated closely with observed data, with the finite difference method showing improved agreement. Discrepancies at the initial times and at stations close to the point of impact were reflected in oscillations at early times which was not supported by experimental observations of the strain waves.

Lee and Kolsky (1972) based their investigation of flexural waves, generated at the junction of two non-collinear rods, on the Timoshenko theory. The transmitted and reflected flexural wave were considered and the shape of the initial pulse was assumed as the integral of the difference between two error functions separated by the pulse length, expressed in an inverted Fourier cosine transform. The shapes of the four waves generated at the junction, two longitudinal pulses and two flexural pulses where both types reflected back along the first rod and also transmitted into the second rod inclined at various angles

to each others, were determined and compared with experiments.

Sagartz and Forrestal (1972) compared the Timoshenko solution with the Euler - Bernoulli solution and with experiments for the flexural waves, propagating from the clamped end of an impulsively loaded semi-infinite cantilever beam. The transform method was used to find a solution for the hyperbolic Timoshenko beam equations and to compare the results with observed data, where the input pulse was assumed in the form of a sine-squared uniform lateral pressure pulse. The effects of shear deformation and rotatory inertia were shown to be especially important at the initial time.

Philips and Crowley (1972) treated pulse propagation in a curved beam by the Timoshenko theory and used the method of characteristics for the numerical solution, where the input pulse was in the form of a half-sine pulse, as in the case of Plass (1958). Similarities to the problem investigated by Lee and Kolsky (1972) were also pointed out. It was concluded that aflexural pulse in a curved beam of moderate curvature was insensitive to the actual beam curvature, as far as the bending moment and shear were concerned . These results are in agreement with the conclusions of Morley (1961) who showed that there was no significant interaction between extension and flexure for small curvature.

Forrestal et.al (1975) checked the accuracy of a two-dimensional elastic-plastic wave propagation computer code TOODY, by comparing its results with those based on Timoshenko beam calculations for an impulsively loaded simply supported beam, where the transient pulse was a sine-squared pressure pulse of very short duration. General agreement between the two theoretical predictions was good except for higher frequency oscillations predicted by TOODY.

Colton and Herrmann (1975) used the Timoshenko beam theory to calculate the beam response, before, during and after fracture. The method of characteristics was employed to obtain strain histories

under localized impulsive loading of a beam of rectangular cross-section, where three models of the fracture were postulated. Comparison of calculated and measured strains showed that a two-stage fracture model approximated the structural response. A similar investigation by Colton (1977) showed that all fractures were initiated by bending stress.

Parker and Neubert (1975) obtained the transient lateral response of a cylindrical rod with free ends to a short duration half-sine pulse of either moment or shear applied to one end. They applied the mode shapes and frequency equations, as given by Huang (1955), as well as the classical separation of variables to obtain modal series solutions involving many modes for the Timoshenko beam theory with time-dependent boundary conditions. The theoretical solutions predicted higher peak values when compared with experimentally observed data reported by Ripperger 1955.

Sun and Huang (1975) developed a higher order beam finite element by increasing the nodal degrees of freedom to three and tested its efficiency when applied to impact problems concerning the response of of a simply supported beam subjected to a sine pulse and the impact of a steel sphere on a cantilever beam, where displacement curves and contact force histories were presented and were found to be in good agreement with existing solutions.

Tanaka and Motoyama (1976) investigated an infinite circular bar subjected to impulsive bending load, using the three-dimensional theory of elasticity and comparison of dispersion relations with those obtained from several approximate theories, showed that the results of the Timoshenko beam theory conformed to those of the exact theory over the whole region for the first mode and over a small region of the second mode. Laplace transform and Fourier transform techniques were used in the analysis. In a second paper of Tanaka and Iwahashi (1977), a similar analysis was presented for a bar of rectangular cross-section. The solution

was obtained by an approximate crosswise superposition of two series solutions. Dispersion curves for the frequency specturm of the bending mode showed a very good agreement for the fundamental branch between the results of the Timoshenko theory and those obtained by the present method.

A controversial brief note by Nicholson and Simmonds (1977) suggested that for an elastic isotropic beam of narrow rectangular cross-section clamped at one end, the Timoshenko beam theory was not more accurate than elementary beam theory. This provoked no less than seven discussion contributions, which were published in the Journal of Applied Mechanics (1977) as a one time exception, since it does not publish discussions on brief notes. In all discussions the importance of the Timoshenko theory as a valuable engineering tool was emphasised and the unusual nature of the chosen example was criticised. Van der Heijden pointed out that the Timoshenko beam theory yields quite accurate numerical results, although it is not a consistent theory from the point of view of asymptotic theories. Koiter agreed with the author's caution in the sense that engineering theories should never be applied indiscriminately, but saw no reason for singling out the Timoshenko theory as a particularly vulnerable case. Reissner pointed out that the problem constructed by the authors was of such a highly unusual nature that the transverse shear strain distribution was assumed uniform across the depth of the beam, in place of a "reasonable" parabolic or near parabolic distrubutions. This ment that tranverse shear deformation effect canceled-out altogether, up to terms of order ε^2. Christensen noted that beam theory was just a one-dimensional specialization of plate theory. Mathematically, the Euler-Bernoulli theory and the Timoshenko beam theory are both of the same order, but with different degrees of generality or completeness. The more complete theory should in general be preferable, even though counter examples may exist.

Schmidt demonstrated that in view of the presence of large longitudinal distributed shearing loads, applied to the upper and lower edges of the bar, the author's loads cannot be regarded as "reasonable" for a beam, as no longitudinal forces on long edges are permitted in the beam theory. Levinson stated that the validity of the Timoshenko theory, with its own valid mathematical structure, rested on how well it compared with experience and not on its mathematical integrity alone.

The problems of elastic wave propagation in rods and beams have been surveyed in many articles such as by Davies, (1956) who discussed in detail dispersion relations together with phase velocities and group velocities. A survey by Abramson (1958) gave extensive information on various types of waves propagated in rods and beams. Two surveys published in 1960 by Miklowitz and by Curtis contained the discussion of the transient wave propagation problem in beams and rods. In 1963 two surveys by Kolsky and Goldsmith reviewed experimental and theoretical advances in the propagation of waves in elastic solids. More recently Scott (1978) presented an annotated bibliography which included a few recent references on flexural wave propagation in rods.

For a more detailed treatment of the theory of wave propagation in elastic solids, one should refer to many valuable books. Kolsky's book (1953) can be considered as the standard book of the modern history of elastic waves. A recent revival of interest in the subject led to the publication of many books in the seventies which included comprehensive treatments of wave propagation problems and a large number of bibliographies. These are the books by Johnson (1972), Graff (1975) and Miklowitz (1978). They presented the continuing and growing interest during the last three decades due to a number of reasons such as the rapid development of computing facilities, the advance of experimental equipment available for producing and detecting stress waves, and the need for information on the behaviour of structures

subjected to impulsive loading.

There is also an overwhelming increase in the literature related to the field of geophysics, acoustic and electromagnetic waves.

2.3. Wave propagation in beams with discontinuities of cross section

Structural units used in many applications are of non-uniform cross sectional areas. The non-uniformity can be either a continuous variation of cross-ection such as tapered bars and truncated cones. or a discontinuous abrupt change in cross-section, such as stepped bars. In addition, nonhomogenities in the modulus of elasticity and material density do exist. Although the problem of elastic wave propagation in a rod with non-uniform cross-section has been a subject of interest and investigation for decades, the problem has received relatively little attention in the literature.

Most of the dynamic investigations of non-uniform rods are related to the analysis of longitudinal and flexural vibration and are based on the one dimensional elementary theory of longitudinal motion and the Euler-Bernoulli theory of lateral motion. However, many structures used in land, sea, air and space vehicles are subjected to impact and transient loading. Many structural units are in the type of beams with constant cross-section over a certain length which changes abruptly to another constant section. These are called stepped beams or beams with discontinuities of cross-section and are of main concern in the present investigation.

Investigations of transient loads in stepped beams are limited to longitudinal wave propagation and torsional waves since they are the simpler form for theoretical treatment. There are some studies related to flexural waves in tapered structures which are based mostly on the Euler-Bernoulli theory and there are some solutions related to flexural vibration in tapered beams based on the Timoshenko theory. However, there is no known research published on the analysis of flexural waves

in a beam with discontinuity of cross-section according to the Timoshenko beam theory, which is the subject of this thesis.

Donnell (1930) investigated the effect of a sudden change in cross-section or material of a bar on a propagated longitudinal wave, which when it arrives at the junction initiates two new waves, a transmitted wave and a reflected wave. When the sudden change was one of area only, Donnell found that for an incident wave striking a reduction in area, the reflected wave was of opposite sign to the original, whereas for a wave striking an enlargement, the reflected wave was of the same sign as the incident wave. The transmitted wave was always of the same sign as the incident wave. Donnell also studied the problem of a gradual change and formulated the differential equation of motion for longitudinal waves in a form which takes this effect into account. Compression force and longitudinal velocity of particles for the bar were presented graphically, and diagrams were constructed for waves produced by variable forces, based on energy consideration.

Angus (1943) derived force-velocity relationships for the elastic impact of a bar composed of several parts of different cross-sections, from analogy with hydraulic equations for water hammer. He presented an example of a bar composed of two cylinders of different diameters moving horizontally at a constant velocity and stopped because of striking a rigid body. It was shown that the stresses could be calculated by the known relation $\sigma = \rho c v$.

Langer (1943) used the general equation of motion for longitudinal vibration to obtain the frequency equation for an oil well pump rod consisting of a string of rods with abrupt changes in cross-section. The resulting natural frequencies were compared with records obtained from magnetic strain gauges located in the string of rods.

Le Van Griffis (1944) discussed the propagation of longitudinal waves in a bar with decreased or increased area which underlay the

conditions of equilibrium of forces and particle velocities. He explained reflections at free and fixed ends, as equivalent to a decrease in section to zero and infinite increase in section respectively.

Van Griffis constructed x-t diagrams with the help of a characteristic propagation velocity $c=\sqrt{E/\rho}$ which determined complete time-space stress function for any case of longitudinal impact and compared the results with measurements using wire resistance strain gauges.

Robinson (1950) discussed the "dynamic effects" in an aircraft under landing conditions and traced the propagation of various kinds of stresses in the structure. He described the use of the method of characteristics for the solution of the equation of motion as a hyperbolic system of partial differential equations. Robinson gave a general solution for shock reflection at discontinuities in connection with abrupt changes at the junction of aeroplane wings, such as in the wing root and in the vicinity of the power plant installation, where there was an abrupt change of characteristics relevant to wave propagation, i.e. stiffness and density.

Fischer (1954) investigated the transmission and reflection of an elastic longitudinal rectangular pulse in a bar with a cylindrical neck or swell of varying length. The transmission and reflection of the pulse in a bar with discontinuity of cross-section was followed up by a modified form of "graphodynmics method" which was applied before by De Juhasz (1942) and Bergeron (1938). In this graphical method force-velocity and space-time diagrams were used to obtain stress-time and displacement-time diagrams. A more extensive study and comparison with experiment was presented in a second paper by Fischer (1959).

Mugiono (1955) used the Euler-Bernoulli equation for the investigation of flexural waves in beams with one and two discontinuities of cross-section and used a travelling wave solution to obtain a

so-called reduction factor as a function of slenderness ratio for the propagation of bending wave in relation to sound transmission through walls in building structures. Calculations and experiments showed a reasonably good agreement for harmonically sinusoidal excitations.

Cranch and Adler (1956) used the simple beam theory to solve the problem of bending vibration of beams having rectangular cross section with any power-width variation where the depth variation was linear, quadratic or cubic. Bessel function solutions were obtained for a truncated pyramid cantilever, a cantilever with parabolic width variation and compound beams of similar halves joined together.

Ripperger and Abramson (1957b) repeated the theoretical solution of the bending wave problem in a bar with discontinuities of cross-section, treated before by Mugiono and added a comparison with the reflection and transmission of longitudinal wave pulses. It was attempted to determine reflection and transmission coefficient of a stress pulse based on steady-state wave propagation. This analysis was successful for longitudinal propagation where the dispersion did not seriously alter the pulse shape, but not for bending waves pulses which are always distorted by dispersion regardless of the pulse length. It was concluded therefore that any comparison of amplitude in bending waves was not a precise method. In order to compare with experimental results, reflection and transmission coefficients originally derived for velocity were related to the corresponding quantities of moments. The discrepancy was too large and it was concluded that a more accurate theoretical analysis was needed, especially when pulses were of short duration. A better agreement between theory and experiment was obtained by Habberstad and Hoge (1971). The problem of reflection and transmission of a longitudinal wave across a sudden change in cross-sectional area was discussed by Burton (1958) where equilibrium conditions for

particle velocities and forces were formulated.

The idea of reflection and transmission coefficient is similar to the idea of stress concentration factor used in the static loading shafts subjected to torsion and bending. Allison (1961) obtained the elastic stress concentration factors vs. diameter ratio in shouldered shafts subjected to pure bending as the quotient of the peak stress in the shouldered shaft to the maximum axial stress in a uniform shaft of smaller diameter, subjected to the same moment.

Taleb and Suppiger (1961) applied the Cauchy function method from the theory of integral equations to obtain the approximate fundamental frequency and modal configuration in a simply supported stepped beam. The solution was based on the elementary Euler-Bernoulli theory of lateral vibrations. The fundamental frequency computed after two iterations for the beam with a jump discontinuity was compared with the exact solution and was found to be only about three per cent above the exact value.

Reed (1962) reported a method for the computation of the amplitudes of the succession of pulses which were produced from the incidence of single longitudinal stress pulse on a zone of many abrupt discontinuities not simply related in their properties. An identifier was assigned to each pulse and described its propagational history. It was used together with a pulse designator to calculate amplitude and arrival times of reflected and transmitted pulses. The numerical method was used to calculate the relative amplitudes of the members of resultant pulse trains for rods with three and six step transitions, for rods with stepped-cone terminations of two to ten discontinuities, and for a continuous linearly tapered cone.

Cone (1963) obtained a theoretical solution for the longitudinal wave propagation across an abrupt change in the bar's cross-section and predicted the ratio between the incident, reflected, and

transmitted waves. The investigation was based on the elementary theory and results were compared with experimental data obtained by strain gauge measurements.

Conway and Dubil (1965) investigated transverse vibrational resonance frequencies of truncated cone and wedge beams for nine possible combinations of the simply supported, clamped, and free end conditons. The Euler-Bernoulli equations were used to obtain solutions in theform of Bessel functions of second order which were approximated by their polynomials and numerical results were tabulated for five modes and for four values of length ratios.

Davids and Kesti (1965) compared the determination of maximum loads under impact using vibration analysis and stress-wave propagation method for the design of long bars and stepped shafts. It was found that for a ramp-type pulse with a rise time t_0, whenever the rise time of the impact pulse exceeded the time required to propagate the length of the bar and back about three times, an almost exact sinusoidal oscillation occured. However, for a step pulse, the peak stress obtained by the stress wave method was almost 50 per cent higher than that from the vibration method. The longitudinal waves in an actuater and pilot shaft combination, designed for impact service, were investigated . An abrupt change of section was shown to be more sucessful in reducing the level of stress than a gradually changing cross-section .

Eddoe (1965) obtained a transient solution of the problem of longitudinal stress waves in a cylindrical rod with several step changes in cross-sectional area, by means of the Laplace transform method. The theory was applied to a rod with a simple neck, formed by two inverse changes in cross-section, where damping and wave dispersion effects were not considered. Results, obtained by strain gauge measurement showed good agreement with the theory.

Kawata and Hashimoto (1965) derived an approximate theory of

dynamic-stress concentration factors by considering notches and shoulders as discontinuities of cross-sectional area in struts. Experimental results for notched specimens of polyurethane rubber, using high-speed photoelasticity, were shown to coincide with theoretical results using one-dimensional theory of longitudinal wave propagation in an elastic bar .

Lindholm and Doshi (1965) were concerned with the propagation of a stress pulse in a continuously nonhomogeneous elastic bar of finite length where the elastic modulus was a function of the position in the bar. The one dimensional analysis for the propagation of longitudinalwaves was synthesized from the eigen functions for the non homogeneous bar by utilizing the principle of virtual work. Numerical results were presented for a finite free-free bar subjected to a pressure pulse and for one complete reflection in the bar. It was shown that the eigen functions satisfied the orthogonality conditions and series expansions were evaluated for the first 30 terms. Based on Laplace transforms,an approximate solution of the same problem was given by Whittier (1965).

Rosefeld and Miklowitz (1965) formulated a general solution for the response of an elastic rod of arbitrary cross-section to mixed end condition loading, where the orthogonality condition of the eigen functions for the displacements with different eigen values for the frequency were employed. Laplace and Fourier transforms were introduced in order to obtain solutions in term of harmonic waves for long-wave effects which governed the long-time, large distance behaviour. It was pointed out that the nature of the results for low frequencies did not depend directly on the boundary shape, but the higher modes had a more complicated structure.

Yang (1966) derived a general differential equation governing discontinuous wave propagation in non uniform Timoshenko beams. A

closed form solution was obtained for a nonuniform beam with a linear variation in cross-section. The method of characteristics was used to formulate expressions for jumps in moment, shear, angular velocity and transverse velocity.

Bruner and Muster (1967) reported the attenuation characteristics of a typical drill-string model as a long bar with spaced discontinuities in cross-section area subjected to plane longitudinal acoustic waves. The analysis was based on mechanical-electrical analogy, used before for single area discontimuities in infinitely long bars by Miles (1946) who showed that the discontiniuty could be represented by a shunt capacitance and by Karal (1953) who represented the discontiniuty by a series inductance, both as functions of area ratio. Bruner and Muster found that attenuation peaks decreased with increasing area ratio and that attenuation occured at frequencies governed by the bar length at the last segment of the system.

Tsui (1968) solved the problem of a projectile impinging upon target as one of longitudinal wave propagation in a finite length bar with power variation in the cross-section. A solution was obtained for a free-free bar subjected to an arbitrary pulse applying the method of separation of variables and the principle of virtual work, as used before by Lindholm and Doshi (1965) for the non-homogeneous bar. The same problem was solved by Handelman and Rubenfeld (1972) using Laplace transform method. The calculations, although standard, were somewhat tedious.

Kenner and Goldsmith (1969) investigated the effect of a thin glue section, joining two adjacent cylindrical bars, on the longitudinal wave propagation. The joint was treated as a short discontiniuty by the one dimensional theory and the effect of eccentric alignments on the wave transmission was also investigated. It was found that a thin insert placed between cylindrical sections disturbed the wave transmission

in varying amounts depending on both the disparity in mechanical impedance ρc_o with the exterior bars and the thickness of the section. The eccentricity distorted the transmitted longitudinal wave very little, but decreased the peak strain up to 10%. The theorectical predictions were tested by experiments performed on aluminium bars glued together using two different adhesives.

Habberstad (1971) formulated a two-dimensional theory for axisymmetric elastic wave propagation by approximations of the Pochhammer-Chree equations governing axisymmetric wave propagation in cylindrical bar,using afirst order finite difference scheme. The numerical analysis was based on a displacement formulation used by Bertholf (1967) to study the same type of waves in uniform cylindrical rod. However, Habberstad used this numerical technique for a bar containing a discontinuity in cross-section and for a bar composed of two materials fused together. Ramamurti and Ramanamurti (1977) solved the same problem by the finite element method.

Mabie and Rogers (1972) obtained the differential equation of motion for a vibrating double-tapered cantilever beam from the Euler-Bernoulli theory of transverse vibration. The frequencies of five modes were tabulated for various taper ratios. The results were obtained by numerical integration.

Mortimer et.al (1972) used three theories to analyse the problem of reflection and transmission of transient longitudinal pulses in shells with discontinuous cross-sectional areas. The three theories used were the bending theory which included the transverse shear, radial inertia, and rotary inertia effect; a modified membrane theory which included bending and rotary inertia, and a uniaxial theory, which included only axial motions. Solutions were obtained by solving each of the three systems of governing equations by the method of characteristics. The longitudinal and circumferential incident, transmitted and reflected

strain pulses as predicted by the bending and membrance theories were shown to be in good agreement with experimental results, whereas the uniaxial theory strain predictions did not agree well with the experiment. In a second paper by Rose et.al (1973) the method of characteristics was used to obtain a numerical solution according to the bending theory for the longitudinal impact of a joint cylinder-truncated cone-cylinder. Good agreement was obtained with experiments carried out for a model consisting of a 1/100 - scale replica of a portion of the Apollo/Saturn V vehicle.

Yang and Hassett (1972) utilized the method of characteristics in the theoretical analysis of the problem of transient stress in axisymmetric bodies of varying areas, such as cones and structures with large step changes in cross-sectional area and with changing impedances.

Rader and Mao (1972) were concerned with the amplification of longitudinal pulses which propagated along tapered elastic bars, which was regarded as a wave guide with continuously varying impedance. A general travelling wave solution representing waveforms propagating in both directions was used where the incident wave generated an infinite sequence of reflected and refracted waves. Experimental results showed that only for very short and very long pulses, did the amplification approach the limiting values given by the theoretical prediction.

Reismann and Tsai (1972) developed an improved theory which accounted for longitudinal as well as radial motions. The theory was applied to two bonded, semi-infinite rods composed of different materials and to a rod of finite length bounded at each end to two semi-infinite rods composed of different materials. The results were compared with the predictions of the elementary rod theory as characterized by the wave equation. For a harmonic excitation, phase velocity vs. frequency plots was presented and it was shown that the improved

theory indicated the existence of two modes.

Koenig and Berry (1973) applied the direct finite analysis, originally developed by Davids and Koenig (1967) to obtain the transient flexural response of a cantilever tapered beam and a composite beam of two different materials, subjected to a step moment input and a step velocity input. The time-histories of bending moment and shear forces were presented graphically.

Lee and Wang (1973) presented a one-dimensional theory which accounted for longitudinal as well as radial and axial shear deformation and their inertias for elastic circular rod with nonuniform cross-section. The theory was an extension of the Mindlin-McNiven theory (1960). The numerical results were obtained by the method of characteristics for several non-uniform semi-infinite and finite rods subjected to either a step or a pulse loading. The geometrical effect of variation of section on the stresses and the effect of the elastic support on the reflection and propagation of the stress were deduced. Predicted and measured results were compared.

Klein (1974) investigated the transverse free vibration of elastic beams with non-uniform characteristics using variational analysis, either as a Rayleigh-Ritz type method or as a finite element type method. The basic assumptions of the analysis were based on the Euler-Bernoulli theory. The case of a simply supported stepped beam was studied as a model for a non-uniform rotor blade. Comparison with experiments indicated that the theory adequately predicted natural frequencies for the first three modes and the mode shapes.

Lee and Sechler (1975) used the one-dimensional theory to examine the longitudinal wave propagation in wedges due to impact at their large end. Closed from solutions were obtained in term of Laplace transforms and Bessel functions.

Gorman (1975) investigated the lateral free vibration of beams

with step changes in the properties of their cross-section and gave extensive tables to obtain the frequencies for 4 modes and various end conditions. The solutions were based on the Euler-Bernoulli theory.

Ramamurti and Ramanamurti (1975) used a finite difference formulation to solve the problem of longitudinal wave propagation in very short bar with discontinuity of cross-section. Due to the symmetry in loading the problem was treated as a two-dimensional one.

Levinson (1976) studied the natural frequencies of a stepped simply supported beam using the Euler-Bernoulli theory. He obtained the frequency equation which was quite complicated to be solved exactly, even for a stepped beam consisting of only two distinct parts. It was concluded that an approximate numerical solution method should be used.

Goel (1976) investigated the transverse vibration of linearly tapered beams and the results for the first three eigen-frequencies for different values of stiffness ratio's and taper ratios were tabulated. The analysis was based on the Euler-Bernoulli equation of motion.

Johnson (1977) studied the problem of longitudinal waves in a bar with step change in cross-sectional area and material and expressions relating the transmitted and reflected wave to the incident wave, using the one-dimensional theory were presented.

Filippov (1977) formulated general solutions for composite rods consisting of finite rods of constant but different thickness and of composite rods with continuously varying thickness. The solutions were based on the one-dimensional theory of longitudinal wave propagation using Heaviside function and Dirac delta function for the applied Laplace transformation.

Vasudeva and Bhaskara (1978) discussed the problem of a pressure pulse in an elastic bar of finite length whose Young modulus, material density and cross-sectional area varied along the length in a general power form. The solution used the elementary theory and Laplace

transformations gave the general expressions for stress. The numerical values were computed by iteration for a half-sine wave pulse and the results agreed fairly well with those of Lee (1974).

Gupta and Nilsson (1978) studied the problem of longitudianl impact between a truncated finite conical rod and a long cylindrical rod, where contact was maintained from the time of impact and the piston-rod system was considered as one structural unit. Two theoretical solutions were obtained, a closed from solution based on one-dimensional wave theory and a numerical finite element solution based on three dimensional axisymmetric model. Finite element results were in good agreement with experimental results, apart from spurious oscillations shown in the finite element solution of impact for pistons with various apex angles.

Nagaya (1979) formulated an approximate numerical method for the dynamic analysis of a tapered Timoshenko beam with moving loads. Hamilton's principle was applied to obtain the equation of motion from the Lagrangian of the Timoshenko beam and using the orthogonality of the eigenfunctions, of first and second kind. In the numerical computation the effect of the inertia force on shear motion was neglected and the approximate solution was found to be larger than with the exact Timoshenko beam with increased velocity of the load.

Hashemi (1979) obtained the frequency equation and point impedance of a stepped beam using the elementary Euler-Bernoulli theory of transverse vibration. The roots of the frequency equations were obtained for the first five modes and various length to width ratios. The numerical results were compared with experimental results.

CHAPTER III

ANALYSIS OF TRANSIENT BEAM RESPONSE

3.1. Derivation of the Equation of motion

The Pochhammer-Chree theory can not be used to find solutions for flexural wave propagation in finite or even semi-infinite beam with arbitrary prescribed displacement or stress distribution on the end cross-section. The Euler-Bernoulli theory is inadequate because it neglects the effects of "rotatory inertia" and "shear deformation" when dealing with the transverse vibration of prismatic bars.

The theory which takes these effects into account is attributed to Timoshenko (1921, 1922, 1928), in the so called Timoshenko beam theory which is widely used for solving problems of flexural vibration of beams and more recently for solving transient flexural wave propagation in beams.

The Timoshenko beam theory includes, in addition to the transverse displacement due to bending which is the only term included in the Euler-Bernoulli theory, the effect of rotatory inertia, originally introduced by Bresse in 1859 and usually attributed to Rayleigh 1894, as well as a second term which takes into account the effect of the non-uniform shear distribution over the cross-section.

The Timoshenko beam equations were originally formulated by Timoshenko using D'Alemberts principle. The same equations, however, can be derived, by using a more general approach from the three-dimemsional theory of elasticity on the basis of Hamilton's principle.

The Timoshenko beam theory is a one-dimensional approximate theory which used two displacement co-ordinates to represent the transverse motion of the beam axis (y), and to account for the rotation of the cross-section (ψ) as shown by the beam element in figure 3.1 of a beam under the effects of bending moment M and shear force Q.

When the beam element is deformed and, for small displacements, the

cross-section of the beam rotates through an angle ψ, while the neutral axis of the beam rotates through a small angle $\partial v/\partial x$, and it is no longer perpendicular to the beam cross-section. These two rotations differ by the angle of the shear, i.e. $\gamma = \frac{\partial v}{\partial x} - \psi$. If u_1 and u_3 are defined as

$$u_1 (x, y, z, t) = - y\psi(x, t)$$

$$u_3 (x, y, z, t) = v (x, t)$$

The non-zero strains are then

$$\varepsilon_{xx} = \frac{\partial u_1}{\partial x} = -y \frac{\partial \psi}{\partial x}$$

$$\varepsilon_{xy} = \gamma = \left(\frac{\partial v}{\partial x} - \psi\right)$$

The shear force is distributed non-uniformly over the cross-section and there is not a single angle for the cross-section. But in order to retain a one-dimensional model, a shear correction factor k^2 is introduced to give an "equivalent" uniform shear, a form of averaging over the cross-section.

The linear constitutive relations for a differential beam element lead to the integrals for the kinetic energy, strain energy and the potential energy of a Timoshenko beam of length L. The kinetic energy T consists of two parts due to translation and rotation

$$T = \int_0^L \left\{ \frac{\rho A}{2} \left(\frac{\partial v}{\partial t}\right)^2 + \frac{\rho I}{2} \left(\frac{\partial \psi}{\partial t}\right)^2 \right\} dx$$

The strain energy for the Timoshenko beam is also made of two parts and can be found from the following relation

$$U = \int_0^L \int_A \frac{E}{2} \varepsilon_{xx}^2 \, dA dx + \int_0^L \int_A \frac{G}{2} \varepsilon_{xy}^2 \, dA dx$$

The shear force-shear strain relation is found using the value of k^2 such that

$$\int_A \frac{G}{2} \varepsilon_{xy}^2 \, dA = \frac{k^2 G}{2} \int_A \left(\frac{\partial v}{\partial x} - \psi\right) dA$$

$$= \frac{k^2 GA}{2} \left(\frac{\partial v}{\partial x} - \psi\right)$$

The strain energy is then formulated as

$$U = \int_0^L \left\{ \frac{EI}{2} \left(\frac{\partial \psi}{\partial x}\right)^2 + \frac{k^2 GA}{2} \left(\frac{\partial v}{\partial x} - \psi\right)^2 \right\} dx$$

From here on the general displacement variable y will be used instead of v, since y is usually used for the location of the beam axis.

The Lagrangian $\mathcal{L}$ is usually used for the difference between the kinetic energy T and the strain energy U

$$\mathcal{L} = T - U$$

When the Timoshenko beam is subjected to external forces such as shear force Q and bending moment M, the work done by these forces W, illustrated in fig. 3.1, can be expressed as

$$W=M_1(0,t)\,\psi(0,t) + Q_1(0,t)\,y(0,t) + M_2(L,t)\,\psi(L,t) + Q_2(L,t)\,y(L,t)$$

The Hamilton's principle implies that all variations vanishes at the arbitrary time limits t_1 and t_2 and can be applied to the Timoshenko beam system to give

$$\delta \int_{t_1}^{t_2} (\mathcal{L} - W)\, dt = 0$$

The expression for $\mathcal{L}$ and W are inserted in the above equation after the variational calculus is performed

$$\delta \int_{t_1}^{t_2} T dt = \int_{t_1}^{t_2} \int_0^L \{\rho A \frac{\partial y}{\partial t} \delta \frac{\partial y}{\partial t} + \rho I \frac{\partial \psi}{\partial t} \delta \frac{\partial \psi}{\partial t}\}\, dt dx$$

After integration by part and using the fact that the variations δy and $\delta\psi$ must both vanish at x=o and x=L, one gets the variation of the kinetic energy as

$$\delta \int_{t_1}^{t_2} T dt = - \int_{t_1}^{t_2} \int_0^L (\rho I \frac{\partial^2 \psi}{\partial t^2} \delta\psi + \rho A \frac{\partial^2 y}{\partial t^2} \delta y)\, dx dt$$

Similarly the variations of U and V are found as

$$\delta \int_{t_1}^{t_2} U dt = - \int_{t_1}^{t_2} \int_0^L \{ EI \frac{\partial \psi}{\partial x} \delta \frac{\partial \psi}{\partial x} + k^2 GA (\frac{\partial y}{\partial x} - \psi)\, \delta (\frac{\partial y}{\partial x} - \psi) \}\, dx dt$$

$$= - \int_{t_1}^{t_2} \int_0^L \{(EI \frac{\partial^2 \psi}{\partial x^2} - (\frac{\partial y}{\partial x} - \psi) k^2 GA - EI \frac{\partial \psi}{\partial x})\, \delta\psi + (k^2 GA (\frac{\partial^2 y}{\partial x^2} - \frac{\partial \psi}{\partial x}) + k^2 AG (\frac{\partial y}{\partial x} - \psi))\, \delta y\}\, dx dt$$

$$\delta \int_{t_1}^{t_2} W dt = - \int_{t_1}^{t_2} (M_1 \delta\psi_1 + M_2 \delta\psi_2 + Q_1 \delta y_1 + Q_2 \delta y_2)\, dt$$

Applying Hamilton's principle and grouping the terms in the above equations:

$$\delta \int_{t_1}^{t_2} (T-U-W)\, dt = \int_{t_1}^{t_2} \int_0^L \{(EI \frac{\partial^2 \psi}{\partial x^2} - \rho I \frac{\partial^2 \psi}{\partial t^2} - EI \frac{\partial \psi}{\partial x} + (\frac{\partial y}{\partial x} - \psi) k^2 GA) \delta \psi$$

$$+ k^2 GA (\frac{\partial^2 y}{\partial x^2} - \frac{\partial \psi}{\partial x}) - \rho A \frac{\partial^2 y}{\partial t^2} - k^2 AG (\frac{\partial y}{\partial x} - \psi)) \delta y\} \, dx dt +$$

$$+ \int_{t_1}^{t_2} \{M_1 (0,t) \delta \psi_1 + M_2 (L,t) \delta \psi_2 + Q_1 (0,t) \delta y_1 + Q_2 (L,t) \delta y_2\} dt = 0$$

Rearranging the equation;

$$\delta \int_{t_1}^{t_2} \mathcal{L}_a dt = \int_{t_1}^{t_2} \int_0^L \{(k^2 GA (\frac{\partial^2 y}{\partial x^2} - \frac{\partial \psi}{\partial x}) - \rho A \frac{\partial^2 y}{\partial t^2}) \delta y + (EI \frac{\partial^2 \psi}{\partial x^2} - \rho I \frac{\partial^2 \psi}{\partial t^2} +$$

$$+ k^2 AG (\frac{\partial y}{\partial x} - \psi)) \delta \psi\} dx dt + \int_{t_1}^{t_2} \{-EI \frac{\partial \psi}{\partial x} \delta \psi - k^2 GA (\frac{\partial y}{\partial x} - \psi) \delta y\} \Big|_{x=0}^{x=L}$$

$$+ \int_{t_1}^{t_2} (M_1 (0,t) \delta \psi_1 + M_2 (L,t) \delta \psi_2 + Q_1 (0,t) \delta y_1 + Q_2 (L,t) \delta y_2) dt = 0$$

Since the variations of the two functions $\delta y(x,t)$ and $\delta \psi(x,t)$ are arbitrary, the necessary conditions for them to vanish are the pair of coupled partial differential equations for $0 < x < L$;

$$k^2 GA (\frac{\partial^2 y}{\partial x^2} - \frac{\partial \psi}{\partial x}) - \rho A \frac{\partial^2 y}{\partial t^2} = 0$$

$$k^2 GA (\frac{\partial y}{\partial x} - \psi) + EI \frac{\partial^2 \psi}{\partial x^2} - \rho I \frac{\partial^2 \psi}{\partial t^2} = 0$$

These are the governing equations for a Timoshenko beam and the boundary conditions at x=0: $(EI \frac{\partial \psi}{\partial x})_1 = -M_1$

$$k^2 GA (\frac{\partial y}{\partial x} - \psi)_1 = -Q_1$$

and at $x = L$: $(EI \frac{\partial \psi}{\partial x})_2 = M_2$

$$k^2 GA (\frac{\partial y}{\partial x} - \psi)_2 = Q_2$$

The Timoshenko beam equation is sometimes also written as a fourth order partial differential equation by eliminating one of the variables ψ or y from the two partial second order differential equation. Uncoupled and written in term of the transverse displacement y

$$EI \frac{\partial^4 y}{\partial x^4} + \rho A \frac{\partial^2 y}{\partial t^2} - \rho I (1 + \frac{E}{k^2 G}) \frac{\partial^4 y}{\partial x^2 \partial t^2} + \frac{\rho I}{k^2 AG} \frac{\partial^4 y}{\partial t^4} = 0$$

Hamilton's principle was applied for the derivation of the Timoshenko equations by the variational method, by several authors, e.g., Carnes (1964); Crandall et.al (1968); Dym and Shames

(1973) and Harrison (1977).

In Hamilton's principle the geometric constraints are embodied in the admissibility conditions, and the dynamic force requirements are embodied in the variational criterion.

3.2. Methods of solution

3.2.1. Transform methods

The problem of transverse wave propagation in an elastic beam can be solved by using Laplace transforms and to a lesser extent Fourier transforms. Solutions have been basically obtained for transverse impact of semi-infinite beams of circular and rectangular cross-section, as was described in section 2.2.2.

Uflyand (1948) was the first to derive solutions employing Laplace transform and contour-integration inversion methods. Results were obtained through convolution for the response to a step input function and inputs having an impulsive time character in the form of a delta function.

The main difficulty is in connection with the treatment of end conditions. Miklowitz (1953a) obtained the Laplace transform for certain types of end conditions and pointed out at the same time that it was much more difficult to obtain the transform for other types of end condition.

The use of transform methods is almost restricted to the study of transverse waves in uniform semi-infinite bars where no discontinuities and wave reflections are involved. However, the problem of eccentric impact of beams is more difficult to handle with Laplace transforms and no solution is available by this method even for the simplest case of a uniform beam .

Transform techniques generally require numerical inversions and numerical integration schemes become more complicated when boundary conditions are incorporated. Closed form solutions provide little

insight into the response of structures and leave much to desired regarding convergence near the wave fronts. Carnes (1964) showed that complex inversion integrals should be evaluated when Laplace transforms are used to obtain solutions for the semi-infinite beam. This is a rather tedious procedure. Transform formulae usually involve infinite integrals and difficult integrations which must be approximated in practical computation. Weinberger (1965) pointed out that transform solutions have the appearance of being exact, whereas in practice they require limiting processes which cannot usually be carried out.

The integral, obtained after lengthy inversions, usually contains different combinations of Bessel functions. When a solution is obtained for a certain type of input, the inversions cannot be used for other types of inputs, In the Laplace transform, for a differant input function, another lengthy transfrom and inversion process must be carried out and the resulting integral must be evaluated separately by numerical means.

Closed from solutions by transform methods are usually restricted to some special cases of transverse wave propagation and in most other cases, one has to resort to a numerical approximation method which will be presented in the next sections. However, Laplace transform methods are useful in producing "exact" solutions for certain problems which can be used for comparison in obtaining the accuracy of other approximate methods. It is known that the Laplace transform method yields solutions in closed form only when the special distribution of variable parameters is restricted to certain power law or exponential formats. Foran arbitrary parameter distribution asymptotic methods could be used but are usually valid only for short times and diverge at intermediate or long times. (Moodie and Barclay, 1976 and Gordon, 1977).

3.2.2. Finite element methods

Finite element methods have been used widely for frequency analysis of flexural vibration of Timoshenko beams and for predicting mode shapes and natural frequencies, as described in section 2.2.1.

Several solutions have been obtained by several authors for axisymmetric longitudinal transient wave propagation problems.

Costantino (1967) used the finite element method to solve wave propagation problems of one-dimensional plane strain and two-dimensional half-space problems. The results were satisfactory for displacement time-histories, but stress-time histories were not as accurate and depended on the spatial variation of stresses as compared to the element size and the traversal time of the stress pulse across the element. Costantino used a system of equations based on the "point mass" system, in contrast to the alternative approach "consistant mass matrix" which is used in structural vibration analysis.

Shipley et.al. (1967) also used finite element formulations for solving axisymmetric wave propagation problems and he found that the analysis modelled the displacement field much more accuratly than the stress field. The stress-time histories showed a predominance of high frequency oscillations in trailing portions of the disturbance and the data were compared with exact solutions.

One of the disadvantages of the finite element model is that computed stresses show severe oscillations - a consequence of a so-called "numerical dispersion". This makes the finite element method less attractive for flexural wave propagation problems, since it becomes difficult to decide whether the oscillation are due to the dispersive nature of the propagated wave or the dispersion is due to numerical inaccuracies. Another problem is the difficulty encountered in representing discontinuities and transient wave fronts. Finite element models also behave like low pass filters having definite passing bands

and cut-off frequencies which depend upon the wave types being propagated, longitudinal or transverse and they depend on the finite element mesh as well.

Belytschko et.al. (1978) showed that the numerical solution oscillated about the analytical solution for a step function input, due to attenuation of all frequencies beyond the cut off frequency in a discrete mesh.

Several authors treated examples of one-dimensional and two-dimensional axisymmetric wave propagation problems by various triangular and rectangular finite element models. In most works, the mass of each element was lumped at its modal points "point mass system". This made the mass matrix diagonal and hence, the associated inversions were made simple. However, this procedure led to poor approximations. Some of the works dealing with axisymmetric longitudinal wave propagations are those of Fu (1970), Buturla et. al. (1974), Holmes et.al. (1976).

The main advantage of finite element methods are their ability to treat geometrically complex structures. A wide range of elliptic and parabolic governing equations have been successfully solved using finite element methods (Zienckiewicz, 1971). However, finite element methods have not yet proven their suitability for the solution of transient flexural wave propagation problems which are governed by hyperbolic partial differential equation systems, in connection with mixed initial and boundary conditons.

3.2.3. Finite difference methods

Finite difference methods are well established and are successfully used in solving wave propagation problems. The solution method has been first discussed in a paper by Courant et.al. (1928). However, its usefulness was helped as by other numerical schemes, by the recent development in large digital computers in both speed and core size. There exist several forms of finite difference approximation

and common approximate techniques are used in finite difference methods. They are extensively treated in several books (Sauer, 1954, Lax, 1958, Richtmyer and Morton 1967; Forsythe and Wasow, 1960).

The essence of the finite difference technique is to replace the differential equations and boundary conditions by simple finite difference approximations, such as Taylor series expansions with truncation at some point to optimize both error and computation requirements. The resulting equations are then numerically integrated to obtain the solution of the problem.

Finite difference methods are easy to programme and capable of solving transient problems which can give information at many frequencies from one computer run, in contrast to steady state solutions. The method is most useful in near field region of sources. Finite difference and finite element methods differ in that the former discretizes the governing partial differential equations or energy functions, whereas the latter discretizes the structure itself.

Cushman (1979) compared the use of finite difference and finite element methods and concluded that for irregular domains, finite element analysis is often easier to use, while for regular domains finite difference methods are more easily programmed. He illustrated for the case of one-dimensional longitudinal wave-propagation, the possibility to generate the standard finite difference scheme as a special case of finite element scheme, simply by applying the finite element discretization process to time as well as to space. However, there was little to be gained with this technique and it involved increased storage and computational requirements. This technique is, therefore, rarely used.

The main disadvantage of the finite difference techniques is its inefficiency in handling discontiniuties in geometry which suggested the introduction of doubtful assumptions of compatibility at the discontinuities and fictitious surfaces at the boundary. This technique

made the results dependent upon the chosen assumption for the displacement values at the junction points. Furthermore, difficulties were experienced in treating material interfaces or indeed any type of discontinuous stresses, which must be averaged. The introduction of artificial viscosity terms into the equations, have the effect of smoothing out the input function over a short distance, but can introduce significeint errors into the analysis. The method has been mostly developed for two-space variable problems.

Karnes and Bertholf (1970) solved the problem of axisymmetric elastic-plastic wave propagation by a two-dimensional finite difference scheme which employed the Von Neuman and Richtmyer method for smoothing shock fronts by an artificial viscosity. The study was an extension of the solution obtained by Bertholf (1967) for the elastic wave propapation problem. The accuracy of the numerical results depended on the number of finite difference increments, or meshes used.

Chiu (1970) used the finite difference scheme to investigate the transmission and reflection of longitudinal stresses in an elastic bar with discontinuities, as a one-dimensional wave propagation problem.

Habberstad (1971) approximated the exact equations of motion governing elastic, axisymmetric wave propagation in cylindrical rod by a first order finite-difference scheme, which was used to study longitudinal wave propagation in a bar composed of two materials (steel and aluminum), and in bars containing a discontinuity in cross-section.

Ramamurti et.al (1975) used the finite difference analysis to solve the problem of axially symmetric impact in very short uniform and stepped beams. The solution was based on a finite difference scheme, as proposed by Alterman and Karal (1970) for wave propagation in semi-infinite bars. The results showed high oscillations and were not compared with any other numerical results or with any experimental results.

Forrestal and Bertholf (1975) used a two-dimensional wave propagation finite difference scheme to obtain strain-time histories for the transverse impact of a beam of rectangular cross-section. The results showed higher frequency oscillations.

Several authors have developed special finite difference schemes for applications in Seismology (Alterman and Lowenthal, 1972; Boore, 1972, Bond, 1978). Ilan et.al. (1979) used finite difference methods to study elastic waves scattered by irregularities (slots) in a stress free surface, a problem particularly important for ultrasonic non destructive testing.

The finite difference methods are mostly used to solve problems in which the response is mostly dominated by axisymmetric motion. However, its application to study flexural wave propagation problems is less feasible. Therefore finite difference methods are used for solving longitudinal axisymmtric wave propagation problems where they are efficient (Swartz and Wendroff,1974)

3.2.4. The method of Characteristics (MOC)

Wave propagation problems are mathematically classified as mixed initial boundary value problems and their governing equations are mostly partial differential equations of hyperbolic type. For hyperbolic systems involving two independent variables, the method of characteristics (MOC) is undoubtedly the most convenient, most effective and most accurate method of solution. Other numerical methods such as finite difference and finite element methods are basically more suitable for hyperbolic equations in higher dimensions where the MOC might be less satisfactory. (Mitchell, 1969).

In the MOC the system of the governing equations is replaced by a system expressed in characteristic co-ordinates,the so called canonical equations. One of the main advantages of characteristics, and a disadvantage of finite differences, is that discontinuities in

the initial values may propagate along the characteristics. This situation is difficult to handle by other than the characteristic net. (Ames, 1977).

The earliest applications of the MOC to linear wave propagation problems are those by Riemann (1860) in gas dynamics by Massau (1889) in hydraulics and Soil mechanics and by Prandtl (1920) in mechanics of plastic metals. The theory of MOC is best described in the works of Courant et.al. (1928); Courant and Friedrichs (1937). Abbott (1966) gave various application examples and Cristescu (1967) and Nowacki (1978) gave detailed description of application examples in the theory of plastic flow under quasi-static and dynamic conditions. In a number of works, Chou and his co-workers used the MOC in a unified manner to solve elastic wave propagation problems with a variety of initial and boundary conditions in beams, plates and shells.

The MOC have been used widely in solving the Timoshenko beam equations as a system of hyperbolic partial differential equations (PDE) governing transverse and bending wave propagation problems due to transverse and eccentric impact, as was described in section 2.2.2.

The principle of domain of dependence in the MOC ensures a unique solution in the region between the characteristic lines with the smallest slope. Furthermore the MOC has the advantage that it follows the physical wave fronts as they are propagated along the beam. The MOC is particularly useful in solving wave propagation problems in finite structures, since reflections from boundaries are automatically absorbed into the solution by the presence of the backward-running characteristic curve at each grid point.

The detailed investigation given by Courant et.al. (1928) for the solution of hyperbolic PDE by the MOC, in which they specified the condition for the stability of the numerical scheme, the so called Courant-Friedrichs-Lewy (C-F-L) stability condition, is particularly

important in obtaining numerical results using finite difference approximations along the characteristic lines in the domain of dependence.

Pfeiffer (1947) was the first to obtain a general solution for the Timoshenko beam equations as a system of first order PDE, using the method of characteristics. Schirmer (1952) used the technique suggested by Pfeiffer to apply the MOC to the Timoshenko beam theory to study bending waves in beams. Leonard and Budiansky (1953) utilized the MOC to analyse travelling waves in beams subjected to lateral loading, governed by the Timoshenko beam theory, but for the rather physically non-realistic assumption of $c_1 = c_2$ which simplified the numerical work involved.

Kuo (1958) solved the problem of bending waves in rods subjected to eccentric impact by MOC in the same way as by Leonard and Budiansky. Plass (1958) used the MOC for Timoshenko beam problems subjected to various type of short half-sine pulse loading and applied more realistic distinct bending wave (c_1) and shear wave (c_2) velocities.

The Timoshenko beam equations have been treated as a system of second order PDE by the MOC in a series of papers, in a unified approach capable of dealing with discontinuities along the characteristics in semi-infinite structures, where no reflections were involved and the emphasis was set on the refinement of the numerical scheme. (Chou and Mortimer, 1965; Chou, 1965; Chou and Koenig, 1966).

Aprahamian et.al. (1971) used the MOC to solve the Timoshenko beam equations for a doubly infinite beam subjected to an impulsive transverse load, which gave excellent agreement with experimental results obtained by holographic interferometry .

Stepanenko (1976) showed how the so called "numerical dispersion" can be minimized, although not completely eliminated in the case of the Timoshenko beam, when explicit finite difference formulations were used for the integration along a characteristic network constructed

with varying steps, peculiar to each type of waves.

The method of characteristics has been used to treat flexural waves in curved bars in a Timoshenko-like theory (Crowley et. al. 1974) and to predict fractures in brittle materials according to the Timoshenko theory (Colton, 1973) as well as for determining the rate of healing of a partially cracked bone with the aid of a combination of longitudinal and Timoshenko-type waves (Philips et. al., 1978).

Axisymmetric elastic wave propagation in beams, plates and shells have been treated by the MOC in a unified manner which could be applied to various plane cylindrical and spherical waves with one-, two- and three displacement variables. (Chou, 1965; Chou and Mortimer 1967; Rose and Chou, 1973).

Mengi and McNiven (1971) obtained the response of a semi-infinite transversly isotropic rod to a time-dependent input using the MOC, which gave an accurate prediction to the response except perhaps for the very front of the wave, which is influenced by the higher branches.

Several problems of axially symmetric wave propagation in non-uniform structures were treated by the method of characteristics (MOC) as was described in section 2.3.

The method of characteristics has also been successfully applied for the prediction of transient responses in multilayered rods and shells. (Chou and Flis, 1975; Ziv, 1975; Mukunoki and Ting, 1980).

In the theory of visco-elastic and plastic wave propagation, the method of characteristics led to the solution of various types of transient response problems.

Lee (1953) obtained the permanent plastic distribution in the corresponding regions of a structure by MOC and the difficulties arising in boundary value problems of the theory of plasticity, were pointed out.

Plass (1955) investigated bending waves in a rod where plastic

stresses were present by the Timoshenko beam theory and relations about plastic flow in a solid exhibiting a strain rate effect. Numerical results were obtained by the MOC.

Bejda (1967) solved wave propagation problems in elastic visco-plastic beams by the MOC and Clifton (1967) used the same method and the one-dimensional theory of rate-independent plastic wave propagation to study longitudinal elastic-plastic waves in long bars.

McNiven used the MOC to obtain the response of an infinite visco-elastic body with an infinitely long cylindrical hole, where the lateral surface was subjected to a uniform pressure.

The problem of one-dimensional wave propagation through a bilinear elastic-plastic specimen in Kolsky's split Hopkinson pressure bar, was investigated by Jahsman (1971) using the MOC.

In his thesis, Ranganath (1971) solved the problem of the transverse impact of an infinite elastic-plastic beam by a semi-infinite elastic rod using the MOC, based on the Timoshenko beam theory. A strain rate independent model was used to describe the material behaviour and a strain hardening criterion was used for the pure bending, based on the quasi-static moment-curvature relation.

The use of the method of characteristics is widespread in fluid mechanics and gas dynamics to predict flow velocity at pipe outlets (Iseman, 1967) and multi-dimensional unsteady flows (Sauerwein, 1967). Sedney (1969) gave a survey of the use of the MOC for non-equilibruim internal flows. Another application field for the method of characteristics is soil mechanics. Streeter et.al. (1974) investigated the wave propagation corresponding to earthquake intensities in a model of unsaturated and saturated soils.

Wylie and Streeter (1976) found the MOC suitable to investigate the transmission of shear waves in soil layers. It has been attempted to extend the application of the method of characteristics to two-

dimensional spatial problems i.e. cases of three independent variables. (Thornhill, 1952).

Clifton (1967) investigated plane stress dynamic deformation of an isotropic-linear elastic solid by a second order explicit method, as proposed by Butler (1960) for integration along the bicharacteristic. Ziv (1969) also studied two-dimensional spatial elastic wave propagation by the MOC. Chang (1972) investigated two-dimensional motion of a cylindrical bar subjected to axisymmetric impact by the MOC.

Haddow and Mioduchowski (1979) used a near characteristic scheme proposed by Sauer (1964) for two-spatial variables and time to obtain numerical results for waves in a plate due to a suddenly punched hole as a uniaxial tension field.

Good agreement with experimental results and with transforms increased the confidence in the results of the method of characteristics. Therefore its results were used to check the accuracy and validity of the results of other numerical methods such as finite difference and finite element methods.

Fu(1970)compared finite element results with MOC results for a circular finite length rod subjected to a suddenly applied uniform pressure. Raney and Howlett (1971) presented a comparison of numerical solutions obtained by finite element, finite difference and the method of characteristics for the axisymmetric response of a cylindrical shell subjected to an initial axisymmetric velocity at its centre. The importance of higher frequency modes was emphasised.

Forrestal and Bertholf (1975) compared the results of finite difference method with the MOC for the transverse impact of a beam of rectangular cross-section.

Belyschko (1978) also compared the results of the three numerical results and pointed out the advantage of the method of characteristics, particularly for solving hyperbolic partial differential equations.

In flexural wave propagation problems, where time and space play similar roles and where characteristics are important, since the motion is governed by a PDE, the finite difference approximation along the characteristics has a powerful potential advantage (Morton, 1976).

3.2.5. Conclusions

In the solution of transient wave propagation problem, closed-form solutions are restrictive and in most cases impossible to obtain. Therefore one has to employ numerical techniques. There are basically two main approaches in numerical solution of elastic wave propagation problems.

(a) The method of characteristics, in which the partial differential equations are reformulated along directions of possible discontinuities and then integrated in these directions.

(b) Discretization methods such as finite difference and finite element methods where the partial differential equations are first discretized in space and then integrated along parallel lines in the time domain.

Discretization introduces dispersion and because of the finite cut-off frequency, high frequency input results in spurious oscillation, which could be reduced by introducing an artificial viscosity term. However, this has two undesirable effects in that the dispersions in the final solution will be increased and rapid changes in the wave fronts will be smoothed. Therefore these methods are unable to predict precisely a very sharp wave front.

After careful considerations, the method of characteristics (MOC) is chosen for the numerical solution of transient flexural wave propagation in beams with discontinuities of cross-section. The method has many advantages and desirable properties, particularly for one-dimensional problems with two independent variables which are governed by hyperbolic partial differential equations.

i) Characteristics are the only lines along which discontinuities in

the wave front may propagate. The characteristic lines represent natural co-ordinates for wave propagation and the progress of the waves or traces of the progress may be followed along these line.

ii) Discontinuities in geometry and material may be incorporated easily in the numerical scheme when the MOC is used.

iii) The MOC is capable of handling arbitrary initial and boundary conditions especially sharp inputs, so long as dependence on only two independent variables is maintained.

iv) Numerical integration by the MOC is stable and conforms the Courant-Fiedrich-Lewy stability criterian. This will be discussed in more detail in section 3.3.3.

v) The method is also known to be accurate since adherence to the stability criterion ensures convergence to the true solution as Δx and Δt approach zero.

vi) Good agreement with some available solutions by transform methods and very good agreement with experimental results has encouraged the use of the MOC to obtain solutions for complicated problems where no other numerical solution can deliver satisfactory results.

vii) The MOC is particularly advantageous in the investigation of finite structures where wave reflections are involved.

Although the MOC is most suitable for one-dimensional spatial problems, finite difference and finite element methods are much more efficient in solving two dimensional spatial problems. The most satisfactory approximation in one case is not necessarily the most appropriate in another case. Furthermore, the choice of the method must depend on the required accuracy, the nature of the structure and its complexities, the importance of shear and rotatory inertia and the type of analysis required, i.e. in time domain or frequency domain. The method of characteristics was found to be most suitable for the problem under consideration.

3.3. Solution to the Timoshenko equations by the Characteristics method

3.3.1. General theory

The method of characteristics (MOC) is used for the numerical solution of first order and second order partial differential equations (PDE) of hyperbolic type.

Consider a quasi linear second order PDE in the form

$$a\frac{\partial 2u}{\partial x^2}+b\frac{\partial^2 u}{\partial x \partial t}+c\frac{\partial^2 u}{\partial t^2}= \bar{f} \qquad (3.1)$$

Where $a,b,c,\bar{f}$ are functions of x,t,u,u_x and u_t; the suffices x and t being used to represent partial derivatives with respect to x and t. This equation is said to be hyperbolic, parabolic or elliptic according as $b^2 - 4ac$ is positive, zero or negative.

For the hyperbolic PDE, there exists two distinct families of real characteristic curves at each point (x,t). For the parabolic case, the two characteristics coincide and they are of no significant value in understanding the behaviour of the solution, whereas the elliptic form of the PDE has no real characteristics.

Knowledge of the characteristics concept is most important for the hyperbolic PDE and the understanding of MOC is a powerful tool in developing numerical solution. The MOC is the natural numerical method for hyperbolic systems in two independent variables. The existence of characteristics gives considerable insight into the expected behaviour of a problem's solution, even before the solution is obtained.

The real characteristics of the PDE are curves in the real domain of the problem and discontinuities propagate along the characteristics. A step-by-step process is usually used in building-up simultaneously the characteristic grid and solving the hyperbolic PDE at the grid points.

For regions in the physical plane where the first derivative of u

exist and are continuous, one may write

$$du = u_x dx + u_t dt \qquad (3.2)$$

$$d(u_x) = u_{xx} dx + u_{xt} dt \qquad (3.3)$$

$$d(u_t) = u_{xt} dx + u_{tt} dt \qquad (3.4)$$

writing equations (3.1) as $\bar{f} = a u_{xx} + b u_{xt} + c u_{tt}$ (3.5)

Equations (3.3) to (3.5) constitute a set of three simultaneous equations for the three unknowns u_{xx}, u_{xt} and u_{tt} in terms of the known functions u, u_x and u_t. They can be written in the matrix form

$$\begin{bmatrix} a & b & c \\ dx & dt & o \\ o & dx & dt \end{bmatrix} \begin{bmatrix} u_{xx} \\ u_{xt} \\ u_{tt} \end{bmatrix} = \begin{bmatrix} \bar{f} \\ d(u_x) \\ d(u_t) \end{bmatrix}$$

The second partial derivatives u_{xx}, u_{xt} and u_{tt} are uniquely determined by this system of equations unless the determinant of the coefficient matrix vanishes. Upon equating this determinant to zero, one finds the characteristic equation

$$\begin{vmatrix} a & b & c \\ dx & dt & o \\ o & dx & dt \end{vmatrix} = o$$

This yields the characteristic equation

$$a(dt)^2 - b(dt)\,(dx) + c\,(dx)^2 = 0 \qquad (3.6)$$

The two roots of equation (3.6) define the characteristics and they are real when equation (3.5) is hyperbolic $\frac{dt}{dx} = \frac{1}{2a}(b \pm \sqrt{b^2-4ac})$ (3.7) When this holds, there is no solution at all unless the other determinants of the system also vanish. This is based on the property that adding a multiple of any row (or column) of a determinant to a different, parallel row (or column) does not change the determinant value. One can write for instance one of the three other determinants as

$$\begin{vmatrix} a & \bar{f} & c \\ dx & d(u_x) & 0 \\ 0 & d(u_t) & dt \end{vmatrix} = 0$$

or $ad(u_x)dt - \bar{f}dxdt + cd(u_t)dx = 0$ (3.8)

Equation (3.7) gives the slope of the characteristics, i.e. the transformation of the PDE into canonical form and (3.8) defines the conditions to be satisfied.

If the characteristics are real and the initial values are prescribed along a non-characteristic curve, the initial-boundary value problem can be solved. Furthermore, it follows that because discontinuities are propagated along the characteristics in the(x,t) plane, finite step input functions may occur and can be handled as will be described later.

A necessary condition for the co-ordinate given in equations (3.7) to be non-singular is that the two real characteristics must be different. Hence, one must take the plus sign in one case and the minus sign in the other. For the hyperbolic case, where $b^2-4ac>0$, second order terms may be reduced to a standard form by one linear transformation at any one particular point; one can write the characteristic ξ = const. and η = const. as roots of equation (3.6), which can be rewritten in the form

$$a\left(\frac{dt}{dx}\right)^2 - b\left(\frac{dt}{dx}\right) + c = 0 \quad (3.9)$$

which gives the slopes of the two families of characteristics

$$\xi = \frac{dt}{dx} = \frac{b - \sqrt{b^2 - 4ac}}{2a} \quad (3.10)$$

$$\eta = \frac{dt}{dx} = \frac{b + \sqrt{b^2 - 4ac}}{2a} \quad (3.11)$$

Along the characteristics, u_x and u_t are connected by the respective equations, obtained from equation (3.8) as

$$\bar{f}dt - a\xi u_x - cu_t = 0 \quad (3.12)$$

$$\bar{f}dt - a\eta u_x - cu_t = 0 \quad (3.13)$$

These two equations, together with the identity relation expressed in equation (3.2), are just sufficient to allow the step-by-step propagation of the solution along the characteristic curves from a non-

characteristic initial curve.

In the present work, the method of characteristics is used to solve the Timoshenko equations as a system of two second order hyperbolic partial differential equations involving two independent variables x and t and two dependent variables.

3.3.2. Numerical techniques

In the theory of elasticity, a beam is a three-dimensional structure and its exact stress and displacement distribution are very difficult to obtain. In a structure, it takes a finite, though small time for any disturbance to be transmitted through it. Excitations are propagated at either one of the two velocities, the dilatational velocity or the equivoluminal velocity.

Because of the difficulties involved in the exact equations of elasticity, one usually needs an approximate governing equation. However, for transient response study, the derived equations must be totally hyperbolic, otherwise their transient response is either meaningless or not obtainable.

The Timoshenko equations are the most suitable approximate equations governing flexural transient response in beams. Although the Timoshenko equations are approximate, they do not alter the hyperbolic nature of the exact elasticity equations and the Timoshenko equations are practically essential for transient analysis.

The Timoshenko equations are totally hyperbolic and involve two governing equations of second order or one fourth order equation. Alternatively, it may be decompcsed into four first order equations. The system with two second order PDE's has certain advantages as compared to the other two systems. The wave velocities associated with each of the variables appear explicitly in the second order equations and the factors governing the propagation of discontinuities also appear explicitly. A suddenly applied disturbance in ψ, or in the moment M,

propagates at the bar velocity c_1, while the disturbance in y, or in shear propagate at the shear velocity c_2.

It is more convenient for the numerical solution to express the second order governing Timoshenko equations in terms of displacement, rather than the mixed stress-displacement formulation.

When the Timoshenko equations are written in this form, they are

$$\frac{\partial^2\psi}{\partial x^2} - \frac{1}{c_1^2}\frac{\partial^2\psi}{\partial t^2} = \frac{k^2AG}{EI}\psi - \frac{k^2AG}{EI}\frac{\partial y}{\partial x}$$

$$\frac{\partial^2 y}{\partial x^2} - \frac{1}{c_2^2}\frac{\partial^2 y}{\partial t^2} = \frac{\partial\psi}{\partial x} \qquad (3.14)$$

where $c_1^2 = E/\rho$ and $c_2^2 = kG/\rho$ (3.15)

In order to use the same notation as in the computer programme which will be utilized for the computation, the dependent variables ψ and y are renamed as u_1 and u_3 respectively and equations (3.14) are rewritten as

$$\frac{\partial^2 u_1}{\partial x^2} - \frac{1}{c_1^2}\frac{\partial^2 u_1}{\partial t^2} = \frac{k^2AG}{EI}u_1 - \frac{k^2AG}{EI}\frac{\partial u_3}{\partial x} \equiv \bar{f}_1$$

$$\frac{\partial^2 u_3}{\partial x^2} - \frac{1}{c_2^2}\frac{\partial^2 u_3}{\partial t^2} = \frac{\partial u_1}{\partial x} \equiv \bar{f}_2 \qquad (3.16)$$

The boundary conditions are usually prescribed in some form of generalized stresses; they may be defined as

$$M = -EI\frac{\partial u_1}{\partial x} \qquad (3.17)$$

$$Q = k^2AG\frac{\partial u_3}{\partial x} - k^2AG\,u_1 \qquad (3.18)$$

To classify the Timoshenko equations according to equation (3.1), one finds $a = 1$, $b = 0$ and $c = -\frac{1}{c_1^2}$ for the first of equations(3.16) and $c = -\frac{1}{c_2^2}$ for the second of equations(3.16). Hence, the inequality $b^2 - 4ac$ is equal to $\frac{4}{c_1^2}$ and $\frac{4}{c_2^2}$ which is greater than zero for both

equation of (3.16). Therefore the Timoshenko beam equations are totally hyperbolic as stated before.

Using equations (3.10) and (3.11), the characteristics are determined as

$$\frac{dt}{dx} = \pm \frac{1}{c_1} \text{ and } \frac{dt}{dx} = \pm \frac{1}{c_2}$$

or

$$\frac{dx}{dt} = \pm c_1 \text{ and } \frac{dx}{dt} = \pm c_2 \qquad (3.19)$$

Hence, there exist four distinct real characteristics for the hyperbolic second order systems with two independent variables x and t and two dependent variables u_1 and u_2.

Since the slopes of the characteristic are constant, the characteristic curves are straight lines in the case of the Timoshenko equations.

For regions in the physical plane, where the first derivatives exist and are continuous, one may write these derivatives using equations (3.3) and (3.4)

$$\begin{aligned} d(u_{i,x}) &= (u_{i,xx})dx + (u_{i,xt})dt \\ d(u_{i,t}) &= (u_{i,xt})dx + (u_{i,tt})dt \end{aligned} \qquad (3.20)$$

where

$$u_{i,x} = \frac{\partial u_i}{\partial x} \quad , \quad u_{i,t} = \frac{\partial u_i}{\partial t}$$

$$u_{i,xx} = \frac{\partial^2 u_i}{\partial x^2} \quad , \quad u_{i,tt} = \frac{\partial^2 u_i}{\partial t^2}$$

Since only continuous u_i are being considered, one can write according to equation (3.20)

$$\begin{aligned} du_1 &= u_{1,x}\,dx + u_{1,t}dt \\ du_3 &= u_{3,x}dx + u_{3,t}dt \end{aligned} \qquad (3.21)$$

Using equations (3.12) and (3.13), the characteristics equation are written as

$$d(u_{1,t}) \mp c_1 d(u_{i,x}) \pm c_1 \bar{f}_1 dx = 0, \text{ along } \frac{dx}{dt} = \pm c_1$$

$$d(u_{3,t}) \mp c_2 d(u_{3,x}) \pm c_2 \bar{f}_2 dx = 0, \text{ along } \frac{dx}{dt} = \pm c_2 \quad (3.22)$$

Equations (3.21) together with equations (3.22) consist of a system of six simultaneous equations which may be used to determine the six variables u_1, $u_{1,x}$, $u_{1,t}$, u_3, $u_{3,x}$ and $u_{3,t}$, if proper boundary and initial conditions are specified.

For the investigation of the propagation of discontinuities, equations (3.16) are written in the following general form

$$\frac{\partial^2 u_i}{\partial x^2} - \frac{1}{c_i^2} \frac{\partial^2 u_i}{\partial t^2} = \sum_{j=1}^{n} (\alpha_{ij} u_j + \beta_{ij} \frac{\partial u_j}{\partial x}) \equiv R_i \quad (3.23)$$

Where $u_i = u_i(x,t)$ but the c_i, α_{ij}, β_{ij} are continuous functions of x only. The solution for $\partial^2 u_i / \partial x^2$ can be obtained from equations (3.23) using equations (3.20), and is written as the characteristic equations

$$d(u_{i,t}) \mp c_i d(u_{i,x}) \pm c_i R_i dx = 0 \quad (3.24)$$

along $(dx/dt) = \pm c_i$ respectively.

In the Timoshenko equations, the dependent variables u_i s of first and second order may suffer discontinuities which will be shown to occur along the characteristic lines. Discontinuities in $u_{i,x}$ and $u_{i,t}$ can occur when a finite step input (or jump input) is applied at a particular x.

To investigate first order discontinuities, that is where

$$[u_i] = 0; \quad [u_{i,x}] \neq 0; \quad [u_{i,t}] \neq 0$$

Let A and B be two points on a c_i^- or c_i^+ characteristic on either sides of a line which is not a characteristic, where

$$[u_i] = u_i(B) - u_i(A) \text{ as } B \to A \quad (3.25)$$

So finite jumps are represented by a square bracket, i.e. $[u_i]$ designates the finite jump of the function (u_i) across $x = \tilde{x}(t)$.

Using Hadamard's lemma which states that $[u_i] = 0$ along $x = \tilde{x}(t)$ implies $[u_{i,t}] + (d\tilde{x}/dt)[u_{i,x}] = 0$, one obtaines

$$[u_{i,t}] = -\frac{d\tilde{x}}{dt}[u_{i,x}] \tag{3.26}$$

Integrating equation (3.24) yields,

$$u_{i,t}(B) - u_{i,t}(A) \mp \int_A^B c_i \, d(u_{i,x}) = \mp \int_A^B c_i R_i dx \tag{3.27}$$

As $B \to A$ and dx approaches zero, the right hand side of equation (3.27) vanishes and the equation is reduced to

$$[u_{i,t}] \mp c_i [u_{i,x}] = 0 \tag{3.28}$$

substituting equation (3.26) into equation (3.28) yields

$$\{ -\frac{d\tilde{x}}{dt} \mp c_i \} [u_{i,x}] = 0 \tag{3.29}$$

since by definition $[u_{i,x}] \neq 0$, one finds

$$\frac{d\tilde{x}}{dt} = \mp c_i \tag{3.30}$$

as lines of the first order discontinuities.

Similarly for second order discontinuities where

$$[u_i] = [u_{i,x}] = [u_{i,t}] = 0$$

$$[u_{i,xx}] \neq 0; \quad [u_{i,tt}] \neq 0 \text{ along } x = \tilde{x}(t)$$

Equation (3.23) can be written for both sides of $x = \tilde{x}(t)$ and taking the difference, one obtains

$$[u_{i,xx}] - \frac{1}{c_i^2} [u_{i,tt}] = 0 \text{ along } x = \tilde{x}(t) \tag{3.31}$$

Using Hadamard's lemma for the first derivatives

$$[u_{i,tt}] = (\frac{d\tilde{x}}{dt})^2 [u_{i,xx}] \tag{3.32}$$

Substituting equation (3.32) in equation (3.31) gives

$$\{ 1 - \frac{1}{c_2^2} (\frac{d\tilde{x}}{dt})^2 \} [u_{i,xx}] = 0 \tag{3.33}$$

But by definition $[u_{i,xx}] \neq 0$, so $\frac{d\tilde{x}}{dt} = \pm c_i$ (3.34)

the equations for the families of lines along which second order discontinuities occur.

Hence, the lines along which first order and second order discontinuities occur, are the characteristic lines $\pm c_i$.

In order to obtain the equations for the discontinuities, each family of characteristics will be treated separately. Along $dx/dt=c_i$ and using equations (3.23) and equation (3.24) with the choice of the lower sign, one has the relation governing the magnitude of the jumps

$$d[u_{i,x}]+c_i d[u_{i,x}] = c_i\{\alpha_{ii}[u_i] + \beta_{ii}[u_i]\}dx \qquad (3.35)$$

In this equation, there is no summation on the i's, since $[u_i] = 0$

Along the characteristics, one has from equation (3.28)

$$[u_{i,t}] = -\frac{dx}{dt}[u_{i,x}] = -c_i[u_{i,x}] \qquad (3.36)$$

Substituting (3.36) in (3.35), gives

$$\frac{d[u_{i,x}]}{dx} + \frac{d[u_{i,x}]}{dx} - \frac{dc_i}{c_i dx}[u_{i,x}] = \beta_{ii}[u_{i,x}] \qquad (3.37)$$

$$\frac{d[u_{i,x}]}{[u_{i,x}]} = \frac{1}{2}(\beta_{ii}dx - \frac{dc_i}{c_i}) \qquad (3.38)$$

Thus may be integrated to give

$$[u_{i,x}] = K_i c_i^{-\frac{1}{2}} \exp \tfrac{1}{2}\int(\beta_{ii}dx) \text{ along } c_i^+ \qquad (3.39)$$

where K_i s are constants to be determined from the boundary and initial conditions.

From equation (3.39) and equation (3.36), the relationship for the discontinuities of $u_{i,t}$ is obtained as

$$[u_{i,t}] = -K_i c_i^{\frac{1}{2}} \exp \tfrac{1}{2}\int\beta_{ii}dx \qquad (3.40)$$

Along the characteristics $dx/dt = -c_i$, the discontinuity equations of $u_{i,x}$ and $u_{i,t}$ are obtained in a similar way. They are

$$[u_{i,x}] = K_i c_2^{-\frac{1}{2}} \exp \tfrac{1}{2}\int\beta_{ii}dx$$

$$\left[{}^{u}i,t \right] = K_i c_2^{\frac{1}{2}} \exp \tfrac{1}{2} \int \beta_{ii} dx \qquad (3.41)$$

These relations are obtained in similar approaches by Chou (1965) and Mengi and McNiven (1970). They were also previously discussed by Leonard and Budiansky (1953) and Jahsman (1958).

The numerical solution of the Timoshenko equations consists of determining the values of the generalised displacements u_1 and u_3 as well as their first derivatives at a position x and at time t. The values of stresses and strains can then be calculated using the raltionships given in equations (3.17) and (3.18). In order to carry out the numerical calculations, the physical x-t plane is divided into a network by characteristic lines, as shown in figure (3.2). On this plane, the line $\frac{dx}{dt} = c_1$ divides the space-time domain into two parts, a domain representing undisturbed particles and a second domain representing rod particles in motion. This second domain is of main interest for the numerical solution. The part of interest is subdivided by means of a primary grid which is formed by means of two sets of parallel lines having equal but opposite slopes $\pm c_1$. Each grid element, or so called mesh has diagonals measuring $2\Delta x$ and $2\Delta t$, as shown in a typical mesh in figure 3.2. Within each mesh, a secondary grid is constructed using characteristic lines with the slopes $\pm c_2$ and drawn from the point at which the unknowns are to be evaluated.

The whole characteristic network can be constructed without the prior knowledge of any of the generalized stresses since the slopes of the characteristics depends only on the material and geometrical properties of the beam. The typical mesh in figure 3.2 shows the primary grid in fine solid lines and the secondary grid in dotted line. As the dotted lines fall within the element, i.e. c_1 is always greater than c_2, the domain of dependence of a point is conserved.

The required properties at point 1 in figure 3.2 may be calculated

if the corresponding values at neighbouring points 2,3, and 4 are known. The characteristic lines of the secondary grid with slope $\pm c_2$ intersects the primary grid at points 5 and 6 as shown in the typical mesh of figure 3.2. The values of the variables at point 5 and 6 are obtained from those at points 2, 3 and 4 by linear interpolation. In order to perform numerical calculation, the characteristic equations (3.22) are written in finite difference form, where only central differences and averaging operations are used.

Consider the typical mesh illustrated in figure 3.1 along $\frac{dx}{dt} = c_1$

$$\{u_{1,t}(1) - u_{1,t}(2)\} - c_1\{u_{1,x}(1) - u_{1,x}(2)\} = -c_1\bar{f}_1\{x(1) - x(2)\}$$

along $\frac{dx}{dt} = -c_1$

$$\{u_{1,t}(1) - u_{1,t}(3)\} + c_1\{u_{1,x}(1) - u_{1,x}(3)\} = c_1\bar{f}_1\{x(1) - x(3)\}$$

along $\frac{dx}{dt} = c_2$

$$\{u_{3,t}(1) - u_{3,t}(5)\} - c_2\{u_{3,x}(1) - u_{3,x}(5)\} = -c_2\bar{f}_2\{x(1) - x(5)\}$$

along $\frac{dx}{dt} = -c_2$

$$\{u_{3,t}(1) - u_{3,t}(6)\} + c_2\{u_{3,x}(1) - u_{3,x}(6)\} = c_2\bar{f}_2\{x(1) - x(6)\} \qquad (3.42)$$

The values of the variables relating to points 5 and 6 are expressed in terms of corresponding values at points 2,3 and 4 by linear interpolation, using the following relationships, derived from the geometry of the typical mesh $\Delta x = c_1\Delta t$

$$\Delta x' = c_2\Delta t'$$

$$\frac{\Delta x'}{\Delta x} = \frac{2\Delta t - \Delta t'}{\Delta t} = \frac{c_2\Delta t'}{c_1\Delta t}$$

Thus $$\frac{\Delta t'}{\Delta t} = \frac{2}{1+\frac{c_2}{c_1}} \qquad (3.43)$$

Hence $$u_{3,t}(5) = u_{3,t}(4) + \{u_{3,t}(2) - u_{3,t}(4)\}\frac{\Delta x'}{\Delta x}$$

$$= u_{3,t}(4) + \{ u_{3,t}(2) - u_{3,t}(4) \} \cdot \frac{2c_2/c_1}{1 + c_2/c_1} \qquad (3.44)$$

To obtain $u_{3,t}(6)$ using equation (3.44), $u_{3,t}(2)$ should be replaced by $u_{3,t}(6)$. Similarly, $u_{3,x}(5)$, $u_{3,x}(6)$ are expressed in terms of $u_{3,x}(2)$, $u_{3,x}(3)$ and $u_{3,x}(4)$.

Equations (3.44) are used to eliminate the values of the variables at points 5 and 6 from the second and third of equations (3.42).

The continuity equations are written according to equations (3.21) for u_1 and u_3 along c_1^- and c_2^- in finite difference form as

$$u_1(1) - u_1(3) = \frac{u_{1,x}(1) + u_{1,x}(3)}{2} \{ x(1) - x(3) \} + \frac{u_{1,t}(1) + u_{1,t}(3)}{2} \{ t(1) - t(3) \}$$

$$u_3(1) - u_3(6) = \frac{u_{3,x}(1) + u_{3,x}(6)}{2} \{ x(1) - x(6) \} + \frac{u_{3,t}(1) + u_{3,t}(6)}{2} \{ t(1) - t(6) \} \qquad (3.45)$$

The four characteristic equations (3.42) and the two continuity equations (3.45) constitute a set of six simultaneous equations which are sufficient for the determination of u_1, $u_{1,x}$, $u_{1,t}$, u_3, $u_{3,x}$ and $u_{3,t}$ in term of previously calculated values at points 2,3 and 4. However to start the numerical calculations, certain initial values along the boundary $x = 0$ have to be specified.

Along the boundary $x = 0$, the two characteristics c_1^+ and c_2^+ are absent and the numerical calculation is carried out in the half mesh 1,2,3 of the main network. If u_1 and u_3 are specified along $x = 0$, the remaining four equations are sufficient for finding the remaining four unknowns $u_{1,x}$, $u_{1,t}$, $u_{3,x}$ and $u_{3,t}$. However, in specifying generalised stresses M and Q along $x = 0$, two new finite difference equations must be obtained from equations (3.17) and(3.18) to replace the missing characteristic equations along c_1^+ and c_2^+. Therefore, the

system of six simultaneous equations necessary for the determination of the six unknowns is again complete.

For the analysis of a finite bar, additional boundary conditions at $x = L$ need to be specified. When the travelling wave reaches the new boundary, it is reflected and a second wave is created. This situation is repeated at each subsequent reflection. In a bar containing a discontinuity of cross section, this situation occurs at an earlier stage, when the wave reaches the position of discontinuity, a part of it will be reflected and another part will be transmitted. Flexural wave are dispersive in nature and these reflections cause additional dispersions which complicate the wave propagation considerably. However, the method of characteristics seems to be the most promising numerical procedure to deal with this complex situation.

3.3.3 Accuracy and Stability

The investigation of accuracy and stability is of great practical interest in numerical solutions such as the method of characteristics which employs finite difference approximation for the governing equations along the characteristic lines.

Courant - Friedrich and Lewy (1928) were the first to propose an explicit finite difference method for solving linear second order PDE. They also discovered the conditional stability of certain finite difference approximations and they proved the convergence of the numerical solution to the exact solution as $\Delta x \to 0$ when $\frac{\Delta x}{c\Delta t} \geq 1$, where Δx and Δt are the space and time intervals respectively. This inequality condition is widely known as C-F-L stability condition. They also introduced the concept of the domain of dependence and pointed out that convergence required that the domain of dependence of the differential equation should always stay within the domain of dependence of the difference equation.

In 1952, Courant et. al presented a difference method for the solution of quasi-linear hyperbolic PDE of first order. They showed that

the error introduced by integration along characteristics with a fixed mesh, in going from the exact solution at time t to the difference solution at time $t + \Delta t$, was of type $O(\Delta t^2)$ which is known generally as first order accuracy method. They showed that the error becomes zero as the mesh size Δt tends to zero.

Second order accurate finite difference formulations have been also suggested and their stability and rate of convergence extensively discussed. (Stetter, 1961; Lax and Wendroff, 1964; Raganath and Clifton, 1972). The stability investigation of mixed-initial boundary value is not as developed as stability and convergence considerations of pure initial value problems (Cauchy problem) for which many researches have been published. (Osher, 1969, 1972; Gustafsson et. al, 1972; Ilan et. al, 1976). This is because initial boundary value problems are much more complicated and only recently were subject to increased interest (Kreiss, 1971, Morton 1976 and Gladwell et. al, 1979). Most of these works areof general theoretical nature and the practical aspects of the stability and convergence has been taken up only recently.

Numerical results can be useful only when the numerical solution converges to the solution of the continuous problem. This convergence condition was supplied by the Lax-Richtmyer(1956) equivalence theorem; "Given a properly posed initial-value problem and a finite difference approximation to it that satisfies the consistency condition, stability is a necessary and sufficient condition for convergence." There are two excellent books which discuss error estimation and stability as related to finite difference approximations to PDE. These are the books of Forsythe and Wasow (1960) and Richtmyer and Morton (1967).

The method of characteristics is exact in itself and when used to the solution of hyperbolic PDE. However, the discretization of the continuous structure by finite difference approximation which are needed

for the numerical solution, must introduce certain inaccuracies. Let us consider the concept of stability and convergence in its relation to error estimation (O'Brien, 1951; Hahn, 1958 and Sedney, 1970).

A difference scheme is called convergence if the solution of the differnce (u_j^n) equation tends to that of the differential equation u(x,t) as Δt tends to zero.

A difference scheme is called stable if solutions of the difference equations are uniformly bounded functions of the initial data for all sufficiently small Δt and all $n\Delta t$ in a given finite interval.

It is clear from the definitions that convergence implies stability. Lax and Richtmyer (1956) proved that the converse is also true, as was described by their equivalence theory.

Let u(x,t) be the exact solution of the PDE

Let u_e be the exact solution of the partial difference equation.

Let u_j^n be the numerical solution of the partial difference equation of the same problem at time $t = n\Delta t$ andposition $x = j\Delta x$, where Δt and Δx are the mesh sizes used in the numerical calculation. Then the error e is given as

$$e = u(x,t) - u_j^n = (u(x,t) - u_e) + (u_e - u_j^n) \qquad (3.46)$$

The error consists of two parts $u - u_e$ is called the truncation or discretization error and investigations of whether and how $(u - ue) \to 0$ as the grid size approaches zero is called the problem of stability and $u_e - u_j^n$ is called numerical error and its main source is round-off error. The convergence and stability depend on the finite difference approximations and upon the initial and boundary conditons.

Forsythe and Wasow noticed that an approximate method applied to a PDE may converge in a satisfactory way to a set of values that has nothing to do with the correct solution of the problem. The mesh size affects the truncation error and round-off error in opposite ways. The first decreases as the mesh size decreases, while the second generally

increases. Therefore one cannot generally assert that decreasing the mesh size always increases the accuracy.

It is always necessary to observe a "stability criterion" to prevent errors from amplifying so much as to make the calculations meaningless. The "stability criterion" usually amounts to a restriction on the permissible size of Δt in terms of the size of the spatial increments. Otherwise the scheme can produce signs of instability.

In one space variable problem, the method of characteristics is inherently stable because it always adheres to the C-F-L stability criterion, which requires $\frac{\Delta x}{c\Delta t} \geq 1$ where c is the largest of the wave velocities. The MOC as an explicit method has an obvious advantage of requiring relatively little computer storage as compared to the implicit method.

Ideally, choosing a mesh size of infinitesimal size produces an exact solution. However, there are several realistic restraints prohibiting the selection of infinitesmally small increments, since this can cause the round-off error to become excessive and dominate the solution, in addition to the increased computer running time.

Finite difference approximations seldom achieve more than a rather modest accuracy. When stability criteria are observed, the rounding off errors are not amplified as time goes on, they merely accumulate in proportion to the square root of the number of steps in the calculation. Nevertheless roundoff error and truncation error are propagated along with the solution. Thus the further the solution goes, the greater the error becomes. Therefore, particular care must be taken in minimizing the error at the beginning, although this disadvantage of error growth is customary to all marching numerical schemes.

In writing the characteristic equations in finite difference form for the mesh points, only central differencing and averaging operations were used and the truncation error is of second order (Δx^2) and the

approximation is called first order accurate.

However, second order accuracy difference methods have been developed by several authors and they are useful in certain cases, particularly by finite difference methods. But this does not necessarily mean improved accuracy. (Lax and Wendroff, 1964; Stetter, 1961; Ranganath and Clifton, 1972).

The central differnce approximations as employed in the MOC are found to be stable and maximum accuracy is obtained by taking $\Delta x = c_1 \Delta t$, for $c_1 > c_2$. In practice, it is better to take $\Delta t = (\frac{1}{c_1})\Delta x$ rather than some smaller value, since a smaller Δt would require additional calculation and round off error. Also for practical considerations, it is desirable to use the largest possible Δt for a fixed Δx. (Fox, 1960).

One can determine the accuracy and the rate of convergence of a numerical scheme by evaluating exact error for two step sizes, one half of each other and then determining the ratio of these errors.

A second method for determining the error requires the numerical evaluation of an exact solution when available for certain cases (Hoffman, 1973). Several authors compared the numerical solution by the method of characteristics with closed form "exact" solutions and obtained excellent agreement. This was outlined in section 3.2.4.

For problems involving one space variable, the numerical scheme adopted is inherently stable. For two space variable transient problems, numerical schemes are not always stable. The question of stability must be established for each problem separately and is usually very difficult.

A second criterion for stability was obtained by Von Neuman and Richtmyer (1950) from a study of error growth which in its necessary aspects was equivalent to the condition given by Courant et. al (1928). The Von Neuman stability criterion is mostly used to study the accuracy of afinite difference approximation when periodic excitations are applied

and it uses the fact that an initial exponential function remains exponential.

Assuming an initial value in the form

$$u(x,0) = u_o e^{ikx} \tag{3.47}$$

Then the solution of (3.47) at $t = \Delta t$ will be

$$u(x,\Delta t) = \sum_p C^p e^{ik\Delta_p x} e^{ikx} u_o$$

$$= (\sum_p C^p e^{ikr_p \Delta t})\, u(x,0) \tag{3.48}$$

and at $t = n\Delta t$ it will be

$$u(x,t) = (\sum_p C^p e^{ikr_p \Delta t})^n\, u(x,0) \tag{3.49}$$

The matrix $\sum_p C^p e^{ikr_p \Delta t}$ is called the amplification matrix.

Von Neuman's condition for stability states that the eigen value of the amplification matrix should not exceed one in absolute value for any real value of $k.\Delta t$. This condition is discussed in the works of (Hahn, 1958; Fox, 1960) and has been applied by many authors. (Chiu and Neubert, 1967; Uckan and Ang, 1971 and Krieg, 1973).

Once the material properties are established, the necessary truncation error depends only on the frequency of excitation. In the case of sinusoidal excitation, the frequency is known. However, if no prodominant frequency exists, as in the case of transient response, the maximum significant frequency should be used and for a larger frequency, a smaller Δt must be used. (Wylies and Streeter, 1976).

Strictly speaking, the study of the truncation errors is only valid if the physical quantities are sufficiently smooth to insure the existence of the Taylor series expansion containing continuous bounded partial derivatives about the point $x_1 t$. Therefore, at the wave front where discontinuities may occur, the truncation error estimates are not expected to hold.

Chou and Greif (1968) showed that the combined characteristic

difference method was adequate in representing discontinuous wave fronts and the error was only 1.2%.

Chou and Flis (1975) also presented the excellent convergence of the method of characteristics as applied to composite material response, whereas finite element methods with a high number of modes showed poor convergence.

Sobel and Geers (1973) showed the unsatisfactory convergence behaviour of conventional finite difference formulations for transient wave type problems.

The rate of convergence depends primarly on the truncation error and if it is known, an extrapolation technique can be employed to achieve a high degree of accuracy with a small amount of calculation. The extrapolation method of Richardson (1911) can be applied to the calculated values at any point.

The error of the numerical calculation e is said to be of h^2-type if it can be expressed in the form

$$e = u - u_j^n = \phi_1 h^2 + \phi_2 h^4 + \phi_3 h^6 + \ldots \qquad (3.50)$$

where h is the mesh size. If two values u_1 and $\bar{u}_1$ are calculated at a given point, with u_1 corresponding to a mesh size h and $\bar{u}_1$ corresponding to $\bar{h}_1$, then one may write (3.50) twice in truncated form

$$u = u_1 + \phi_1 h^2$$

$$u = \bar{u}_1 + \phi_1 \bar{h}_1^2$$

Elimination of ϕ_1 gives the extrapolated value of u

$$u = (\bar{h}_1^2 u_1 - h_1^2 \bar{u}_1)/(\bar{h}_1^2 - h_1^2) \qquad (3.51)$$

This formula is called the h^2-type two point extrapolation. Similarily if calculations with three different mesh size h_1, $\bar{h}_1$, $\bar{\bar{h}}_1$ are performed, a three point h^2-type extrapolation formula can be obtained.

Although the finite difference equations involve errors of h^2 - type there is no proof that the error in the calculated values of u_1 itself is

also of the h^2-type, since the round-off error might influence the error type of the numerical solution. Therefore, the type of error should be investigated in each case.

A detailed investigation of error estimation by extrapolation technique applied to finite differencing technique as used in the method of characteristics with error estimation of h-type and h^2-type has been presented by Roberts, 1959· Chou et.al, (1967) presented error estimation for blast waves; Hoffman (1973) for irrotational and rotational flows and Lister (1960) for isentropic flows.

Ripperger (1967) suggested the use of changing mesh sizes where the numerical procedure could be started by a very small mesh size and then increased to a coarser mesh. This scheme was particularly useful in high rate strains in materials with yield stress significantly lower than the applied stress. The author checked the accuracy of the numerical results by halving the final mesh and found the difference between the two solutions to be in the fifth and sixth significant digits.

In the present numerical analysis of the transient flexural wave propagation according to Timoshenko equations it is sufficient to use the C-F-L stability criterion and a small time increment is required to maintain a value of 1 for $\Delta x/c_1\Delta t$. The characteristic lines of the primary grid are $dx/dt=\pm c_1$ and the interval of dependence of any point is bounded by the lines through it at slopes of $\pm c_1$. Consequently, the points used in the finite difference scheme must, for convergence, always remain in an interval as large as that bounded by $\Delta x/\Delta t \geq c_1$.

It is desired to select the largest mesh size with a minimal acceptable error. This is accomplished by choosing a mesh size in such a manner that any further reduction in this quantity will not alter the solution significantly.

The choice of the correct mesh size has to be decided for each individual problem, depending upon the type of loading and the rise time, the end conditions and the size and positon of discontinuity.

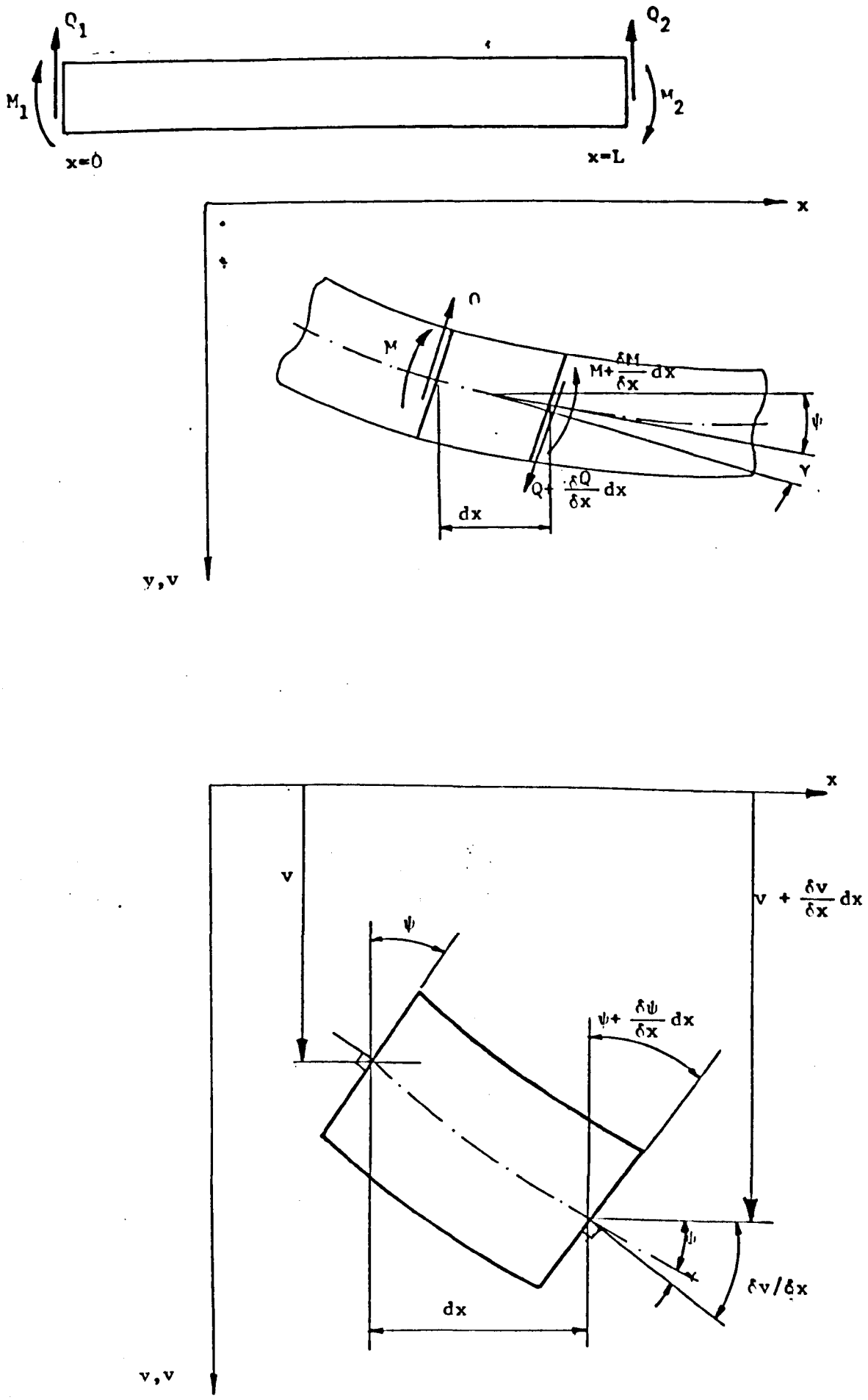

FIG. 3.1 TIMOSHENKO BEAM AND TIMOSHENKO ELEMENT

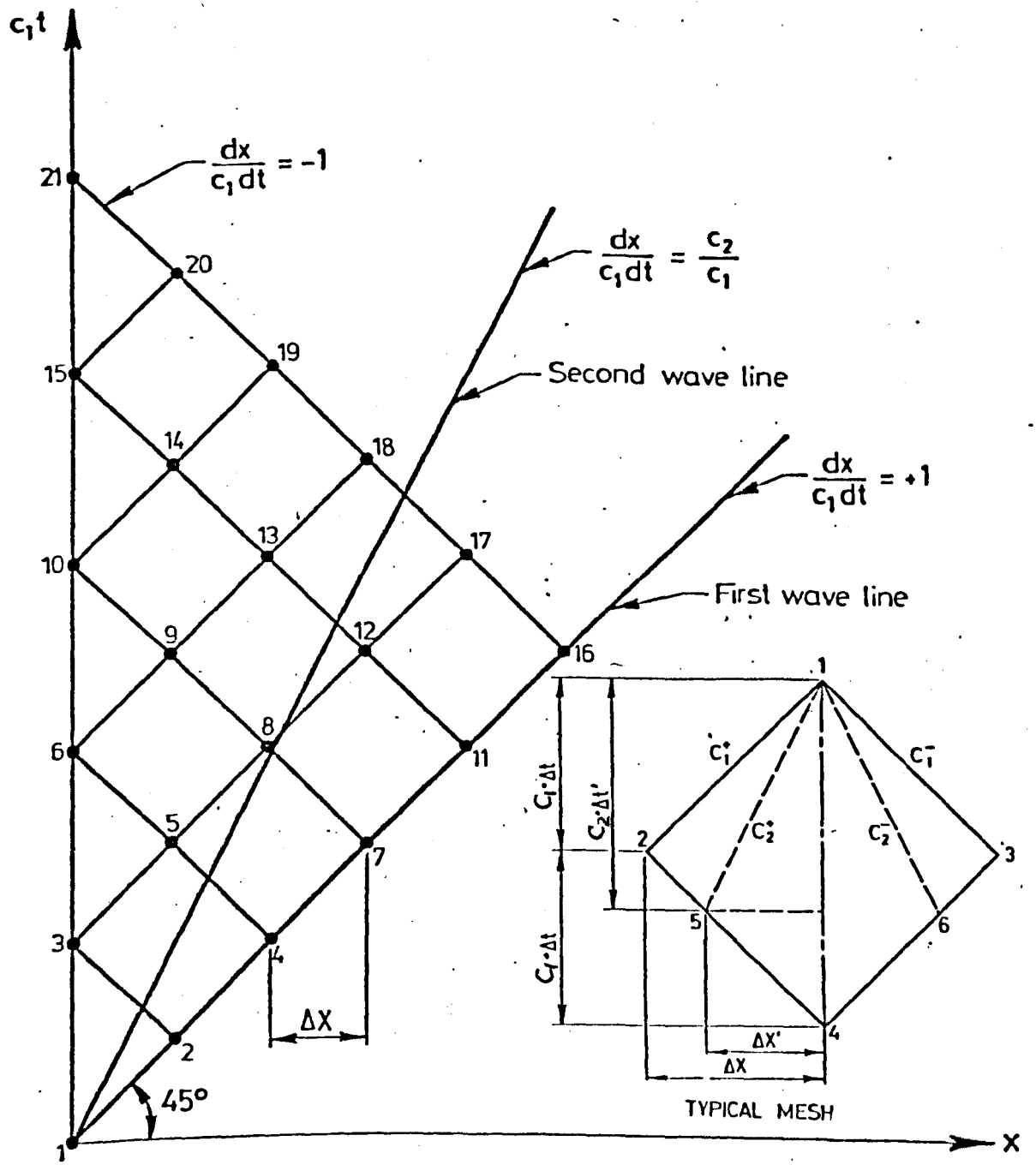

FIG. 3.2 CHARACTERISTIC NETWORK

CHAPTER 1V

COMPUTER CODE FOR TRANSIENT FLEXURAL WAVE PROPAGATION

The computer programme employs the method of characteristics for the study of transient response in beams subjected to eccentric impact with zero initial conditions and time varying boundary conditons.

The present programme is based on a computer code, MCD1T-21, written by Mortimer and Hoburg (1969) and capable of handling semi-infinite regions of various structures such as shells, Mindlin plates, bars and Timoshenko beams.

The MCD1T-21, a general-purpose computer code designed to solve one dimensional elastic wave propagation problems governed by one, two or three coupled second order hyperbolic partial differential equations, uses a system involving two independent variables, one space and the other time. The dependent variables are the generalized displacements and the coefficients of the displacements and their first spatial derivatives are functions of the spatial variable. The general theory is given in the work of Chou and Mortimer (1966) where a system of n equations is analyzed by the method of characteristics, yielding closed form equations for the physical characteristics, the characteristic equations, and the relations governing the propagation of discontinuities.

The governing equations are one of the following forms

$$\frac{\partial^2 u_1}{\partial x^2} - \frac{1}{c_1^2}\frac{\partial^2 u_1}{\partial t^2} = f_1\frac{\partial u_1}{\partial x} + f_2 u_1 \qquad (4.1)$$

or

$$\frac{\partial^2 u_1}{\partial x^2} - \frac{1}{c_1^2}\frac{\partial^2 u_1}{\partial t^2} = f_1\frac{\partial u_1}{\partial x} + f_2 u_1 + f_5\frac{\partial u_3}{\partial x} + f_6 u_3$$

$$\frac{\partial^2 u_3}{\partial x^2} - \frac{1}{c_2^2}\frac{\partial^2 u_3}{\partial t^2} = h_1\frac{\partial u_1}{\partial x} + h_2 u_1 + h_5\frac{\partial u_3}{\partial x} + h_6 u_3 \qquad (4.2)$$

$$\text{or} \quad \frac{\partial^2 u_1}{\partial x^2} - \frac{1}{c_1^2}\frac{\partial^2 u_1}{\partial t^2} = f_1\frac{\partial u_1}{\partial x} + f_2 u_1 + f_3\frac{\partial u_2}{\partial x} + f_4 u_2 + f_5\frac{\partial u_3}{\partial x} + f_6 u_3$$

$$\frac{\partial^2 u_2}{\partial x^2} - \frac{1}{c_1^2}\frac{\partial^2 u_2}{\partial t^2} = g_1\frac{\partial u_1}{\partial x} + g_2 u_1 + g_3\frac{\partial u_2}{\partial x} + g_4 u_2 + g_5\frac{\partial u_3}{\partial x} + g_6 u_3 \qquad (4.3)$$

$$\frac{\partial u_3}{\partial x^2} - \frac{1}{c_2^2}\frac{\partial^2 u_3}{\partial t^2} = h_1\frac{\partial u_1}{\partial x} + h_2 u_1 + h_3\frac{\partial u_2}{\partial x} + h_4 u_2 + h_5\frac{\partial u_3}{\partial x} + h_6 u_3$$

One can see that the Timoshenko beam equations as given in equations (3.16) correspond to equations (4.2) and the coefficient f_i and h_i are obtained by the equality of the two systems

$$f_2 = \frac{AGK^2}{EI} \quad , \quad f_5 = -\frac{AGK^2}{EI}$$

$$f_1 = f_6 = 0$$

and $\quad h_1 = 1$

$$h_2 = h_5 = h_6 = 0$$

For zero initial conditions and a semi-infinite beam, three boundary conditions are specified along the line $x = 0$, in the following form

$$A_1\frac{\partial u_1}{\partial x} + A_2 u_1 + A_3\frac{\partial u_2}{\partial x} + A_4 u_2 + A_5\frac{\partial u_3}{\partial x} + A_6 u_3 + A_7\frac{\partial u_1}{\partial t} = b_1(t)$$

$$B_1\frac{\partial u_1}{\partial x} + B_2 u_1 + B_3\frac{\partial u_2}{\partial x} + B_4 u_2 + B_5\frac{\partial u_3}{\partial x} + B_6 u_3 + B_7\frac{\partial u_2}{\partial t} = b_2(t) \qquad (4.4)$$

$$C_1\frac{\partial u_1}{\partial x} + C_2 u_1 + C_3\frac{\partial u_2}{\partial x} + C_4 u_2 + C_5\frac{\partial u_3}{\partial x} + C_6 u_3 + C_7\frac{\partial u_3}{\partial t} = b_3(t)$$

Where A_i, B_i, and C_i are constants ($i = 1....7$) and $b_1(t)$, $b_2(t)$ and

$b_3(t)$ are functions of time at $x = 0$,

For the Timoshenko beam u_2 is always equal to zero and $b_2(t) = 0$. The second of equations (4.4) is determined as

$$B_4 u_2 = 0 \text{ , so } B_4 = 1$$

where $B_1 = B_2 = B_3 = B_5 = B_6 = B_7 = 0$ and the three equations of (4.4) reduce to two and all terms in u_2 vanish.

For properly posed $b_1(t)$ and $b_3(t)$, the constants A_i and C_i can be determined in non-dimensional form in accordance with the various types of end conditions.

In the present work the MCD1T-21 computer code has been modified and further developed to solve one dimensional transient flexural wave propagation problems in finite beams and finite beams with discontinuities of cross sections.

The present TMOTCU computer code consists of three programmes: (a) the TMOTCU-1 programme for flexural wave propagation in semi-infinite beams. (b) TMOTCU-2 programme for flexural waves in finite beams, and (c) TMOTCU-3 programme for flexural waves in finite beams with discontinuities of cross sections.

TMOTCU-1,2 programmes have been used for checking the accuracy of the present programmes where present numerical results are compared with results obtained by other authors for semi-infinite and finite beams.

However, for finite beams with discontinuities of cross sections, there are no theoretical or expiremental results available and the numerical results were compared with experimental results obtained during the present investigation.

TMOTCU programmes are written in Fontran 1V and are run on CDC 7600 computer, which has approximately 29 significant figures. Thus, round-off error was assumed to be negligible.

TMOTCU-1 consists of a main programme and 17 separate subroutines, employed for evaluation of the variables of each point in the

characteristic network.

For the TMOTCU-2, 4 additional subroutines are needed to include the effect of the second boundary, and 4 further subroutines are required to take the effect of the discontinuity into consideration. Thus, TMOTCU-3 consists of the main programme and 25 subroutines. The number of the input cards is also different for each individual problem.

The subroutines may be divided into two classes, as presented in figure 4.1: the first-level and the second-level subroutines. Each of the first-level subroutines is used to evaluate a different point in the physical plane. The second-level subroutines are general in nature. Their purpose is to define quantities or perform tasks which are needed for several types of points. Some second-level subroutines reamin the same regardless of the type of problem or boundary conditions and are called invariant. Other second-level subroutines are used to define the problem and boundary conditons and thus are completely dependent upon the nature of the particular problem. These are called user-specified.

For each new point, the main programme decides the point type and calls the corresponding first-level subroutine. Each first level-subroutien, in turn calls those second-level subrountines necessary to evaluate qualities at the new point, as illustrated in figure 4.1.

Second level subroutines

Boundary condition time functions subroutines

These three fortran subroutines specify the three time-dependent functions b_1, b_2 and b_3 which form the right-hand sides of the three boundary condition equations (4.4) for a semi-infinite beam at $x = 0$.

A second similar set of three subroutines is needed to specify the three time-dependent functions at second boundary of a finite beam, at $x = L$.

Discontinuity values subroutines

These two subroutines are used to assign the values of the dis-

continuities in $\frac{\partial u_1}{\partial x}$, $\frac{\partial u_2}{\partial t}$, $\frac{\partial u_3}{\partial x}$ and $\frac{\partial u_3}{\partial t}$ which may occur along the c_1^+ and c_2^+ characteristics. These values are determined as described in section (3.3.2).

Printout quantities subroutine

This subroutine is written to obtain the desired output. Any of the quantities calculated at the mesh points and for any functions of those quantities, such as bending moment and shear force, may be printed out, as specified in dimensional and/or non-dimensional form.

Governing equation coefficient definitions subroutines

These three Fortran subroutines are used to specify the coefficients $f_1 \ldots\ldots f_6$, $g_1 \ldots\ldots g_6$ and $h_1 \ldots\ldots h_6$ in the governing differential equations.

Solution matrix subroutine

This subroutine calculates the coefficient of the solution matrix for the quantities at all points other than the first point in terms of known quantities previously evaluated. During its execution, the simultaneous solution subroutine is called to solve the system.

Simultaneous solution subroutine

This subroutine solves "n" equations in "n" unknowns by a matrix inversion technique. No zeros may appear along the diagonal of the determinant (or matrix) of the coefficients of the unknowns.

First level subroutines

First point subroutine

This subroutine calculates the quantities at point 1 in figure 4.2. The subroutine is called only once, at the beginning of evaluation of quantities in the physical plane.

The quantities at point 1 and 2 are to be evaluated simultaneously and a total of 18 unknowns exist: u_i, $u_{i,x}$ and $u_{i,t}$ $(i = 1,2,3)$ at point 1 and at point 2. The 18 needed equations are obtained as follows:

2 compatibility equations along each of the lines: 1-2, 2-3, 2-6.

1 Compatibility equation along each of the line: 1-7, and 2-4.

3 Continuity equations along 1-5.

2 Continuity equations along 2-3.

1 Continuity equations along 2-4.

3 boundary conditons at point 1

The compatibility relations are defined as those differential relations between the first derivatives of the dependent variables u_i that necessarily must be satisfied along the characteristic lines. They are also called characteristic equations.

The 6 continuity equations are written using equations (3.21) and are used to eliminate the 3 displacement variables u_1, u_2 and u_3 at point 1 and at point 2, leaving a system of 12 equations in 12 unkowns, where the compatibility equations are written according to equations (3.22). After a solution for the 12 derivatives is obtained, the 6 continuity equations are used to calculate the displacement variables at point 1 and 2. The first point subroutine calls the following second level subroutines during its execution. (see Fig. 4.1)

(A) The boundary condition time function subroutine.

(B) The discontinuity values subroutine.

(F) The governing equation coefficient definitions subroutines to specify the compatibility equations.

(C) The simultaneous solution subroutine to solve the 12 equations in 12 unknowns.

(D) The printout quantities subroutine.

The description of all subroutines is given in the general form for three displacement variables and their spatial and time derivatives, although for the Timoshenko beam u_2, $u_{2,x}$ and $u_{2,t}$ are all set equal to zero.

Input point subroutine

The input point subroutine is called at the beginning of each new

$\frac{dx}{c_1 dt}=-1$ characteristic line. It is used to define and print out the quantities specified at a point on the first discontinuity line.

Boundary point subroutine

This subroutine is called at the end of each line. It is used to calculate quantities at the points on the boundary x = 0 which satisfy the equations along left running characteristic directions and which satisfy the boundary condition equations. The 9 equations used to calculate the 9 unknowns at point 1 of figure 4.3, in a way similar to that used in the first point subroutine, are obtained as follows

2 compatibility equation's along 1-3.

1 compatibility equation along 1-4

2 continuity equation's along 1-3

1 continuity equation along 1-4

3 boundary conditions at point 1

Ordinary point subroutine

This subroutine is used for each point after an input point and before a boundary point, except for points complicated by the crossing of the second discontinuity lines. The 9 equations used to calculate the 9 unknowns at point 1 of figure 4.4 are obtained from compatibility and continuity conditions along the characteristic lines. The system is reduced to 6 equations with 6 unknowns and is solved simultaneously as in the previous subroutines.

Case I subroutine

The case I subroutine is used for points complicated by the crossing of the second discontinuity line with both of the lines $\frac{dx}{c_1 dt}=-1$ in the manner shown in figure 4.5. After solution for the quantities at point 1 (Fig. 4.5a), dicontinuities in $\frac{\partial u}{\partial x}3$ and $\frac{\partial u}{\partial t}3$ are added to the calculated values so that the calculation may proceed to the quantities at point 1' (Fig. 4.5b). For each of the two points 1 and 1', a system of 9 equations in 9 unknowns is solved, just as for an ordinary

point. The printout subroutine is only called once at point 1'.

Case II subroutine

The Case II subroutine is used for a set of points complicated by the crossing of c_2^+ second discontinuity line in the manner shown in figure 4.6. The procedure for this case is similar to that used in that used in the case I subroutine, with quantities at both points 1' being calculated in the same subroutine, as shown in fig. 4.6b and 4.6c. The same second level subroutines are called during execution for each of the two blocks.

Finite beam

For transient flexural wave propagation in a beam of finite length ℓ, the reflected wave from the other boundary at x = L must be considered. In addition to the initial and boundary conditions at x = 0, a second set of end and boundary conditions at x = L must be specified. In the programme TMOTCU-2 developed for the finite beam, there are 21 separate subroutines. 17 of these subroutines are the same as used for the semi-infinite beam and are as described before. Additional modifications are needed in the main programme to provide the requirements for calling the following subroutines at the end of the beam (x = L). Figure 4.7 shows the characteristic network for a finite beam.

Beam end point subroutine

The beam end point subroutine is used to calculate quatities at the points on the boundary x = L such as point 1 of the typical mesh represented in figure 4.7. The 9 equations needed to claculate the 9 unknowns are similar to those of the boundary point subroutine, which are the following

2 compatibility equation's along 9-1

1 compatibility equation along 6-1

2 continuity equation's along 9-1

1 continuity equation along 6-1

3 boundary conditions at point 1

The contition at the end of the subroutine are formulated in such a way that the required subroutine, to calculate the variables at the next point backwards along the beam, is called.

Beam end boundary condition time function subroutine

These three subroutines are used to specify the three functions $e_1(t)$, $e_2(t)$ and $e_3(t)$ which form the right-hand sides of the three boundary condition equations corresponding to $x = \ell$.

$$D_1\frac{\partial u_1}{\partial x} + D_2u_1 + D_3\frac{\partial u_2}{\partial x} + D_4u_2 + D_5\frac{\partial u_3}{\partial x} + D_6u_3 + D_7\frac{\partial u_1}{\partial t} = e_1(t)$$

$$E_1\frac{\partial u_1}{\partial x} + E_2u_1 + E_3\frac{\partial u_2}{\partial x} + E_4u_2 + E_5\frac{\partial u_3}{\partial x} + E_6u_3 + E_7\frac{\partial u_2}{\partial t} = e_2(t) \qquad (4.5)$$

$$P_1\frac{\partial u_1}{\partial x} + P_2u_1 + P_3\frac{\partial u_2}{\partial x} + P_4u_2 + P_5\frac{\partial u_3}{\partial x} + P_6u_3 + P_7\frac{\partial u_3}{\partial t} = e_3(t)$$

Where $D_1 \ldots D_7$, $E_1 \ldots E_7$ and $P_1 \ldots P_7$ are constants and they are determined together with $e_1(t)$, $e_2(t)$ and $e_3(t)$ in just the same way as described for the boundary conditions $x = 0$.

Finite beam with discontinuity of cross-section

The computer code TMOTCU-2 is further developed to write TMOTCU-3 computer code for studying transient flexural wave propagation in finite beam with discontinuity of cross section at any position along the beam and with any area ratios of the cross section. In figure 4.8, the characteristic network of a finite beam with discontinuity of cross section are represented, together with a typical mesh at the area discontinuity, where reflection and transmission of

the incident wave occur. The basic subroutines are identical to those of TMOTCU-2 and in addition, 4 subroutines are developed in order to incorporate the matching conditions at the discontinuous cross sectional area. Thus TMOTCU-3 employed a total of 25 subroutines.

The continuity of velocity and angular velocity from region 1 to region 2 are (see Fig. 4.8)

$$\left(\frac{\partial u_1}{\partial t}\right)_1 = \left(\frac{\partial u_1}{\partial t}\right)_2$$

$$\left(\frac{\partial u_3}{\partial t}\right)_1 = \left(\frac{\partial u_3}{\partial t}\right)_2 \qquad (4.6)$$

$$\left(\frac{\partial u_2}{\partial t}\right)_1 = \left(\frac{\partial u_2}{\partial t}\right)_2 = 0$$

The equilibruim of bending moment and shear forces at the area of discontinuity are written as

$$E_1 I_1 \left(\frac{\partial u_1}{\partial x}\right)_1 = E_2 I_2 \left(\frac{\partial u_1}{\partial x}\right)_2$$

$$K^2_1 A_1 G_1 \left\{\left(\frac{\partial u_3}{\partial x}\right)_1 - (u_1)_1\right\} = K^2_2 A_2 G_2 \left\{\left(\frac{\partial u_3}{\partial x}\right)_2 - (u_1)_2\right\}$$

$$\left(\frac{\partial u_2}{\partial x}\right)_1 = \left(\frac{\partial u_2}{\partial x}\right)_2 = 0 \qquad (4.7)$$

It is assumed that the beam was made of the same material throughout its length and that the discontinuity is due to the change in dimensions only. This assumption simplifies the problem in the way that the characteristic lines remain straight and with the same slope along the whole beam, since $c_1(1) = c_1(2)$, and $c_2(1) = c_2(2)$. However the extension of this programme for the case of discontinous beam which is made of two different materials, should not represent any additional difficulties, except that the computation would

require major alterations due to the different values of the propagation velocities c_1 and c_2 in the two materials.

The additional subroutines required for the TMOTCU-3 computer code are the following

Discontinuity subroutine

This subroutine is used for the calculation of a typical point at the area discontinuity, as shown in figure 4.8. It solved 18 equations in 18 unknowns. These are obtained as follows

2 compatibility equations along each of 9-1 and 3-1'

1 compatibility equation along each of 6-1 and 4-1'

3 continuity equations along each of 5-1 and 5'-1'

Six additional equations are obtained from the matching condition as given in equations (4.6) and 4.7), which are used to eliminate the variables at point 1'. The six continuity equations are applied at point 1 and 1' to obtain the displacement variables u_1, u_2 and u_3, leaving the system of 6 equations which are solved simultaneously.

Discontinuity solution matrix subroutine

This subroutine is similar to the solution matrix subroutine described before. The discontinuity of the cross section is considered in determining the coefficients of the solution matrix for the quantities at points 1 and 1', in terms of the known quantities at the neighbouring points.

Case I discontinuity subroutine

This subroutine is similar to case I subroutine and is used for points at the area discontinuity complicated by the crossing of the c_2^+ line with both of the lines $\frac{dx}{c_1 dt} = -1$ of the block. The discontinuity solution matrix subroutine is used to set up the system of simultaneous equations and the same second level subroutines are called as in the case I subroutine.

Case II discontinuity subroutine

This subroutine is used for a set of points complicated by the crossing of the c_2^+ line in the same way as shown for case II subroutine in figure 4.6. In the first block at the area discontinuity, the discontinuity solution matrix subroutine is used, whereas in the second block which is not at the area discontinuity, the solution matrix subroutine is used.

At the end of the beam, at x = L, the subroutines described before for the case of finite beam are used. However, the change in the geometry of the second region due to the discontinuity of cross section, has to be considered.

TMOTCU-3 computer code for transient flexural wave propagation in beams with discontinuity of cross section is the most comprehensive version of the three TMOTCU programmes and actually incorporate the other two versions. TMOTCU-3 is listed in Appendix A.

The sequence of the numerical calculation is as follows:

1. For each problem studied, one set of input cards is required and the initial conditons utilized by the programme are zero. From the initial conditions, boundary conditions and equations governing the propagation of discontinuities, the values of the nine variables u_i, $u_{i,t}$ $(i = 1,2,3)$ are known at points 1 and 2 of the characteristic network represented in figure 4.7. The values of the variables at point 3 are then computed through a simultaneous solution of the governing characteristic equations and boundary conditions.
2. The computation then proceeds to the $\frac{dx}{c_1 dt} = -1$ characteristic line through point 4. The values of the nine variables are then computed at point 5.
3. The known variables at points 3 and 5 are used to compute the variables at point 6 through a simultaneous solution of the governing characteristic equations and boundary conditions.

4. The computation then proceeds to the $\frac{dx}{c_1 dt} = -1$ characteristic line through point 7. Knowing the values of the variables at point 4,5 and 7, the values are then computed at point 8.

5. This process continues by solving sets of simultaneous equations to obtain the values fo the variables at points 8, 9 and 10, in that order. Again, the computation shifts to the next $\frac{dx}{c_1 dt} = -1$ characteristic line and solves for the values of the variables at the mesh points along this line (e.g., 12, 13, 14 and 15). This procedure continues until the values along the $\frac{dx}{c_1 dt} = -1$ characteristic through the Mo^{th} point are obtained.

6. The number of lines to be evaluated Mo can be increased for a calculation of longer time history, or decreased due to computer memory space requirement limitations and computer run time. This is achieved by changing Mo in the common statement.

7. The output of the programme includes a preliminary printout listing of all input data which was read into the main programme. The printout of the quantities at mesh points will then begin as specified in the printout quantities subroutine which can be altered to give the output at the required points in time and space.

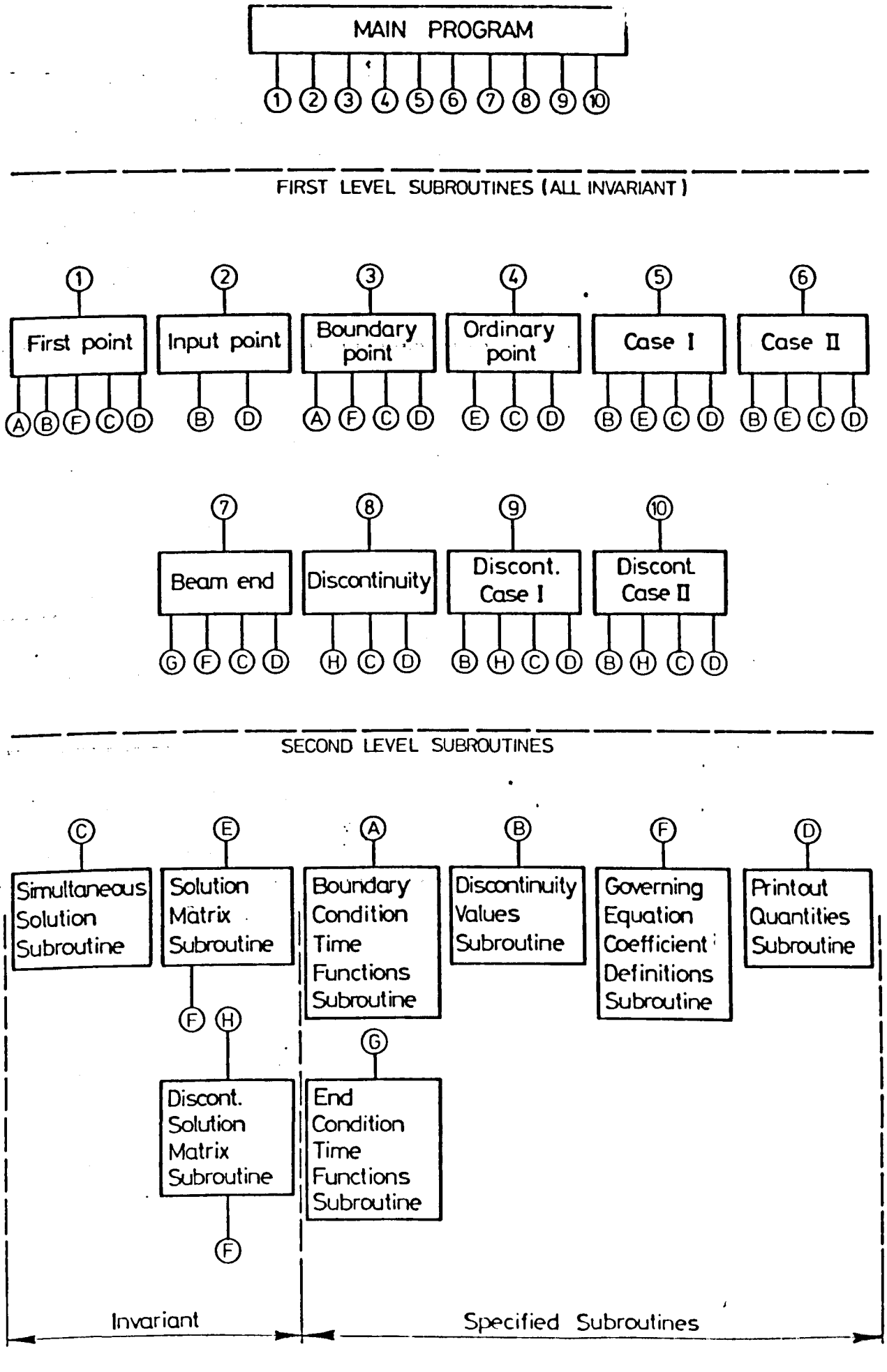

FIG. 4.1. BLOCK DIAGRAM OF THE PROGRAM

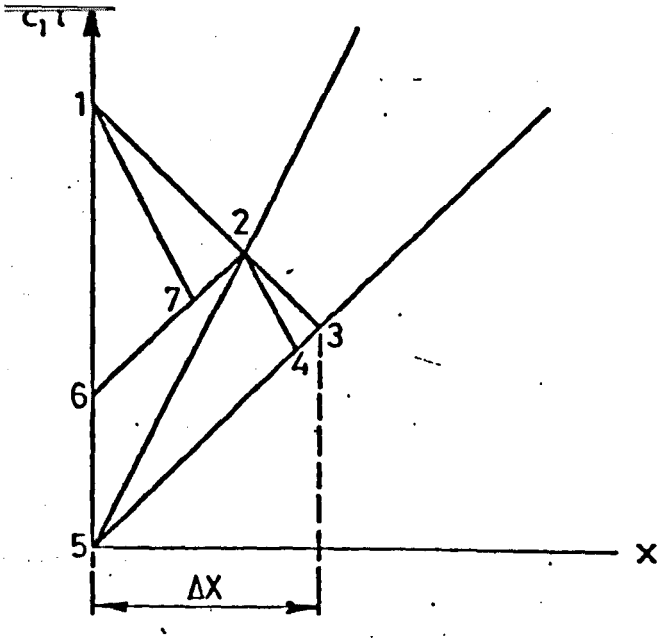

FIG. 4.2. THE FIRST POINT

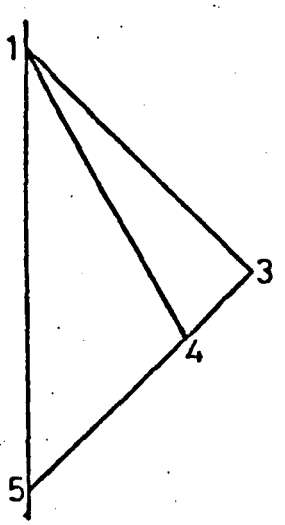

FIG. 4.3 A BOUNDARY POINT

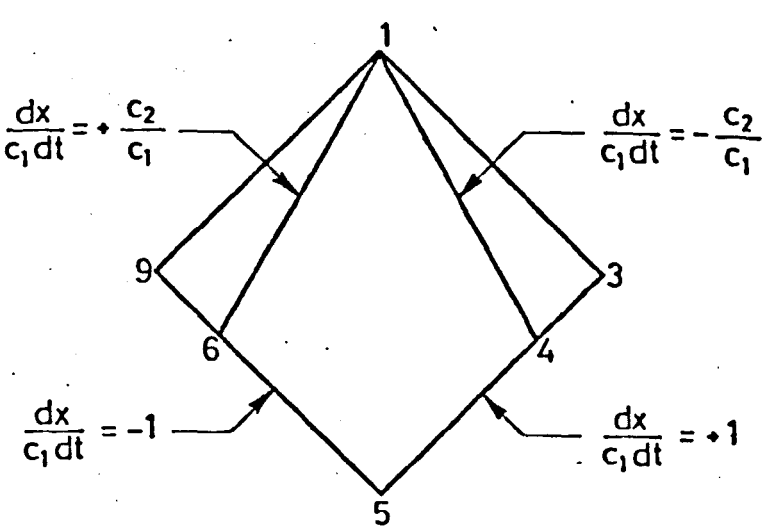

FIG. 4.4. AN ORDINARY POINT

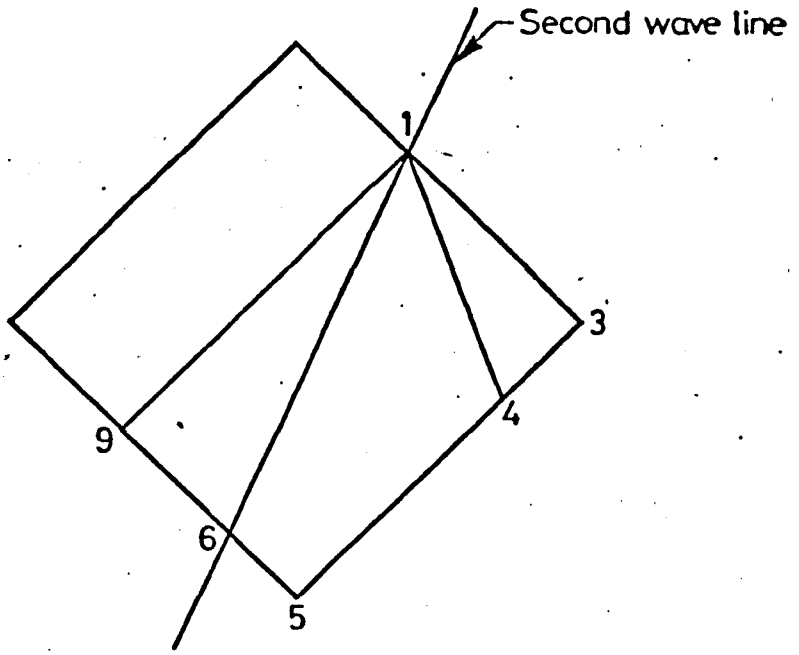

a) Evaluation at point 1

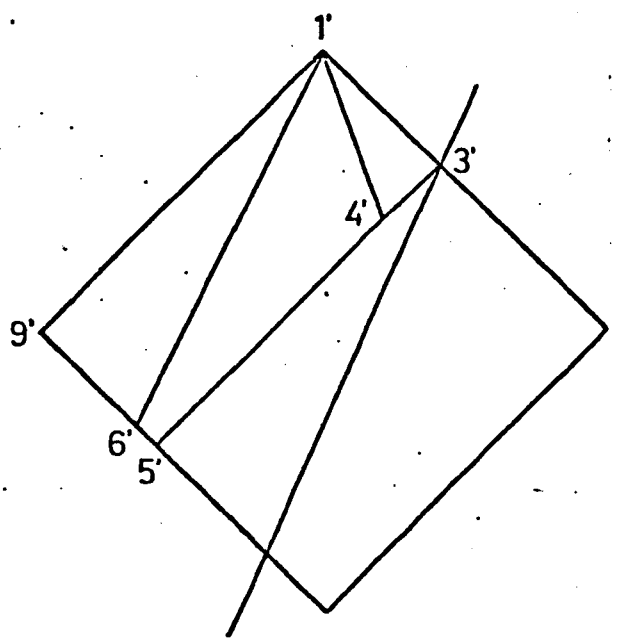

b) Evaluation at point 1'

FIG 45 A CASE I POINT

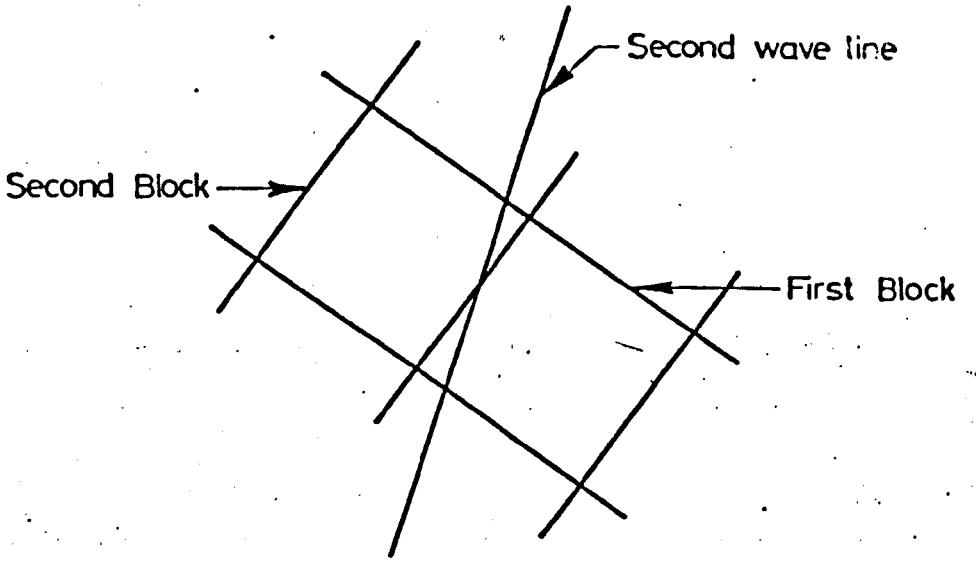

a) Occurrence of a case II set of points

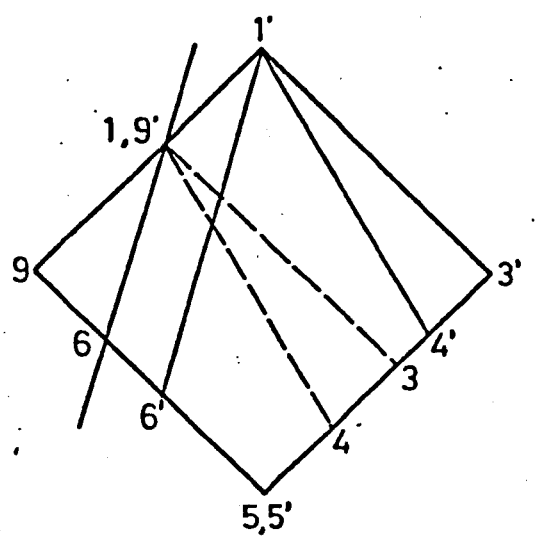

b) Evaluation at points 1,1', First Block

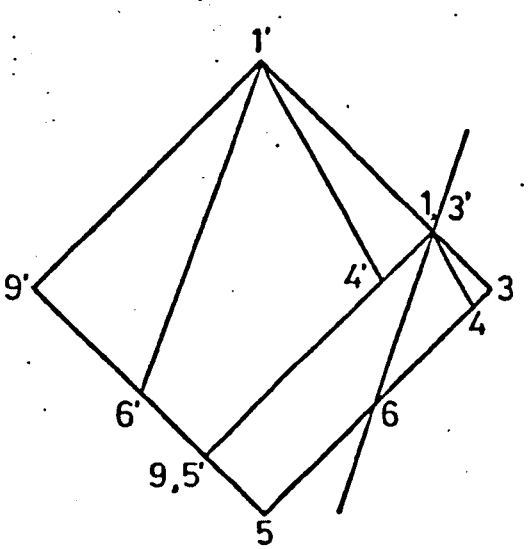

c) Evaluation at points 1,1', Second Block

FIG. 4.6 A CASE II POINT

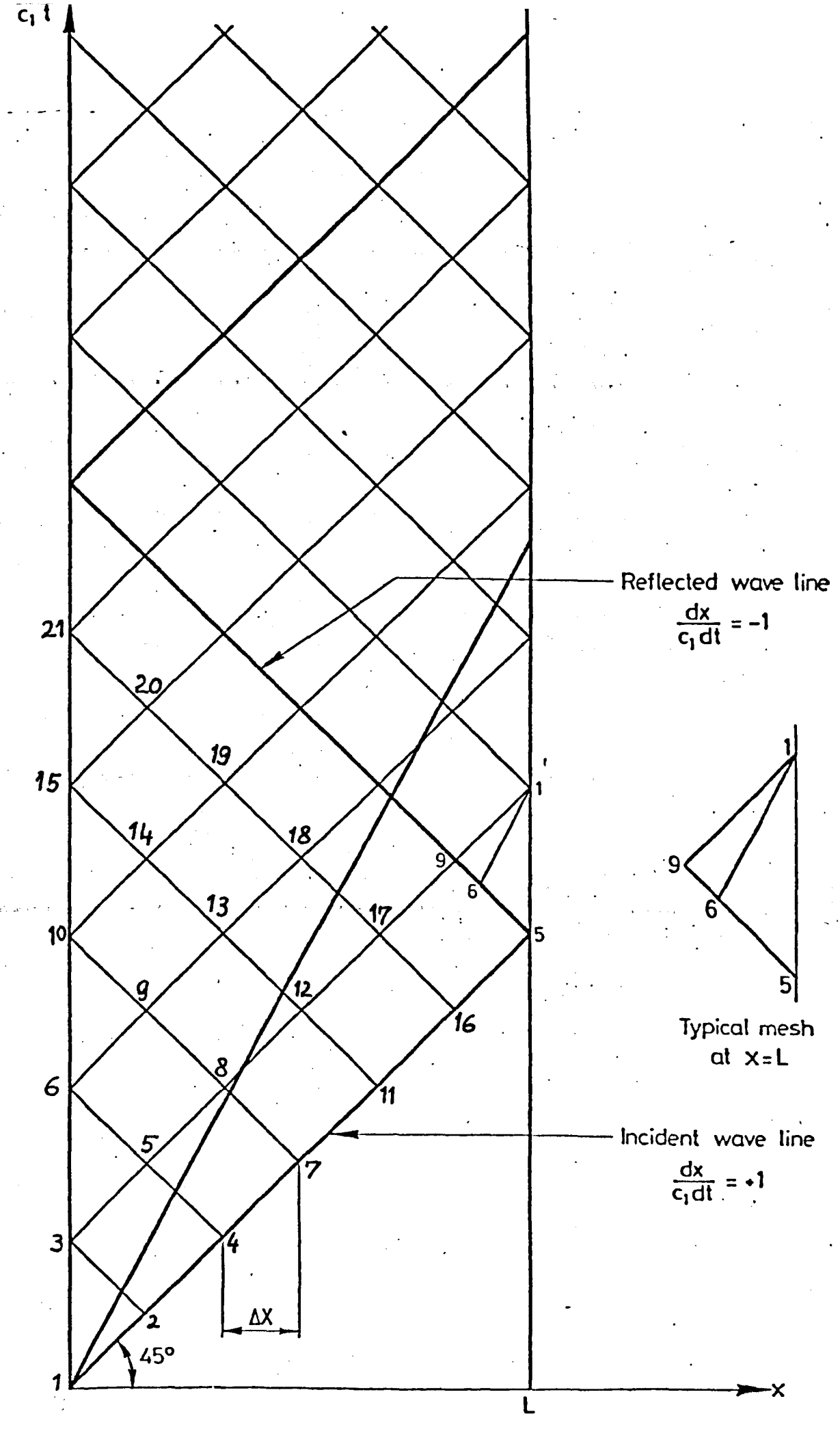

FIG. 4.7 FINITE BEAM CHARACTERISTIC NETWORK

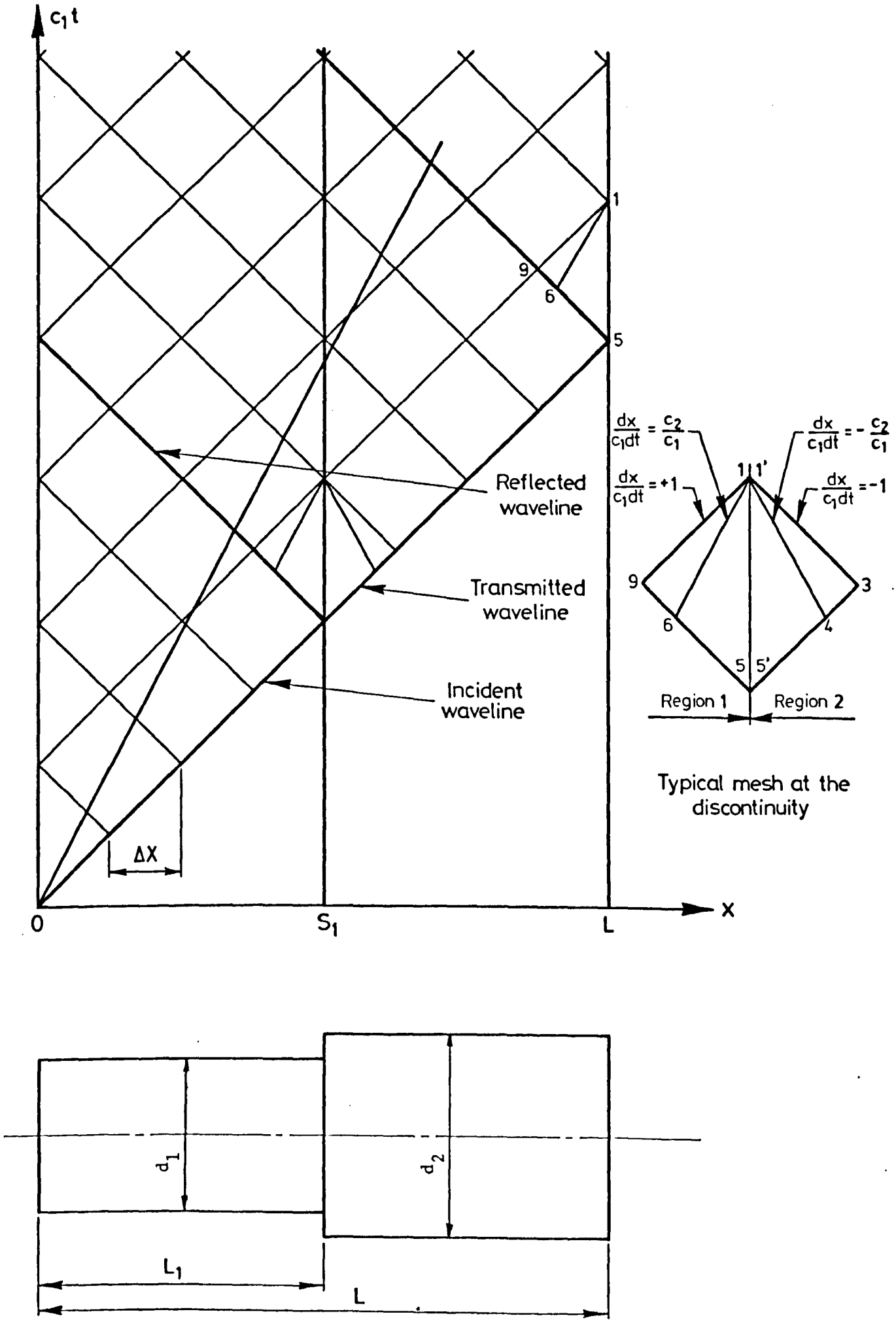

FIG. 4.8. DISCONTINUITY AND CHARACTERISTIC LINES

CHAPTER V

NUMERICAL RESULTS FOR FLEXURAL WAVE PROPAGATION IN BEAMS

5.1. The shear coefficient k^2

Timoshenko (1921) defined k^2 as the ratio of average shear strain across a section to the shear strain at the centroid, a coefficient which takes into account the shear stress distribution over the cross section of the beam. Under static conditions and assuming a parabolic distribution of the shear stress, the shear coefficient which depends on the shape of the cross section, was given by Timoshenko (1921) as 2/3 for rectangular cross section and as 3/4 for circular cross section. This definition neglects the effect of warping of the cross section on its rotatory inertia and taking this effect into account, Göns (1931) derived an approximate fromula for k^2 by the principle originally suggested by Föppl (1897) where the work done by the forces warping an element must be equal to the potential energy due to shearing distortion. The shear stress distribution was again taken as parabolic distribution. Göns obtained the values $k^2 = 5/6$ for rectangular section and $k^2 = 9/10$ for circular section.

The values of the shear coefficient k^2, which is based on the static parabolic distribution, is suitable for very low frequencies and slender beams, but in the higher modes, the shear stress distribution is largest near upper and lower surfaces and k^2 must be modified in order to obtain the best results which the Timoshenko equations are capable of achieving.

In a second paper, Timoshenko (1922) used $k^2 = 8/9$ for a fixed-fixd beam of rectangular cross section in order to bring the prediction of his frequency equation into close agreement with the two-dimensional theory of plane stress. Furthermore, Timoshenko suggested, although not shown in the paper, that the value of k^2 can be derived for a

beam of rectangular cross section by comparison of the two theories just mentioned and the following expression can be derived where ν denotes Poisson's ratio

$$k^2 = 5(1 + \nu) / (6 + 5\nu) \qquad (5.1)$$

A more accurate expression can be derived for a bar of circular cross section by equating the expressions of the frequency equations from the Pochhammer-Chree and Timoshenko theory for flexural waves in an infinite beam. The shear coefficient k^2 is then determined as

$$k^2 = 6(1 + \nu)^2 / (7 + 12\nu + 4\nu^2) \qquad (5.2)$$

where a series expansion for the Bessel functions appearing in the exact frequency determinant should be employed. Therefore, in higher modes the shear coefficient k^2 is not only dependent on the shape of the cross section but also depends on the Poisson's ratio and the frequency.

There have been since many attempts to obtain the value of the shear coefficient by various theories and there is no general agreement in the literature about the exact effects of the cross section geometry and of mode number on the evaluation of k^2 value which tends to vary between 0.667 and 1.0 and numerous attempts have been made to evaluate k^2 theoretically and experimentally.

Sutherland and Goodman (1951) presented various methods of obtaining the shear coefficient k^2 for beams of rectangular cross section. One method was based on the prediction by the exact solution of the general elasticity equation that the wave velocity in a thin rectangular beam must approach that of Rayleigh surface waves for small wave lengths and k^2 was determined as 0.8696 for $\nu = 1/3$. A second method described by the authors was based on thickness shear mode of vibration with the circular frequency $\pi c_s / r\sqrt{12} \hat{=} c_s \sqrt{k^2}/r$, which gives $k^2 = \pi^2/12 = 0.8225$. This value was also obtained by Mindlin and Deresiewitz (1954) who suggested that if this value is used, the

Timoshenko equations give good results in agreement with experiment for both low and high frequencies.

The value of k^2 was obtained experimentally in connection with Young's modulus measurement from flexural vibrations and comparison with theoretical derivation was made (Göns, 1931; Pickett, 1945; Spinner et. al., 1960; Nederveen et. al., 1964 and Ritchie, 1973).

A new approach to the derivation of the shear coefficient was adopted by Cowper (1966) who derived the Timoshenko equation by integration of the equations of the three dimensional theory of elasticity and obtained a general formula for k^2 and various cross section configurations. Their expressions for a rectangular cross section and for a circular cross section are respectively

$$k^2 = 10(1 + \nu) / (12 + 11\ \nu) \qquad (5.3)$$

$$k^2 = 6(1 + \nu) / (7 + 6\ \nu) \qquad (5.4)$$

In a second paper in 1968a, Cowper showed the k^2 values derived by his expression for a thin beam were in close agreement with the thickness shear mode theory. Cowper also pointed out that although his results were derived from the lowest mode of vibration, they also were applicable to higher bending modes.

Spence and Seldin (1970) pointed out that since only the product of k^2G can be determined from flexural resonances , the relative error in G is as severe as the relative error in k^2. They obtained experimentally $k^2 = 0.873$ for a rectangular cross section and $k^2 = 0.923$ for a round bar, where $\nu = 0.287$.

Carnegie and Thomas (1972) investigated the dynamic behaviour of turbine blades, modelled as cantilver beams of rectangular cross section and noted the marked effect of shear and rotatory inertia in the higher modes. k^2 was chosen as 0.834 which is close to the values of Cowper and Mindlin.

Alami and Atzori (1974) matched the results of the Timoshenko

equations to the results based on a three dimensional form of extended Rayleigh-Ritz energy method and concluded that the flexural frequencies of a simply supported Timoshenko beam are better expressed with two different values for the shear coefficient in the two branches of the flexural modes.

Ghosh (1974) presented the effect of various values of k^2 on frequencies of vibration and mode shapes up to the 5th mode and concluded that the frequency ratios of the higher modes were lower, the greater the k^2 values. The effect of variation of k^2 was most significant in the higher modes.

Kaneko (1975) gave a comprehensive review of the history of the Timoshenko shear coefficient and its estimation and based his calculation on the values suggested in general terms by Timoshenko (1922).

Hsu (1975) suggested a modification of Cowper's theory, which led to k^2 - values greater than unity, where k^2 was defined as the effective shear coefficient since it included the effect of pressure gradient over the beam cross section. Hsu agreed with the opinion expressed by one reviewer of his brief note that since his derivation was based only on deflections, there is no guarantee that the stresses resulting from the present approach agree with the Timoshenko theory. Although this newly suggested value, which is greater than unity, may include some effect not included in the Timoshenko theory, it is not useful for the Timoshenko equations.

Downs (1976) used Hsu's value to obtain agreement with the additional shear oscillation frequency mode in a uniform simply supported Timoshenko beam. However, the value of k^2 greater than unity does not give any reasonable comparison with the basic modes of the flexural motion of the beam.

Rosinger and Ritchie (1977) assessed experimentally the k^2 values derived by Kaneko and obtained excellent agreement between theory

and experiment for the first six natural frequencies .

Stephen (1978) showed that the value of k^2 as obtained by equating the Timoshenko phase velocity prediction to the exact phase velocity as calculated by Hudson (1943) was only suitable for long wave length propagation and should not be used for the approximate discription of flexural wave motion according to the more important first frequency spectrum. He also found that for higher frequencies the k^2 value differed little from the value given by Kaneko.

In a second paper in 1980, Stephen obtained the shear coefficient employing the distribution in a beam performing flexural vibration and subjected to uniform body force or gravity loading. The derived expressions were compared with those of Cowper and Kaneko for several cross sections.

Table I presents the various values used for the shear coefficient for circular and rectangular cross sections. In most cases the expressions for k^2 were evaluated for the Poisson's ratio $\nu = 0.29$, usually found in the literature for steel.

Ideally, one should use different values for the shear coefficient k^2 depending on the frequency range. However, in order to keep the concept of single correction factor for each cross section and material i.e. if k^2 is to be taken as constant, and choose atthe same time a suitable value for transient loading, the values used in this thesis were based on the derivation of Cowper (1966) which were derived by integration from the three dimensional theory of elasticity. The Cowper k^2 values are close to most k^2 values except the ones based on the parabolic static shear distribution which are unsatisfactory for impact loading with a wide range of high frequency spectrum.

The values used for the shear coefficient in this thesis are unless otherwise stated, as defined by equations (5.3) and (5.4) and are for $\nu = 0.29$: $k^2 = 0.8856$ and 0.8492 for circular and rectangular cross section respectively.

5.2. Comparison of the transient response with results obtained by other solution methods and with experiments

The computer code MOTCU-1 for a semi-infinite beam and TMOTCU-2 for a finite beams were both checked for accuracy by comparing their numerical results with various experimental, numerical and exact solutions available in published papers, reports and Ph.D. theses.

The cases considered were those of a semi-infinite beam subjected to a ramp platform bending moment, a semi-infinite beam subjected to a half-sine input bending moment and a cantilever beam subjected to a ramp platform bending moment at the free end. The beams in all these cases were of circular cross sections except the cantilever beam which was of rectangular cross-section.

The developed computer code is applicable to problems of eccentric impact where a bending moemnt is applied at one end of a free-free, simply supported, or cantilever beams. The boundary conditions can be formulated in terms of bending moment, shear force, angular velocity and transverse velocity.

The TMOTCU-1 to 3 computer programmes are equally applicable to problems of lateral impact of finite Timoshenko beams with various end conditions. The case of lateral impact of a simply supported beam of rectangular cross section is also investigated.

Computer processing time for the problems just described on a CDC-7600 computer was from 30 seconds to 110 seconds depending on the mesh size and the time span for which the bending moment distribution was evaluated. In most cases, the discussion is confined to bending moment distribution due to its importance in engineering problems. However, the time wise distribution of θ, ω and v are all included in the programme output.

5.2.1. Semi-infinite beam subjected to eccentric impact

The results of the present numerical solution by the method of characteristics were compared with a solution by Kuo (1958) who investigated the bending stresses in a bar subjected to eccentric longitudinal impact, induced by a striking bar of the same dimensions and material. The properties and dimensions are given in Table II, for a low carbon mild steel bar with a slenderness ratio L/r = 100 where L is the length of the beam and r its cross sectional radius of gyration.

Kuo based his theoretical solution by the method of characteristics on a physically unrealistic value of $c_1 = c_2$ and therefore the bending moment time distributions of this case were plotted in non-dimensional form at two beam stations $\bar{x} = 0.1$ and 0.3 where $\bar{x} = x/L$.

Kuo also obtained a modal super position solution which was based on the value $c_2/c_1 = k^2G/E = 0.3$. The coefficients required for the present numerical solution are listed in table III and boundary conditions corresponding to a ramp platform bending moment at the end of the free-free beam are according to table IV for a maximum unity input bending moment

$$\bar{M}(0,\bar{t}) = 10\ \bar{t} \text{ for } 0 < \bar{t} < \bar{t}_o$$

$$\bar{M}(0,\bar{t}) = 1 \text{ for } \bar{t} > \bar{t}_o$$

$$\bar{Q}(0,\bar{t}) = 0 \text{ for all } \bar{t}$$

The non-dimensional mesh size $\Delta\bar{x} = \Delta x/L$ was chosen as 0.01 and corresponded to a time step of 1.22285 μs. Figure 5.1 shows the time distribution of the bending moment at beam stations $\bar{x} = 0.1$ and $\bar{x} = 0.3$ in non-dimensional form for $\bar{M}$ vs. $\bar{t}$, where $\bar{M} = ML/EI$ and $\bar{t} = c_1 t/L$. The time history was limited as by Kuo to the initial stress build up with $\bar{t} = 2.4$ (i.e. $t \simeq 293.5\mu s$).

The comparison between the present results and Kuo's solution, as shown in figure 5.1, is good as both curves are reaching the same peak value. However, there is a small shift at the initial portion

of the present curve which starts at $\bar{t} = 0.1$ for $\bar{x} = 0.1$ and at $\bar{t} = 0.3$ for $\bar{x} = 0.3$. These points represent the earliest possible arrival of any bending wave. Therefore, the present curves can be considered to give a better picture of the wave propagation than Kuo's curve which start at a later position and Kuo mentioned this phase shifting when he compared his theoretical results with experimentally observed data. At the beam position $\bar{x} = 0.3$, Kuo's theoretical solution shows large oscillations starting at $\bar{t} = 1.8$ and there is no logical explanation for their appearance in the case of a semi-infinite beam, where no reflections are considered, unless they are caused by numerical instability.

Kuo suggested that the beam response was not particularly sensitive to the change in k^2G/E and that curves based on taking a higher value k^2G/E invariably lead ahead of those based on a lower value. The curves obtained by TMOTCU-1 for $k^2G/E = 0.3$ and 1.0 were presented in figure 5.2 and showed that the effect of the change in k^2G/E upon the bending moment distribution is significant and cannot be neglected.

The effect of varying the rise time of the ramp platform moment are presented in figure 5.3 for the beam stations $\bar{x} = 0.1$ and 0.3. Three different rise times $\bar{t}_o = 0.025$, 0.1 and 0.4, as well as a step input moment, were considered. The step input moment required a smaller mesh size of $\Delta x = 0.0025$ for the numerical solution. It is seen that there is a large difference between the initial portions of the curves, and the amplitude increases as the rise time is decreased and approaches the step input response curve as a limiting value. The difference between the later portions of the curves is much smaller and the amplitude becomes almost constant as time progesses and approaches slowly the initial value of the input bending moment.

5.2.2. Semi-infinite beam subjected to short bending wave pulse:

Figures 5.4 and 5.5 compare the theoretical results of the present work with experimental results obtained by Ripperger (1955) for the eccentric impact of a steel ball of ½ in.dia on the end of a cylindrical steel bar of 0.516 inch diameter. The pulse shape for the applied bending moment was approximated for the numerical solution by a half sine wave, obtained by the superposition of solutions for the continued sine wave differing at the start by half the period, as given in Table IV. The pulse duration was assumed as t_r=14.28μs and the sine input function was

$$M(0,t) = 27.14 \sin(\pi t/14.28)$$

The material properties and the dimensions of the beam are given in Table II and the required coefficient for the initial and boundary conditions are given in Table III.

The agreement between the numerical results obtained by TMOTCU-1 programme and the experimental data of Ripperger is good as shown in figure 5.4 for beam stations x/d = 2 and 6; and in figure 5.5 for beam stations x/d = 10 and 22 where d is the bar diameter. The results are presented in nondimensional form for the bending wave $\bar{m}$ vs. $\bar{T}$ where $\bar{m} = \frac{M.d}{EI}$ and $\bar{T} = \frac{c_1 t}{d}$. The range of the time for the bending moment pulse was much shorter than the time it takes the reflected pulse to reach the considered position and the response was the same as for a semi-infinite free beam.

Various authors used Ripperger's experimental data to check their theoretical solutions. Plass (1958) obtained good agreement for his numerical solution by the method of characteristics. Plass defined $C = c_1^2/c_2^2 = E/k^2G$ and assumed C = 4 for ν =0.3 and k^2 = 3/4. The exact value of C is obviously 3.467. In Plass's work C was an important parameter used for establishing the limits of the transform solution and for evaluating the integrals for one case to compare with the

numerical results of the MOC. The value $C = 4$ gives $c_1 = 2c_2$ and was seemingly chosen for convenience in obtaining transform solutions, but it does not correspond to the properties of the material.

Parker (1973) compared analytical results obtained by a modal solution with augmented series, with the experimentally observed data of Ripperger. Parker was able to present good time-wise agreement, but the amplitude of his analytical predictions were much higher, some of them were more than twice the recorded response. Parker suggested the following explanation: "The fact that the amplitude of the experimentally recorded pulse drops off more rapidly than the analytical predictions may be due to internal damping, strain rate effects, or limitations of the experimental appratus with regard to frequency response". This explanation can not be considered as convincing for the very large deviations of the analytical solution from experimental results. One is inclined to believe in the inadequacy of analytical modal solutions for impact problems of short duration, particularly eccentric impact where flexural dispersive waves are to be considered.

Even the use of a large number of modes, as by Parker who used up to 800 modes did not seem to improve the usefulness of the method for this kind of problem.

5.2.3. Cantilever beam

The accuracy of TMOTCU-2 computer programme was checked by comparing its results with an example solved by Koenig and Davids (1968) for a cantilever beam subjected to a ramp platform bending moment at its free end, where the effect of reflected waves in a very short cantilever beam of 1.5 inch length and 1 in x 1 in cross section. The value of 1.0 lb.in end moment with a rise time $t_o = 5.174\mu s$ was assumed. The property data are listed in Table II and the required coefficients for the numerical solution are given in Table III.

The results of the present method are in a very good agreement

with those obtained by Koenig and Davids by a so called "Direct analysis" which was based on a finite difference scheme.

Figures 5.6 and 5.7 show the bending moment and shear force distributions at position x = 0.5 inch of the cantilever beam in comparison with the results obtained by Koenig and Davids. Both results are in very good agreement and x is measured from the built-in end.

The reflected bending wave from the built-in end of the cantilever beam arrives at the station x = 0.5 in. at t = 13 μs after which oscillations with a large amplitude are noticed. The peak at t = 23 μs is considerably larger than the peak at t = 15 μs and both peaks are larger than the unity input bending moment.

Figure 5.7 shows the effect of reflected waves on shear force distribution which causes the shear force to take on values other than zero as time increases, whereas in a semi infinite beam, the value of shear force would approch zero with increased time.

In order to compare the wave propagation in cantilever beams with other end conditions a numerical solution was obtained by the use of TMOTCU-2 for a second much longer cantilever beam and its bending moment time history are compared with free-free and simply supported end conditions, as presented in figures 5.13 and 5.14 for various beam stations and discussed in section 5.3.3.

5.2.4. Lateral impact of simply supported beam

Dengler et. al (1952) studied analytically and experimentally the problem of lateral impact of a beam of uniform rectangular cross section. The beam was simply supported at the ends and was struck transversly at the mid span by dropping a steel ball.

The beam length was sufficient to ensure that reflection from the beam end did not return to the beam station considered within the time span considered at beam stations x/h = 4 and x/h = 8 for which the bending moment prediction $\bar{m} = \frac{M.h}{E\ I}$ vs. time t are presented .

The authors used the Hertzian theory for the theoretical predictions of the force-time history and observed close correlation between theoretical and experimental results.

The analytical closed form solution was derived for an infinitely long beam and contained complicated contour integrations and their evaluations caused several difficulties due to singularities at both ends of the integration interval.

The properties and dimensions of the mild steel square beam are given in Table II and the coefficient required for performing the numerical solution by the method of characteristic are listed in Table III. The shear force applied at the centre of the beam was assumed to be of a half sine form with an amplitude of 15.6 lb and a duration of 14 μs, as given in a general form in Table IV.

Comparison of the present results with those of Goland et. al. are shown in figure 5.8 for the positions measured from the point of impact. The comparison showed the excellent reproduction of the transient components of the records in the theoretical solution obtained by the TMOTCU-2 computer program. The agreement of the present numerical results with the experimental observation was as good as the agreement of the analytical results obtained by Duhamel integrals.

Forrestal and Bertholf (1975) compared the Goland et. al solution with their numerical solution for a lateral impact problem obtained by two dimensional finite difference method. They found general agreement between the two sets of results except for higher frequency oscillations predicted only by the numerical solution.

The two dimensional solution is only suitable for flexural wave propagation in beams of rectangular cross-section which could be solved as a plane strain problems. However, flexural waves in beams of circular cross section are three-dimensional problems and cannot be solved by the two-dimensional finite difference method.

Furthermore, in order to apply the finite difference scheme even to rectangular beams, one needs to assume the input to be in the form of Dirac delta functions or sinosoidal functions which are not always adequate for the prediction of the input force. Other difficulties are involved in handling discontinuities and boundary conditions which dictate the introduction of a fictitious viscosity term in order to reduce the spurious oscillations.

All these factors made the finite difference scheme unsuitable for solving various types of flexural wave propagation problems in Timoshenko beams particularly in beams with discontinuities of cross sections. Therefore, it was decided to use the numerical solution by the method of characteristics throughout the present work.

5.3. Finite beams subjected to end moment impacts

5.3.1. Free-free beam

The problem of a free-free finite beam subjected to a ramp platform end moment suddenly applied at $x = 0$, was solved by the method of characteristics. The moment time relations at various stations along the beam are plotted. For a semi-infinite beam, the value of the bending moment would approach the value of the maximum input moment. However, for the finite beam the bending moment reaches higher values due to reflection from the end of the beam.

The material properties used for the numerical computation are those of mild steel, which are listed in table II, together with the geometrical data of the cylindrical beam. The bending moment time relations in non-dimensional form are shown in figures 5.9 and 5.10 for beam stations $\bar{x} = 0.1$, 0.3 and 0.5.

The ramp platform input bending moment $\bar{M} = ML/EI$ was assumed to reach the value of unity after a rise time $\bar{t}_o = \frac{c_1 t}{L} = 0.1$ (equivalent to 12.285 μs). It is seen that until reflected bending waves have reached the beam station under consideration, the curves of the semi-

infinite and finite free-free beam are identical, that is until $\bar{t} = 1.9$ for $\bar{x} = 0.1$, $\bar{t} = 1.7$ for $\bar{x} = 0.3$, and $\bar{t} = 1.5$ for $\bar{x} = 0.5$. After that time, the effect of the reflections is manifested in the oscillations occuring in the bending moment distribution as time progresses. It was found that the value of the bending moment immediately after the time required for the reflection to reach the corresponding position did differ, although in a very small amount not noticable on the graphs, from the value of the bending moment in a semi-infinite beam. However, much larger differences are noticed at later stages. For the positions $\bar{x} = 0.1$, the first two alternating bending moment peaks appear at $\bar{t} = 3.6$ and $\bar{t} = 3.7$. A much larger oscillation in the value of the bending moment distribution is seen at about $\bar{t} = 4.5$ and $\bar{t} = 5.0$ where $\bar{M} = 1.17$ and $\bar{M} = 0.88$ respectively. The number of alternating peaks in the bending moment distribution increases and appears at earlier times at the positions $\bar{x} = 0.3$ and $\bar{x} = 0.5$.

The effect of the reflected wave is considerable and must be taken into consideration. Furthermore, the difference between the moment-time relations in a finite beam and a semi-infinite beam at various stations increases as the number of reflections reaching the considered positions increases. The time history of the bending moment was obtained for $\bar{t}$ up to 7 which includes 2-3 reflections. The mesh size used for the numerical evaluation was $\Delta\bar{x}=0.0025$. The required constants A_i and C_i at x=0 and D_i and P_i at x=L are given in Table III for a ramp platform bending moment applied at x = 0, as given in Table IV.

5.3.2. Simply supported beam

The same ramp platform bending moment of $\bar{M}= 1$ and rise time $\bar{t} = 0.1$ was applied at $\bar{x} = 0$ of a simply supported beam of the same properties and dimensions as the one used in section 5.3.1. The required coefficients A_i, C_i, D_i and P_i for the numerical solution are listed

in Table III and the time history of the bending moment at the beam stations $\bar{x} = 0.1$, 0.3 and 0.5 is presented in figures 5.11 and 5.12.

Comparison of the bending moment distribution in the beam when the ends are simply supported with those of the free-free beam show that the value of the bending moments in the simply supported beams is much smaller and the build-up is much slower. However, both sets of results show a similar pattern in the initial build up, but deviate more and more from each other as time progresses.

In figures 5.11 and 5.12, the effect of the change of mesh size is investigated. Three different mesh sizes of $\Delta\bar{x} = 0.005$; 0.0025 and 0.00125 are used in order to check quantitatively the difference between the three curves obtained by different mesh sizes, chosen by successively decreasing the mesh size to half its value.

The difference between the three curves with various meshes for the beam position $\bar{x} = 0.1$ is seen to be very small (about 1%) until the time $\bar{t} = 3.6$. The maximum error occured at $\bar{t} = 5$ and $\bar{t} = 6.3$ and had the value of about 5% when the difference is related to the initial unity input value of the input moment. The maximum error within the time span considered for the bending moment-time relation at beam stations $\bar{x} = 0.3$ and $\bar{x} = 0.5$ had the values of 5% at $\bar{t} = 6.6$ and 7% at $\bar{t} = 7.0$ respectively.

It is noticed that the maximum amplitude occured at the same instant by all three mesh sizes and the maximum differences were concentrated at the peak values. Furthermore, the difference between the bending moment values obtained by two successive mesh sizes was decreasing and the error accumulation was not increasing as time progresses. A smaller mesh size always requires a longer processing time in the computer and can be considered as a serious limitation which restricts the use of the method of characteristics to relatively short periods of time due to economic considerations. However, with

the vast increase in processing speed of modern computer, this disadvantage has become less significant.

5.3.3: Effect of end conditions

In addition to the cases of a free-free beam and a simply supported beam previously discussed, the case of a cantilever beam subjected to a ramp platform input bending moment at the free end $x = 0$ was also considered. The bending moment distribution of all three types of boundary conditions are plotted together with the curve of a semi infinite free beam in figures 5.13 and 5.14 for beam stations $\bar{x} = 0.1$, 0.3 and 0.5.

The bending moment at each considered station of the cantilever beam is exactly the same as that of the free beam until the time after reflections from the built-in end have reached that position.

All compared sets of results were obtained using the same mesh size of $\Delta\bar{x} = 0.0025$, corresponding to a real time step of 0.306 μs and the computer code specially developed for finite beams (Programme TMOTCU-2) as described in chapter 4.

The alternating sense of the bending moment was clearly noticed and indicated the presence of higher frequencies due to superposition of propagated and reflected waves. In all cases the dispersion, the velocity of propagation being a function of wave length, is clearly demonstrated. The fluctuations at beam positions $\bar{x} = 0.3$ and $\bar{x} = 0.5$ are more dominant than at $\bar{x} = 0.1$.

In comparison with the moment time relations in beams with various end supports, it is seen that the higher peaks are reached at earlier times due to reflection from the free end, whereas the build up in the simply supported beam was the slowest. In the case of the cantilever beam the highest peak value of $\bar{M} = 1.19$ was reached at $\bar{t} = 5.6$ within the time considered and at beam position $\bar{x} = 0.1$. It is expected that several reflections should be considered for the estimation of the maximum stresses in the structure.

The boundary conditions are prescribed in generalized displacement variables and generalized velocities. The generalized stresses are also used as boundary conditions and are of practical importance in the present solution of the flaxural wave propagation problem according to the Timoshenko beam equations.

The number of generalized stresses can be equal to or greater than the number of generalized displacements. However, the number of generalized stresses used as a boundary condition is equal to the number of generalized displacements. Therefore, in the case of the Timoshenko beam, one needs to specify only two boundary conditions at $x = L$, in addition to two initial conditions for y and ψ. A properly posed boundary condition is to specify generalized stresses or generalized displacement. At a particular position, one may specify either stresses or displacements, but not both.

Properly posed initial and boundary conditions are those which assure a unique solution of the equations.

At a free (unsupported) end, the bending moment and shear force are zero ie. $M = Q = 0$, and at a simply supported end, the bending moment and transverse velocity are zero, i.e. $M = v = 0$. For the case of the built-in end of a cantilever beam, the transverse and angular velocities are both zero, i.e. $v = \omega = 0$. Various types of loading can be applied to various types of end conditions. Plass (1958) used generalized stress boundary conditions and Boley (1955) used generalized displacement formulations at the boundaries. Chou (1965) discussed in his report both types of boundary conditions.

5.4. Finite beams with discontinuties of cross section

5.4.1. Free-free beam

5.4.1.1. The variation in diameter ratio

The computer programme TMOTCU-3, based on the method of characteristics and described in chapter 4, was developed to solve

the system of Timoshenko beam equations (4.3) subject to the conditions of equilibrium of forces and moments and continuity of displacements, as given in equations 4.6 and 4.7.

The values of the coefficients A_i and C_i at x = 0 together with the D_i and P_i at x = L are exactly the same as the ones used for the finite free-free beam and are given in Table III.

The TMOTCU-3 programme included special subroutines to evaluate the values of M, Q, W and V at $x = L_1$, where the radius of the beam was changed from R_1 to R_2, L_1 being the length of the beam in region 1 with a radius R_1, as illustrated in figure 4.8.

The bending moment distribution was obtained numerically until the non-dimensional time $\bar{t}$ of about 2, corresponding to a real time of 245 μs, where $\bar{t} = \frac{c_1 t}{L}$ and with a bar velocity of c_1 = 5111 m/s and L = 0.625m. All parameters and material properties of the beam are given in Table II.

The mesh size used for the numerical solution was $\Delta\bar{x} = 0.25 \times 10^{-2}$ which is ½ the mesh size required for the finite beam and 1/4 the mesh size required for the semi-infinite beam.

The adequacy of the present mesh size was checked by carrying out numerical solutions with a mesh size $\Delta\bar{x} = 0.125 \times 10^{-2}$ and it was found that the effect of the change in mesh size was mainly concentrated at the points of peak values and the maximum difference was less than 5%, whereas solutions based on a larger mesh size of $\Delta\bar{x} = 0.5 \times 10^{-2}$ were found to deviate from the present result and reduced the effect of reflected and transmitted pulses through the position of discontinuity.

Furthermore, the difference between the results based on $\Delta\bar{x} = 0.25 \times 10^{-2}$ and $\Delta\bar{x} = 0.125 \times 10^{-2}$ did not accumulate as time progressed and therefore the mesh size $\Delta\bar{x} = 0.25 \times 10^{-2}$ was considered small enough to give satisfactory results for the finite beams with discontinuity

of cross section.

The discontinuity of cross section was introduced at the middle of the bar, i.e. $L_1 = 0.5L$ and the diameter ratio DR was varied. Five different cases of DR = 0.9, 1.0, 1.1, 1.5 and 2.0 were investigated, where $DR = R_2/R_1$ and with $R_1 = 12.5$mm. The case DR = 0.9 corresponded to a beam where the diameter of the second region was smaller than the first region; and DR = 1.0 was the case of the continuous beam without any discontinuity. All other cases were with an increased diameter in the second region.

The bending moment responses of the cases discussed were presented in figure 5.15 for beam stations $\bar{x} = 0.1$ and 0.2 and in figure 5.16 for beam stations $\bar{x} = 0.4$ and 0.6, where the position $\bar{x} = 0.6$ was in the second region i.e. after the position of discontinuity.

It is seen that the bending moment in the second region with an increased diameter are much smaller than the stresses in the first region. The curves of $\Delta\bar{x} = 0.6$ for DR = 0.9, 1.0 and 1.1 were presented in figure 5.17 separately from the curves for DR = 1.5 and 2.0, given in the second graph of figure 5.16, due to the different scales needed.

The values of the bending moment at $\Delta\bar{x} = 0.1$ for all beams with discontinuity showed oscillations starting at about $\bar{t} = 1.4$ and there were alternating signs of oscillations within the range of $\bar{t} = 2$, whereas the curves of $\bar{M} - \bar{t}$ for a finite beam presented in figure 5.9 showed the first oscillation at $\bar{t} = 3.5$. This indicated clearly the effect of reflected waves from the position of discontinuity arriving at position $\Delta\bar{x} = 0.1$ after the time $\bar{t} = 1.4$.

The deviation from the $\bar{M} - \bar{t}$ curve corresponding to the finite beam with DR = 1.0 became larger with increased diameter ratio which also resulted in an increased amplitude.

The bending moment distribution at the position $\bar{x} = 0.6$ after

introducing the discontinuity, presented in figures 5.16 and 5.17, indicated an increased oscillation with decreased diameter ratio with a maximum amplitude for $R_2 = 0.9R$, ten times the maximum amplitude in the bar with $R_2 = 2R_1$. This showed a significant effect on the bending moment time history.

Figures 5.18 and 5.19 showed the effect of the change in diameter ratio for a second set of beams with the discontinuity positioned at $L_1 = 0.3L$, i.e.nearer to the end $x = 0$ where the input ramp platform bending moment was applied.

The response curves were of the same pattern as those for the discontinuity at $L_1 = 0.5L$, except that the oscillations appeared earlier and with larger peak values. The earlier arrival of the reflected waves is easily explained by the shorter distance to be travelled from the new positions of discontinuities.

The effect of the variation in diameter ratio on the peak values of bending waves was demonstrated in figure 5.20 which presented peak values of the bending moment versus diameter ratio for the beam stations $\bar{x} = 0.1$, 0.2, 0.4 and 0.6 of the free-free beam subjected to a ramp platform end moment with a rise time $\bar{t}_o = 0.1$ and with the discontinuity positioned at $L_1 = 0.3L$. This graph was derived from the curves of figures 5.18 and 5.19 and showed that the peak values increased with increased diameter ratio for all beams at beam positions $\bar{x} = 0.1$, 0.2 and 0.4, whereas for the beam station $\bar{x} = 0.6$, the peak values decreased with increased diameter ratios.

5.4.1.2. The effect of change in the discontinuity position

The bending moment distributions are presented in figure 5.21 for length ratios $LR = 0.2$, 0.3 and 0.5, where $LR = L_1/L$ and for a diameter ratio $DR = 1.5$

All curves are for bending waves transmitted through the discontinuity of cross section except for the curve $LR = 0.5$ at beam station $\bar{x} = 0.4$ which was for a reflected wave from the discontinuity.

At position $\bar{x}$ =0.4 the amplitudes of the alternating oscillations increased with increased length ratio and the arrival of the pulse was also directly related to the position of the discontinuity, since a reflected pulse from a position of discontinuity nearer to $\bar{x}$ =0.4 was manifested in larger peak values with alternating signs. However, the same conclusion could not be derived from the curves for the beam position $\bar{x}$ = 0.6 which showed the maximum amplitude for the response curve of the beam with LR = 0.3, whereas the other two curves had their maximum amplitude for LR = 0.2 and 0.5 were showing amplitudes of the same magnitude. This could be caused for example by the superposition of a transmitted wave through the discontinuity and a reflected wave from the end of the beam for LR = 0.3; whereas the case of smaller amplitudes could be due to the arrival of reflected and transmitted waves of compression and tension cancelling each other.

5.4.1.3 The shear force distribution

Figures 5.22 and 5.23 illustrated the shear force distributions for various diameter ratios DR = 1.0, 1.1, 1.5 and 2.0 with the discontinuity at the middle of the beam L_1 = 0.5L. The non-dimensional shear force $\bar{Q}$ is plotted at the positions $\bar{x}$ = 0.1, 0.2, 0.4 and 0.6.

The effect of the ramp-platform bending moment input on the shear force time history is seen to cause much larger oscillations in the shear force than in the bending moment response itself. There was a sharp jump in the value of the shear force at $\bar{t}$ = 0.2 for beam station $\bar{x}$ = 0.1 due to the input bending moment and several oscillations with alternating signs started after $\bar{t}$ = 1.1 due to the arrival of reflected waves from the position of discontinuity and increased with increasing diameter ratio. This showed that the amplitude of the reflected wave increased when the diameter of the second region increased, i.e. the amplitude of the transmitted wave decreased since the total of the reflected and transmitted wave should be related to the incident wave

which is the same for all the different discontinuities due to the input bending moment and the diameter of region 1 having the same values. However, the relation was not easily obtainable due to the dispersion of transient flexural waves.

The effect of reflection and transmission of transient waves was strongly manifested in the shear force distribution curves, since in comparison with bending moment responses, the shear force responses represent a lower derivative of the displacement variable.

5.4.2. Simply supported beam

5.4.2.1. The variation in diameter ratio

Figure 5.24 demonstrated the transient bending moment response $\bar{M}$ due to a ramp-platform bending moment input with a rise time $\bar{t}_o = 0.1$ as in the case of the free-free beams. The discontinuity was positioned at $L_1 = 0.5L$.

The bending moment distribution was presented for beam station $\bar{x} = 0.4$ and 0.6 before and after the discontinuity and the curves were similar to those of figure 5.16.

It is seen that the oscillations and peak values increased with increased diameter ratio for beam station $\bar{x} = 0.4$, whereas for the beam station $\bar{x} = 0.6$ the amplitude of the bending wave increased as the dimension of the cross section in the second region became smaller.

The second graph of figure 5.24 illustrated only the bending moment time histories for the beams with diameter ratios DR = 1.5 and 2.0, whereas the curves for DR = 1.0 and 1.1 reached much higher peak values and were off the scale. This is in agreement with the fact that a greater percentage of the incident wave is reflected with increased diameter in the second region. This is closely connected to the use of beams and tubes with discontinuities of cross section for the purpose of filtering various frequency spectrums.

The peak values of the oscillations in the simply supported beam

were smaller than those of the free-free beam represented in figure 5.16 for the same beam stations.

5.4.2.2. The shear force distribution

The shear force distribution was presented in figure 5.25 for beam stations $\bar{x} = 0.4$ and 0.6 for various diameter ratios DR = 1.1, 1.5 and 2.0.

The large fluctuations in the values of the shear forces $\bar{Q}$ were directly proportional to increased diameter ratio.

The maximum value of the shear force was reached for $\bar{x} = 0.4$ at $\bar{t} = 0.8$ and alternated its value to a similar value of opposite sign at $\bar{t} = 1.15$

At the position $\bar{x} = 0.6$, the peak values of the alternating oscillation were reached at $\bar{t} = 1.15$ and 1.45 and were followed with several smaller oscillations.

Authors	Year	Expressions for k^2 ..	ν	Shear coeff.	
				○	▨
Timoshenko	1921	-	-	0.750	0.667
Timoshenko	1922	-	-	0.952	0.889
Göns	1931	-	-	0.901	0.833
Olsson	1934	rectangle: $20(1+\nu)/(24+15\nu)$	0.3	-	0.912
Pickett	1945	circle: $\frac{24.612(1+\nu)}{29.538+5.942\nu+64.077\ \nu^2}$	0.33	0.850	0.833
Davidson et. al	1946	-	-	0.80	-
Sutherland et. al.	1951	rectangle: $16[1-(1-2\nu)k^2/2(1-\nu)]\cdot(1-k^2)=(2-k^2)^4$	0.33	-	0.870
Mindlin et. al.	1954	-	0.33	0.847	0.823
Gaines et. al.	1966	-	0.30	0.90	0.833
Cowper	1966	circle: $6(1+\nu)/(7+6\nu)$ rectangle: $10(1+\nu)/(12+11\nu)$	0.29	0.8856	0.849
Spence et. al.	1970	-	0.33	0.850	0.873
Carnegie et. al.	1972	-	-	-	0.834
Ritchie	1973	-	0.304	-	0.833
Kaneko	1975	circle: $6(1+\nu)^2/(7+12\nu+4\nu)^2$ rectangle: $5(1+\nu)/(6+5\nu)$	0.29	0.923	0.866
Rosinger et. al.	1977	circle: $6(1+\nu)^2/(7+12\nu+4\nu)^2$ rectangle: $5(1+\nu)/(6+5\nu)$	0.292	0.924	0.866
Stephen	1980	circle: $6(1+\nu)^2/(7+12\nu+4\nu^2)$ rectangle: $\frac{5(1+\nu)^2}{6+11\nu+\nu^2(5-m^4+\frac{90m^5S}{\pi^5})}$			

TABLE I: Comparison of shear coefficient values

Problem & Author / Parameter	Semi-infinite free-free		Cantilever beam	Simply supported	Finite beam &
	Kuo (1961)	Ripperger (1955)	Koenig (1968)	Goland et.al (1955)	various end cond.
Density ρ	0.8×10^{4} kg/m^3	0.283 lb/in^3	0.3 lb/in^3	7.187×10^{-4} lbs^2/in^4	0.8×10^{4} kg/m^3
Modulus of Elast. E	209×10^{9} N/m^2	30×10^{6} psi	30×10^{6} psi	30×10^{6} psi	209×10^{9} N/m^2
Poisson's ratio ν	0.3	0.29	0.3	0.29	0.3
Modulus of Rigid. G	80.38×10^{9} N/m^2	11.628×10^{6} psi	11.538×10^{6} psi	11.628×10^{6} psi	80.38×10^{9} N/m^2
Shear corr. coeff. k^2	0.78	0.886	0.833	0.8687	0.886
Longt. wave vel. c_1	5111 m/s	202.35×10^{3} in/s	196.57×10^{3} in/s	200×10^{3} in/s	5111 m/s
Shear wave vel. c_2	2790 m/s	118.553×10^{3} in/s	111.26×10^{3} in/s	112.92×10^{3} in/s	2983.5 m/s
Beam length ℓ	0.625m	36.12 in.	1.5 in.	96 in.	0.625m
Beam dia. d	25mm	0.516 in.	-	-	25mm
Beam height h	-	-	1.0 in.	1.0 in.	-
Beam depth b	-	-	1.0 in.	1.0 in.	-
Cross-sect. Area A	490.87 mm^2	0.209117 in^2	1.0 in^2	1.0 in.^{2}	490.87 mm^2
Cross-sect. Moment of area I	19.1748×10^{-9} m^4	0.384×10^{-2} in.^{4}	0.08333 in.^{4}	0.08333 in.^{4}	19.1747×10^{-9} m^4
E I	4007.525Nm^2	104.3975×10^{3} lb in^2	2.5×10^{6} lb in^2	2.5×10^{6} lb in^2	4007.525 nm^2
k^2AG	30.776×10^{6} N	2.1537×10^{6} lb.	9.6112×10^{6} lb	9.5636×10^{6} lb	34.958×10^{6} N
Rise time of inp. moment tr	12.228 µs	-	5.174 µs	-	12.228 µs
Slenderness ratio L/r	100	280	6	384	100
k^2AG/EI	7680m^{-2}	20.6268 in^{-2}	3.8445 in^{-2}	3.825 in^{-2}	8723m^{-2}
Mesh size Δx	0.0025m	0.0516 in	0.003125 in	0.025 in.	0.0025 m
Duration of $\frac{1}{2}$ sine inp.	-	14.28 µs	-	14 µs	-

TABLE II: Material properties and parameters of various examples for the Timoshenko beams

End cond.		Type of load*	Generalised fct.	i	Coefficients of equations 4.4**						
					1	2	3	4	5	6	7
Free end x=0,L	I	$\dot{M}(x,t) = M_o$	$b_1(t) = M_o/EI$	A_i, D_i	-1	0	0	0	0	0	0
		$\dot{Q}(x,t) = 0$	$b_3(t) = Q/k^2AG=0$	C_i, P_i	0	-1	0	0	+1	0	0
	II	$M(x,t) = 0$	$b_1(t) = M_o/EI=0$	A_i, D_i	-1	0	0	0	0	0	0
		$Q(x,t) = Q_o$	$b_3(t) = Q/k^2AG$	C_i, P_i	0	-1	0	0	+1	0	0
	III	$\omega(x,t) = \omega_o$	$b_1(t) = \frac{\partial\psi}{\partial t} = \omega_o$	A_i, D_i	0	0	0	0	0	0	+1
		$Q(x,t) = 0$	$b_3(t) = Q/k^2AG$	C_i, P_i	0	-1	0	0	+1	0	0
	IV	$M(x,t) = 00$	$b_1(t) = M_o/EI$	A_i, D_i	-1	0	0	0	0	0	0
		$v(x,t) = v_o$	$b_3(t) = \frac{\partial y}{\partial t} = v_o$	C_i, P_i	0	0	0	0	0	0	+1
Simply Supported end x=0,L	V	$M(x,t) = M_o$	$b_1(t) = M_o/EI$	A_i, D_i	-1	0	0	0	0	0	0
		$v(x,t) = 0$	$b_3(t) = \frac{\partial y}{\partial t} = v_o$	C_i, P_i	0	0	0	0	0	0	+1
	VI	$M(x,t) = 0$	$b_1(t) = M_o/EI$	A_i, D_i	-1	0	0	0	0	0	0
		$Q(x,t) = Q_o$	$b_3(t) = Q_o/k^2AG$	C_i, P_i	0	-1	0	0	+1	0	0
	VII	$\omega(x,t) = \omega_o$	$b_1(t) = \partial\psi/\partial t$	A_i, D_i	0	0	0	0	0	0	+1
		$V(x,t) = 0$	$b_3(t) = \partial y/\partial t=0$	C_i, P_i	0	0	0	0	0	0	+1
	VIII	$M(x,t) = 0$	$b_1(t) = M_o/EI$	A_i, D_i	-1	0	0	0	0	0	0
		$v(x,t) = v_o$	$b_3(t) = \partial y/\partial t=v_o$	C_i, P_i	0	0	0	0	0	0	+1
Built-in x=0,L	IX	$M(0,t) = M_o$	$b_1(t) = M_o/EI$	A_i	-1	0	0	0	0	0	0
		$Q(0,t) = 0$	$b_3(t) = Q/k^2AG=0$	C_i	0	-1	0	0	+1	0	0
		$\omega(L,t) = 0$	$b_1(t) = \partial\psi/\partial t$	D_i	0	0	0	0	0	0	+1
		$v(L,t) = 0$	$b_3(t) = \partial y/\partial t$	P_i	0	0	0	0	0	0	+1

* The loading can take any specified form such as step, ramp platform, sinosoidal or exponential.

** For the Timoshenko equations the coefficients $B_4 = E_4 = 1$ and all other B_i and E_i are zero.

TABLE III Specified boundary conditions and the corresponding coefficients.

Input functions	Time interval	Illustration
Step input $b_i(t) = Y_o = \text{const.}$ Y_o is one of M,Q,ω,V	$t \geq 0$	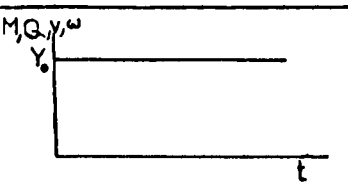
Ramp platform $b_i(t) = Y_o t / t_o$ $b_i(t) = Y_o$	$0 \leq t \leq t_o$ $t > t_o$	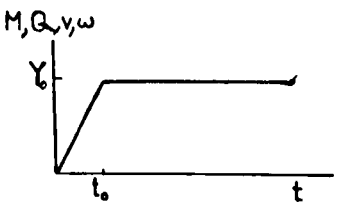
Sinosoidal input $b_i(t) = Y_o \sin \frac{2\pi t}{t_o}$	$t \geq 0$	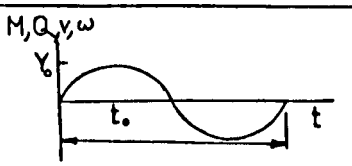
Half sine input super position of two cont. sine fct. differing by $\frac{t_o}{2}$	$0 \leq t \leq \frac{t_o}{2}$	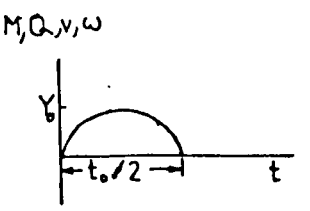
Trapezoidal input The difference of two ramp platform fct. diff. by pulse duration t_d	$0 \leq t \leq t_d$	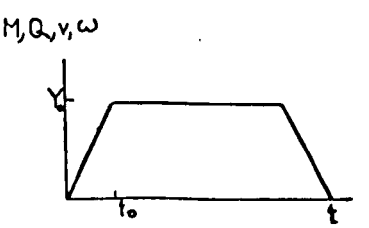
* The initial conditions for M,Q,ω,V are zero		

TABLE IV: Time variation of the input functions

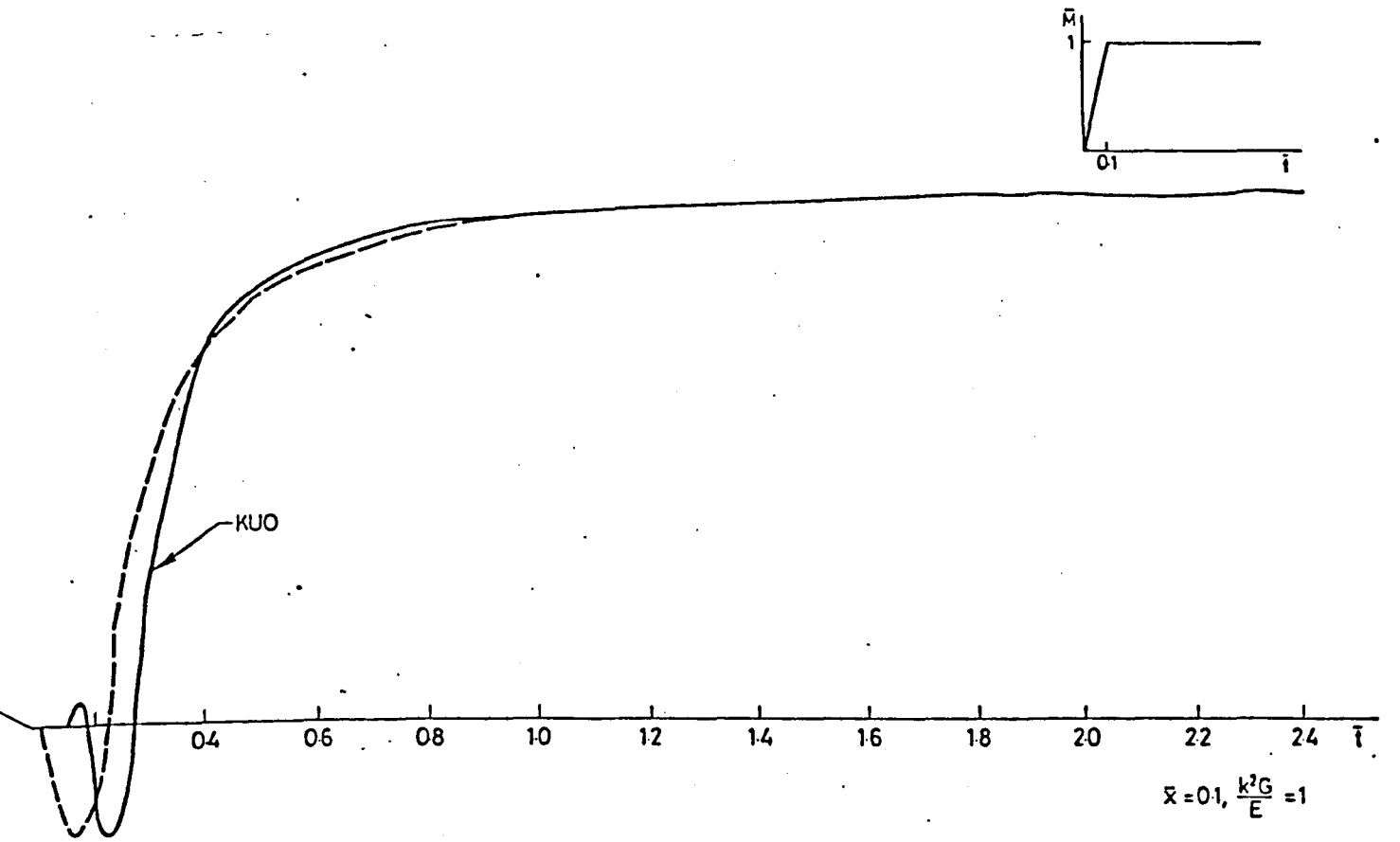

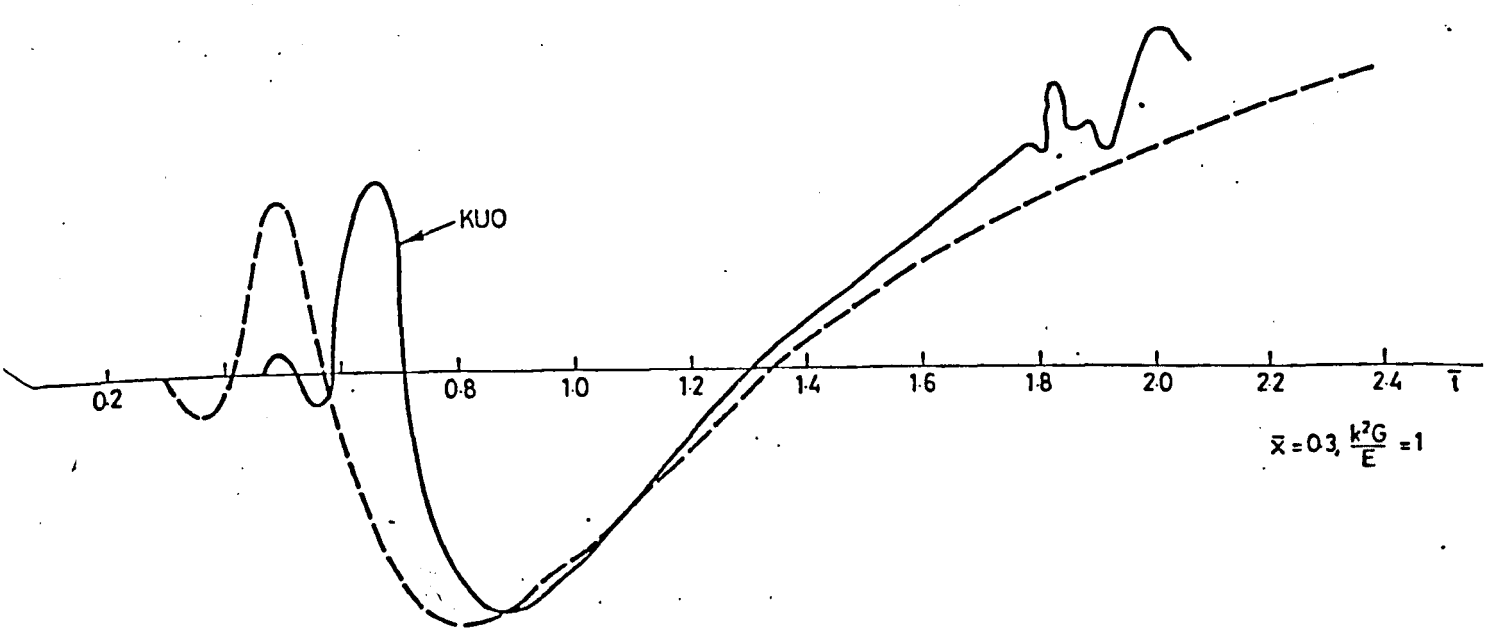

FIG. 5.1 DIMENSIONLESS M-t CURVES
Free-Free semi-infinite beam
subjected to end moment

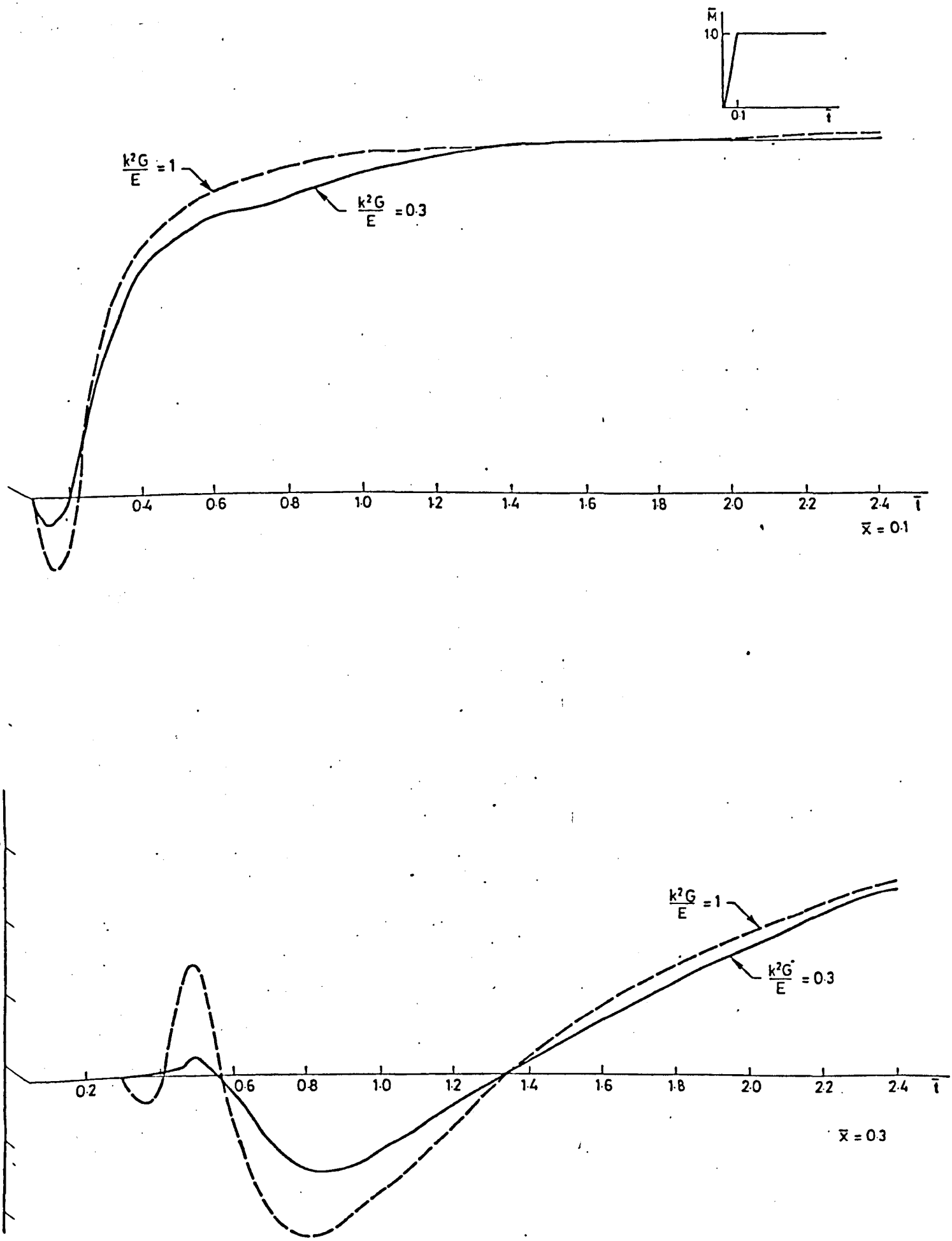

FIG. 5.2. EFFECT OF CHANGE OF $\frac{k^2G}{E}$

Free-Free semi-infinite beam subjected to end moment

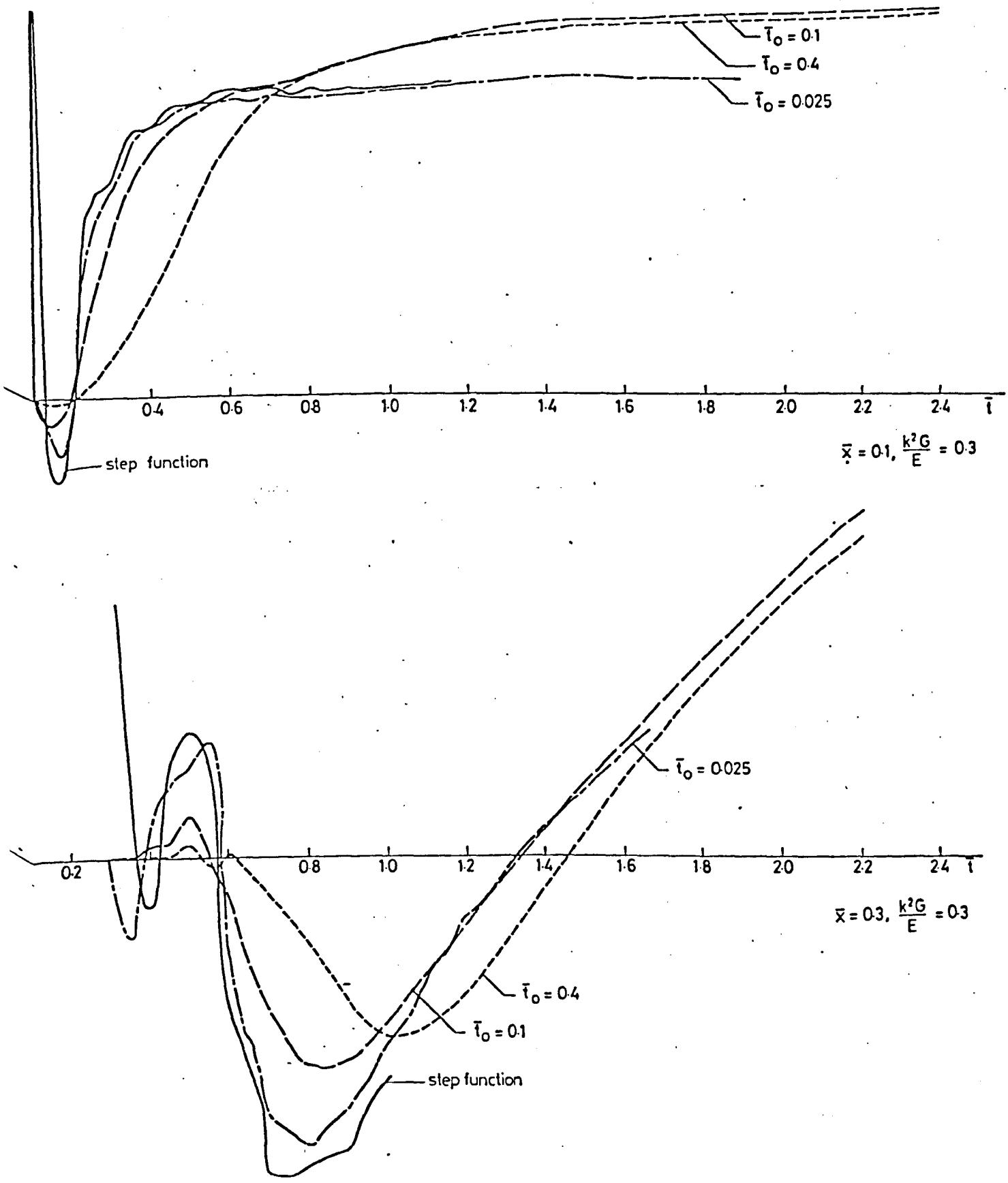

FIG. 5.3 EFFECT OF RISE TIME $\bar{T}_o$

Free-Free semi-infinite beam subjected to end moment

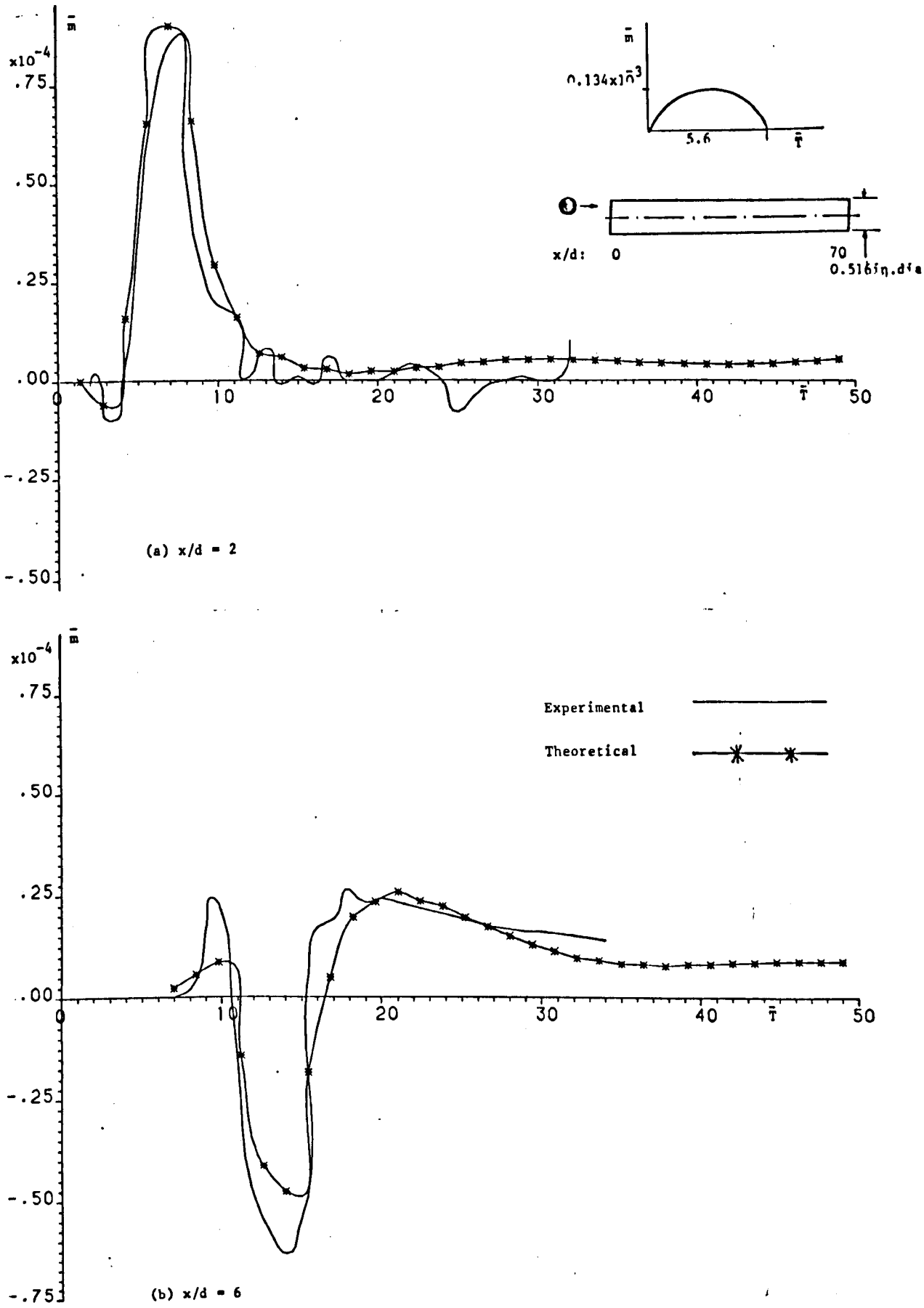

FIG. 5.4 MEASURED AND CALCULATED HISTORIES OF THE BENDING MOMENT FOR A 36.12 INCH LONG FREE-FREE CYLINDRICAL BEAM SUBJECTED TO ECCENTRIC IMPACT

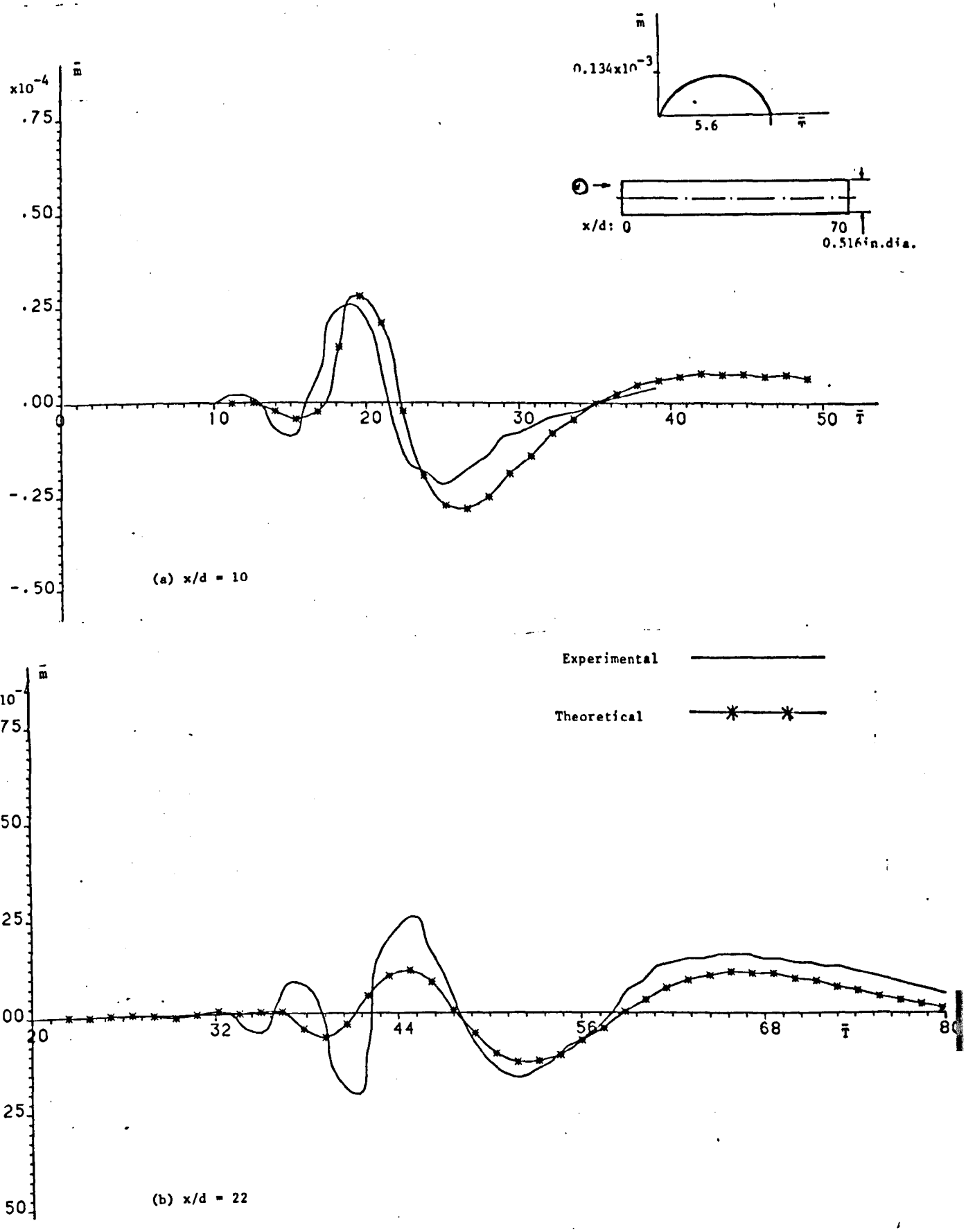

FIG. 5.5 MEASURED AND CALCULATED HISTORIES OF THE BENDING MOMENT FOR A 36.12 in. LONG FREE-FREE CYLINDRICAL BEAM SUBJECTED TO ECCENTRIC IMPACT

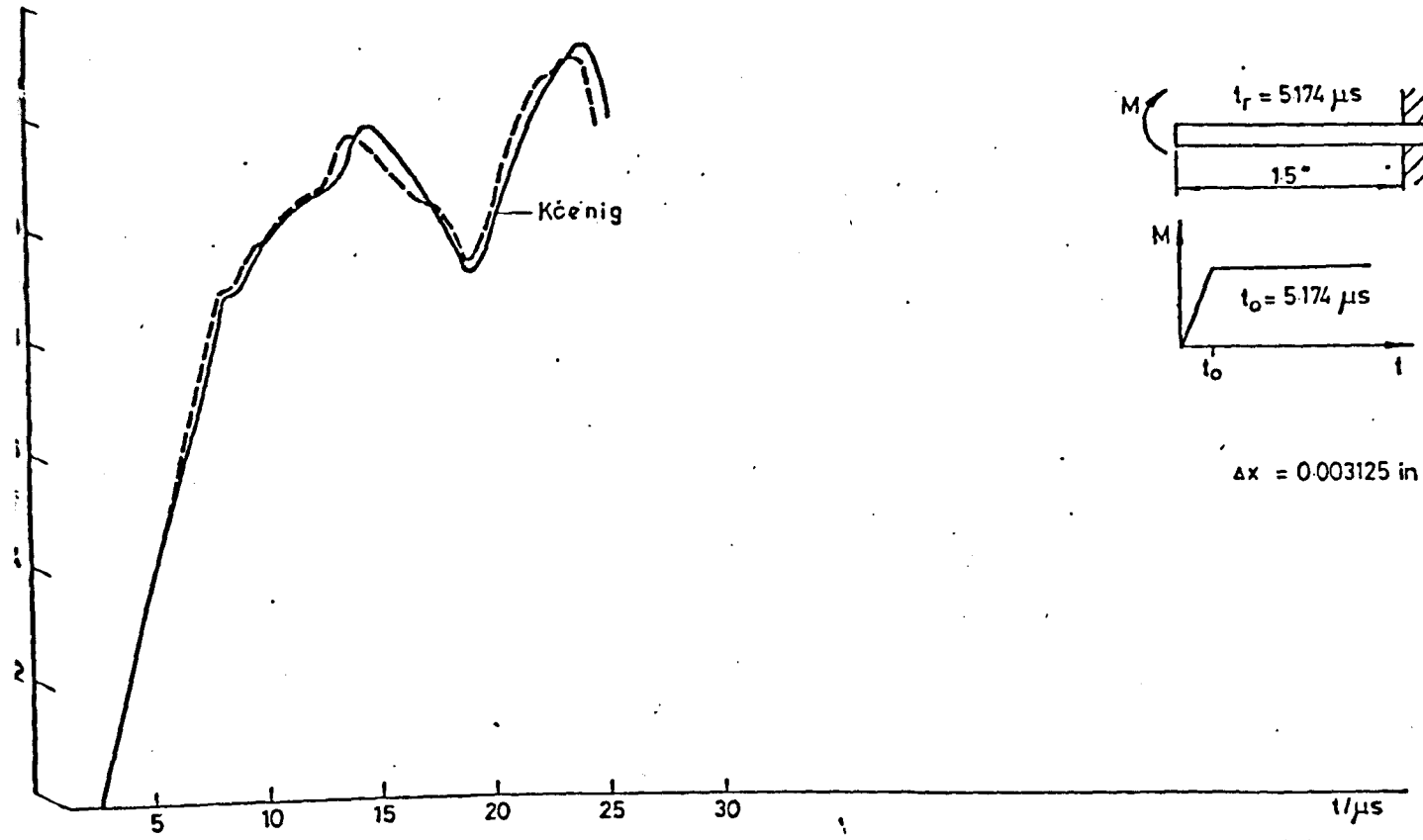

FIG. 5.6 M VS. t'

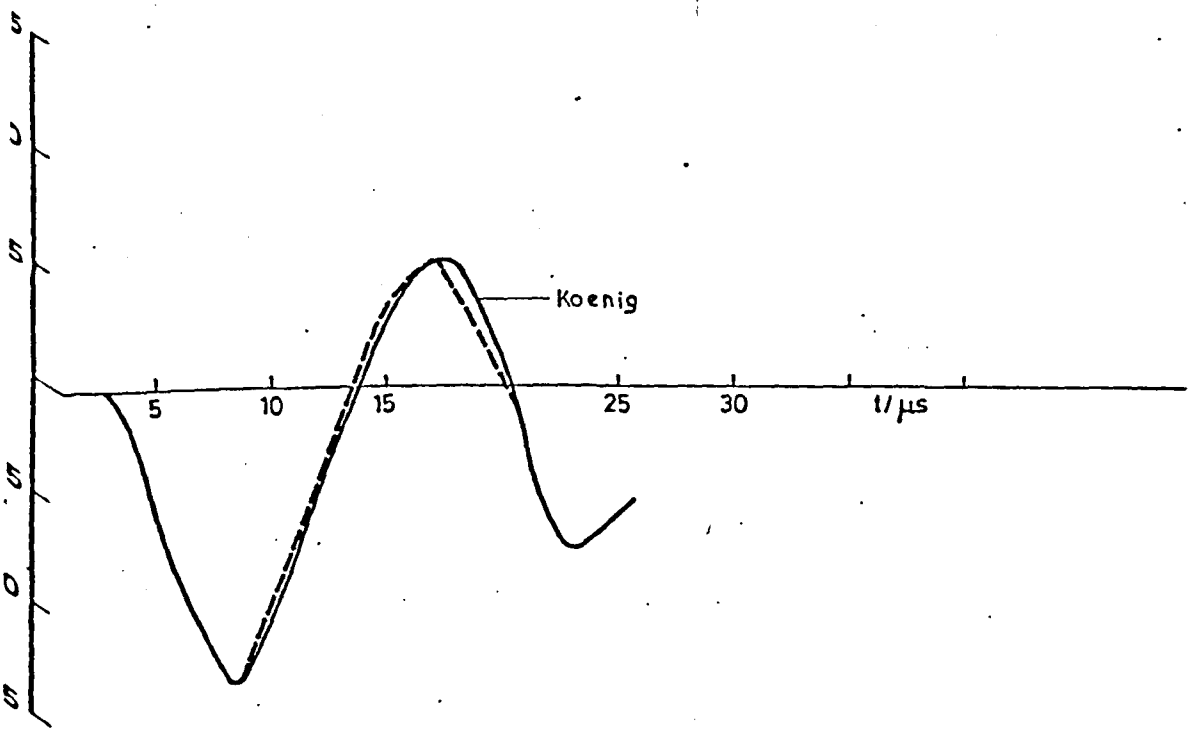

FIG. 5.7 Q VS. t
CANTILEVER BEAM

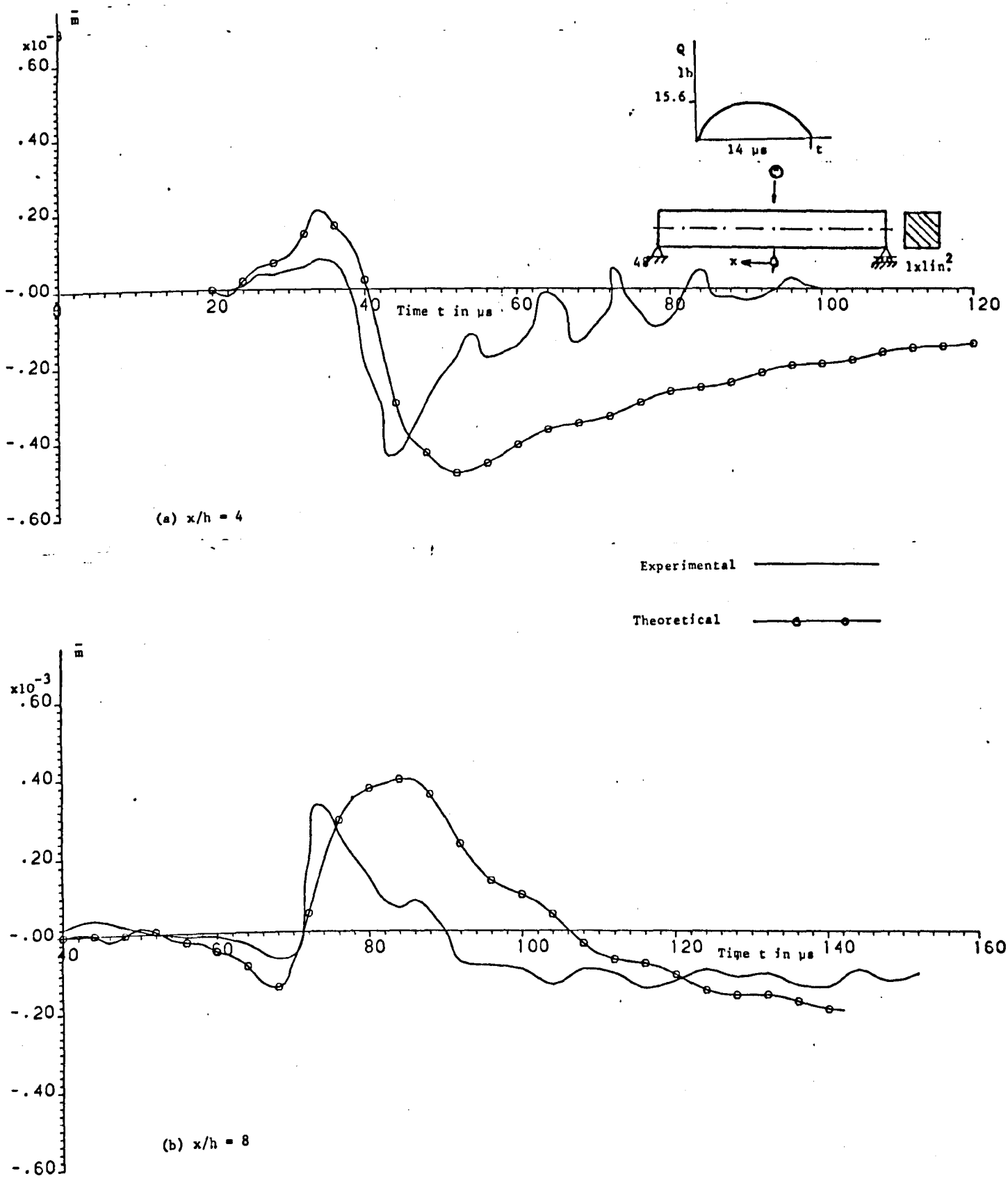

FIG. 5.8 MEASURED AND CALCULATED HISTORIES OF THE BENDING MOMENT FOR THE 96 in. LONG SIMPLY SUPPORTED BEAM SUBJECTED TO TRANSVERSE IMPACT BY A 5/32 in. DIAMETER STEEL BALL DROPPED FROM 2.0 INCH HEIGHT

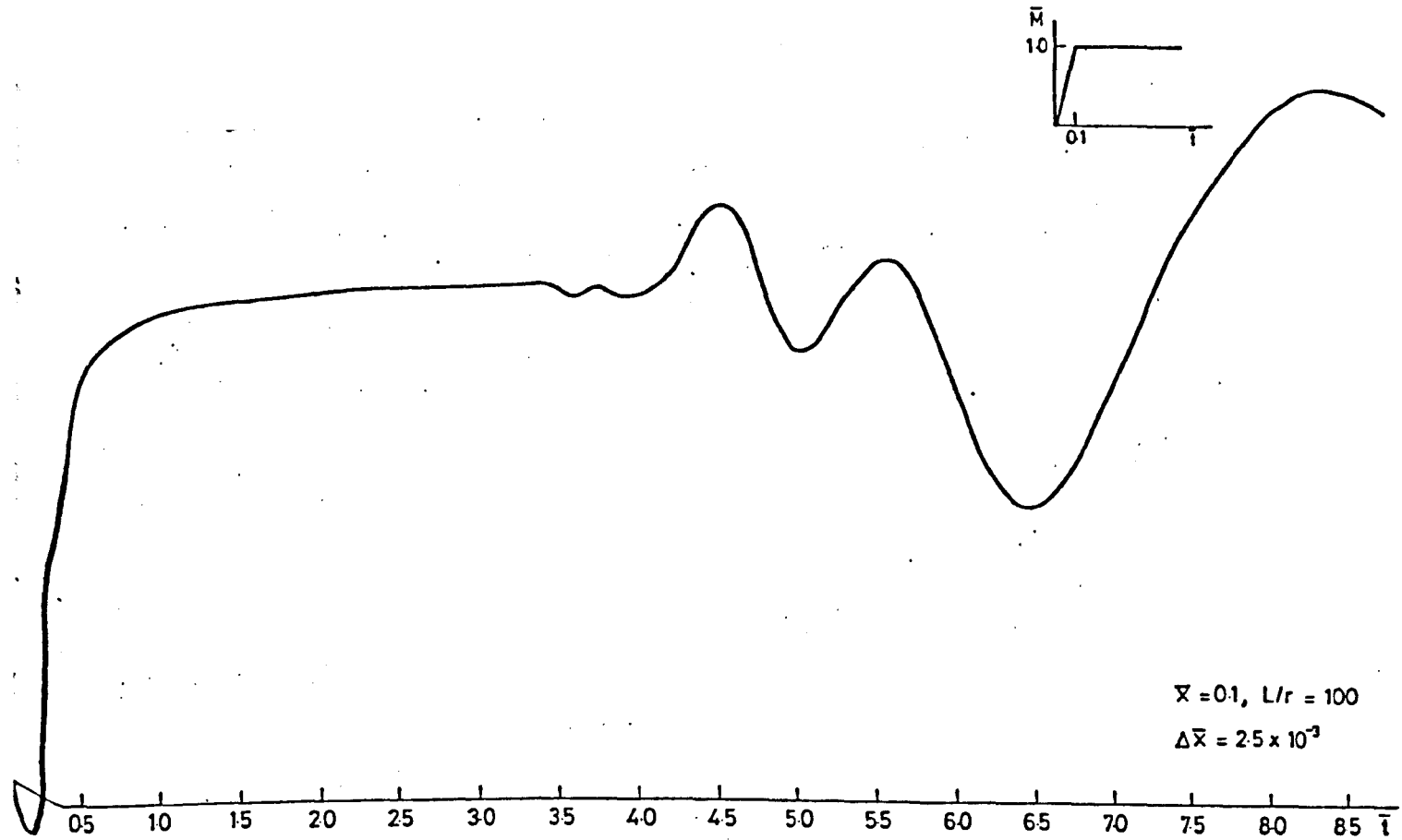

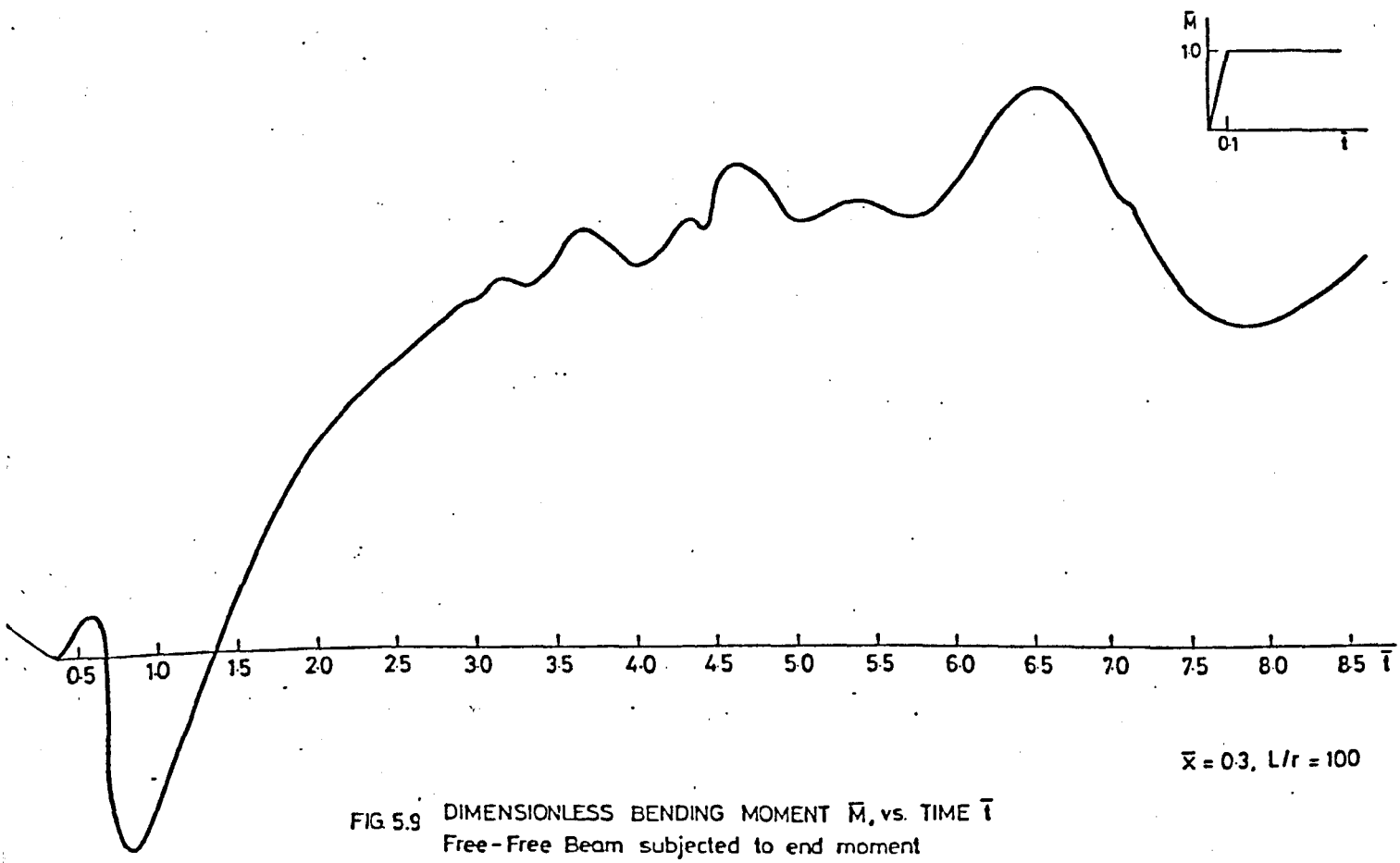

FIG. 5.9 DIMENSIONLESS BENDING MOMENT $\bar{M}$, vs. TIME $\bar{t}$
Free-Free Beam subjected to end moment

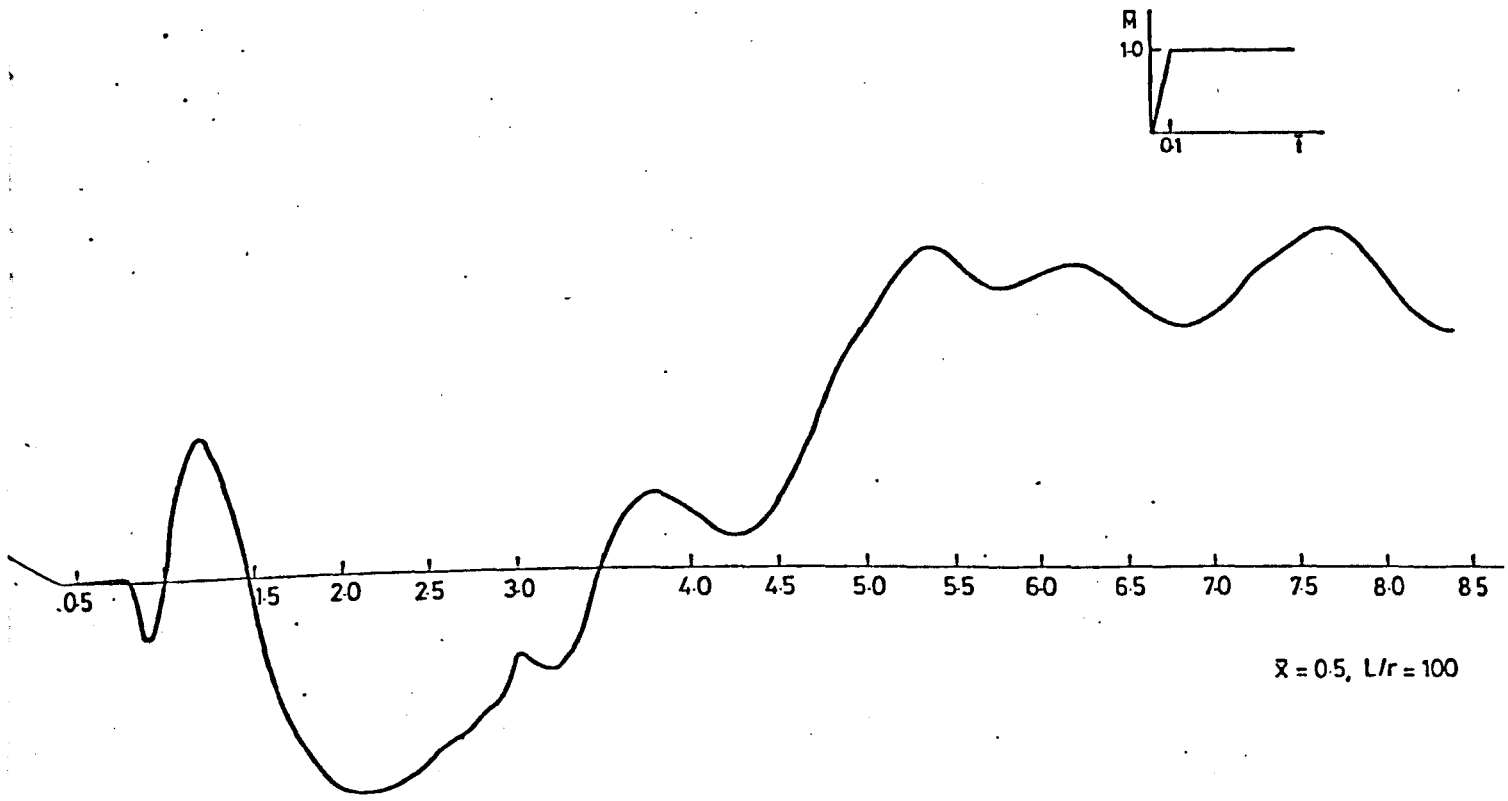

FIG. 5.10. DIMENSIONLESS BENDING MOMENT $\bar{M}$, vs. TIME $\bar{t}$
Free-Free Beam

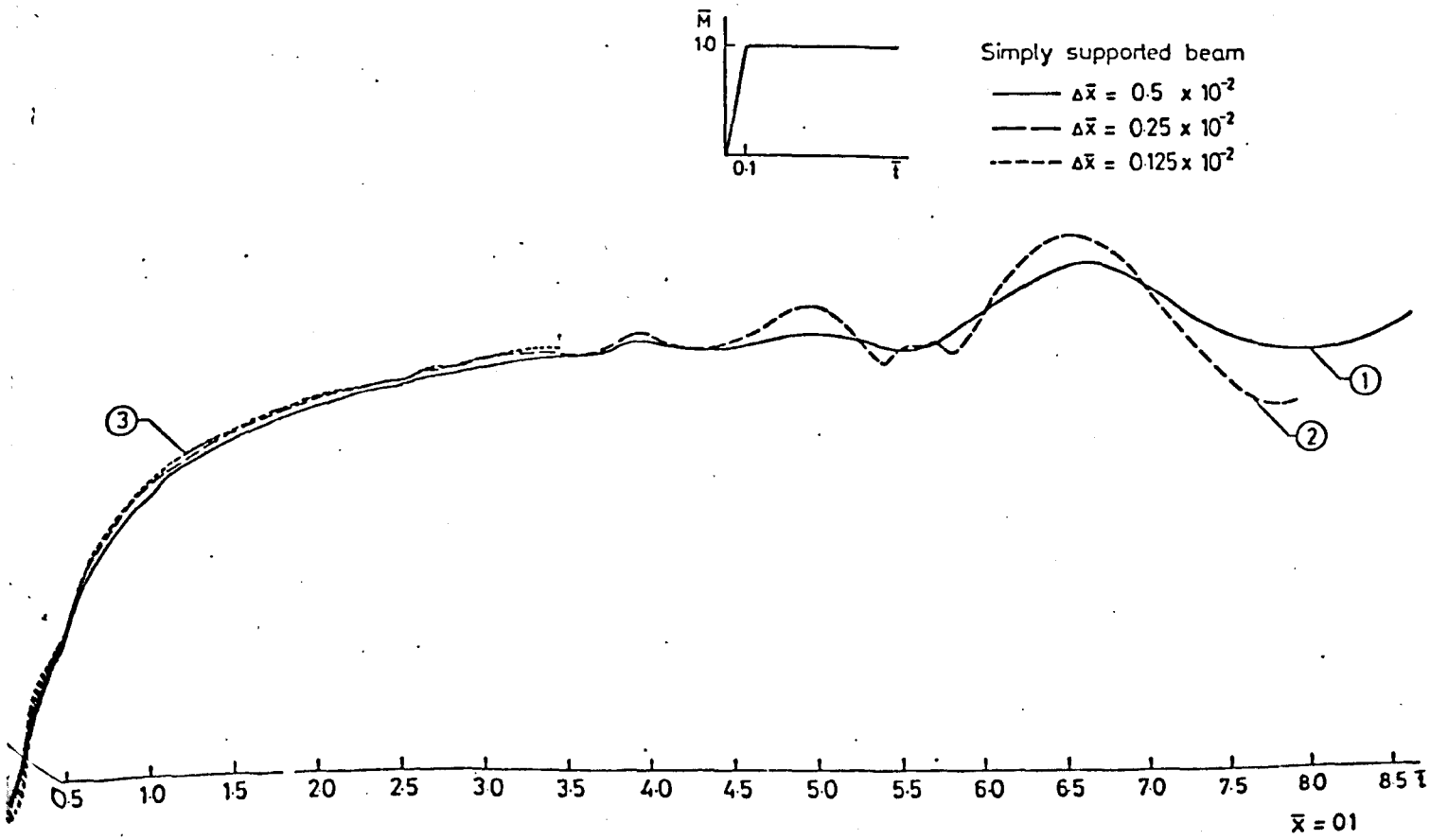

FIG. 5.11. EFFECT OF MESH SIZE $\Delta\bar{x}$
Simply supported beam

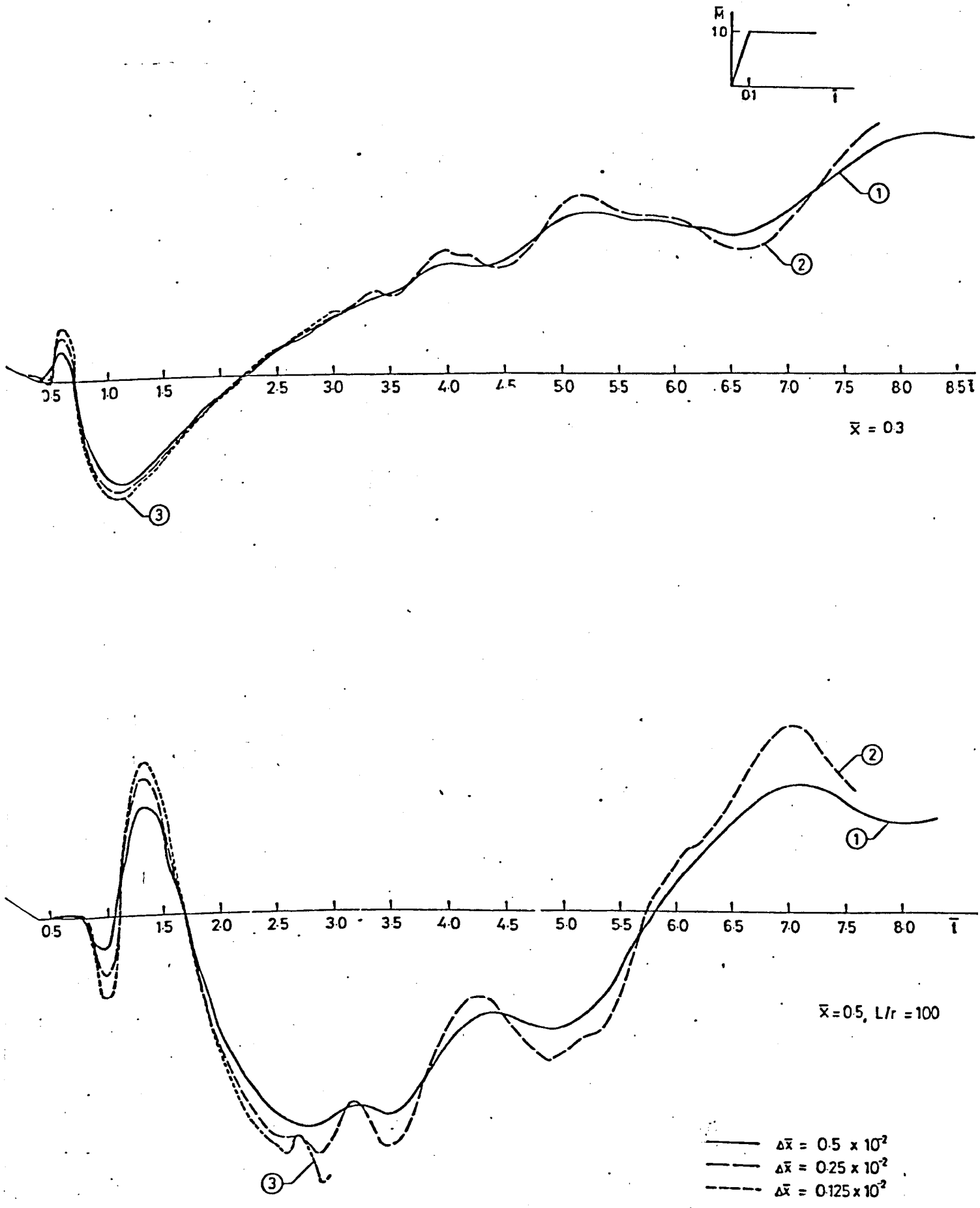

FIG. 5.12. EFFECT OF MESH SIZE $\Delta\bar{x}$
Simply supported beam

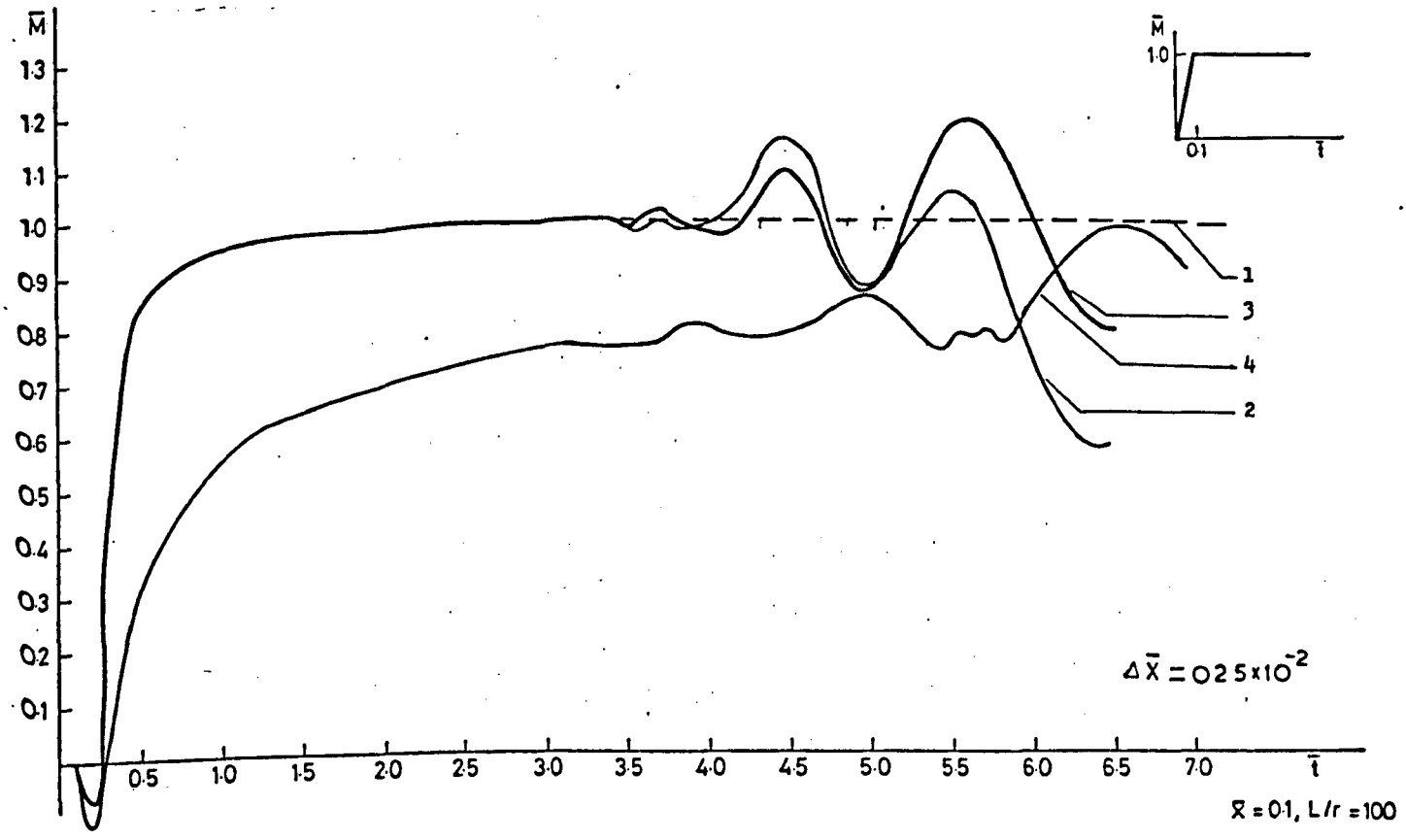

1 Semi-infinite free 2 Free-free
3 Free-fixed 4 Simply-supported

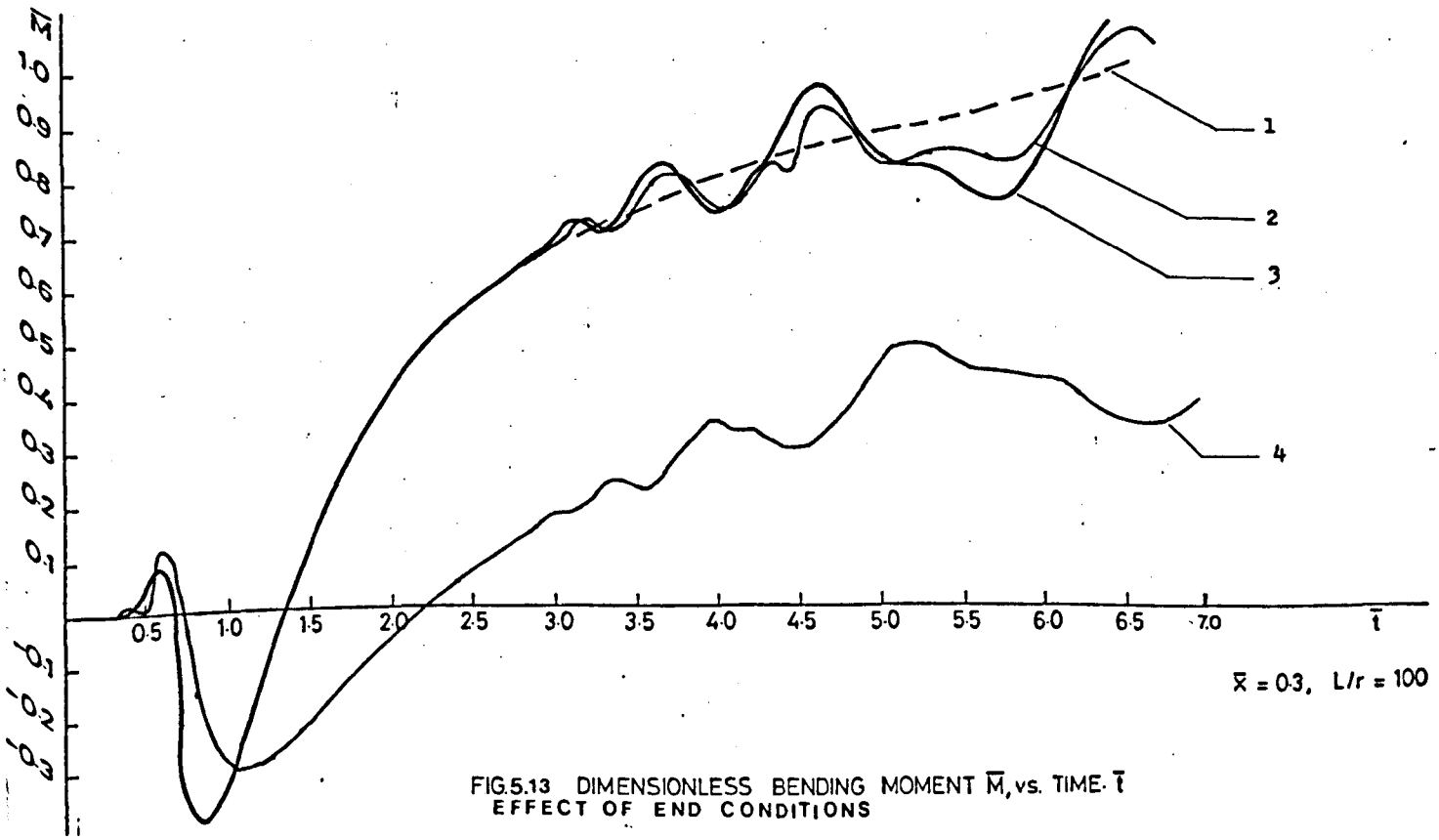

FIG.5.13 DIMENSIONLESS BENDING MOMENT $\bar{M}$, vs. TIME $\bar{t}$
EFFECT OF END CONDITIONS

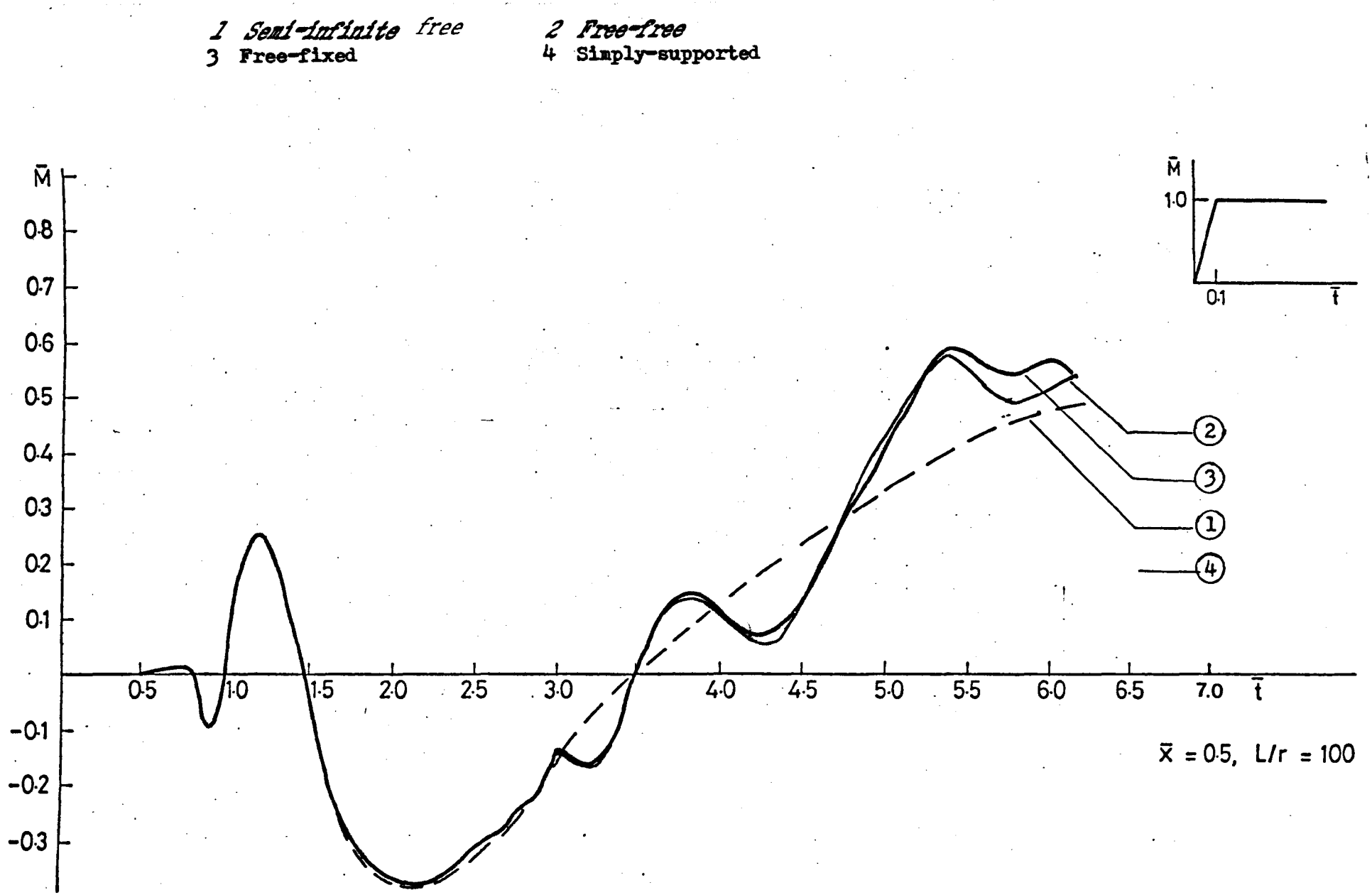

FIG.5.14 DIMENSIONLESS BENDING MOMENT $\bar{M}$, vs. TIME $\bar{t}$

EFFECT OF END CONDITIONS

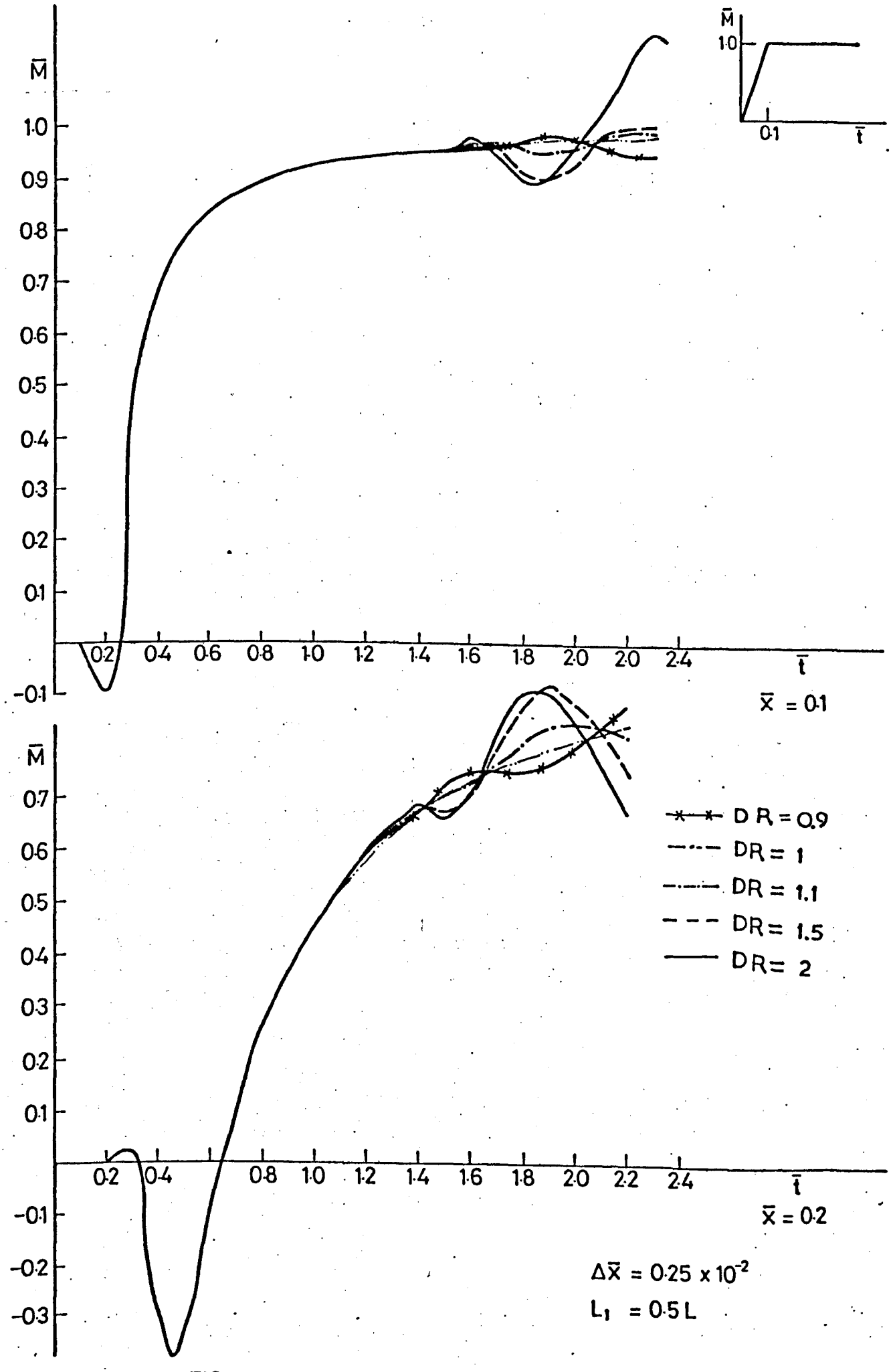

FIG. 5.15 EFFECT OF DIAMETER RATIO DR

Free - Free beam

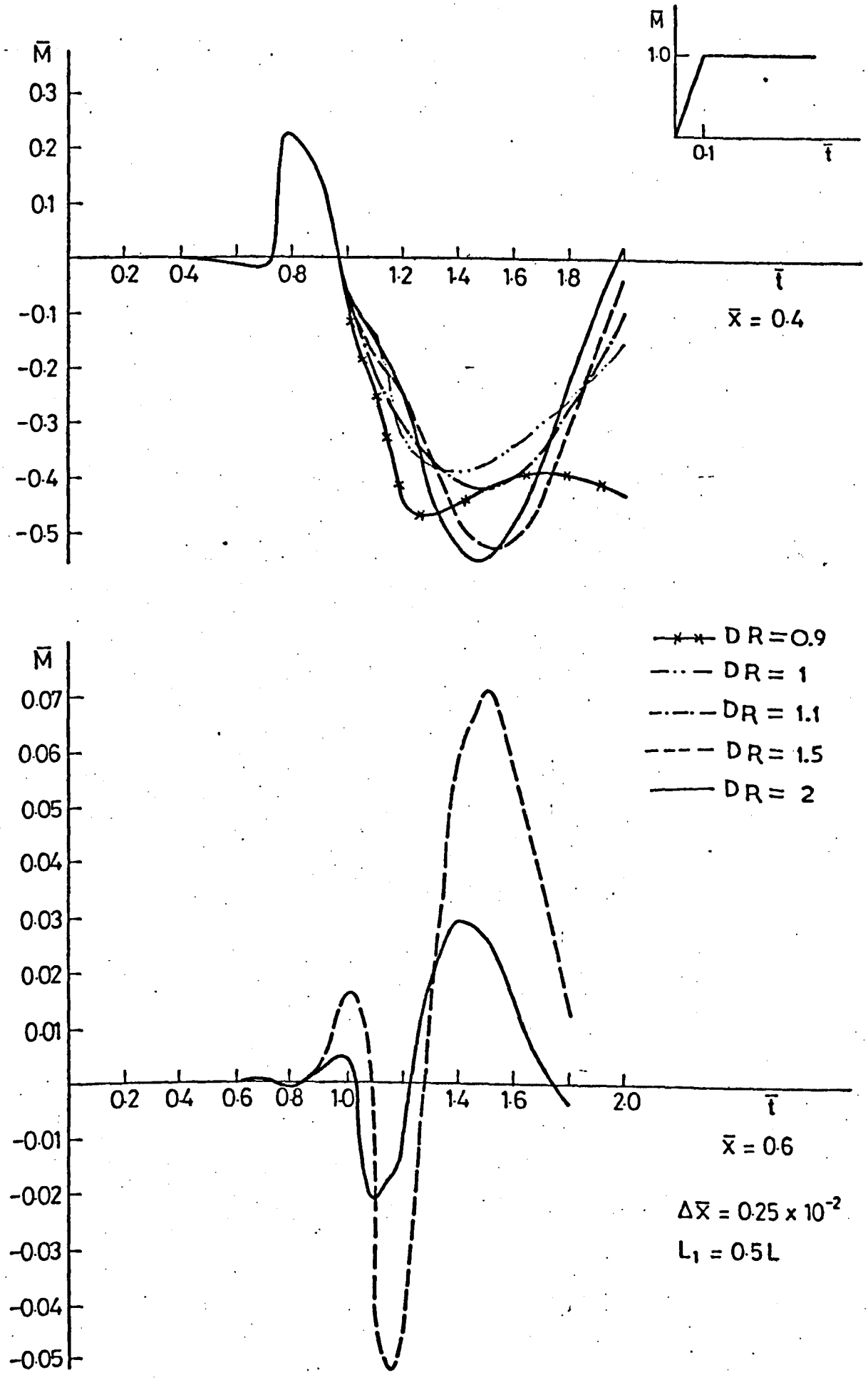

FIG. 5.16 EFFECT OF DIAMETER RATIO DR

Free - Free Beam

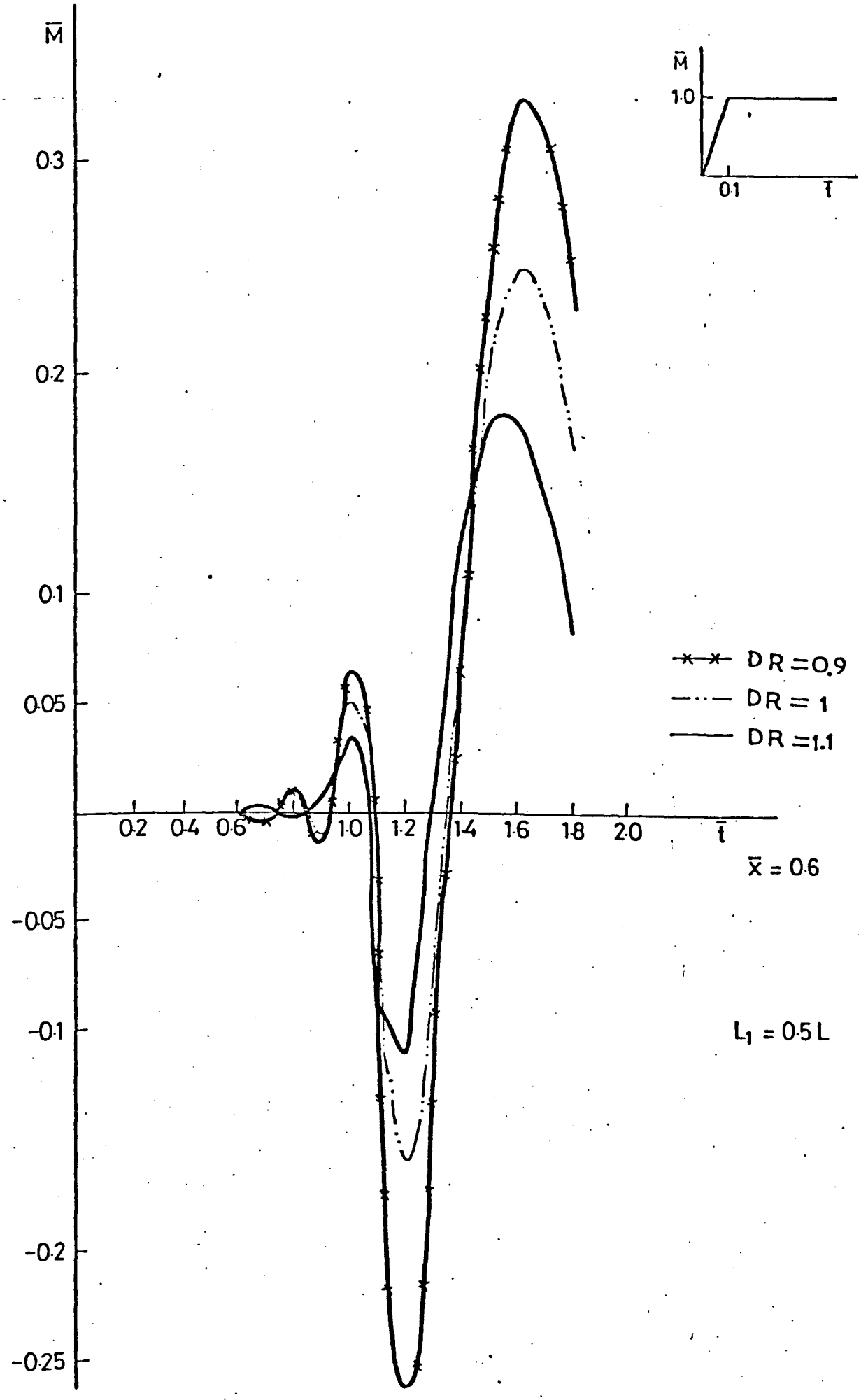

FIG.5.17 EFFECT OF DIAMETER RATIO DR AT $\bar{x} = 0.6$

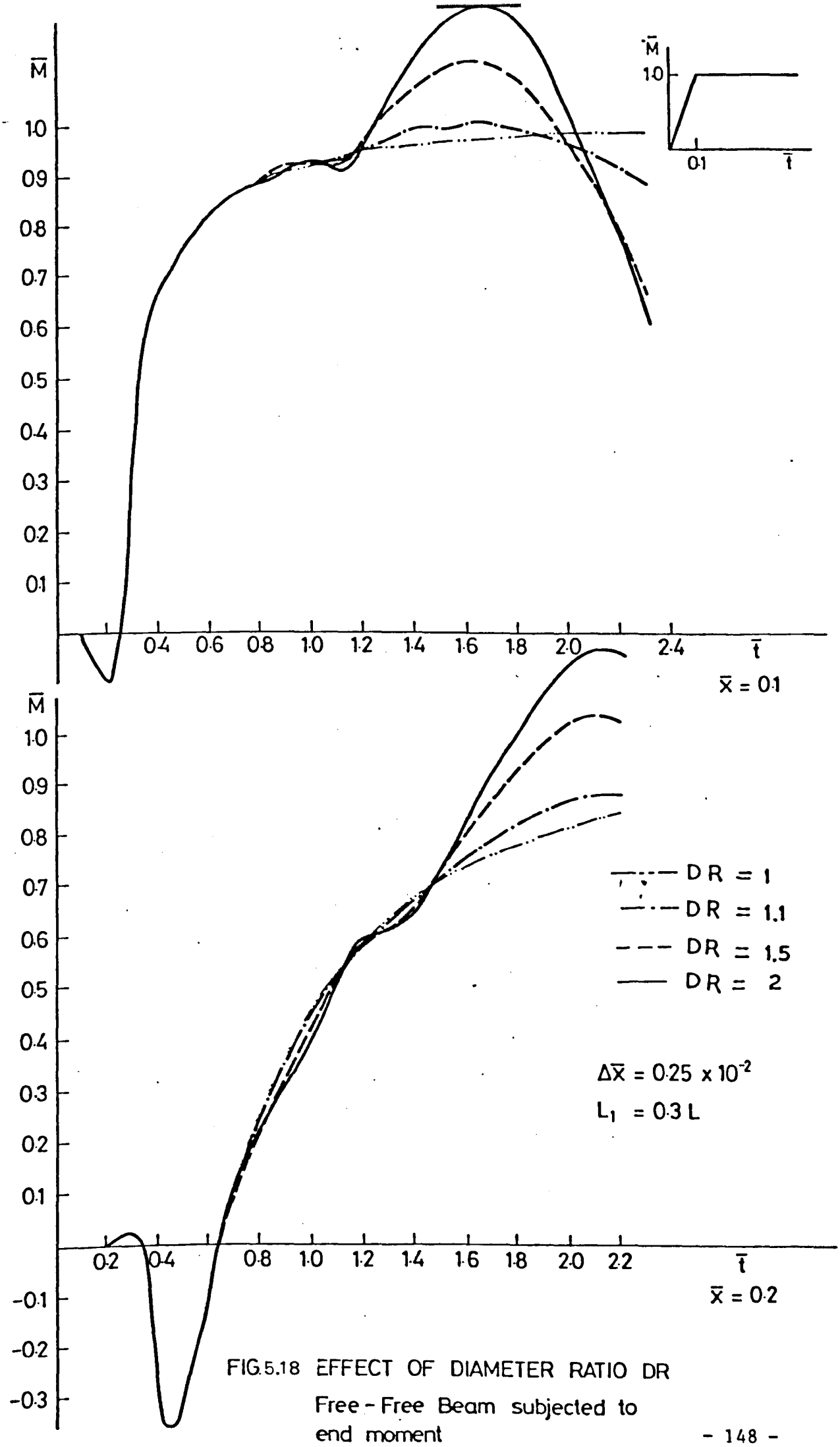

FIG.5.18 EFFECT OF DIAMETER RATIO DR

Free - Free Beam subjected to end moment

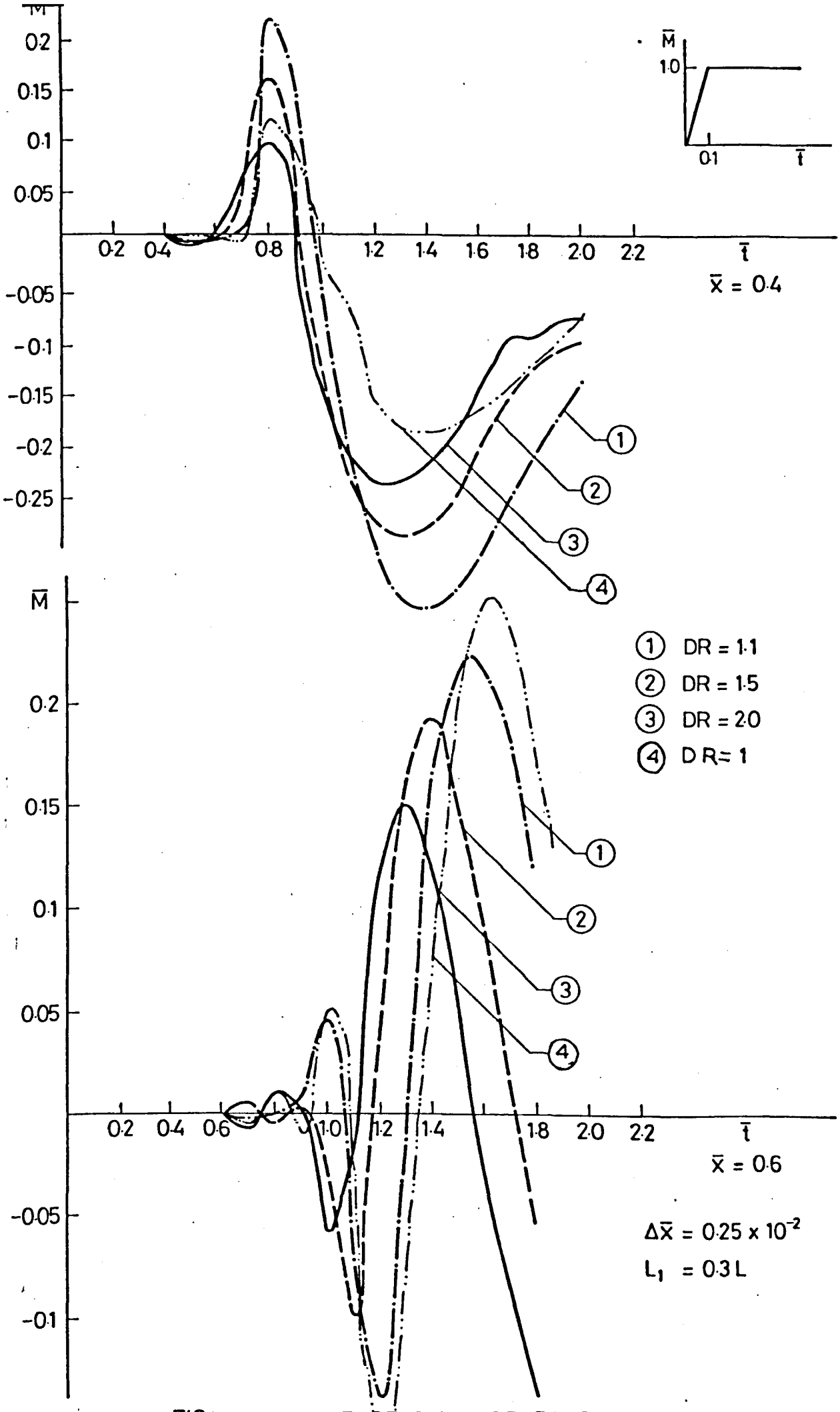

FIG.5.19 EFFECT OF DIAMETER RATIO DR

Free - Free beam

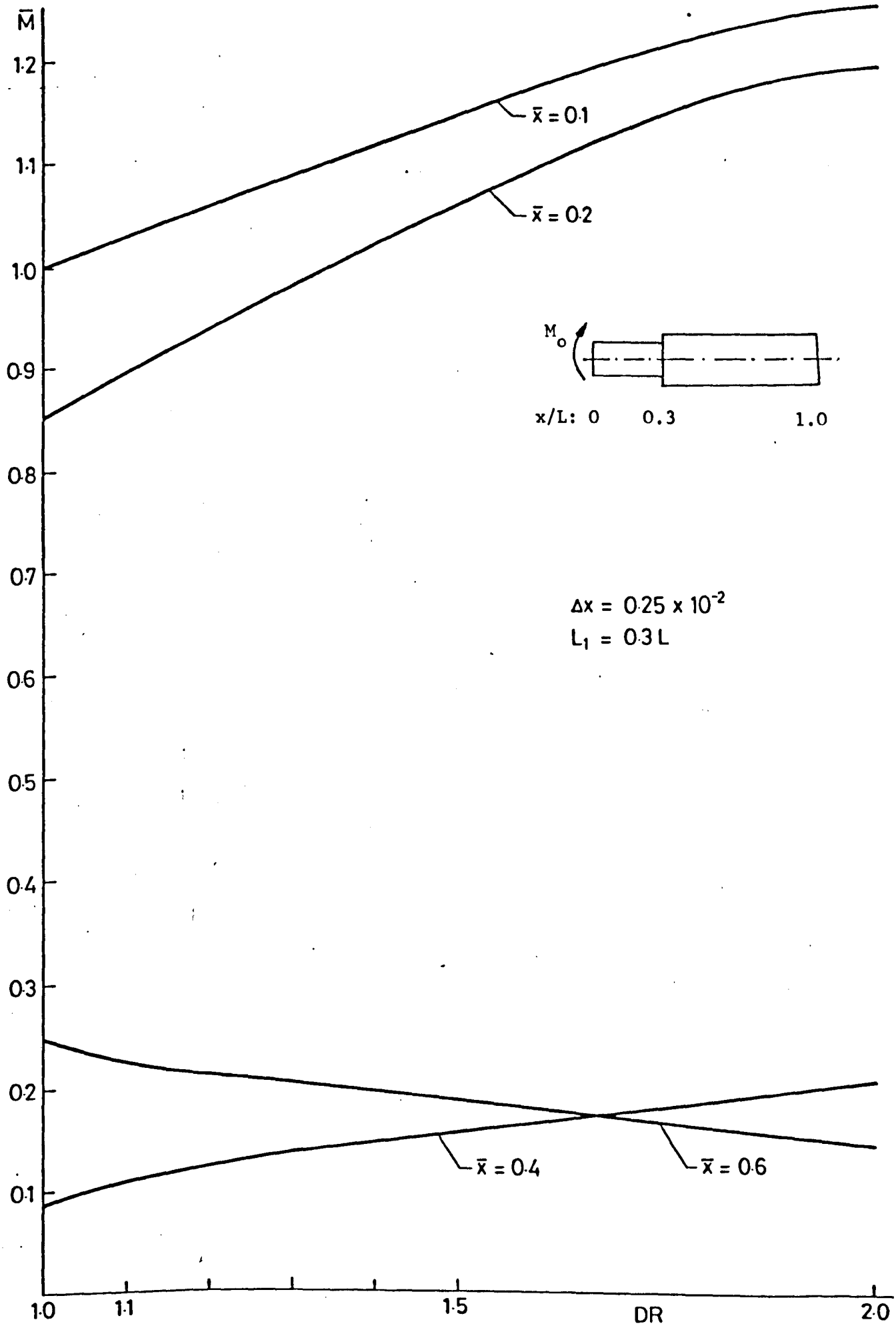

FIG.5.20 PEAK VALUES OF $\bar{M}$, vs. DIAMETER RATIO
Free-free finite beam with discontinuity

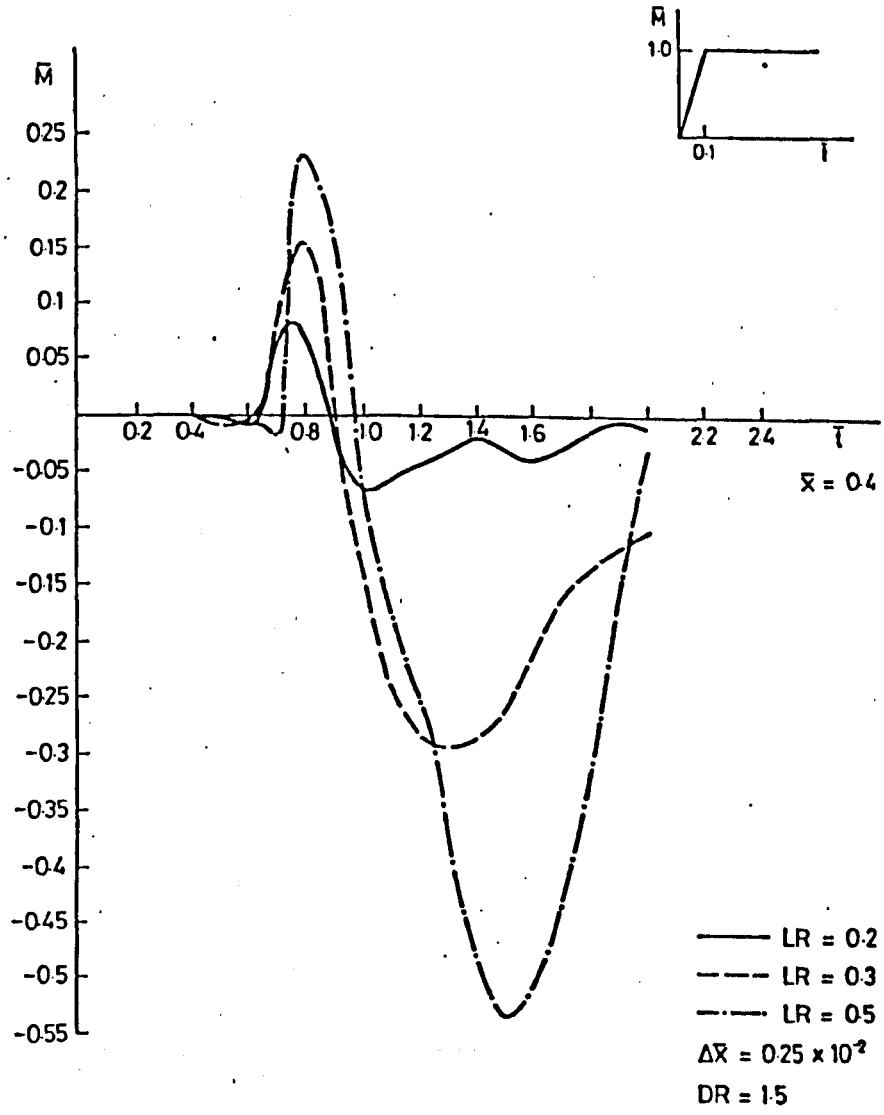

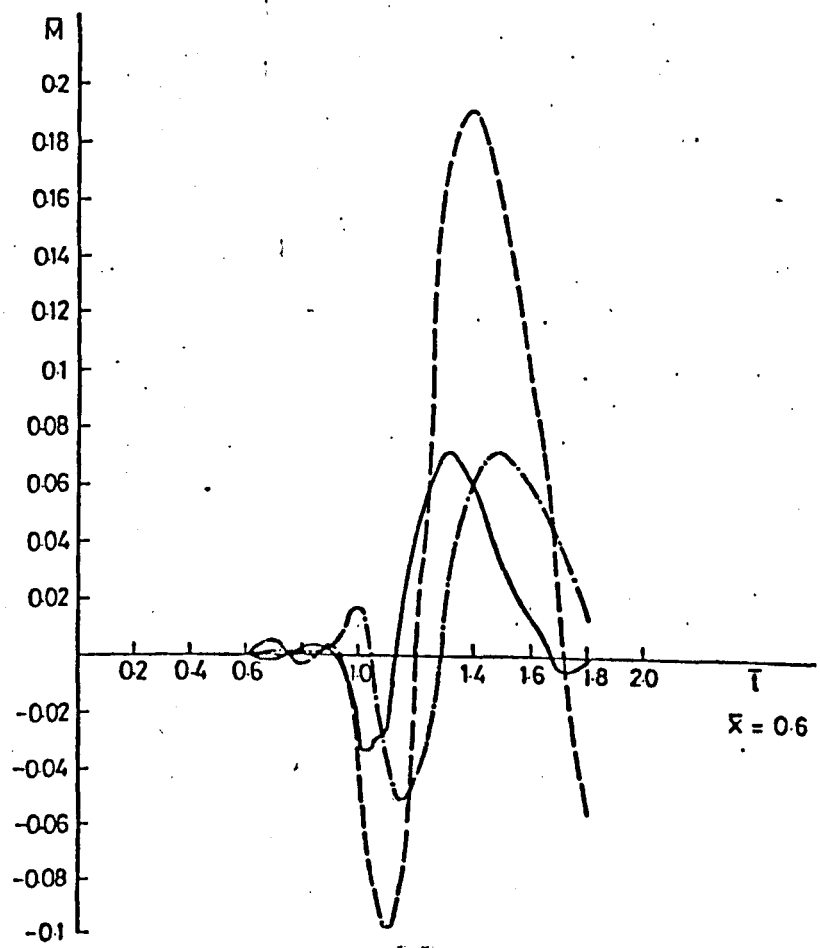

FIG. 5.2.1 EFFECT OF LENGTH RATIO LR

Free - Free Beam

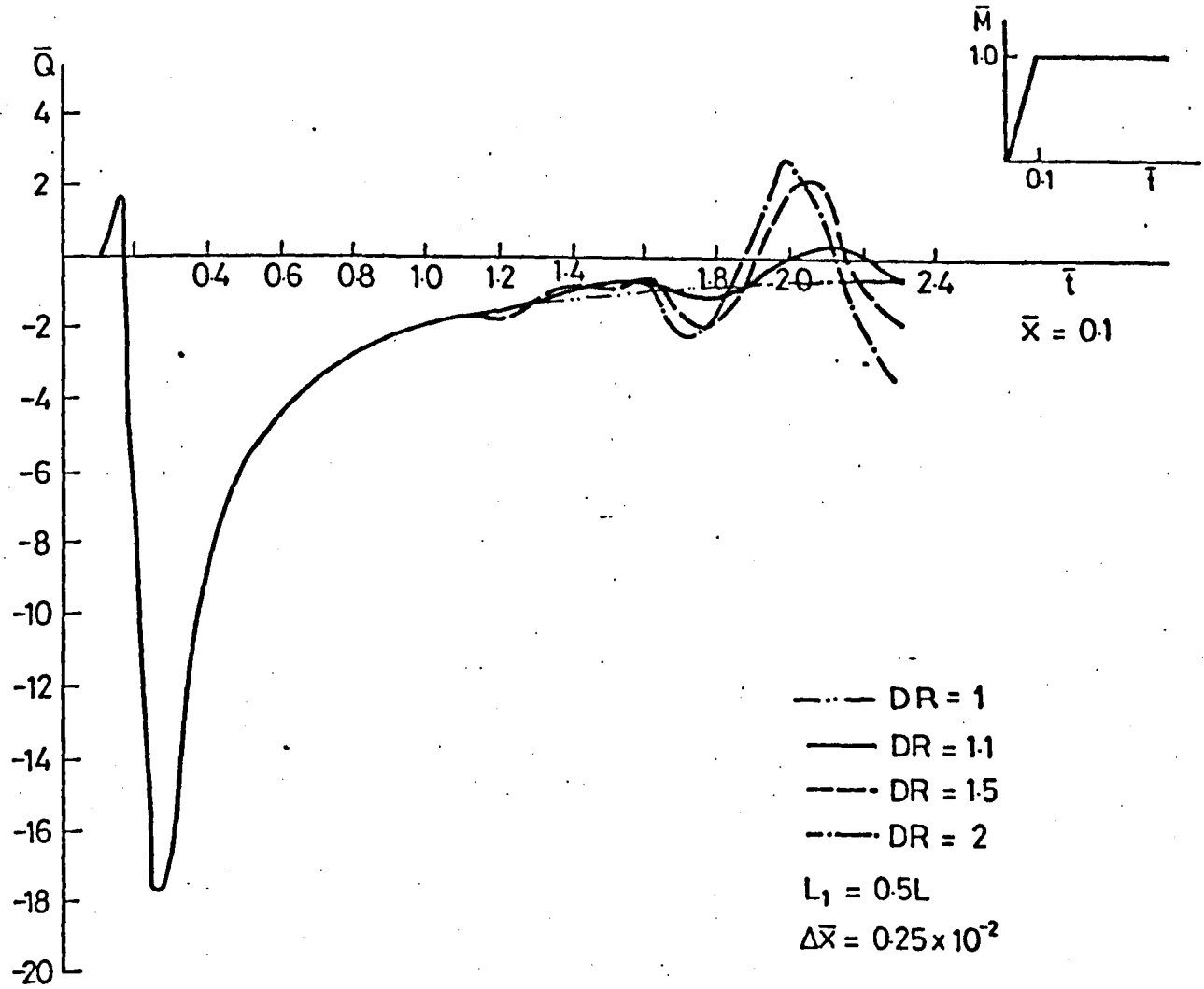

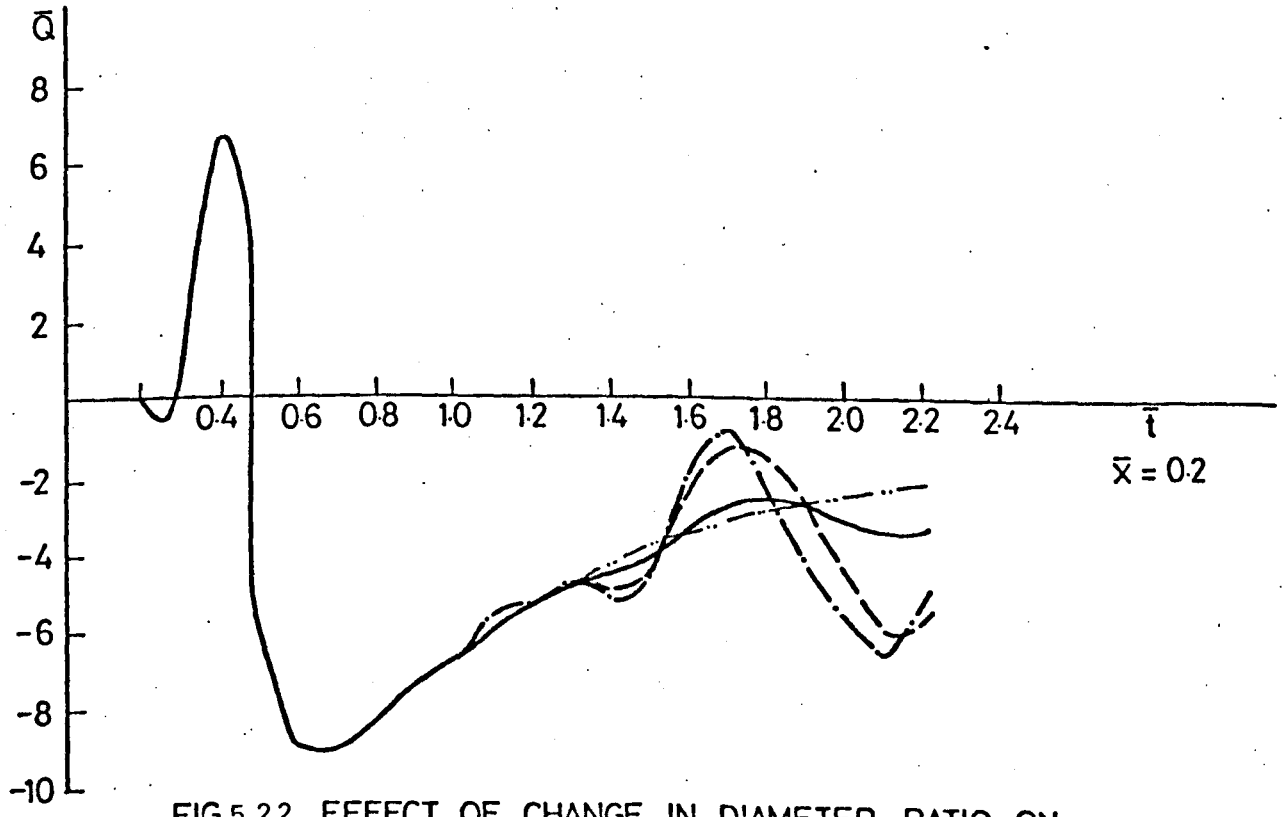

FIG.5.22 EFFECT OF CHANGE IN DIAMETER RATIO ON SHEAR FORCE

Free - Free Beam subjected to end moment

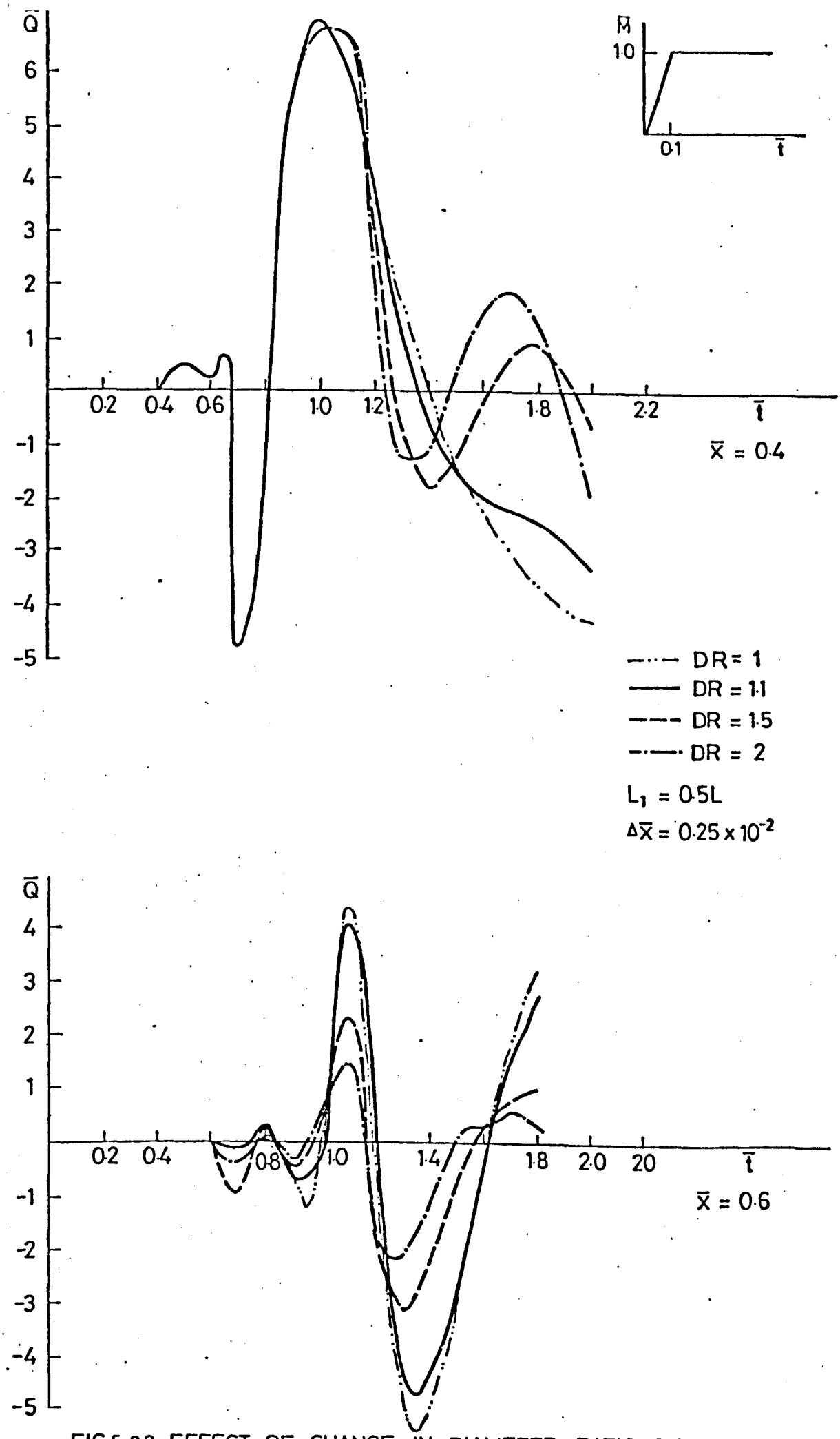

FIG.5.23. EFFECT OF CHANGE IN DIAMETER RATIO ON SHEAR FORCE

Free - Free Beam

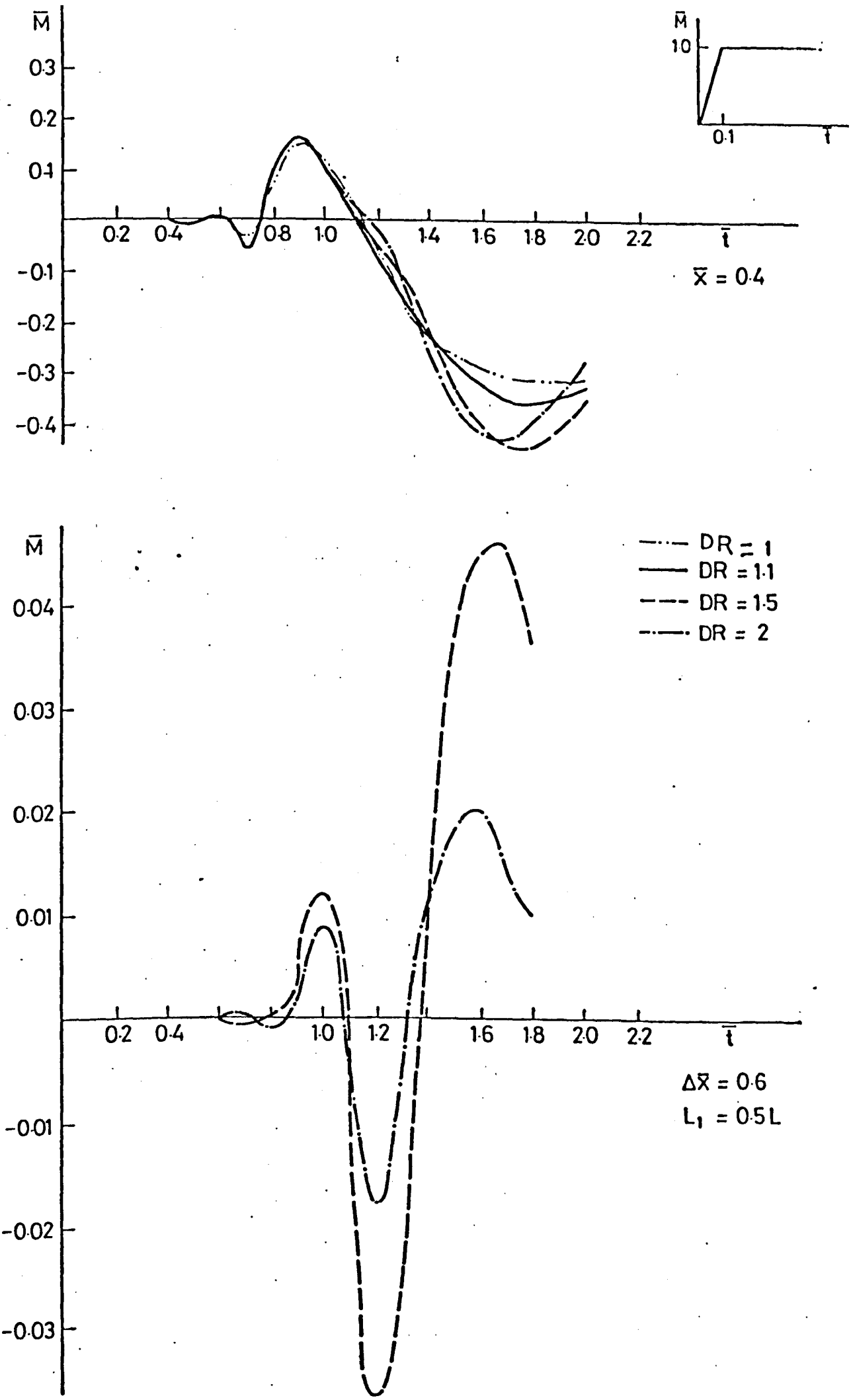

FIG 5.24 EFFECT OF CHANGE IN DIAMETER RATIO DR

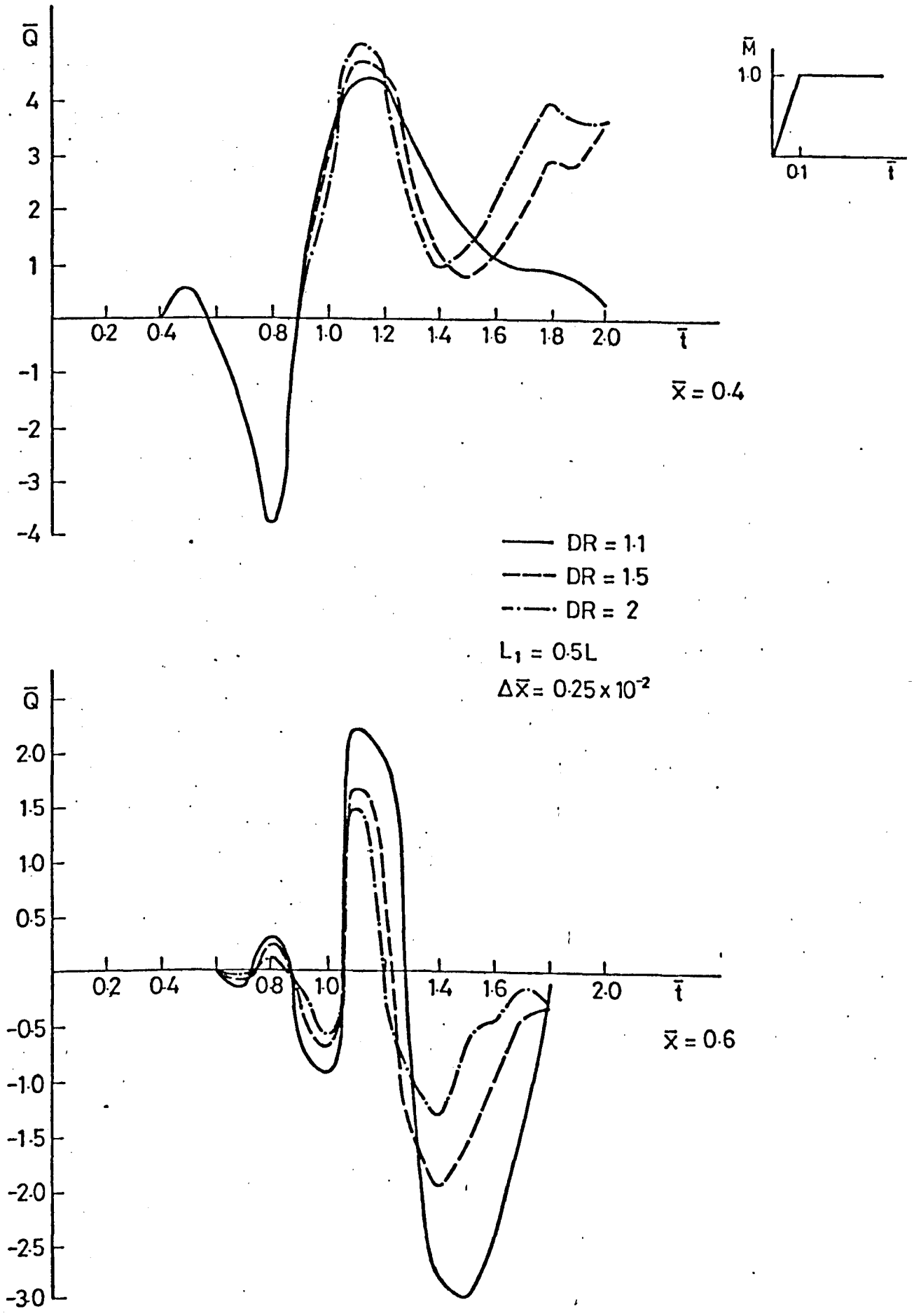

FIG 5.25 EFFECT OF CHANGE IN DIAMETER RATIO ON SHEAR FORCE

Simply supported Beam

CHAPTER VI

EXPERIMENTAL STUDIES ON TRANSIENT WAVES

6.1. Historical background

More than 100 years ago, theoretical investigations of longitudinal and transverse wave problems were extensively developed as was discussed in chapter 2 and section 2.1.

However, the experimental work was lagging behind the theory and early investigations were limited to the measurement of over all effects such as the time of impact and impact velocity.

The use of strain gauges from the forties onwards gave an important boost to the experimental work and the continuous measurement of forces and strains became possible.

By the end of the fifties most of the phenomena related to longitudinal wave propagation were experimentally studied. However, the investigation of flexural wave problems was far from complete. This caused a revival of interest in this field and experiments for various types of impact using strain gauges and to a less extent photo elastic methods.

The experimental studies of flexural waves have been mostly concerned with uniform and infinite structures, but these experiments provide the basis for further work to study the behaviour of nonuniform structures. This made it possible to carry out the present experimental investigation of flexural waves in beams with discontinuities of cross section subjected to transient loading.

Classically, there are two cases of impact where it is possible to calculate the stresses set up during collision, assuming there are no permanent changes in the dimensions of the colliding bars i.e. no plastic deformations.

The first case was investigated by St. Venant (1867) and was that of longitudinal impact of two long uniform bars. According to

St. Venant, the elastic impact initiates in each of the colliding bodies a rectangular pulse travelling away from the plane of contact and the duration of impact is equal to the time taken by the wave to travel twice the length of the shorter bar. However, this is only true if the ends of the bars are perfectly plane and meet instantaneously over their full area.

St. Venant treated the two bars as a single body during the collision. In each bar, the impact was assumed to initiate a rectangular stress pulse travelling away from the plane of contact and the magnitude of the longitudinal stress can be derived from the relationship between the pressure p and the particle velocity $\dot{u}$.

$$p = \rho c_o \dot{u}$$

The condition of perfect plane impact is almost impossible to realise in experiments.

The second case was that of colliding bodies where the surfaces are spherical, cylindrical or ellipsoidal and has been treated by Hertz (1882). The Hertz theory is based on a quasi-static model and obtains, for elastic conditions, a relation between the distance α through which the colliding bodies are pressed together and the force of impact F

$$F = k \alpha^{3/2}$$

where k is a constant depending on the elastic constants of the colliding bodies and their geometry in the region of contact.

For crossed cylinders of radius r and both of the same material with a Poisson's ratio ν and a Young's modulus E,

$$k = 2E \sqrt{r/3 \ (1-\nu^2)}$$

The Hertz theory should only be used as guide lines since the theory uses assumptions which break down at high velocities where the Hertz contact time could serve only as a lower bound on the contact time. For the case of a sphere striking a beam, the motion of the beam reduces the force, but the contact time remains about the same.

Finally it could be concluded that the theory of St. Venant applies to impact between the end faces of long rods, whereas the Hertz theory applies when the time of transit of an elastic wave through the colliding bodies is small compared with the time of contact as in the case of two colliding spheres (Goldsmith and Lyman, 1960).

Sears (1908) showed that both these theories were complementary and when the ends of long rods were rounded, the history of their impact could be deduced by combining the theories of St. Venant and Hertz, where the last theory was applied to the region immediately around the surface of contact. Sears carried out the first experiments confirming the theory just described(Sears,1912) .

Later calculations and comparison with strain measurements demonstrated the need to introduce a gradually rising wave front, as Sears had proposed, rather than the abrupt jump of the Saint-Venant theory.

To follow up the experimental research on wave propagation in solids during the past 30 years, one must select from several hundreds of published papers, theses and reports.

Most of the reported experimental studies have been concerned with longitudinal wave propagation in various types of structures. Experimental investigations of flexural wave propagation are mainly concentrated on various types of transverse impact problems, whereas flexural wave propagation due to eccentric impact are not plentiful and where reported seldom match theoretical predictions to any desirable degree of accuracy.

In this chapter, some of the experimental studies and applications of longitudinal and flexural waves in rods will be reviewed. No attempt will be made to be comprehensive, but merely to bring out results and investigations in areas related to the theoretical work of the present investigation.

Comprehensive reviews of experiments in impact loading are given in several excellent books by Kolsky (1953), Goldsmith (1960), Johnson (1972), Bell (1973), Graff (1975) and Miklowitz (1978).

Several articles reviewed the experimental studies elastic wave propagation. Some of these are the surveys by Ripperger (1952), Davies (1956), Kolsky (1958), Curtis (1960) and Rawlings (1963).

A large number of experimental studies have been concerned with plastic deformation of beams subjected to high velocity loading due to longitudinal and transverse impacts. However, these investigations are beyond the scope of the present work and will be not discussed here.

6.2. Longitudinal waves due to impact

6.2.1. Longitudinal impact of two bars

Based on the earlier theoretical studies, Sears (1907) was the first to provide experimental results for the problem of longitudinal impact of two metal rods with rounded ends. The rods were of 1/2 inch diameter with rounded ends of 1 inch radius for the curvature. Two rods of equal length were suspended by fine cords and in their lowest position, the rods were co-linear and just in contact. The impact velocity was ca. 5 in/s.

Sears was able to obtain the velocity of propagation, as given by St. Venant ($c_o = \sqrt{E/\rho}$), by observing the duration of longitudinal impact ($t = 2L/c_o$). Sears found that the impact duration was slightly greater than the time required to travel twice the length of the bars and attributed the difference to the so called "end effects".

To obtain a more accurate estimate for the duration of impact, Sears suggested a combination of the Hertz theory and the St. Venant theory. This gave a better agreement with experimental results, where the time of contact was measured electrically. The investigations of Sears enabled him to explain some earlier doubts casted on the theory because of disagreement with previous experimental results.

Ramsauer investigations (1909) gave more strength to the conclusions reached by Sears where the propagation of stress waves and the time of contact between two rods was discussed.

The longitudinal impact of a bar with a shorter bar as a striker showed that the duration of impact increased with increased cylinder length ℓ, without being zero for $\ell = 0$. There was an additional compression time depending on the form and the size of the rounded ends. The deflection of the bar was measured by an optical method.

Tschudi (1921) used an electrical condensor circuit to measure the duration of impact in three sets of cylinders of equal lengths. He suggested that the duration of impact was not a linear function of striker length, but there was a factor due to the initial velocity of impact which had to be taken into account. Wagstaff (1924) conducted similar exp

The measurement of strain changes in time became only possible after the introduction of strain gauges and Fanning and Bassett (1940) were probably the first to use strain gauges (originally called electrically strain sensitive strips) for the measurement of longitudinal strains.

A similar arrangement to that of Sears was used for the longitudinal impact of two rods 1.167 inch in diameter and 6 ft. long where one end of the bar was flat and the other was a spherical surface. The results were in agreement with those previously published by Sears (1908 and 1912).

De Forest (1941) was able to confirm qualitatively the St. Venant theory for longitudinal impact of two long bars suspended as bifilar pendulum and one bar was allowed to swing into collision with the other. However, it was pointed out that the most complete solution was given by Sears.

Dohrenwend and Mehaffey (1943) used strain gauges for dynamic measurements in a longitudinal impact of two bars and described the equipment used successfully for dynamic stress analysis and the important contribution of electrical resistance strain gauges.

Recently the longitudinal impact of two bars has found various applications such as determining the yield stress of metals at various stress levels and strain rates, as by Suh (1967) who employed for this purpose the longitudinal impact of a long steel bar with a shorter bar. At the opposite end of the long bar, a truncated cone was machined and supported against a rigid wall. The stress wave amplitude could be amplified to varying degrees by truncating the cone at different places. The change in the shape of the reflected wave from the conical end was measured.

Cunningham et. al (1970) used a photomultiplier tube and a laser light source to record stress optical data associated with a moving stress wave. The stress wave was generated either by dropping or by pneumatically driving a 1/8 inch steel ball or a 1/8 x 2 inch steel cylinder.

Nevill et. al (1972) performed experiments for wave propagation, attenuation and dispersion in steel, epoxy and steel-epoxy composite specimens. The rods were subjected to axial impact by a striker propelled at velocities of the order of 75 fps from an airgun. The strikers were of varying length and of 0.382 inch diameter.

Matsumoto and Simpson (1977) used the longitudinal impact of two finite elastic cylinders to investigate the acoustic radiation and found that the noise generation was assoiciated with the injection of air into the region between the impact surfaces just after impact seperation. Three foil strain gauges were mounted symmetrically around the cylinders and the transient acoustic pressures were measured using 1/4 inch condensor microphone with the associated cathode follower.

6.2.2. The Hopkinson pressure bar

The longitudinal impact of long cylinderical bars was used by Hopkinson (1913) to obtain pressure-time curves and impact duration of short pulses generated by a rifle bullet fired at, or gun cotton

detonated near one end of the bar. At the other end of the bar, a short piece of the same bar was in firm contact and when the pulse passed the joint, the end piece flew off trapping the whole momentum within it and leaving the long bar at rest.

The end piece was caught up in a ballistic pendulum in a form of a box and by taking end pieces of different lengths, Hopkinson was able to obtain the pressure-time curve over the corresponding intervals.

Landon and Quinney (1923) carried out further experiments with the Hopkinson pressure bar technique and discussed the effect of the change of bar length and bar diameter on the variation of the mean pressure. The authors also discussed the effect of coned bar on the propagated longitudinal wave.

Although the Hopkinson pressure bar technique is simple, it has a basic short coming in that the shape of the input pressure pulse is not known and only its duration can be determined together with its maximum value.

In the same experiment, Davies (1948) introduced the displacement measurement technique by using the bar as the earthed member of a parallel-plate condensor. The radial and axial displacement were separately determined.

Voltera (1948) used the Davies technique for obtaining strain- time curves for copper and polythene specimens.

Kolsky (1949) proposed a further modification of the Hopkinson pressure bar technique and called it the split Hopkinson bar. The new method consisted of sandwiching a short cylindrical specimem of test material between two long rods of high strength steel. The stress pulse was initiated in one of the elastic bars by a detonator and the amplitude of the pulse was measured by a cylindrical condensor microphone. The displacement of the free end of the extension bar was measured with a parallel plate condensor.

The split Hopkinson pressure bar (SHPB) has been widely used in dynamical studies of material properties and to obtain yield point and it has been shown that in cases where an impact load of 100 μs duration was applied, the stress required to initiate yield was about double those required under normal static conditions.

Davies and Hunter (1963) used the SHPB to obtain displacement-time relations for disk shaped specimens of copper, aluminum, magnesuim, zinc, brass and polymers.

In later experiments, strain gauges were used to measure the incident, reflected and transmitted waves and to determine the dynamic stress-strain relations for the tested materials. This new form of the SHPB was used by Lindholm (1964) for testing three annealed face centred cubic metals, namely lead, aluminum and copper.

Conway and Jakubowski (1969) suggested the use of the shorter cylindrical bars for the longitudinal impact which were positioned directly below and parallel to and slightly beyond a longer bar in order to ensure an accurate alignment for the classical Hopkinson pressure bar. Strain gauge records provided the essential data for axial strains.

Nicholas (1971) discussed the validity of the SHPB technique and carried out experiments involving the variation of input stress, gauge length and material behaviour. The results were compared with theoretical predictions which were obtained using the method of characteristics.

Bertholf (1974) used the split Hopkinson pressure bar (SHPB) to demonstrate the feasibility of a two-dimensional numerical analysis. An axial stress of 1 kbar amplitude was applied to the end of one of two elastic bars of 1 inch diameter. The elastic specimen had an impedance appr. 1/6th that of the steel bar.

Goldsmith and Katsamanis (1979) conducted a Hopkinson-bar type tests with spherical strikers to investigate strain pulses in thin rectangular specimens of polymethyl methacrylate (PMMA) and polycarbonate of

bisphenol (lexan). The initial and rebound velocities of the spheres as well as strain histories were measured. The stress intensity factor at the tip and the nominal stress at central holes were ascertained by means of a shadowgraphic technique.

6.2.3. Longitudinal impact of spheres on bars

The generation of a longitudinal stress wave in bars by the impact of an elastic sphere has been originally used by Hopkinson and was described in the previous section. The same arrangement approach is used for studies of longitudinal wave propagation.

Crook (1952) investigated the impact of a hard sphere on a metal cylinder within the ranges of the theories of elastic impacts due to St. Venant and Hertz. A steel spehere of 100 gm was freely suspended and allowed to fall against an anvil supported by Piezo-electric crystal for force measurements.

The calculated impact velocities from experimental force-time curves agreed with values obtained from the fall of the sphere.

Ripperger (1953) conducted an extensive investigation of pulses in rods resulting from spherical ball impact. The rod diameter ranged from 1/8 in. to 1/2 in. and various impact ball diameters as well as various impact velocities were considered.

The strain signals were detected by piezoelectric strain gauges and the pulse shape had a general half-sine form at positions starting at several diameters from the impact end.

Longitudinal pulses in a narrow rectangular bar, generated by a 1/2 inch diameter ball bearing, were studied by Cunningham and Goldsmith (1958). They showed excellent agreement between the experimental results of two measurement methods for the force-time curves. One method used strain gauges and the other method used piezoelectric crystals.

Barton et. al (1958) obtained experimental results for the longitudinal impact of an elastic sphere on an infinitely long cylindrical

steel bars. The spheres with diameters ranging from 1 in. to 2 in. were dropped from the height of 7.5 cm to 30 cm to impact longitudinally a 1 in. in diameter bar.

Strain gauges were placed at a position 6 inch from the impact end and the experimental results showed good agreement with theoretical predictions based on the Hertzian contact theory. A slightly shorter pulse was predicted than observed and the peak amplitudes were also slightly different.

Ramamurti and Ramanamurti (1977) studied longitudinal waves in short bars with hemispherical ends. The specimens were made of araldite, mild steel and aluminum and composite solid and hollow bars.

The impact pulses were generated by the impact of a hard steel ball of 50 mm diameter and the strains were measured at various axial locations with strain gauges.

6.2.4. Longitudinal waves in beams with discontinuities of cross section

The measurement of axial strain in bars with discontinuities of cross section could only be achieved after the introduction of electrical resistance strain gauges in the forties.

De Forest (1941) observed the propagation of longitudinal waves in a bar with a discontinuity of cross section at the middle and used strain gauges for the dynamic measurements. The bar was 8 ft. long and had a diameter of 1 11/16 in. for half of its length and 9/16 in. diameter for the other 4 ft. Three strain gauges were axially mounted on the bar, one 2 ft. from each end and a third very close to the shoulder at the centre.

The impact was applied at both ends by a 1/2 ft. long bar travelling at 5 fps.

Fehr et. al (1944) investigated the dynamic stresses in tensile test specimens and obtained stress vs. time curves with strain gauges cemented on the large diameter section of the bar. The results were in

fair agreement with the theoretical predictions of Donnell (1930) for longitudinal strains in a bar with two discontinuities of cross section.

Le van Griffis (1944) discussed the problem of an impact applied to the end of a bar with increased or decreased cross section. The conditions for transmitted and reflected waves were derived by equating impulse and momentum change for the particles on each side of the discontinuity.

The author also pointed out that a fixed end was equivalent to an infinite increase in cross section, whereas a free end was equivalent to a decrease in cross section to zero.

Van Griffis constructed the x - t diagrams for the wave propagation in the tensile test specimen and in its holders.

Fischer (1954) studied the change of the shape of a transmitted wave travelling along an obstacle in the bar, consisting of a part with reduced or increased area, called neck and swell respectively. Oscillograms were obtained using strain gauges, cathode ray oscillograph and moving film camera. The agreement between measurements and theory proved to be fairly good. x - t diagrams were used extensively for the graphical treatment of the effect of the change in area ratio on the amplitudes of the transmitted and reflected pulses.

Ripperger and Abramson (1957b) presented experimental results for longitudinal waves encountering a discontinuity in a rod in the form of a step change in cross-sectional area. A pulse propagated from the large end towards the small end was shown to retain its shape and duration with only the amplitude being affected by the discontinuity.

Becker (1962) used strain gauge recordings of longitudinal waves in beams with discontinuities of cross section for impedance measurements. Two long elastic cylinders were ballistically suspended and formed the hammer and wave guide. The rounded ends of the bars were replaced by plane ends to obtain a transient wave approaching step loading. A 6 in. long 5/16 in. diameter cylinder was end mounted on the 1/2 in. diameter

wave guide.

Mechanical driving point impedance characteristics were derived from the normalized incident and reflected wave form. The importance of transient loading for dynamic measurement was further emphasised in a second paper by Becker and Conway (1964).

Cone (1963) studied the longitudinal wave propagation across an abrupt change of cross section and used embeded strain gauges in an aluminium filled epoxy model.

By making some corrections in the magnitude of the experimental data to allow for suggested attenuation in the bar, Cone was able in most cases to obtain better agreement in comparison with predictions based on one dimensional theory.

In an investigation by Beddoe (1965), a falling weight struck an upright standing bar and generated a longitudinal wave propagating up the rod where strain gauges provided the recordings. The bar was 8 ft. long and 0.25 inch in diameter. The author obtained good agreement between theory and experiment.

Kawata and Hashimoto (1965) used photo elastic methods for longitudinal wave measurements in a polyurethene rubber struts of rectangular cross section with necks and notches. An approximate formulation was derived for the dynamic stress concentration factor by considering the notches as discontinuities in the cross sectional area.

Mortimer et. al (1968) considered the response of stepped shells subjected to axial impact by shells of identical material properties and uniform cross section. The impact velocity was measured by a photodiode system and strain gauges measuring longitudinal strain were mounted on the shell at various distances from the impacted end.

The experimental results for longitudinal and circumferential strains were compared with analytical results and were in good agreement.

In a second paper Mortimer et. al (1972) investigated in a similar

set up, the longitudianl impact of thin cylindrical shells with cross sectional area discontinuity. Experimental incident, transmitted and reflected strain and stress ratios were measured and they correlated well with the predictions of the "bending" and "membrane" theories, but then the results were not in agreement with the predictions of the "uniaxial" theory.

A similar experimental study was carried out by Rose et. al (1973) for the axial impact of a thin finite joined shell consisting of a cylinder-truncated cone - cylinder, which was a 1/100 scale replica of a portion of the Apollo - Saturn V vehicle.

Habberstad and Hoge (1971) performed an experimental work similar to that of Ripperger and Abramson (1957b) and were able to obtain better accuracy. A steel ball of 1/2 inch diameter was propelled by an air gun and impacted longitudinally the small end of a 1/2 in. diameter bar, machined from a 3/4 in. bar diameter with a total length of 36 in.

Yang and Hassett (1972) obtained good agreement in comparing longitudinal stress waves in bars with step changes in area, in cylindrical-cylindrical shells and in truncated cones. A striker was accelerated by a high pressure airgun to produce a transient input pulse of 50 μs duration and the data were recorded by foil strain gauges.

Rose and Mortimer (1973) pointed out the usefulness of longitudinal elastic wave propagation in nondestructive testing. The effect of notches in a thin aluminum tube on the transmission and reflection of an ultrasonic signals was investigated.

Johnson and Mamalis (1977) investigated the fracture of rectangular perspex stepped bar subjected to end loading by a detonator. High-speed photographic records showed the growth of cracks and spalls.

Barez et.al. (1980) investigated the longitudinal wave propagation in circular bars with discontinuity of cross section and material. They showed that the predictions of the axisymmetric theory were no more accurate than those of the elementary model when compared with experimental results.

6.3. Flexural waves due to impact

6.3.1. Transverse impact

6.3.1.1. Transverse impact of a steel ball on a beam

The criterion for checking the validity of approximate theories describing the transverse impact of structures must be the degree of their agreement with experimental results. Transverse impact tests have been conducted under conditions where the anti-symmetrical wave components are predominant.

The analysis of the process on the basis of the three-dimensional theory is not feasible as was pointed out earlier and the analysis by means of the plane stress solution is limited and too cumbersome and the only other practical alternative theory with reasonable prospect of accuracy is the Timoshenko beam theory which takes into account the rotatory inertia and transverse shear. In most cases the Timoshenko theory predictions were in fair agreement with experimental results.

The analysis of bending waves has been restricted in almost all known publications, to uniform structural element where the comparison with theoretical predictions has been conducted within a short period of time in order to ignore the effect of reflected waves.

As early as 1849, Cox investigated the problem of central impact of a beam with a steel ball suspended as a pendulum and the deflection was measured for various ratios of beam mass to sphere mass. The impact velocity and beam cross section and length were also varied.

In 1913, Timoshenko investigated the transverse impact of a beam with a steel ball using the Hertzian theory of contact combined with the lateral vibration theory to obtain predictions for the local deformation and beam deflection. The specimen used was a simply supported beam of 1 cm x 1 cm square cross section.

A similar investigation was carried out by Mason (1936).

Tuzi and Nisida (1936) used photoelastic method to study transverse

stresses in a phenolite simply supported beam which was struck at the centre. The experimental values of the maximum dynamical stresses were about 70 - 80% of the calculated one.

Hoppman (1952a) investigated the response of multi span beams subjected to a transverse impact by a solid steel sphere of 1 inch diameter and 5.66 fps impact velocity. He measured the bending strains by strain gauges and the maximum displacement was measured with a micrometer. The input pulse was approximated by a half sine wave for the theoretical study. A similar study was carried out by that author (1952 b) for the transverse impact of a sphere on a column.

Goland et. al (1955) measured the transverse waves in a simply supported beam of rectangular cross section subjected to a lateral impact by dropping a steel ball bearing from a known height on the top surface of the beam. Strain gauges were used for strain measurements at two stations along the beam and a force gauge measured the force-time history. Most of the content of the latter paper was included in a report published by three authors Dengler et. al (1952) and more details were presented in section 5.2.4. of the present work where the results of the report were used for comparison purposes.

Cunningham and Goldsmith (1956) reported on the oblique impact of steel ball 1/2 inch in diameter, on a beam. Strain gauges were used to record the outer fibre strains and it was seen that the peak amplitude undergoes inversion as it propagated along the beam. In addition, the presence of high frequency components became more noticeable with distance of propagation.

In a second publication, Goldsmith and Cunningham (1956) provided parallel information on the kinetic history of the same problem. The beam deflections at the centre of the beam were measured and showed the excitation of higher modes.

The displacement time records of longitudinally prestressed beams

of aluminum and steel were obtained by Mori (1957). He used a capacitance type pickup and a single sweep generator for the recordings in the beams subjected to lateral impact produced by a small hammer driven by a motor striking the beam at the centre every two or three seconds.

A study of the transverse impact of an elastically connected double beam system was provided by Seelig and Hoppmann (1964). A half-sine pulse was produced by a 2 inch diameter steel ball with a rubber impact head. The input pulse was recorded by a piezoelectric force gauge and the bending waves were measured by strain gauges cemented to each beam of square cross section 1/2 inch x 1/2 inch and c. 40 inch long.

Schwieger (1965) investigated the elastic central impact of a spherical mass on a steel beam. The bending wave stresses were visualized by applying photoelastic coatings and by means of polarized light using a reflection method. Experimental data were obtained for impact force and contact time for various impact velocities. The experiments verified the use of the Timoshenko method for the prediction of maximum bending strains only under the point of contact, but not at other positions along the beam even when reflections were not considered.

Kuske (1966) presented a comprehensive study of photoelastic metheds applied in dynamic stress analysis and obtained experimental results for flexural waves in a beam of Lakutherm -x 30 subjected to a transverse impact by a 1 gram weight.

The application of laser holography to record bending waves was presented by Aprahamian (1971). A long beam of rectangular cross section was struck at its centre by a ballistic pendulum employing steel spheres of various diameters.

The fringe pattern provided a measure of deflection and holograms were used for plotting the displacement curve along the beam.

6.3.1.2. Transverse impact of a bar on a beam

In addition to the use of spheres as striker, cylindrical bars have also been used in some investigations. The striker had the form of thick short cylinder in some cases as a bar with a length several times its diameter and impact of varying duration and longer than where a sphere is used can be achieved. The most common arrangement for this type of impact is the drop test where the striker falls freely from a certain height to strike the beam transversely.

One of the earlier tests was carried out by Arnold (1937) who obtained bending strains and bending stresses at the centre of an I - beam using a extensometer for the measurement. The 8 feet long I - beam with a cross sectional area of 11.05 $in.^2$ was subjected to a central impact of a 470 lb. weight with an impact velocity of 11 fps.

Vigness (1951) used an experimental method similar to that of Dohrenwend for the impact of a cantilever beam at its clamped end. The impact pendulum consisted of a hammer as a thick cylinder suspended by wires. The strains were measured at various locations and streak photographic recording of displacement was made for the free end of the cantilever beam.

Schulze (1953) investigated the transverse impact of a steel beam 4m long and of square cross section 5 cm x 5 cm. The striker was a thick steel cylinder with the height equal to the diameter and with rounded impact end. The dispersion of the flexural wave was investigated using strain gauges for the measurement.

The drop test method was used by Emschermann (1954) to produce transverse waves in a steel beam of rectangular cross section. Strain gauges were mounted at various positions to record the strains for various impact masses and impact velocities.

A second optical method was used for the stress measurement in a transparent specimen. The experimental results were in good agreement with predictions based on the Timoshenko beam theory.

A photo elastic method was also used by Durelli (1957) to study the transient stress and strain distributions in a simply supported beam subjected to central impact. The beam was made of plastic with good photo elastic properties and fringe patterns were obtained for the entire beam at four instances after impact. The strain-time curve was derived from the displacement-time curve assuming uniform strain distribution.

Flynn and Frocht (1961) used streak photography to determine the stress pattern in a uniform bars of Bakelite under longitudinal and transverse impact.

Odaka and Nakahara (1967) performed experimental work on a simply supported beam 3m long and 25mm x 25mm cross section subjected to central impact by a steel cylinder 20mm in diameter and 1m long, dropped from 1m height. Four strain gauges were mounted at various stations to obtain strain recordings.

A similar investigation was carried out by Ranganath (1971) who used a cylindrical rod with a rounded end as a striker accelerated by a gas gun. The beam and the bar were sufficiently long so that no reflection reached the recording position during the 100 μs after impact which was used for the bending strain measurement by foil strain gauges.

Yew and Chen (1978) studied longitudinal and flexural waves in an aluminum bar 2.5m long and 18mm in diameter subjected to a transverse central impact by a hammer.

The analytical predictions were obtained using a fast Fourier transform in the frequency domain and phase velocity vs. frequency curves were presented using the Timoshenko beam equations for flexural waves.

6.3.1.3. Other types of transverse impact

In some cases, airgun pellets have been used for the generation of transient pulses of very short duration. Another method is the use

of electrical methods such as conductors and electromagnetic drive unit which are more common in fequency analysis.

Dohrenwend et. al (1943) presented a theoretical and experimental study of transverse impact of steel cables, steel beams and steel plates.

A steel beam 15 ft. long of rectangular cross section 1/2 in. x 1/4 in. was struck by an 8 oz. ball-pointed hammer. The initial velocity was approximated by an exponential function.

In a second test a 1/16 inch in diameter steel beam was struck by a 0.6 gm pellet fired from an airgun at a velocity of 200 fps. The strains were measured at various beam positions with the aid of strain gauges.

Zemanek et. al (1961) studied the transverse waves generated in a beam by electromagnetic drive unit where up to 306 resonant frequencies were excited and the resulting phase velocity was computed. The experimental data were compared with predictions of three different beam theories and showed excellent agreement with the exact theory and the Timoshenko beam theory.

Forrestal and Bertholf (1975) conducted experiments on long aluminum bars of rectangular cross-section 50.8mm x 19.05mm subjected to a central sine-squared current-time pressure pulse of 4 μs duration. The loading was produced by two closely spaced parallel conductors and bending strains were measured with strain gauges mounted on both beam surfaces. The results were in good agreement with predictions based on the Timoshenko theory and on a two dimensional elasticity theory.

6.3.2. Eccentric impact

6.3.2.1. Eccentric impact of a steel ball on a beam

The ecentric longitudinal impact of a steel sphere on steel bars has been used to generate bending pulses of very short duration in the range of few microseconds.

Investigations showed that the Timoshenko bending theory provided

an excellent approximation of the flexural wave propagation.

Ripperger (1955) carried out a series of measurements for bending waves in cylindrical bars of 1/2 inch diameter subjected to eccentric impact of steel balls of different sizes. The impacts generated Hertzian pulses with durations ranging from 3.5 μs to 30 μs. Strain gauges were mounted at several locations along the beam to measure the bending strains.

The results of this work were used by Ripperger and Abramson (1957a) to discuss the dispersion of flexural waves in beams subjected to eccentric impact by a sphere.

Ripperger's results were used in chapter 5, section 5.2.2. of the present work as a test for the validity of solutions obtained by the method of characteristics based on the Timoshenko beam theory.

Goldsmith et. al (1972) investigated the elastic waves generated by strikers consisting of steel bars with diameters from 1/8 in. to 1/2 in. and fired from an airgun at a predetermined pressure against the carefully positioned target. The specimens were one solid circular rod and two tubes all made of aluminum and 84.5 inch long and were subjected to eccentric impact.

The strains were measured with foil strain gauges at various positions and the relation between transverse and longitudinal strains was discussed. The alternate stress pattern of antisymmetric waves due to eccentric impact was observed.

6.3.2.2. Eccentric longitudinal impact of two bars

Most of the longitudinal impact investigations have been concentric impact producing longitudinal waves and only few experimental works on eccentric longitudinal impact producing flexural waves are known.

Davidson and Meier (1946) investigated the propagation of transverse waves in prismatical bars due to eccentric impact as an unwanted phenomenon in the percussion drilling of rock. Tests were conducted on

prototype tools of 4 to 8 inches diameter and 30 to 40 feet long which were impacted by a model drilling tool made from 3/4 inch diameter steel bar.

Kuo (1958) subjected a long cylindrical bar to eccentric longitudinal impact with a second bar of equal length and diameter. The two bars each 8 feet long and 1 inch in diameter were suspended by wires at two points.

The strain measurement was carried out at various positions along the beam using strain gauges. The dispersion of the input pulse into a variable frequency harmonic wave train was evident. The results of the work were later published in two papers (Kuo, 1959 and 1961). More details of Kuo's experiment were presented in section 5.2.1. of the present work.

Stephenson and Wilhoit (1965) also studied the propagation of bending waves in a rod. A rod 30 feet in length and 2 inch in diameter was used with eight strain gauge stations. The sudden application of the bending moment at one end of the bar was achieved by the rapid unloading due to fracture of a tensile loading piece attached to the beam end. The great length of the bar was useful in establishing the wave front velocity.

6.3.2.3. Transient bending waves in bars with discontinuity of cross section

The study of wave propagation problems in more complex structures, such as the waves around surface obstacles and irregularities have been limited in almost all known literature to longitudinal waves. Even in simple uniform structures, the investigation of flexural waves is complicated by dispersion and has been restricted to semi-infinite models where reflections need not be taken into account.

In the present, experimental techniques are sufficiently well established to permit detailed investigations of problems such as the

effects of nonuniformities in cross sectional area and elastic properties on the transmission and reflection of bending waves.

There have been few experimental studies of flexural waves in curved beams and T-joined and L-joined frames which will be reviewed in this section.

Mugiono (1955) was first to investigate flexural waves in rods with discontinuities of cross sections as part of an acousto-dynamic study of building structures. The testbars were of aluminum and 3 to 4m long with a diameter D_2 = 40mm and diameter ratios D_2/D_1 were taken as 2, 5 and 11.4.

Specimens with necks and double discontinuity of cross section were excited sideways with a permanent dynamic system attached to the small end of the bar. A crystal microphone was positioned at the middle of the first portion of the bar to measure continuously the acceleration of the steady state bending wave. The experimental results were used to obtain a reflection coefficient.

Ripperger and Abramson (1957 b) studied the reflection and transmission of transient bending waves at a discontinuity of cross section in a circular bar supported on rubber pads and subjected to eccentric impact by a 1/2 ich steel ball fired from a spring powered gun. The test specimen was 32.5 inch long and had a diameter of 1/2 inch in the first half of its length and a 3/4 inch diameter in the rest with strain gauges mounted on both sections of the beam. The experimental results for the bending waves were only briefly discussed because it was realised that the theoretical predictions of Mugiono on the basis of the Euler-Bernoulli theory were inadequate for the transient bending wave comparison.

The theoretical aspects of the previous two publications were discussed in more detail in section 2.3 of the present work.

Lee and Kolsky (1972) performed experiments for longitudinal and

flexural waves in two rods joined end to end at an angle. A longitudinal incident wave was produced by firing a projectile of the same diameter as the bar.

When a stress wave impinged on the junction, it generated four pulses, namely longitudinal and flexural pulses which were transmitted into the second rod and two similar waves that were reflected back .

The comparison of experimental results with predictions based on the Timoshenko theory were generally in good agreement, but showed some significant variations.

Philips and Crowly (1972) investigated pulse propagation in curved beams subjected to a half-sine bending moment input by using simulated photoelastic fringe patterns. Test beams of rectangular cross sections were curved beam with severe bend and a quarter-turn bend. The authors concluded that the propagation of a predominantly flexural pulse in a curved beam of moderate curvature was insensitive to the actual beam curvature as far as bending moment and shear force were concerned.

In a second study of the same problem, Crowly et. al (1974) used a pulsed ruby laser as a light source to obtain isochromatic fringe patterns for three models of Homalite 100, impacted longitudinally with a soft lead pellet. Strain gauges were also used for supplementary experimental data.

Atkins and Hunter (1975) obtained experimental results for elastic wave propagation in L-joint and T-joint models of equal square cross section of 25mm x 25mm and 1.219m long.

A steel projectile was driven forward in a tube of compressed air to impinge longitudinally one end of the joined frames. The longitudinal wave produced at the right angle joint a transverse wave which was propagated into the second bar. Both types of strains were measured separately by strain gauges.

The agreement between experimental results and theoretical

predictions was generally satisfactory except at peak amplitude where the theoretical value exceeded the experimented one by ca. 25%.

6.3.3. Fracture of brittle materials due to bending waves

One example for the manifestation of flexural waves is the brittle fracture occuring in specimens under load where the growth of the fracture results in a very sudden change in the stress field.

Miklowitz (1953b) was seeking an explanation for the fact that when a specimen was broken in tension two fracture surfaces instead of one were found to occur. Miklowitz suggested that this effect was the result of the fact that when a specimen breaks in tension, and the fracture starts at some point off the axis of the bar, a flexural pulse as well as an extensional pulse is generated at the fracture surface.

The superposition of extensional and flexural pulses can cause the build up of stresses in excess of the longitudinal stress at which fracture originally took place and hence a second fracture can be produced at a point remote from the initial one. The specimen was made of plexiglass.

Several examples of dynamic fractures in metal specimens were described by Rinehart and Pearson (1954).

Tsai and Kolsky (1966) studied the generation of the fracture pulses produced in a glass block when fracture takes place under the conditions of a Hertzian type impact between a steel ball and a large glass plate.

Philips (1970) reinvestigated the problem of brittle fracture of a glass rod under simple tension, originally set by Miklowitz. A glass specimen of circular cross section was mounted in a tensile test machine and the load was increased until fracture occured. The specimen length was from 8 to 18 inch.

The two types of waves generated were longitudinal and flexural waves and the output of strain gauges at various positions gave a highly satisfactory agreement with the predictions of the Timoshenko

beam theory, although many simplifying assumptions were made.

Bodner (1973) repeated the experiments of Philips and used long bars of square cross section subjected to pure bending

Nasim et. al(1971) observed the spalling of curved perspex bars subjected to axial impulsive loading and noted its independence of curvature.

Colton (1973) performed experiments on infinite beams and plates loaded with sheet explosives. It was found that all fractures were initiated by bending stresses.

The strains on the surface of the Linen phenolic specimens were measured with strain gauges and a second photoelastic method provided qualitative strain measurements. The beam was 50 cm long and had a cross-section of 25.4mm x 6.4mm.

The effect of the initial central fracture was approximated by a two stage fracture model that specified the bending moment distribution at the fracture point and its reduction to zero behind the fracture front.

The experimental results were in good agreement with predictions by the method of characteristics using the Timoshenko beam theory.

Recently Philips et. al (1978) conducted experiments on an aluminium bar containing a bandsawed edge crack. The bar was struck longitudinally by a shorter bar of the same material. Both bars were of 25.4mm square cross section, with the aim to diagnose bone fracture healing.

Strain gauges were mounted on opposite sides of the bar between the impact end and the crack location to monitor initial compressive strain and reflections containing symmetric and antisymmetric components.

Kida and Oda (1982) used photoelastic methods to study the fracture behaviour of brittle plaster cantilever beams subjected to transverse impact at their free end by a sphere of 50.8 mm dia. and 0.53 kg mass.

An extensive review of dynamic fracture is included in several recent papers by Kolsky (1970, 1971, 1976).

6.4. Experimental methods in stress wave detection

6.4.1. Mechanical methods

The simplest mechanical method of measurement was devised originally by Hopkinson (1913) and was described in section 6.2.2. It is based on the trap of the momentum of the pulse in a detachable time piece which is in close contact with the specimen and to measure this momentum by a ballistic pendulum. The technique was extended by Rinehart and Pearson (1954) to be used with specimens in the form of plates or blocks.

The method is simple and direct and can be used successfully when large stress amplitudes are to be recorded. Its disadvantages are that it does not give an accurate delineation of the pulse shape and the method can not be used for weak stresses and where the decay is too rapid since a useful pressure time curve can not be constructed.

After the development of modern electrical and optical methods, the mechanical methods provide a useful check on the stress-time curves obtained experimentally since the momentum can generally be derived from this curve by integration. However, one should realise that a simple relation does not always exist between the "shapes" of these different quantities.

Davies (1948) modified the Hopkinson method and investigated the validity of the basic assumption of the uniformity of the stress and displacement over the cross section for an input transient pulse.

The mechanical measurement method has been described in several books and publications such as by Davies (1956), Kolsky (1958), Johnson (1972) and Graff (1975).

6.4.2. Optical methods

Optical methods of measurement have been successfully used for the direct determination of longitudinal and torsional displacements of bars under transient loading.

One of the most popular methods is the photo elastic method in which the model must be of photo elastic material; these materials usually exhibit viscoelastic behaviour when high frequency components are present.

Interferometric techniques such as shadow techniques and Schlieren optics require the specimen surface to be highly polished and optically flat. These conditions are hardly met in practice.

Another method, called a diffraction grating method, uses the coating of the surface with a birefringent grating.

The technique of holographic interferometry which employs a pulsed ruby laser as a coherent light source is probably the most advanced optical method and it has been used for transient wave propagation studies. Most of the difficulties involved in this method such as stability and fringe interpretation could be reduced by the proper choice of equipment and optical arrangement.

The optical method provides two dimensional stress analysis and can be used for longitudinal stress wave study.

However, if longitudinal and flexural waves are present the flexural components of the stress can not be studied because after the passage of the longitudinal wave the bar undergoes an axial displacement which will be superimposed to some degree on the flexural wave pattern and cause complications in the analysis.

Optical methods do not provide a complete solution of dynamic loading since the results are only obtained at a particular time, but they are most helpful to provide a qualitative visualization of the problem.

The description of the optical method has been brief and for more details, one should consult one of the following references, Dove and Adams (1964), Dally and Riley (1965) and Robertson and King (1974).

6.4.3. Electrical methods

6.4.3.1. Condenser gauges

The condenser gauge operates on the basis of capacity changes which can be achieved by a change in the spacing of the condenser plates or a change in their area when a narrow air gap between the plates is used as dielectric medium.

One surface of the specimen itself may serve as one plate of the condenser. This was successfully used by Davies (1948) in his modification of the Hopkinson pressure bar.

There are many difficulties in the use of condenser gauges. The passive capacitance of connecting cables reduces the useful capacitance variation of the gauge and extremely high carrier frequencies are required to avoid excessive values of circuit impedance. This makes it difficult to use the condenser gauges for the measurement of sharp pulses of short duration. Additional difficulties are involved in the calibration of the gauge.

Therefore, it is not surprising that condenser gauges are no longer used for strain measurements in transient type loadings.

6.4.3.2. Electrical resistance strain gauges

These gauges are shortly called strain gauges and are probably more widely used than any other device in the measurement of strains in transient wave problems. A strain gauge uses the fact that the electrical resistance of a wire depends on its longitudinal strain which was first described by Lord Kelvin (1856). But the first practical application of strain gauges in dynamical measurement was due to Datwyler and Clark (1938).

In addition to their simplicity and their excellent frequency response, the strain gauges have the advantage of recording directly a particular component of the pulse i.e. separate flexural or longitudinal strain detection which is achieved by using a combination of

strain gauges in circuit connections in a Wheatstone bridge and potentiometer.

The disadvantages are that the initial rise is not instantaneous since the leading edge of the pulse takes a finite time to traverse the length of the gauge. The size of the strain gauge means that it gives an integrated value for the strain over the area. However, very small strain gaugesafew millimeters long are used to counter this disadvantage.

A particular care should be taken in mounting the strain gauges on the surface of the specimen in order to avoid failure at high frequency response due to the properties of the thin adhesive layer.

Furthermore, the strain gauge recordings on the outer surfaces of the specimen can give the transient response of the structure adequately only if a uniform stress distribution over the cross section can be assumed. However, this is one of the assumptions upon which the one dimensional theory of wave propagation is based. Therefore, it does not represent any additional restriction to the experimental results when compared with the predictions of the Timoshenko theory.

Piezoelectric gauges are also sometimes used for dynamic strain measurement. Although they have a much higher sensitivity than wire strain gauges, the piezoelectric strain gauges are difficult to calibrate and they produce a considerable reinforcement at the point to which they are attached. Furthermore, the piezoelectric crystal gauges are expensive and are most frequently used for triggering purposes.

Since the forties, the use of strain gauges for dynamic strain measurement and various aspects of its development have been described in several publications.

Döhrenwend (1943) described the use of strain gauges for strain recordings in the problem of longitudinal impact of two bars where the strain gauges were connected in a potentiometer circuit and the problems

of instrumentation were discussed.

Fink (1950) discussed the calibration of strain gauges used in dynamic measurement when arranged as a Wheatstone bridge circuit for recording longitudinal strain. The accuracy was sufficient for a dynamic strain pulse with a rise time not less than 17 μs.

Krafft (1955) showed that the longitudinal impact of two flat ended bars did not produce a smooth square wave of strain but rather a constant strain plus significant high frequency fluctuation which he managed to reduce by greasing the colliding surfaces.

Cunningham and Goldsmith (1959) concluded from measurement of waves generated in a bar by longitudinal impact of a steel ball that the static gauge factor was applicable in measuring impulsive strain with rise times not less than 7 μs

The errors in the rise time display due to the basic rise time of strain gauges were investigated by Taylor (1966) who showed that the accuracy was improved considerably by using strain gauges with a gauge length of about 5mm and experimental results with an error of ca. 2% were readily obtained.

Oi (1966) was able to show that strain gauges could even be used satisfactorily to record steep strain waves with rise times much smaller than was possible in previous works. An expression for the rise time of bonded strain gauges was given as

$$\tau_{rc} = \tau_{rw} + \tau_{rg}$$

where τ_{rc} was the total rise time and indices w and g corresponded to the rise time of the strain wave and the strain gauge respectively.

Oi obtained an approximate formulation for a strain gauge with the length L as

$$\tau_{rg} < 0.5\ \mu s + 0.8\ L/c_o$$

This gave a cut off frequency $f_c > 360$ kHz for L = 3mm when the strain gauge was mounted on steel.

Bickle (1970) reinterpretted Oi's experiments and showed that the 0.5 μs additive constant in Oi's expression could be greatly reduced to 0.1 μs. Another 0.1 μs was added due to the rise time of the instrumentation system.

Bickle suggested an elimination of the 0.8 L/c_o term and used instead an analytical compensation technique based on the differentiation of the output signal of the strain gauge using positive feedback. However, this operation is difficult to perform on experimental data, since differentiation is fundamentally a noise-amplifying process and furthermore, the process was generally inherently unstable.

Atkins (1971) showed the advantages of the use of strain gauges in comparison with the use of accelerometers as transducers for the measurement of strains in impacted frames made of 1 in square section mild steel bars formed as L- and T-joints. The results were recorded on a tape recorder and simultaneously monitored on an oscilloscope.

Watson (1972) was able to remove the instability from the process of computing a continuous time derivation of analog data. He presented an analytical example for the averaging of an elastic pulse and used the frequency domain analysis because of difficulties involved in a real time domain analysis.

Troke (1976) discussed the use of 1/4 bridge, 1/2 bridge and full Wheatstone bridges for the measurement of longitudinal and flexural wave propagation problems. He presented expressions for the use of shunt calibration technique for producing equivalent tension and compression strains where the different response of the strain gauge to compression and tension was considered.

Lundberg (1977) presented a large number of experiments for longitudinal waves travelling between two strain gauge positions and the results were evaluated for a very short interval in the real time domain using analogue and digital techniques. The errors were estimated

as less than 10%.

A thorough discussion of the various types of strain gauges, their circuit connections, temperature compensations, proper calibration and recording techniques are contained in many text books.

The Handbook of Shock and Vibration, edited by Harris and Crede (1961) has a number of chapters devoted to experimental methods using strain gauges. Some books are devoted entirely to strain gauges such as the books of Perry and Lissner (1962) and Neubert (1967). Several other books cover photo-elastic methods and strain gauge techniques. These are the works of McMaster (1963), Dove and Adams (1964).

Two recent publications on the use of strain gauges in dynamic measurements are a manual of the SESA (1979) and a D.I.Y. strain gauge transducer by Pople (1980).

CHAPTER VII

EXPERIMENTAL INVESTIGATION OF TRANSIENT FLEXURAL WAVES

7.1. Experimental setup

7.1.1. The impact mechanism

The impact method is considered as the simplest method of producing pulsed loading. An impulsive load is usually of the order of microseconds and it requires a finite rise-time to reach its highest value. A pulse is considered transient when it is short compared with the fundamental mode of the bar.

The impact can be achieved by a sphere impinging on the bar and the resulting pulse can be predicted by the Hertzian theory. An impulse can also be produced by the longitudinal, central or eccentric impact of two bars of the same diameter. The rise time of the pulse depends on how rapidly the end faces come into contact and this has led to experimental difficulties. To overcome these difficulties many workers have used bars with rounded ends. These types of impacts are called low velocity impact.

Other forms of impact, so called high velocity impact, are those of bullets fired against targets and the use of explosives. These require great care to be reproducible in the shape and amplitude of the pulses. The specimens are usually destroyed after each test and high velocity loadings are more used in plastic wave propagation studies.

The advantages of low velocity loading are that the same specimen can be used over and over again and when the end of the bar is rounded they can be easily repeated to reproduce exactly the same pulse. Furthermore, the duration and amplitude of the stress pulse can be varied by changing the impact velocity and the length of the striker.

It will be assumed that the one-dimensional theory is sufficient to describe the flexural wave propagation in the bar and that the stress is uniformly distributed across any section of the bar. It has been

shown experimentally (Davies, 1948) and theoretically (Prescott, 1942) that the stress and displacement become uniform over the cross section when the pulse had travelled a distance equal to four or five times the diameter of the bar from the point of impact.

In this work, the bending wave was produced by the eccentric longitudinal impact of a bar 1.0m long and 25mm in diameter with longer uniform bars and with bars of discontinuous cross section. The test bar and the striker were both suspended horizontally by fine wires from a suitable dexion framework.

The two bars were of mild steel and were free to swing in the direction of their length and to collide end to end. The end face of the test bar was flat and the impact end of the striker was rounded. The test bars were suspended by fine piano wires, 0.0167 inch in diameter, looped around the bar at about 40mm from both ends and the wires were attached to threaded hooks after passing through small bolts which were used for coarse horizontal adjustment. Finer adjustments could be made with the locking nuts on the threaded hooks.

The striker was also ballistically suspended with similar fine wires passing through two eye pieces bolted on the top of the striker at about 25mm from both ends. The upper ends of the wire were attached to threaded hooks fixed on the same dexion frame work.

The general arrangement of the test rig is shown schematically in figure 7.1 and is photographed in figure 7.2.

The striker could be adjusted to any desired eccentricity and the eccentricity was measured directly by tracing the off-centre position of the impact. The plane end face of the test bar was covered by a hi-spot engineers blue and after each impact the plane end was pressed against a white piece of paper to produce an indentation which showed a spot locating the position of the impact. This method was considered more accurate than the usual method of measuring the difference in the

heights of the two bars when in rest. The second method involves a certain amount of inaccuracy due to the stretching of the piano wires during the swing.

The horizontal positions of the test bar and the striker were so adjusted that they just touched each other when in rest position.

The impact was achieved by pulling back the striking bar a given distance, 180mm in most experiments, to produce a loading pulse of a given amplitude.

The linear elastic behaviour and small deformations were guaranteed through small impact velocities and various impact velocities could easily be achieved by pulling back the striker to different distances.

A release mechanism was devised to hold the striker at the desired distance by a spring force which was released to allow the striker to swing freely as a pendulum and to collide eccentrically with the test bar. The simple release mechanism contributed to the accuracy and reproducibility of the results.

When the striker rebounded, it was prevented from making the second contact and hence the test bar was loaded only once per impact.

7.1.2. The strain-gauge circuits

The use of electrical methods, especially the strain gauges, for the measurement of dynamic transient strains has the advantage, in addition to its simplicity, of obtaining directly the time dependence of the variables such as strain-and stress-time curves.

In the present work, bending strains and longitudinal strains were measured separately using the same strain gauges but in different bridge connections. The metal surface of the mild steel test bars was properly prepared for mounting the strain gauges using Loctite, IS496-Cyanoacrylate, adhesive.

The strain gauges were mounted diametrically opposite to each other at each gauge point at several positions along the test bars, as shown

in figure 7.3. The strain gauges were so connected in Wheatstone bridges to be sensitive either to symmetrical (longitudinal) strain components or to antisymmetrical (bending) strains. Each Wheatstone bridge contained two active strain gauges positioned at the same gauge point and two dummy strain gauges, cemented to a piece of mild steel, provided the temperature compensation.

The strain gauges used for the uniform bars were type N11-FA-8 of Showa measuring Inst.co. Ltd. with a gauge length of 8mm and 119.8Ω resistance. However, for the test bars with discontinuity of cross section, strain gauges with a gauge length of 4mm and 120Ω resistance were used. These were type 4/120/EC foil strain gauges of Tinsley Telcon Ltd. The gauge factors of the strain gauges were 2.10 and 2.07 respectively. The block diagrams of the Wheatstone bridges for longitudinal and bending strain measurements are both shown in figure 7.4. The use of two active gauges doubles the sensitivity of the Wheatstone bridges and eliminates the nonlinearity effect involved in the use of one active strain gauge.

To calculate the output of the Wheatstone bridge circuits used for both static and dynamic measurements the following general equation can be used (Dove and Adams, 1964 and Pople, 1976)

$$\frac{e_o}{e_i} = \frac{R_{g1}}{R_{g1} + R_{g2}} - \frac{R_{g4}}{R_{g4} + R_{g3}} \qquad (7.1)$$

For a symmetrical bridge with $R_{g1} = R_{g2} = R_{g3} = R_{g4} = R_g$ and with one active arm $R_{g1} = R_g + \Delta R_g$, the output voltage, e_o, is directly related to strain

$$e_o = \frac{\Delta R_g}{4R_g} - \left[1 - \frac{\Delta R_g}{2R_g}\right] e_i \qquad (7.2)$$

$$e_o = \frac{GF\times\varepsilon}{4 + 2GF\times\varepsilon} e_i \qquad (7.3)$$

where GF = the gauge factor ($\Delta R_g/R_g\varepsilon$)

R_g = the gauge resistance

e_i = the imput voltage

The dynamic sensitivity of the Wheatstone bridge can also be written in terms of the current to the bridge (I) and the strain in each bridge arm

$$e_o = \frac{GFxIxR_g}{4}(-\varepsilon_1 + \varepsilon_2 - \varepsilon_3 + \varepsilon_4) \qquad (7.4)$$

The net strain (ε_{net}) depends upon the number of guages being strained and the strain in each gauge.

Two active gauges were used for the measurement of axial strain (Fig. 7.4a) and for the measurement of bending strain (Fig. 7.4b). The active strain gauges were connected in such a way that their output was additive. This helped to reduce the nonlinearity for axial strain and to eliminate it for bending strain (Troke, 1976), with a sensitivity twice as large as that of the one-arm unbalanced bridge. The net strain for both 1/2 bridges is $\varepsilon_{net} = 2\varepsilon_1$.

The dynamic sensitivity of the 1/2 bridge used for axial strain measurement where two opposite arms are unbalanced, is

$$e_o = \frac{GF \times \varepsilon}{2 + GF \times \varepsilon} e_i \qquad (7.5)$$

The dynamic sensitivity of 1/2 bridge used for bending strain measurement where adjacent arms are unbalanced, is

$$e_o = \frac{GF \times \varepsilon}{2} e_i \qquad (7.6)$$

The calibration of the strain gauge circuits was achieved using the shunt calibration method. It involved the production of a known change in resistance by means of a parallel resistor or resistors with one of the active gauges. The change in resistance produced by connecting a shunt resistance, as shown in fig. 7.4(a), is computed as follows

$$\frac{1}{R_{(g + sh)}} = \frac{1}{R_g} + \frac{1}{R_{sh}} \tag{7.7}$$

or

$$R_{(g + sh)} = \frac{R_g R_{sh}}{R_g + R_{sh}} \tag{7.8}$$

$$\Delta R_{ba} = R_{(g + sh)} - R_g \tag{7.9}$$

$$\Delta R_{ba} = \frac{-R_g^2}{R_g + R_{sh}} \tag{7.10}$$

substituting into

$$GF = \frac{\Delta R_g / R_g}{\varepsilon} \tag{7.11}$$

$$\varepsilon_{eq} = \frac{R_g}{GF(R_g + R_{sh})} \simeq \frac{-R_g}{GF \times R_{sh}} \tag{7.12}$$

where ε_{eq} is the equivalent strain, defined as the strain required in the single gauge to produce the same signal as is produced by connecting the shunt resistance R_{sh}.

When the output of two gauges is made additive in the Wheatstone bridge, as was the case with 1/2 bridges used in the measurements, then the deflection per unit of strain is twice that when only one gauge is active and the strain that must be applied to each of the two gauges to produce a signal equal to the calibration signal is

$$\varepsilon = \frac{R_g}{GF(R_g + R_{sh})} \times \frac{1}{2} \simeq \frac{R_g}{GF \times R_{sh} \times 2} \tag{7.13}$$

7.1.3. The measurement instrumentation

The electrical output of the strain gauge and the bridge circuit is comparatively small and considerable amplification is required to drive the commonly used oscilloscopes.

The strain gauge circuits were connected to shielded and earthed leads. The leads of the Wheatstone bridge circuits at locations to be measured were plugged in to 3A10 transducer amplifiers manufactured by Tektronix Inc.

Two 3A10 amplifiers were used and they were mounted in a Tektronix power supply unit type 129 plug-in unit. The 3A10 transducer amplifier exhibited a bandpass with a drop of 3dB at 10 megahertz and selectable upper and lower frequency cutoff. A variable, calibrated DC-voltage source is also provided by the 3A10 unit for powering the strain gauge bridge.

With only two 3A10 amplifiers available, never more than two Wheatstone bridges could be connected during one impact and the impact had to be repeated for a complete set of results from all strain gauge locations.

Signals representing the strains at several positions along the test bars were recorded by direct measurement and also by the use of digital transient recorders of the type DL901 manufactured by Data Laboratories Ltd.

In the direct measurement system, the outputs of the two 3A10 amplifier units were fed into a 3A6 dual trace amplifier which was incorporated in the Tektronix dual beam storage oscilloscope type 564B together with a 3B3 time base unit.

A permanent record of signals on the oscilloscope screen was obtained using a Polaroid oscilloscope camera type A, supplied by Telequipment Ltd. The film used was type 47 high speed polaroid Land film, with ASA exposure index of 3000 in bright sun and produced black and white positive prints.

In the second measurement system, the signal output of the 3A10 amplifiers was fed into the two DL901 transient recorders. The transient recorder is a digital instrument and during recording each sample of the signal is converted into a digital number and stored in the memory.

The DL901 has 1024 words of memory, and the amplitude resolution is to one part in 256 (8 bits). It is necessary to select a suitable

sampling rate to avoid the occurance of 'aliasing' because of too slow sampling rate. Sampling at 2 μs intervals provides for example 500 words in 1 ms trace.

The output of the two transient recorders was fed into the two channels at the 3A3 unit of the storage oscilloscope and could be photographed with the polaroid camera as in the first system of measurement. In addition, the DL901 provided the signal input for a two channel 26000A3 XY-plotter which was used for the simultaneous recording of the strain time history of two locations.

The output of the DL901 can also be recorded on cards or tapes to provide data input to a digital computer such as the HP-Fourier analyser.

The two DL901 units were used in the single shot mode to record and digitise the single transient signal at two locations and to store in the memory. The trigger signal was taken from the signal itself and the pre-trigger recording mode made it possible to obtain the wave form both before and after the trigger. Figure 7.5 shows the measurement instrumentation used for the two measurement systems and Fig. 7.6 represent their block diagram.

In the first direct measurement system, an external trigger signal was needed to initiate the operation oscilloscope time base. This trigger signal was obtained from a piezoelectric crystal gauge mounted on the test beam near the impact end.

7.1.4. Experimental procedure and preliminary measurements

The eccentric impact of a bar by a striker must induce a stress system which has both symmetrical and antisymmetrical components.

The objective of this study was not to investigate the problem of eccentric impact from a comprehensive point of view, but rather to concentrate on the investigation of the beam in bending, i.e. to study the antisymmetrical flexural strain wave propagation along the beam through-

out the impact cycle, together with the complexity of wave interaction due to the bending wave reflections from boundaries and discontinuities.

These bending waves were recorded as rapidly changing strains for any given location and time in the form of photographs and plots.

The experiments confirmed that, due to eccentric impact, longitudinal and bending waves were, in general, superimposed on each other. However, the Wheatstone strain gauge circuits facilitates their separate measurements.

A preliminary measurement of longitudinal strain was needed to determine the input pulse due to eccentric impact. This was employed to obtain the applied axial force and the applied bending moment.

The input pulse shape was determined from the recording of the longitudinal wave at the first position along the uniform cylindrical beams and the beams with discontinuity of cross sections.

After the preliminary measurements of longitudinal waves, most of the measurements were concentrated on the bending waves.

The impact test was carried out by adjusting the bar and the striker to be just in contact when hanging freely and by drawing back the striker through a known distance (in most cases a distance of 18cm) and allowing it to swing back by gravity using a specially devised release mechanism. The radius of swing for the striker was 1.3m.

When the striker rebounded after the strain pulse returned to its impact end, it was prevented from making a second impact by holding it back and the specimen was loaded only once per impact. The linearly elastic behaviour and small deformations were guaranteed through small impact velocities. The impact end of the striker was slightly rounded in order to make the pulse easily reproducable.

In most experiments, the transient recorder DL901 was used to record the single transient signal using the "pretrigger mode" where the trigger was taken from the signal itself. The oscilloscope had

two time-base generators. The trigger signal initiated the operation of the first time-base generator which then provided a preset delay interval before triggering the second time base. This resulted in a single sweep of the oscilloscope beam trace at the sweep rate of the second time base. The use of varying sweep rates of 5ms and 10ms allowed the recording of longitudinal and bending strains and overall trace durations of 5 and 10ms were obtained, although the working range was usually 1ms.

The measurement of both longitudinal and bending strains was made on cylindrical test bars using strain gauges. The dimensions of the rod and the locations of the strain gauges were shown in figure 7.3. In order to produce the bending strain, the striker was allowed to strike as far off centre as possible and the maximum eccentricity was always smaller than the radius of the test bar.

Figure 7.7a shows the pulse shape of a longitudinal pulse measured at the position x/d = 12 of the uniform test bar subjected to the eccentric impact of a striker 1m long. The input compressive pulse takes 90 μs to reach its maximum amplitude and remains at this value until the arrival of the reflection from the far end of the striker which is the shorter of the two colliding bars. When the reflection in the 1m striker has returned to the contact point, the pressure decreases and soon after this the contact between the two bars ceases. The pulse duration was typically 390 μs and agreed very well with estimation based on $t = 2L/c_1 = 389$ μs with a strain of about 50 μ strain (με) in good agreement with $\varepsilon = \frac{1}{2E}\rho v c_1 = \frac{v}{2c_1} = 47.8\ \mu\varepsilon$.

The variation of the striker length affects the input pulse considerably. Figure 7.7b shows that when a shorter striker 31cm long was used, the pulse duration was much shorter and the amplitude started to decrease as soon as it reached its maximum value after about 100 μs.

The record shows the longitudinal strain measurements at two positions

along the uniform test bars, at x/d = 12 and 84.

The short striker could not provide an input pulse of trapezoidal shape approximately obtainable with the striker of 1m. The 1m striker was therefore used throughout the experiments in order to compare the results with theoretical predictions.

The trace in figure 7.8a covers a duration of about 5ms and shows the reflecting longitudinal strain waves from the end of the uniform test bars of 3m length where each reflection is accompanied by a change of sign. The strain measurement was carried out at the position x/d = 12 from the impact end. It is seen that the reflection of the input compressive wave from the far end arrives at this position as a wave of tension. However, soon after its arrival, the strain wave is relieved and its spreading is terminated by a compressional strain wave arriving from the near end of the test bar. The duration between two peaks of the same sign corresponds to the strain wave travelling twice the bar length.

The bending strain measurement of position x/d = 12 is shown in figure 7.8b and is obtained by the same pair of strain gauges used to measure the longitudinal strain of figure 7.7a, but with a Wheatstone bridge connection as shown in figure 7.4b to cancel the symmetrical strain components. The bending pulse shape is markedly different from the longitudinal pulse at the same position and the bending strain has changed drastically after travelling a distance of 12 diameters and shows a considerable negative portion as opposed to the positive (compression type) bending strain input.

Two traces of strain and time base calibrations are shown in figures 7.9a and 7.9b respectively.

The calibration of the strain was carried out by photographing and plotting a signal of known amplitude with all instrument controls set the same as for the actual impact strain measurements. This signal

was obtained by switching a fixed resistance of known magnitude parallel to the active legs of the longitudinal and bending strain bridges in a so called shunt resistance calibration. The resistances were provided by a resistance box containing several resistances and two resistance boxes (Box A and Box B) were used. The exact values of these resistances were measured by a logarithmic LCR Bridge type B500 of Wayne Kerr Co. Ltd.

The calibrations were made at frequent intervals during the measurement and a photograph of a voltage change display is shown in figure 7.9a.

The calibration was carried out during each set of experiments for each strain gauge circuit and the equivalent longitudinal and bending strain was deterimined for the strain gauges specified in Table V and as they were actually connected and used at the various positions along each of the test bars.

The exact values of the shunt resistance used and the corresponding equivalent strains are given in Table VI.

The sweep speed calibration was made by means of a sinusoidal signal generated by a function generator (Feedback FG 600) with a frequency of either 1 or 10 kHz. The sinusoidal wave was used to check the accuracy of the time base which was found to be accurate and it was assumed that subsequent sweep would be unchanged.

The sweep speed calibration was used to determine the duration of pulses and times of wave arrivals at the various gauge positions. An example of the sweep speed calibration is shown in figure 7.9b for a 1 kHz sine wave.

The experimental results were checked by repeating the impact at least three times at each station and for each set of recordings. It was found that repeat measurements of the strains at a gauge position were practically identical for a given set of conditions and the strain profile could be reproduced almost exactly with negligibly small variation in the strain amplitude. Figure 7.10a represents the impact

strain repeated 5 times as photographed at positions x/d = 4 from the impact end of a circular test bar with discontinuity of cross section.

The repeatability of the impact was particularly important since several impacts were needed to obtain a complete set of results from all strain gauge locations where only a simultaneous measurement of two gauge points at each run was possible.

However, the limitation of the measuring equipment was not a serious disadvantage since the eccentric impact was easily reproducable.

By varying the velocity of the striker it is possible to produce pulses of various amplitude. Figure 7.10b presents the recordings of three different pulse shapes obtained simply by pulling back the 1m striker to the distances of 14cm, 18cm and 22cm from the impact end of the test bar. It is seen that the longitudinal pulse in all three cases has the same length since the pulse length is independent of the impact velocity.

It was decided to use a constant impact velocity corresponding to drawing back the 1m striker a distance of 18cm which produced a low velocity impact of ca. 0.5 m/s.

The longitudinal impact strain as measured at the position 1 (x/d=4) of the circular bar with discontinuity of cross section introduced at the middle of the 2m long test bar is shown in figure 7.11a and the eccentric impact had an eccentricity of 7.85mm. These measurements of the symmetrical strain near the impact end were used to calculate the total force of impact and then multiplying this force by the eccentricity of the impact, the applied bending moment could be obtained.

Comparing the impact strain recorded in figure 7.11a with the impact strain in figure 7.7a, it is seen that due to the partial reflection of the compressive wave from the position of discontinuity which reaches the gauge position before the reflected wave in the striker reaches that position, there is a minor pressure increase.

This difference from the pulse shape in the uniform circular bar can only be explained in terms of wave reflections at the discontinuity of cross section where the diameter of the test bar is increased by 1/4 of its value (from 25.4mm to 31.75mm).

The effect of the eccentricity variation and the sensitivity of the bending strain measurement bridges was checked in the results presented in figure 7.11b.

An almost central impact was carried out and the bending strain at gauge position 1(x/d = 4) and the longitudinal strain at gauge position 2(x/d = 32) of the circular test bar with discontinuity of cross section are shown in figure 7.11b for an overall duration of 10ms.

It was necessary to enlarge the scale of channel I five times to show the small trace of the bending strain whereas the longitudinal strain retained its original intensity. The recorded bending strain due to central impact comprised only $\pm$5% of the bending strain which could be produced by eccentricity of 7.85mm used in most measurements. Therefore, the bending strain bridges were considered to produce a very good symmetrical strain cancellation especially when one realises that it is extremely difficult to produce a perfect central impact.

Figure 7.12a shows the longitudinal impact strains at the gauge positions x/d = 4 and 32 in the test bar with the discontinuity of cross section situated at the middle of the bar (x/d = 40).

It is seen that whereas the pulse shape at position I cannot reach anywhere near its original input value, as was explained in figure 7.8a, the impact strain at the position near the middle of the bar is allowed to reach almost its original amplitude. There is sufficient time before the reflection of the travelling wave from each end of the bar arrives at that position. This result is in complete agreement with the theory of strain wave propagation.

The pulse shape of the bending wave is much more complicated since

the velocity of flexural waves in steel bars is strongly dependent on the wave length of the harmonic components in any input resulting from the impact.

The recordings of bending wave measurement in position 1 and position 2 of the 2m long bar, described in the previous paragraph, are shown in figure 7.12b. It is seen that the bending wave undergoes considerable dispersion as it travels along the bar and it is clear that there is no definite velocity of propagation for bending strain wave pulses.

At position 1 ($x/d = 4$) the original pulse shape is still recognisable whereas the bending strain wave at position 2($x/d = 32$) has undergone considerable dispersion and shows negative and positive peaks within the duration of the original positive input pulse.

The plots corresponding to figure 7.12a and 7.12b obtained by the xy-plotter are presented in figure 7.13 and figure 7.14 respectively.

7.2. Measurement of material properties

7.2.1. Young's modulus and density measurements

In order to determine the density of the test bar made of mild steel, the weight of a piece of the test bar was obtained using a precision scale. The dimensions of the same piece were measured using a micrometer and the density was calculated as the ratio of the weight to the volume which was found to be

$$\rho = 0.777 \times 10^4 \text{ kg/m}^3$$

The modulus of elasticity E was determined by static and dynamic measurements.

The static value of the Young's modulus E was obtained from an ordinary tensile test where a tensile test specimen was prepared from the same mild steel as the test bars. The static loading was carried out on Amsler tensile machine and an extensometer was used for the elongation measurement.

The modulus of elasticity E was obtained as the slope of the linear

portion of the stress strain diagram in accordance with Hooke's law.

The static value of the Young's modulus was

$$E = 2.06 \times 10^{11} \text{ N/m}^2$$

The dynamic value of the elastic constant can be obtained by two methods, the wave propagation methods and vibration method.

In the wave propagation method, the measured value of the propagation velocity is used to obtain the value of the elastic constants.

The three types of elastic waves, extensional, torsional and flexural, can be propagated along a solid isotropic homogeneous solid rod. The velocity of propagation depends on the elastic constants and the density of the material.

The velocity of longitudinal wave propagation was measured and found to be $c_1 = 5140$ m/s. The description of the wave velocity measurement is included in the next section.

Using the known relationship $c_1 = \sqrt{E/\rho}$ or $E = c_1^2\rho$, the dynamic modulus of elasticity can be obtained as

$$E = 2.05 \times 10^{11} \text{ N/m}^2$$

The Poisson's ratio μ for the mild steel test bars was assumed as $\nu = 0.29$ and the value of the dynamic modulus of rigidity G can be obtained from

$$G = \frac{E}{2(1 + \nu)} = 0.796 \times 10^{11} \text{ N/m}^2$$

This value of G is used to obtain the shear wave velocity $c_2 = \sqrt{k^2 G/\rho}$ which is for $k^2 = 0.886$

$c_2 = 3011$ m/s

The wave velocity method is known to be extremely accurate and has been widely used in obtaining the dynamic value of elastic constants.

The vibration methods and particularly resonance methods are also common in obtaining elastic properties of materials.

In the resonant method, an oscillating force of fixed amplitude and varying frequency is applied to a mechanical system and the resonant

frequency of the resulting vibration is dependent on the elastic properties of the system.

The longitudinal, torsional and flexural vibrations are used in the resonant method to determine the elastic constants of metals and some of the early works have been described by Kolsky in his book in 1953.

Goens (1931) solved the Timoshenko's equation relating Young's modulus to the flexural resonance frequency for bars of different cross section.

Pickett (1945) had further simplified Goen's solution and obtained the following simplified formulation for E

$$E = \left[\frac{2\pi L^2 f}{r m^2}\right]^2 \rho T$$

where f is the flexural resonance frequency, r is the radius of gyration, m is a constant which has higher values for higher modes with m = 4.730 for the fundamental mode, where T is a correction factor which varies with r/L and μ.

Spinner et. al (1960) carried out careful measurements of mechanical flexural and longitudinal resonance frequencies for steel rectangular and cylindrical specimens. They showed that the theoretical correction factors of Goen's were in fair agreement with experimental results, with the numerical solution obtained by Tefft (1960).

Cowper (1968) pointed out that the measurements of Hardie and Parkins (1968) of the influence of shear and rotatory inertia on the value of the Young's modulus was inaccurate since they used an inadmissionable averaging method for the frequency which assumed that shear and rotatory inertia effects reduce the frequencies of all higher modes by the same percentage, contrary to the Goen's correction factors.

Ritchie's work in 1973 gave experimental support to Cowper's criticism and showed that the Timoshenko theory must be used in calculating the Young's modulus for beams vibrating in their higher

modes as is the case in transient loading.

One of the disadvantages of the resonance frequency method is the loss of energy at the supports and the difficulty of realizing ideal boundary conditions. This was demonstrated by Rosinger and Ritchies (1974) for the case of a cantilever resonant beam, where the relationship between the experimentally measured resonant frequency and Young's modulus of the material deviated from theoretical predictions based on ideal boundary conditions.

A different approach to the determination of dynamic elastic constants is their analyses from the view point of microseismology in a so called pulse method, a form of the wave propagation method. In this method, a travelling pulse along the specimen is detected by the receiving crystal with the arrival times giving the velocity of propagation.

The pulse method has been used by Hughes et. al (1949); Kolsky (1954) and Bell (1960). These works were reviewed by Bell (1973)

The basic difficulty lies in the interpretation of the experimental results, where a number of separate transmitted and reflected pulses are detected at the end of the rod.

In a more recent paper, Goldsmith and Katsamanis (1979) used the wave propagation method to obtain the dynamic Young's modulus of perforated polymeric bars.

7.2.2. Wave velocity measurement

The wave velocity measurements were carried out for longitudinal waves travelling along uniform circular test specimens and circular specimens with discontinuities of cross section.

The wave velocity was measured by two observations of either the recording of the strain at one location or the strain pulse recordings of two strain gauges positioned at a known distance.

In the first method, the interval between two consequative pulses

of the same sign represented the time required for a pulse to travel twice the length of the bar. The wave velocity is obtained from each of the strain pulse traces shown in figure 7.15a for two positions along a circular rod 3.295m long with the discontinuity of cross section at 1m from the impact end. The calculation of the wave speed was based on the corresponding plot obtained by the xy-plotter, where the sweep time of 5ms was prescribed by a distance 36.2mm long and the distance between two peaks of the same sign was 9.3mm. The travelling time t was found as

$$t = \frac{9.3 \times 5}{36.2} = 1.28 \text{ ms}$$

and the wave velocity c_1

$$c_1 = \frac{2 \times 3.295 \times 10^3}{1.28} = 5148 \text{ m/s}$$

In the second method, the wave velocity between two strain gauges was obtained by dividing the distance between the gauges by the difference in arrival times of the pulse as monitored by each strain gauge circuit connected for longitudinal strain measurement and recorded simultaneously in the oscilloscope trace shown in figure 7.15b for two strain gauges 1.8m apart.

The travelling time t was 0.35ms and the wave velocity

$$c_1 = \frac{1.8 \times 10^3}{0.35} = 5143 \text{ m/s}$$

The wave velocity measurements were utilized in the two circular test specimens with discontinuity of cross section and in the uniform circular rod and although some variations in pulse velocities were found from test to test, where values between 5120 m/s to 5160 m/s were observed for the longitudinal wave velocity c_1. An average value of c_1 = 5140 m/s was obtained which was well within experimental error.

The error is mainly introduced in the measurement of arrival times and it can be concluded that the longitudinal pulses are travelling with the wave velocity c_1 in the cylindrical specimen.

The effect of the reflection at the shoulder can be observed

from the comparison of the oscilloscope traces of longitudinal strain pulses in the unifrom circular rod (figure 7.8a) and the recordings of the pulse shapes in the two circular rods with discontinuities of cross section (figure 7.12a and figure 7.15a).

In the strain pulse recording shown in figure 7.8a for the uniform bar at strain gauge laocation x/d = 12, the time required for the first reflection of the input compressive wave from the far free end, due to applied bending moment at x = 0, to arrive at the strain gauge location as a tension wave, was found to be t = 1.05ms corresponding to a longitudinal wave velocity to 5142 m/s.

The reflection arrives at the strain gauge position after the contact with the striker ceased and the amplitude of the input pulse dropped to zero.

The results shown in figures 7.12a and 7.15a are for the test bar with discontinuity of cross section at x/d = 40, at a distance of 1m from the impact end, with an increase in cross section causing a partial reflection of the incident wave of the same sign. The reflection from the discontinuity arrives at the strain gauge location before the reflection from the end of the striker has returned to initiate the amplitude decrease. This was seen as a small increase at the end of the impulse shape noticable only in the test specimen with discontinuitv of cross section.

The arrival of the reflections from the far end of the two stepped bars corresponded to the same longitudinal wave velocity of 5138m/s.

The recordings of the strain gauge location at 0.8m from the impact end are represented by the lower traces of figures 7.12a and 7.15a. It is seen that the reflection of the input compressive pulse arrives at the strain gauge as a tension pulse before the original pulse has dropped to zero in the shorter bar whereas the arrival time in the longer bar was after the input pulse has reached the zero position and the effect of the reflections from the position of discontinuity is clearly demonstrated.

The experimentally observed value of the longitudinal wave velocity and Young's modulus are in good agreement with values found in the literature as can be seen from the values of c_1, E, G, ν and ρ listed in table VII, where the experimentally obtained results in the present thesis are within the range of values found in standard textbooks and well known references related to the field of stress waves in solids.

The travelling of the longitudinal wave along the bar with a constant velocity and the interactions of incident, transmitted and reflected waves can best be represented by a space-time diagram, as illustrated in figure 7.16 for the 2m long test bar with a change of its diameter at the middle from 25.4mm to 31.75mm.

The simple x-t diagram showed the propagation of the longitudinal wave in the striker and in the test bar where its arrival at each strain gauge location could easily be traced.

The arrival times of the compressive strain pulse are calculated from the instant of impact t = 0 when the 1m long hammer struck the test bar. At $t = L_1/c_1$, the pulse arrived at the position of discontinuity and the reflection from that position travelled back as a compression wave and arrived at the impact end at $t = 2L_1/c_1$, causing a small increase in the strain amplitude.

At time $t = L/c_1$, with $L = L_1 + L_2$, the compression wave arrived at the far end of the test bar and was reflected as tension wave to travel back to the impact end arriving at $t = 2L/c_1$, where at the same time a second reflection from the position of discontinuity also arrived.

7.3. Steady state vibration test

The purpose of the vibration test was to investigate how accurately the support of the test bars by fine thin wires reflected the free-free boundary conditions.

A free-free condition implies that there shall be no constraint on the beam. In practice, however, the weight of the beam must be supported and

and some loss of energy is expected at the support and constraint.

The support of the beam at the nodal points is obviously ideal, but the position of these points is not known exactly before the experiment is performed and, in any case, their position varies with each mode.

The use of a suspension which is very"soft" in the direction of displacement in vibration, achieved by hanging the beam by two vertical wires with virtually no constraints, but prevented vertical movement and the location of the wires near the end of the test bar was found to have an insignificant effect on the frequency. (Traill - Nash, 1953 and Hearmon, 1958).

The principle of the method was to excite and detect resonance in a test piece of the same material as the one used in the flexural vibration test, where the resonance frequency was monitored and measured.

The test bar was 1.09m long and had a diameter of 25.4mm and was supported by two thin wires at 15mm from each end.

The following instruments were used for the resonance test

i) Frequency oscillator Model E 503 of Goodmans Industries Ltd. with continuous frequency control from 5 cycles to 50 kc.

ii) Charge amplifier type CA/03 of D.J. Birchall

iii) Shaker type 10 of LWG Dynamic System Ltd.

iv) Pickup tranducer typer AQ 20 Accelorometer of Enviremental equipment Ltd.

v) Feedback digital frequency meter type FM610

vi) Storage oscilloscope type 564B of Tektronix Ltd.

The output of the oscillator was amplified through the power amplifier and was fed to the Shaker, whose mechanical energy in turn was transmitted to the specimen simply by holding the driver manually against the specimen. As the oscillator frequency was scanned, it reached one of the flexural resonance frequencies of the specimen and gave a large increase in the

amplitude of its vibration.

The resonance of the beam was detected by the pick-up tranducer which was mounted on one end of the beam and the output was fed into the oscilloscope. The excitation method used was found to produce satisfactorily the flexural modes of the free vibration. This was checked by removing the exciter at resonance and observing on the oscilloscope screen the drift in the resonance frequencies which was found to be negligibly small.

The purpose of the frequency counter, connected to the oscillator, was to provide a more accurate reading than the one possible by reading the oscillator scale directly. The same procedure was repeated for the higher flexural modes. The block diagram of the arrangement is shown in figure 7.17.

The specimen may be caused to resonate in different ways, longitudinally, flexurally (or transversely), and torsionally. However, longitudinal resonance generally occurs at very high frequencies compared to the bending vibration and the flexural vibrations are more easy to excite .

A more accurate method to obtain the various types of vibration and their overtones is the so called "probing" where the pick-up transducer is held against different parts of the specimen while it is vibrating in resonance and the resulting pattern of changes in the Lissajous figures seen on the oscilloscope establishes the type and higher modes of the particular resonance frequency.

The electrical phase relationships of the Lissajou figures seen on the scope are an exact reflection of the mechanical phase relationships existing in the specimen while it is in resonance (Spinner and Tefft, 1961).

In the experiment carried out to obtain the resonance frequencies, the use of a fixed pick-up transducer was found to give accurate results. At the fundamental flexural resonance frequency, the ends of the specimen are oscillating in the same direction (in phase) while the centre of the specimen is oscillating in the opposite direction.

One of the difficulties of the resonance method is that the coupling

between the driving system and the specimen may result in a change in resonant frequency. The simple method of holding the driver against the specimen was found not to affect the resonance frequency in any serious way.

The other difficulty is related to the realisation of ideal boundary conditions which is more difficult in the case of pinned ends and almost impossible in the case of clamping ends. This difficulty causes the measured resonance frequency to deviate from theoretical prediction. (Rosinger and Ritchie, 1975).

The damping in the beam also causes the experimentally observed resonance frequency to differ from theoretical prediction. Fortunately, this effect was very samll at low damping and could be ignored.

The first five flexural frequencies were measured and compared with theoretical predictions based on the elementary Euler-Bernoulli theory and the Timoshenko bending theory.

The frequency values are listed in table V111, together with the material properties of the mild steel test beam.

The frequency ratios and the precentage deviation of experimental and theoretical values are presented in figure 7.18a and figure 7.18b respectively where it is seen that for the free-free end condition, experimental and theoretical resonance frequencies of the fundamental flexural mode and its four overtones are almost identical. However, the deviation for the case of pinned-pinned ends (simply supported) is more pronounced, since this condition is more difficult to realise practically.

The Euler-Bernoulli theory for flexural vibration is formulated in the differental equation

$$\frac{\partial^4 y}{\partial x^4} + \frac{\rho A}{EI}\frac{\partial^2 y}{\partial t^2} = 0$$

The natural frequency of flexural vibration is obtained by calculating the roots of the frequency equation for a cylindrical beam

$$fn = \frac{\beta_n^2}{2\pi}\sqrt{\frac{EI}{\rho A}}$$

so that $$f_1 = \frac{(417303)^2 r}{4\pi L^2}\sqrt{E/\rho}$$

where $\beta_n L$ = 4.7303; 7.8539; 10.996; 14.137; 17.279 for the modes n = 1; 2; 3; 4 and 5 respectively in the case of a free-free beam and $\frac{I}{A} = \frac{R^2}{4}$ for circular cross-section.

The effect of shear distortion and rotatory inertia, which are taken into consideration in the Timoshenko theory, is to reduce the natural frequencies. (Ayre and Jacobson, 1950).

Haybey (1976) pointed out that frequency difference between measured and calculated Euler-Bernoulli values for the lower modes in the free-free configuration is proportional to a^2/L^2. The relationship was obtained by Rosinger and Ritchie (1977), where a was the beam width or the rod diameter.

The theoretical calculations according to the Timoshenko theory used the Göns correction factors to obtain the lower modes for the free-free end conditions

$$f_1 = \frac{d}{L^2}\sqrt{\frac{E}{1.262\ T_1\rho}}$$

$$f_2 = \frac{d}{L^2}\sqrt{\frac{E}{0.166\ T_2\rho}}$$

$$f_3 \quad \frac{d}{L^2}\sqrt{\frac{E}{0.043\ T_3\rho}}$$

Where T_1 = 1.002; T_2 = 1.0059 and T_3 = 1.0116.

The flexural resonance frequencies obtained by the Timoshenko theory differed very little from the predictions of the Euler - Bernoulli theory for the uniform beam tested, with a slenderness ratio of L/R = 85.8.

The results based on the Timoshenko beam equation for flexural vibration were slightly smaller than those given by the Euler-Bernoulli theory and the first were nearer to the experimental observations, as can

be seen from table VIII, where the difference between the three sets of results is less than 1% and the agreement with experimental results is very good.

However, in the higher modes of vibration, the effects of shear and rotatory inertia increase with the order of the mode.

The resonance flexural vibration method has been widely used to obtain the dynamic Young's modulus and the value of the shear correction factor k^2 for beams of circular and rectangular cross sections, as was described in section 5.1.

A detailed theoretical investigation of the flexural vibration of beams with discontinuity of cross section is included in appendix B, where the Euler-Bernoulli theory is considered to give satisfactory results for the lower modes of the flexural vibration for the beams with large slenderness ratio.

7.4 Experimental results

7.4.1. Free-free beams subjected to eccentric impact

7.4.1.1. Bending strains in uniform beam of circular cross-section

The experimental investigations of flexural transient waves are of relatively recent origin due to the complexities of bending strains and the difficulties involved in the analysis, where the bending strain is the strain due to the applied bending moment.

The bending strains in the various test beams were all produced by the low velocity eccentric impact of the 1.0m long striker. In the immediate vicinity of the impact point, the bending strain is three dimensional and the wave is not only propagated but also reflected from all surfaces.

It is quite possible that, at the point of impact, a plastic flow causes a localized damage. However, this damage is not easily detectable and was not considered. The measurements were carried out at positions along the beams starting at distances of 4 times the diameter of the beam

where the bending strains were regarded as completely elastic.

The input pulse consisted of a longitudinal and a flexural transient wave of finite rise time of 0.09ms and each type of wave was measured separately using different connections of the same strain gauges ; with most of the experiments concentrated on the bending strain observations.

Figure 7.19(a) shows the recording of the bending strains at position 1 and position 2 of the uniform beam of circular cross section (Test beam I of Fig. 7.3) where the two positions along the beam correspond to 0.3m and 2.1m from the impact end respectively.

The output of the oscilloscope for position 1 is magnified twice in the vertical and horizontal scales in figure 7.19(b) and the trace shows that a considerable part of the incident compressive bending strain has been changed into tensile bending strain.

At position 2 the bending wave oscillates more rapidly and several peaks of alternating signs and increased amplitude can be seen in the time progress of the impact strain.

The bending strain at position 1 has a compressive peak of about 89 microstrain at about 0.7ms and the peak of the compression strain at position 2 is about 52 microstrain as compared to the peak of the input bending strain of about 113 microstrain. In the discussion the positive sign means bending strain of compressive type and negative sign means bending strain of tensile type.

All oscillograms are presented on a strain time basis. The strain scale was calculated from the strain gauge data using the shunt calibration and employing the static gauge factor given by the manufacturer. The anti-symmetric strain component due to bending was obtained as half the total of the strains measured at the upper and lower surface of the bar, assuming a uniform strain distribution across the section of the test beams.

7.4.1.2. Beam with discontinuity of cross section at the middle

The bending strain-time results are recorded for six positions along the short stepped beam of 2m length with the discontinuity of the cross section at the middle where the diameter of the cross-section was increased from 25.4mm to 31.75mm ($d_2 = 1.25d_1$). Two pairs of strain gauges were located at 0.1m from each end of the beam (position 1 and position 4) and two other pairs of strain gauges were situated at 0.8m from each end (position 2 and position 3). Two additional pairs of strain gauges were cemented immediately before and after the shoulder of the test beam (position 5 and position 6). The position of the strain gauges and the dimensions of the beam are illustrated in figure 7.3(a).

The pulse shape of the input bending moment was obtained from the longitudinal strain measurement at position 1, used first to obtain the input force as 4831.5N and for an eccentricity of e = 7.85mm, the input bending moment was 38Nm and the corresponding input bending strain was found to be 115με.

A simultaneous recording of the output bending strain of each position together with position 1 was carried out and the reproducibility of the impact was found to be very good. Another set of measurements included the signal output of each two of the strain gauge bridges connected for bending strain time history observations.

Typical traces of the oscilloscope are shown in figures 7.20 and 7.21. The upper and lower traces in figure 7.20(a) correspond to the output of the strain gauges at position 1 and position 2 respectively where positive signals indicated as before negative strains. A portion of the same two signals are shown with enlarged scale in both axis in figure 7.20(b).

Figure 7.21 shows the strain gauge data obtained at position 3 and position 4 (Fig. 7.21a) and position 5 and position 6 (Fig. 7.21b) for an eccentric impact with e = 8.30mm.

The peak strain measured at 0.1m from the impact end (position 1)

was 108 microstrain and the pulse shape of the input pulse was still recognisable at this station.

However, at position 2, the bending wave had already several peaks of alternating sign and was more widespread over a longer time span.

At positions 3 and 4, situated on the larger diameter of the stepped beam, the bending strains were much smaller and more oscillatory in type as can be seen from figure 7.21(a).

Fig. 7.21(b) shows that an increase of 25% in diameter resulted in a drastic decrease in the propagated bending strain. The peak strain immediately before the shoulder was 51με and decreased to 18με immediately after the change of the cross section, a reduction of about 65% in the peak of the bending strain was caused by the relatively small change of the diameter.

The history of bending strain was plotted at the same time using the xy - plotter and a typical plot of the strain gauge outputs at positions 1 and 2 are presented in figure 7.22. These plots are particularly useful for direct comparison with theoretical solutions. They have the advantage of easier evaluation and are considered more accurate. Therefore the estimation of the peak strains and time location were mostly based on the plots rather than on the photographs of the oscilloscope traces.

7.4.1.3. Longer beam with discontinuity of cross section

The bending wave propagation was investigated in a second longer beam with discontinuity of cross-section (Test beam III) with a total length of 3.295m and a change of diameter from 25.4mm to 31.75mm ($d_2 = 1.25d_1$) at 1.0m distance from the impact end. Four pairs of strain gauges were located along the test beam and their positions are shown in Fig. 7.3.

Strain gauge data are presented in figure 7.23 and were obtained from the four stations, and the first three positions were exactly at the same distance from the impact end as in the shorter stepped beam

discussed in the previous section.

The comparison of the strain gauge data obtained from test beam 2 with those of test beam 3 provides useful information regarding the effect of the discontinuity on the bending wave where the reflected wave in the longer beam arrives considerably later at the gauge stations than in the shorter stepped beam.

In position 1 (Fig. 7.23a) the peak strain at 410μs after the wave front arrival is about 97 microstrain due to an eccentric impact with the 1.0m long striker and an eccentricity of e = 7.5mm. The small alternating oscillations arrive at later times when compared with the trace obtained from the same position of the shorter beam and therefore these oscillations are due to reflections from the far end of the beams. The effect of the reflection from the position of discontinuity is shown as a sudden abrupt change in the slope of the main pulse at the same instant in both test beams.

The similarity between the lower traces of Fig. 7.20(a) and 7.23(a) should be noted with differences starting at about 1ms from the bending wave arrival.

The first part of the output at position 3 is similar to the trace of position 2 except the amplitude decrease due to the effect of discontinuity and the earlier arrival of the smaller oscillations.

At position 4 it became more difficult to distinguish between the components of the transmitted bending wave through the cross section change and the reflections from the far end of the test beam.

Figure 7.24 presents an enlarged recording of the bending strain time history at positions 1 and 3 on the two parts of the stepped beam. No attempt was made to obtain the velocity of propagation since the transient bending wave is composed of components with different frequencies and different velocities of propagation clearly shown in the dispersion of the input bending wave even within short distances of propagation.

Therefore there is no significance in attempting to obtain velocities of propagation except that one should notice that any flexural disturbance was propagated with velocities lower than the bar velocity c_1 and in most cases longer sweeptimes were required to trace the bending wave arrival as compared with sweep times for tracing the longitudinal wave propagation.

7.4.1.4. Stepped beam subjected to eccentric impact at the larger end

The 2m long beam with the discontinuity of cross section at the middle (Test beam II of fig. 7.3) was subjected to eccentric impact at its larger end with an eccentricity of e = 9.5mm. The distances of the strain gauges from the large end were exactly the same as from the smaller end due to the symmetrical arrangement of the strain gauges along the test beam. However, positions 1,2,3,4,5 and 6 in the beam loaded at the large end correspond to positions 4,3,2,1,6 and 5 shown in figure 7.3 respectively.

Figure 7.25 shows the traces of bending strain at positions 1,2 and 3 and there is a clear similarity with Fig. 7.20 and 7.21 for the same test beam loaded eccentrically at its small end. The striker was the same as before, a 1m long bar with 25.4mm diameter.

The peak strain of the bending pulse is 78με at position 1 and at position 2 a peak strain of opposite sign with an amplitude of -41.6με can be seen in the lower trace of Fig. 7.25(a).

On the second part of the test beam with a reduced cross section the traces of the bending strains with increased amplitude and oscillations are illustrated in the lower traces Figs. 7.25(b) and 7.26(a) for position 3 and position 4 respectively where the upper trace of both figures represented the bending strain time records at position 1 near the impact end.

The bending strain at the two stations in the neighbourhood of the discontinuity, immediately before and after the change of cross section, is illustrated in figure 7.26(b) where a sharp increase in the bending

strain is noticable and peak strains are more than doubled due to a 25% reduction in diameter. The peak strain at position 5 was 23με and at position 6 about 56 microstrain (με).

7.4.2. Simply supported stepped beam of circular cross section

The effect of end conditons was investigated in a set of experimental results obtained for a short stepped beam simply supported at both ends and the strain gauge data obtained from the six stations along the beam are shown in figures 7.27 and 7.28.

The simple support was achieved by resting the test beam on two V-slots each consisting of two ball bearings mounted on an aluminum block and the blocks were mounted on an angle iron of about 1.0m height, bent in L-shape at its lower end and bolted on a concrete base to provide rigidity for the support.

The ends of the test beam were secured with collar brackets against horizontal movement and were supposed to allow rotation but no deflection.

The input bending moment was produced by the impact of the same 1.0m striker supported as before by thin wire and allowed to swing freely as a bifilar pendulum. The input transient bending moment had the same trapezoidal shape as for the case of the free-free beam and its value is obtained by measuring symmetrical strain, calculating the total force of impact and multiplying this force by the eccentricity of the impact.

The traces of the strain gauge data were similar to the trace obtained for the free-free beam and show that fixing the ends of the bar by collar brackets when resting on the V-slots had very little effect on the form and the amplitude of the transmitted and reflected bending wave pulse.

This suggests that the end supports did not satisfactorily produce the required simple support and the end conditions were merely free-free but now realized by resting the bar on V-slot ball bearings instead of the hanging thin wires.

7.4.3. Free-free stepped beam of rectangular cross section

The bending wave propagation was investigated in a free-free beam of rectangular cross section with a change of the height from 36.44mm to 50.8mm and with the same width over the whole length of the test beam,which is called test beam IV and illustrated in figure 7.29.

The change of the cross section was introduced at 1.0m from the impact end and the total length of the beam was 1.885m. Two pairs of strain gauges were located at the first portion of the beam at 0.1m and 0.8m position 1 and 2 from the impact end and a third pair of strain gauges was cemented on the larger cross section at 0.2m from the position of the discontinuity of crosss section (position 3).

The effect of the change of cross-section was investigated by two pairs of strain gauges located at 5mm distance from both sides of the position of discontinuity (position 5 and position 6.)

The test beam was hung edgewise with thin wires in exactly the same way as the test beams of circular cross-section pulled back a distance of 18cm and allowed to swing freely to impact the stepped beam of rectangular cross section.

The bending strains obtained at position 1 and position 2 are shown in figure 7.30 and traces of bending strains at positions 3,5 and 6 are shown in 7.31 as typical traces for the performed experiments.

The peak strain reaches 68 microstrain ($\mu\varepsilon$) at about 390μs at position 1 and reaches -36$\mu\varepsilon$ at 750 microsecond at position 2, and the dispersion of the bending wave is clearly demonstrated.

The effect of the change of cross section on the bending wave propagation is shown in the traces obtained from the strain gauges at position 5 and position 6 illustrated in figure 7.31(b). The increase of the cross section caused a drastic decrease in the transmitted bending wave where the amplitude of $\pm$49 microstrain was reduced to about $\pm$5 microstrain.

The bending strain build up at position 3 on the larger cross section must therefore be caused by reflection from the far end of the test beam.

The similarity with the strain gauge data of the circular beam with discontinuity of cross-section should be noticed with the discontinuity of cross-section affecting the transmitted bending wave more strongly in the beam of rectangular cross-section with abrupt change in the width than in the beam of circular cross section with abrupt change of diameter.

Each set of experiments was repeated at least three times and the bending strain amplitude against time at each position of strain gauges was measured with reference to the strain gauge output of the position nearest to the impact end (position 1) and the results showed a high degree of consistancy and were satisfactorily repeatable.

All experimental results were plotted using the xy - plotter in addition to their recording with the aid of the cameras.

The calibration of the horizontal axis was checked continuously and the shunt resistance calibration was carried out and repeated continuously for each strain gauge bridge connections.

Gauge type / Gauge Specific.	N-11-FA-8	4/120/EC(a)	4/120/EC(b)
Nominal resistance (Ω)	119.8	120	120
Gauge length (mm)	8	4	4
Gauge factor	2.10	2.07	2.11
Material alloys	-	Epoxy backed Copper-Nickel	Epoxy backed Copper-Nickel
Other specifications	Temp. Comp.	Temp. Comp.	Temp. Comp
Manufacturer	Showa	Tinsley Telcon	Tinsley Telcon
Test bar	uniform circ. bar	stepped bar of circular sect.	stepped bar of rectang. sect.
Batch No.	-	T 14 97	T 2078
Bridge supply voltage	5V DC	5V DC	5V DC

TABLE V Foil Strain gauge Specifications

	Shunt resistance (1)	Shunt resistance (2)	Shunt resistance (3)
Resistance Box A			
Nominal resistance (kΩ)	220	470	1000
Exact resistance (kΩ)	219.4	483	1056
Equivalent strain x 10^6 in bending strain bridge:			
N-11-FA-8 Strain gauge	129.97	59.04	27.0
4/120/EC(a) Strain gauge	132.07	60.0	27.45
4/120/EC(b) Strain gauge	129.57	58.87	26.93
Resistance Box B			
Nominal resistance (kΩ)	220	470	1000
Exact resistance (kΩ)	242	514	1095
Equivalent strain x 10^6 in bending strain bridge			
N-11-FA-8 Strain gauge	117.83	55.49	26.04
4/120/EC(a) Strain gauge	119.74	56.39	26.47
4/120/EC(b) Strain gauge	117.47	55.32	25.97
Resistance Box A			
Nominal resistance (kΩ)		470	
Exact resistance (kΩ)		483	
Equivalent Strain x 10^6 in longitudinal Strain bridge			
N-11-FA-8 Strain gauge		59.04	
4/120/EC(a) Strain gauge		60.0	
4/120/EC(b) Strain gauge		58.86	

TABLE VI Shunt resistance calibrations

Reference	$\rho/10^{4}$ kg/m^3	$E/10^{9}$ N/m^2	$G/10^{9}$ N/m^2	ν	c_1 [m/s]
Kolsky (1953)	0.78	206	79.46	0.29	5190
Markham (1957)	0.7825-0.784	197.47-213.19	79.086-82.119	0.286-0.292	5018-5219
Spinner et.al (1960)	0.7846-0.7854	204.44-207.29	80.53-8064	0.269-0.285	5152-5199
Baumeister & Marker Handbook (1967)	0.783	197.197-206.85	75.845-82.051	0.283-0.292	5018-5155
Johnson (1972)	0.775	204	80.85	0.271	5150
Graff (1975)	0.796	207	80.23	0.29	5060
Rosinger et.al. (1977)	0.7851	208.4	82.09	0.292	5152
Measured & used in this work	0.777	205.6	79.69	0.29	5120-5160

Table VII Physical properties of mild steel

Mode number n	1	2	3	4	5
Free-free end					
$\beta_n \ell$	4.7303	7.8539	10.996	14.137	17.279
Measured freq. values f_n	- 97.38	268.05	524.77	863.51	1279.87
Theor. frq. (E.B.)	97.87	269.83	528.92	874.251	1306.048
Theor. frq.(Timos.)	97.77	268.99	525.84	-	-
Theor. frq. ratio f_n/f_1	1.0	2.757	5.410	8.933	13.340
Exp. frq. ratio f_n f_1	0.995	2.739	5.362	8.823	13.077
prect diff f_e/f_t %	0.995	0.993	0.992	0.988	0.980
Pinned-pinned					
$\beta_n \ell$	3.142	6.283	9.425	12.566	15.708
Measured frq. f_n	42.10	173.92	347.80	641.38	1047.25
Theor. frq. (E-B)	43.185	172.69	388.58	690.74	1079.35
Theor. frq. ratio	1.0	3.999	8.998	15.995	24.994
Exp. frq. ratio	0.975	4.0273	3.054	14.852	24.250
prect. diff. f_e/f_t	0.975	1.007	0.895	0.929	0.970
ℓ = 1.09m; E = 2.056×10^{11} N/m^2; $\rho = 0.77743 \times 10^4$ kg/m^3					

TABLE VIII Comparison of theoretical and experimental results of flexural resonance frequencies

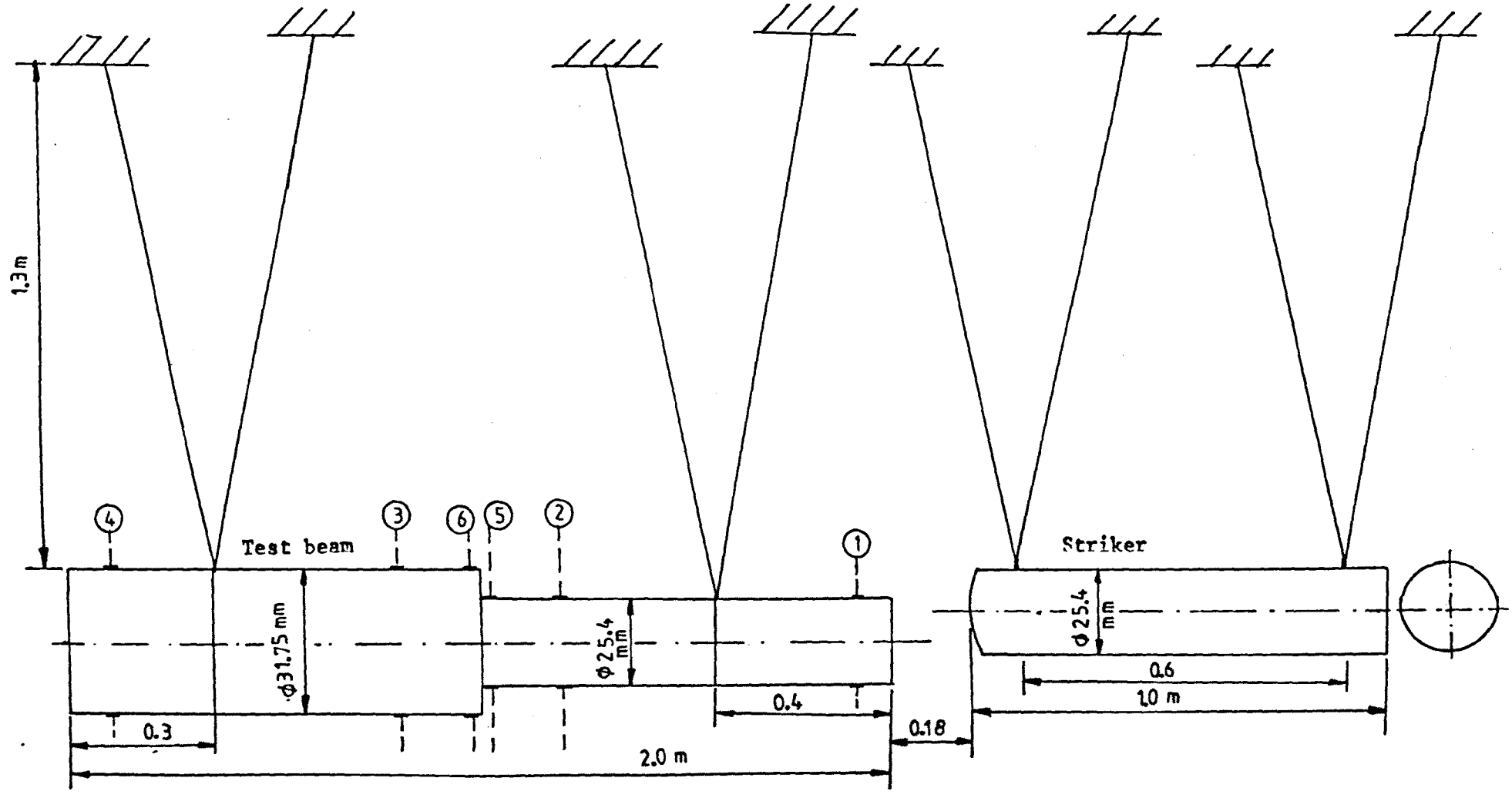

FIG. 7.1. SCHEMATIC OF IMPACT APPARATUS SHOWING STRAIN GAUGE LOCATIONS

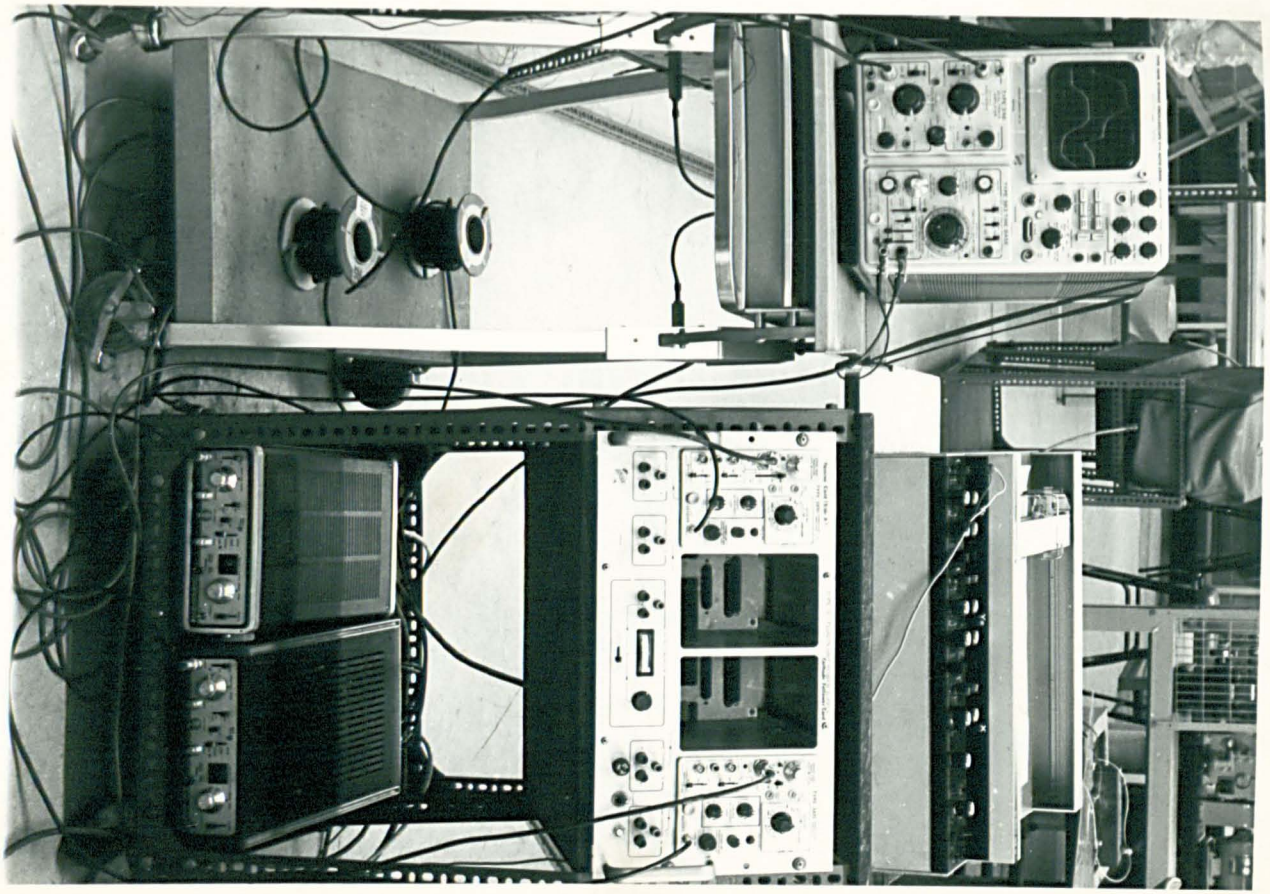

FIG. 7.2 PHOTOGRAPH OF EXPERIMENTAL ARRANGEMENT

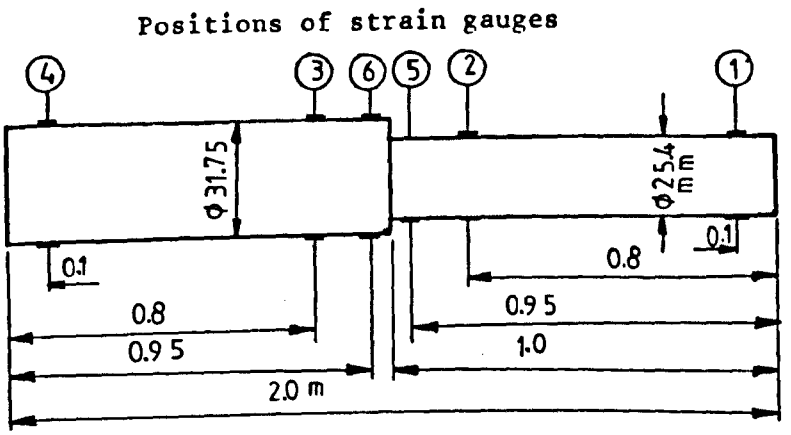

a. Short stepped beam (Test beam II)

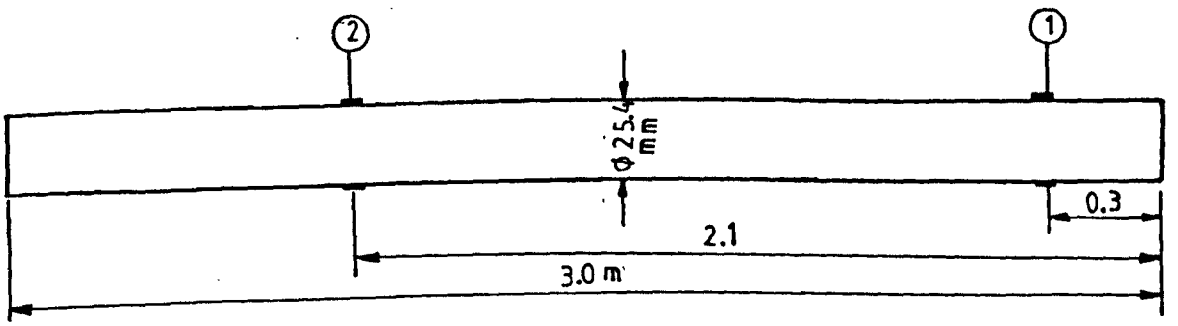

b. Uniform beam of circular cross section (Test beam I)

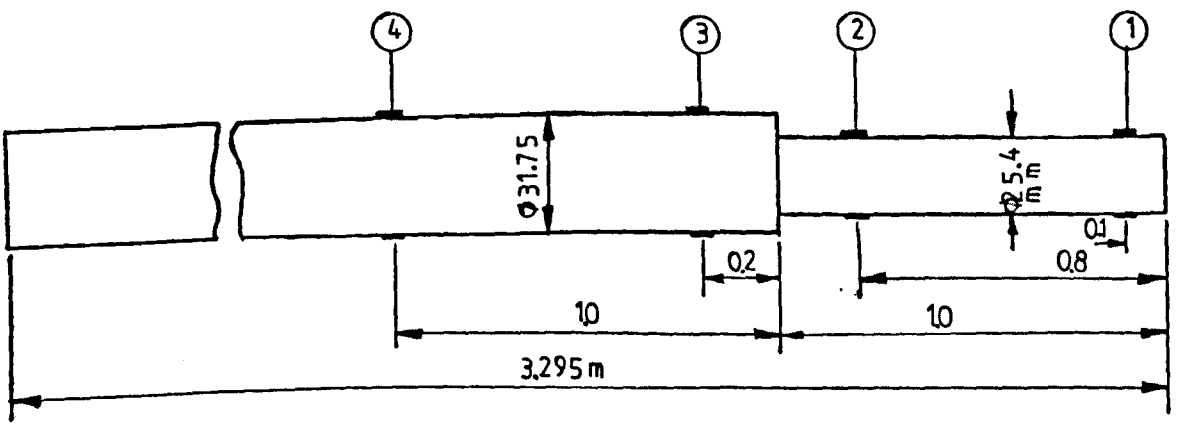

c. Long stepped beam (Test beam III)

FIG. 7.3. TEST BEAMS AND STRAIN GAUGE LOCATIONS

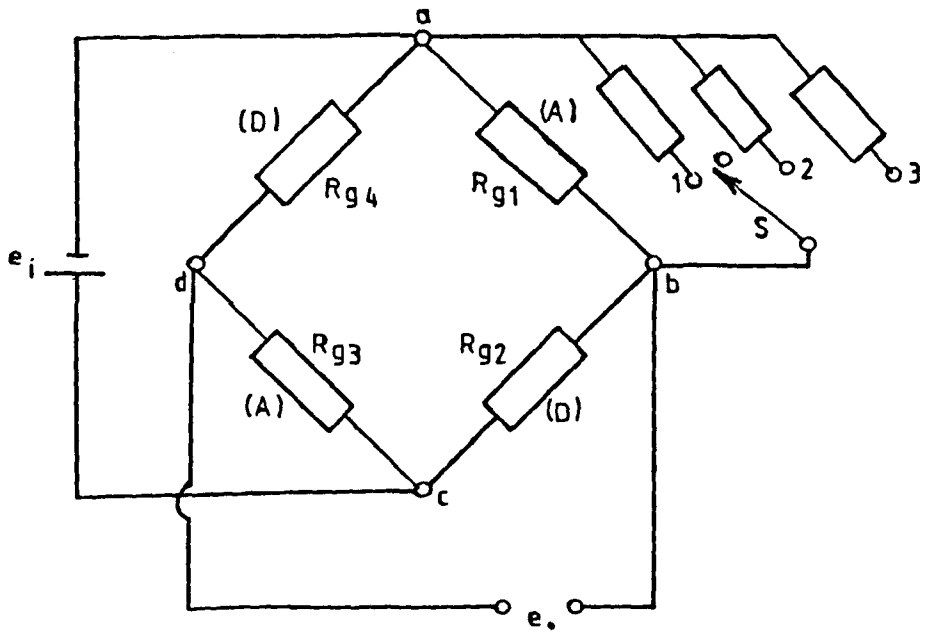

A a. Axial strain measurement

(A) : Active strain gauges

(D) : Dummy strain gauges

R_{gi} : Strain gauge resist.

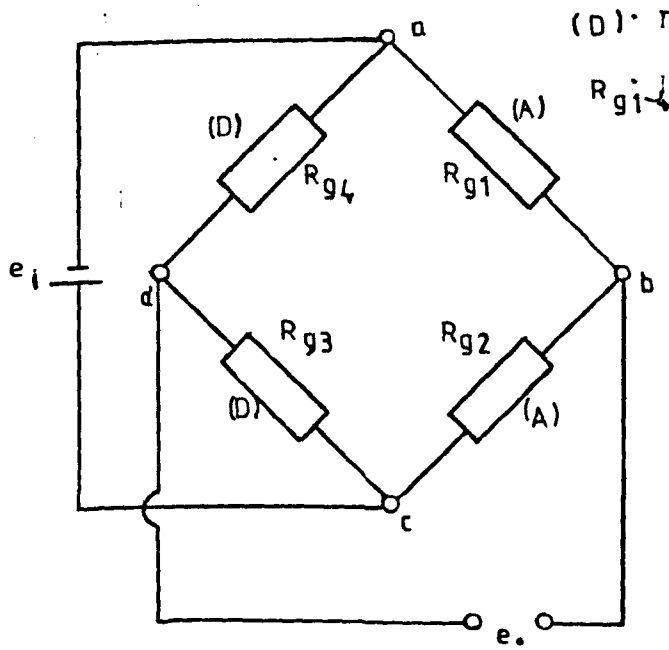

b. Bending strain measurement

FIG. 7.4. STRAIN GAUGE LOCATIONS IN WHEATSTONE BRIDGE CIRCUITS

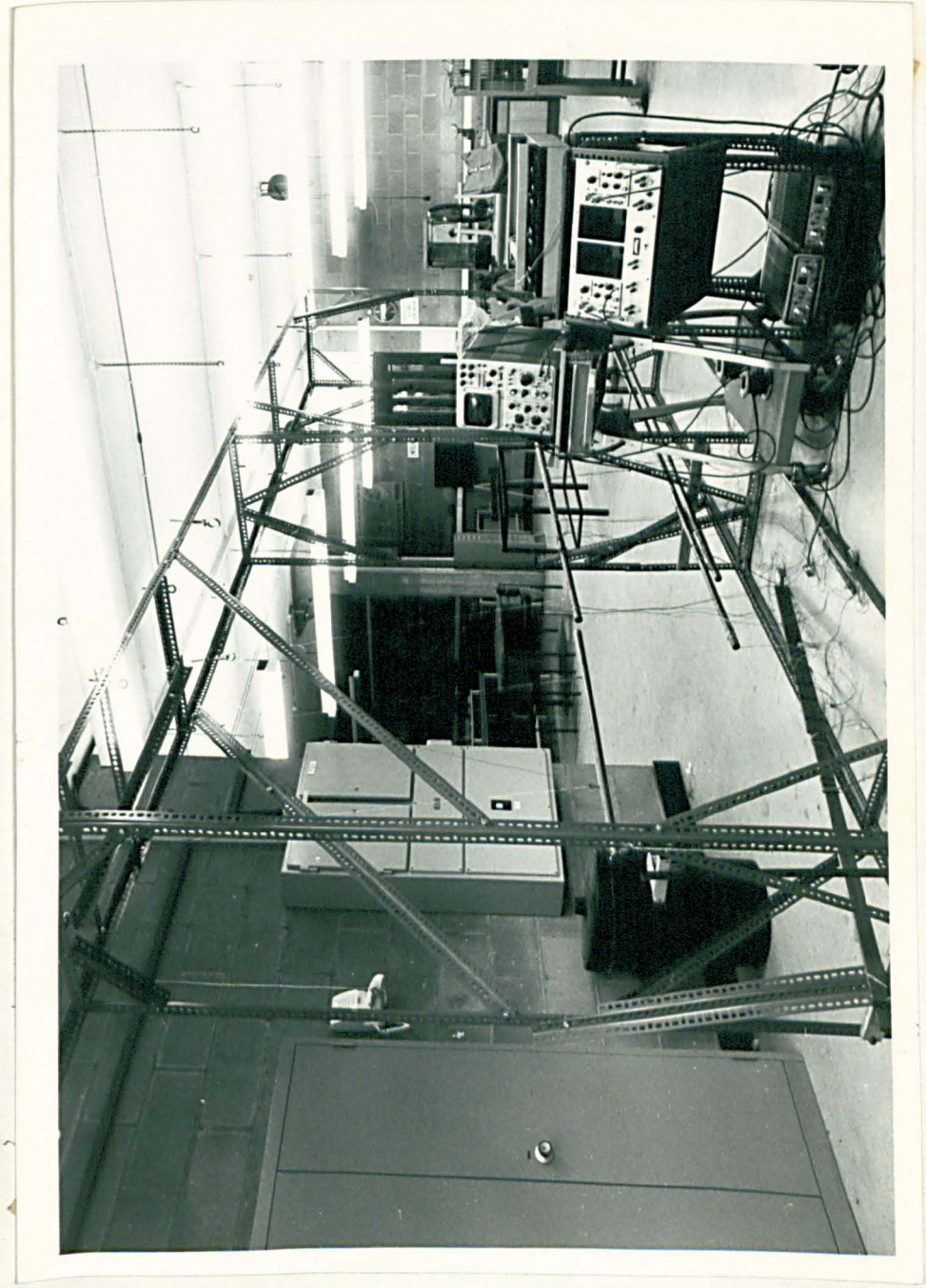

FIG. 7.5 PHOTOGRAPH OF THE MEASUREMENT EQUIPMENT

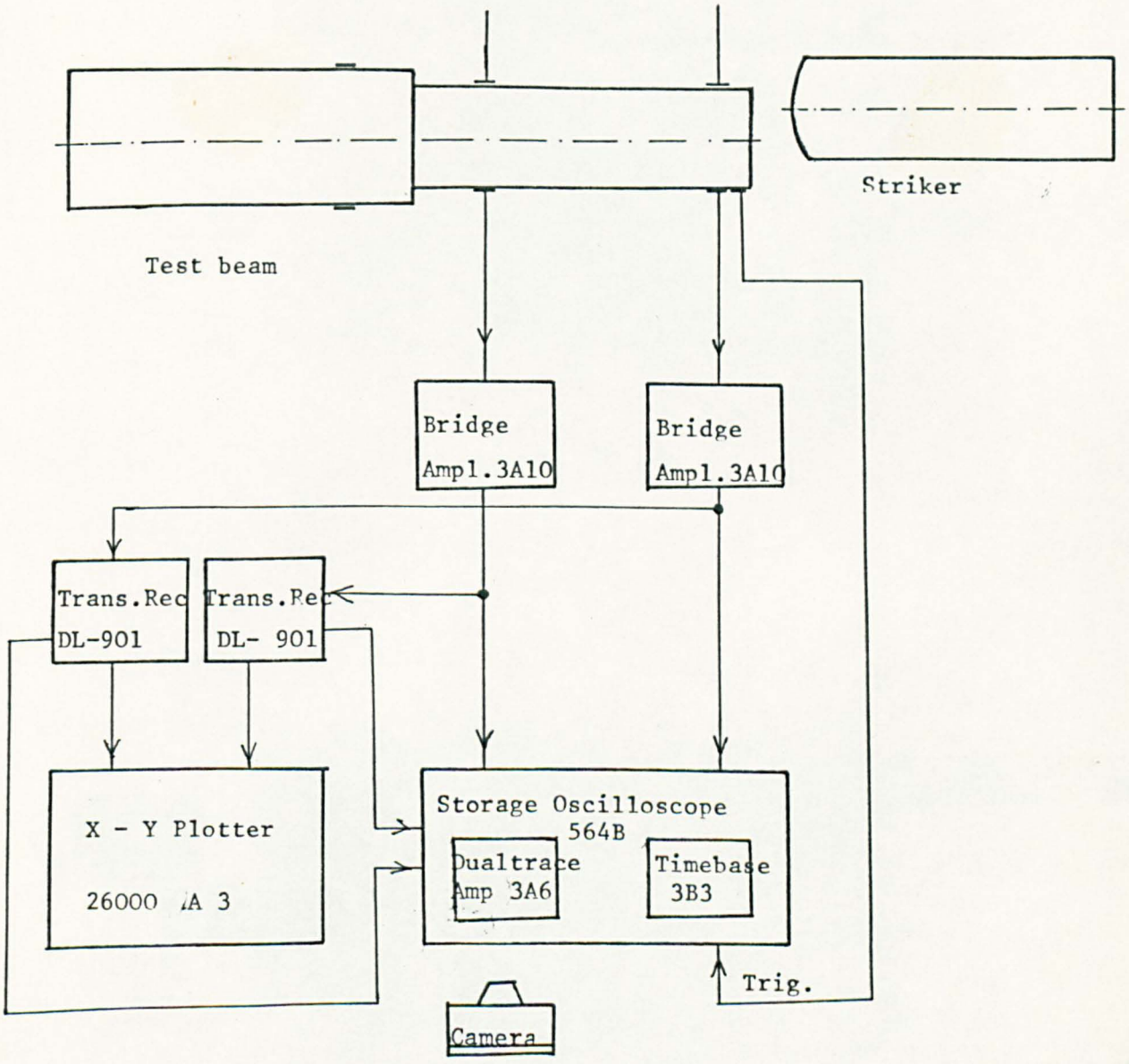

FIG. 7.6. BLOCKDIAGRAM OF MEASUREMENT EQUIPMENT

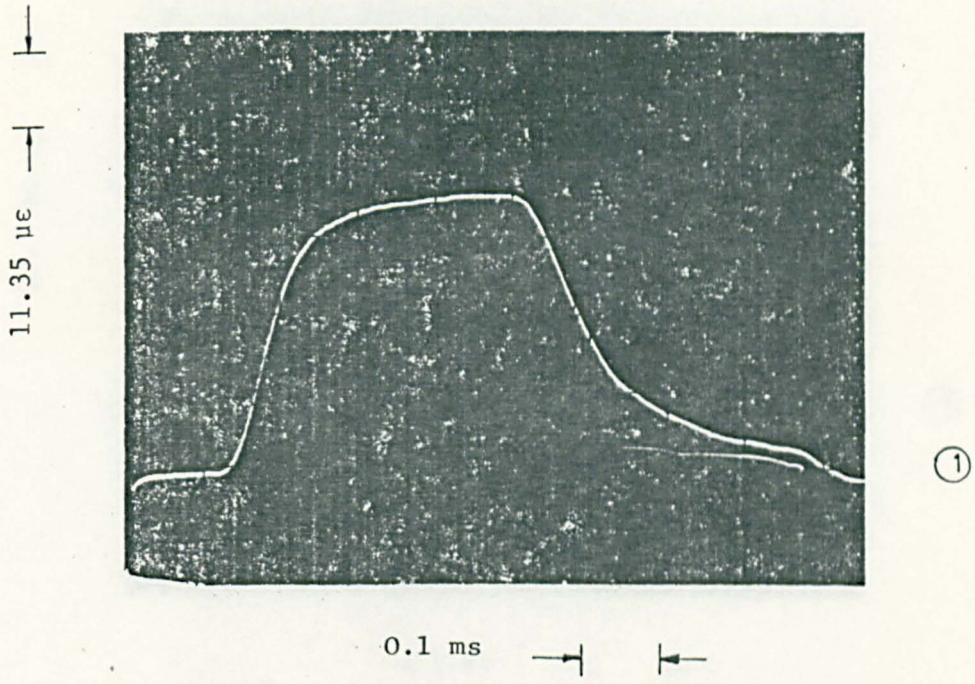

(a) Input pulse due to 1.0 m long striker

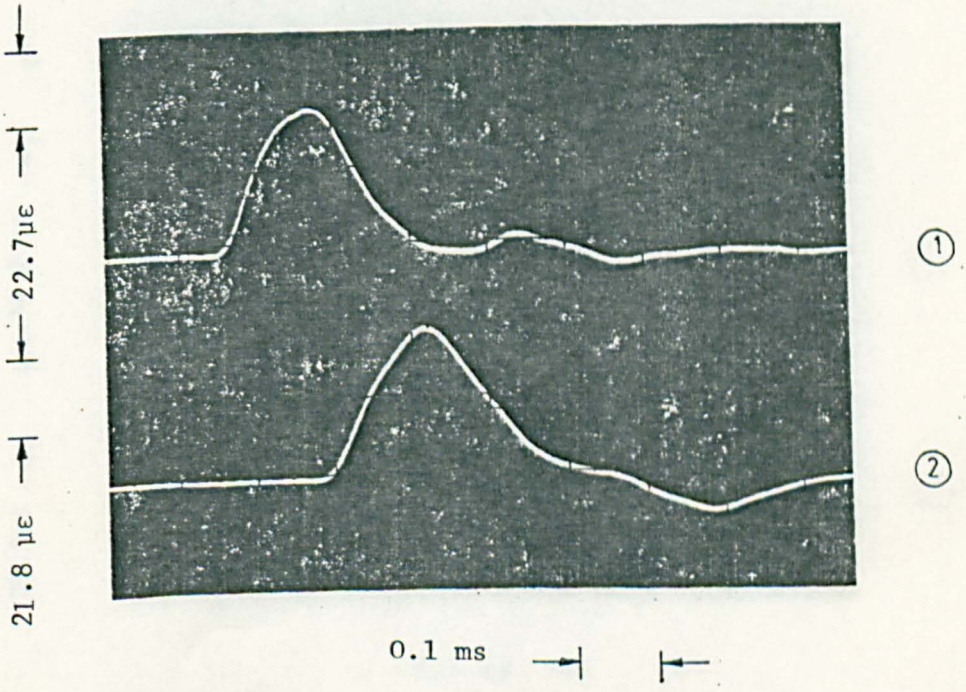

(b) Input pulse due to 0.31 m long striker

FIG. 7.7 LONGITUDINAL STRAIN-TIME VARIATIONS WITH STRIKERS LENGTH

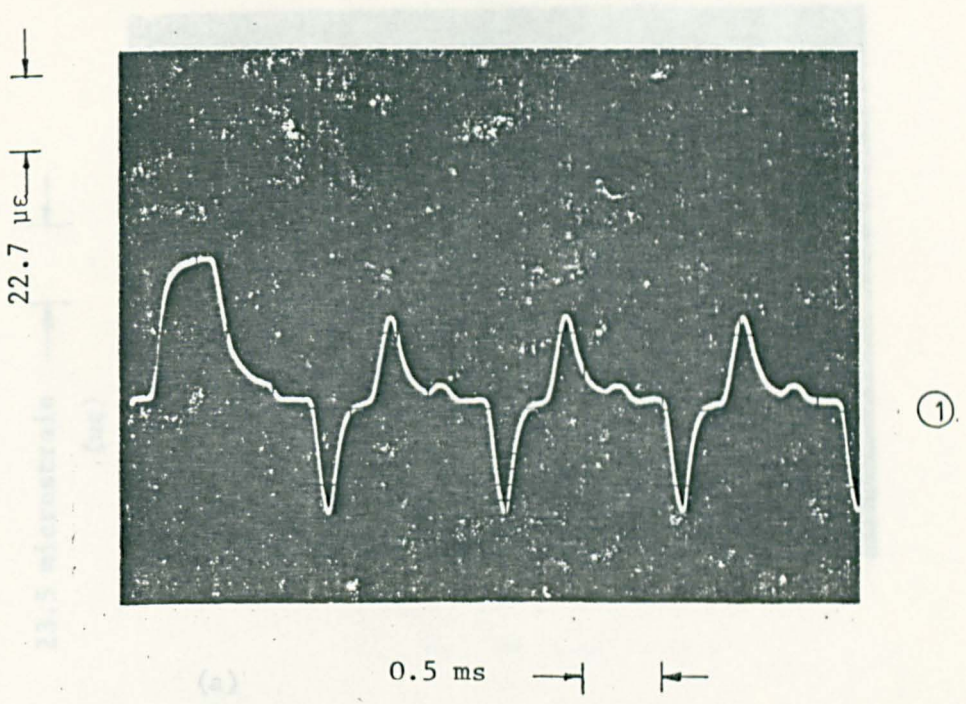

(a)

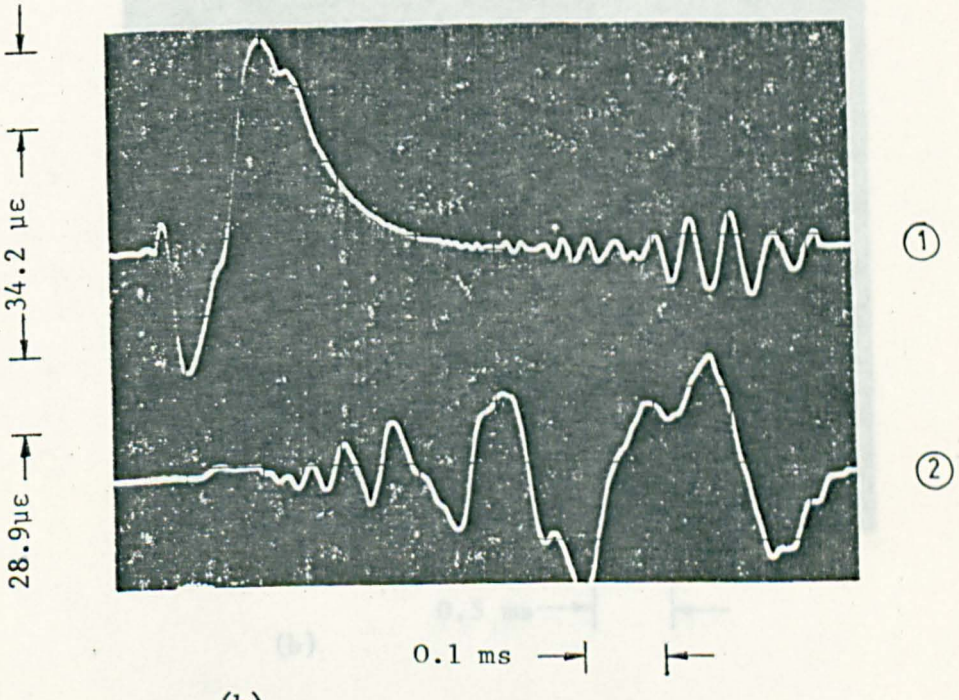

(b)

FIG. 7.8 LONGITUDINAL(a) AND BENDING(b) STRAIN-TIME RECORDS FOR THE UNIFORM TEST BEAM(I) OF CIRCULAR CROSS SECTION STRUCK BY THE 1.0m STRIKER

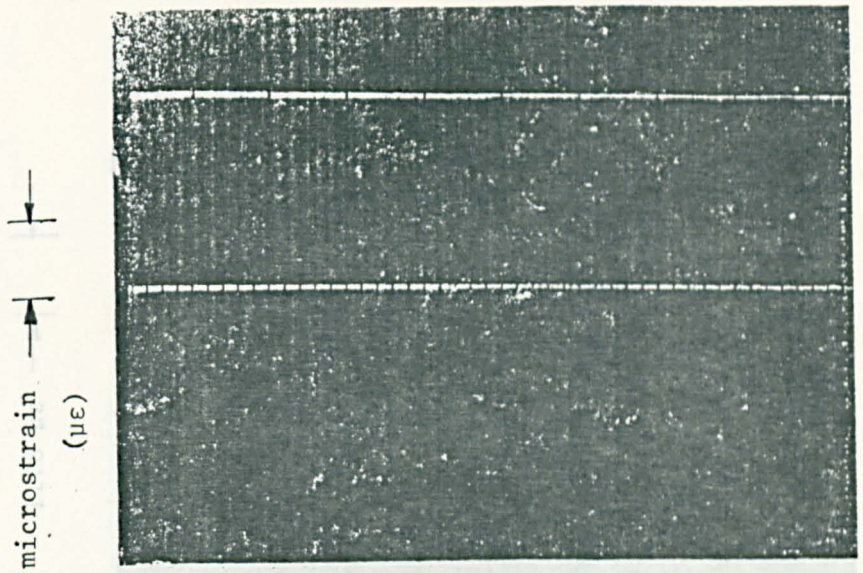

(a)

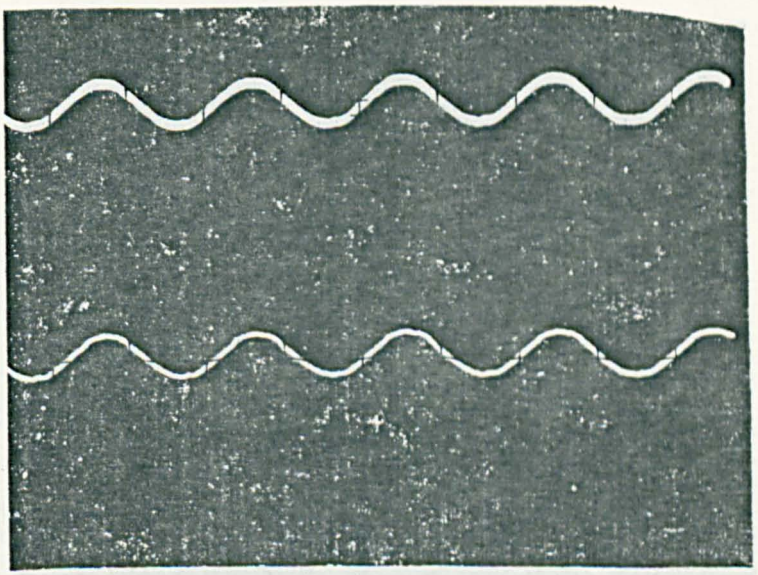

(b)

FIG. 7.9 CALIBRATION OF VERTICAL OUTPUT (a) AND SWEEP RATE (b) FOR THE STORAGE OSCILLOSCOPE TEKTRONIX 564B

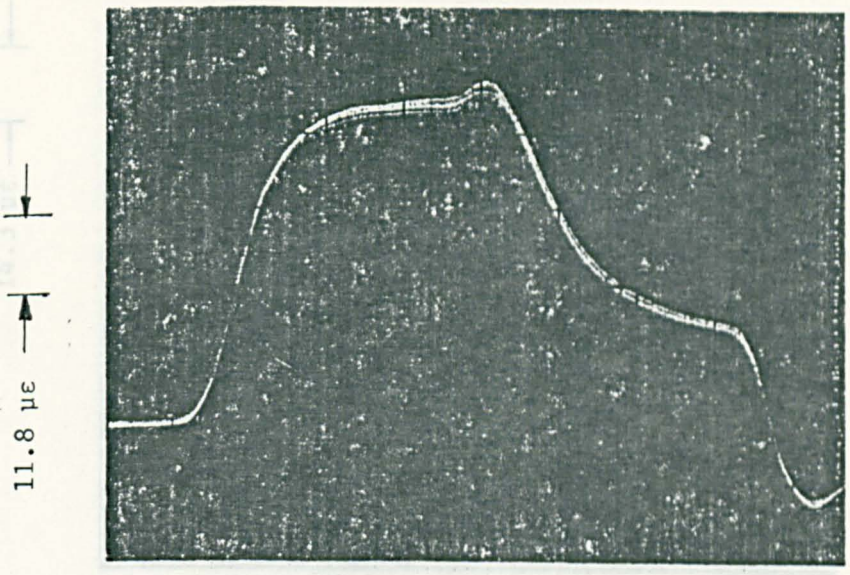

(a)

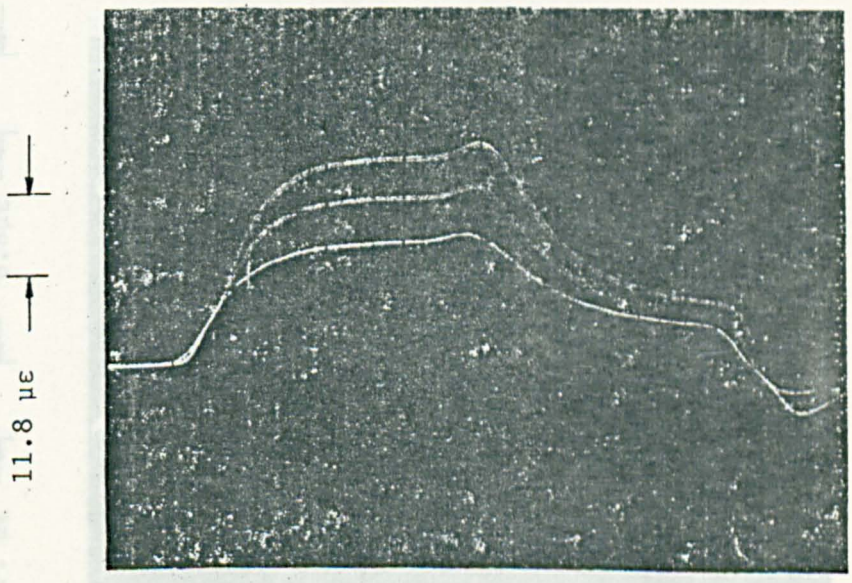

(b)

FIG. 7.10 REPRODUCIBILITY (a) AND AMPLITUDE VARIATION (b) OF INPUT PULSE WITH INPUT VELOCITY AT 4 BAR DIAMETERS FROM IMPACT

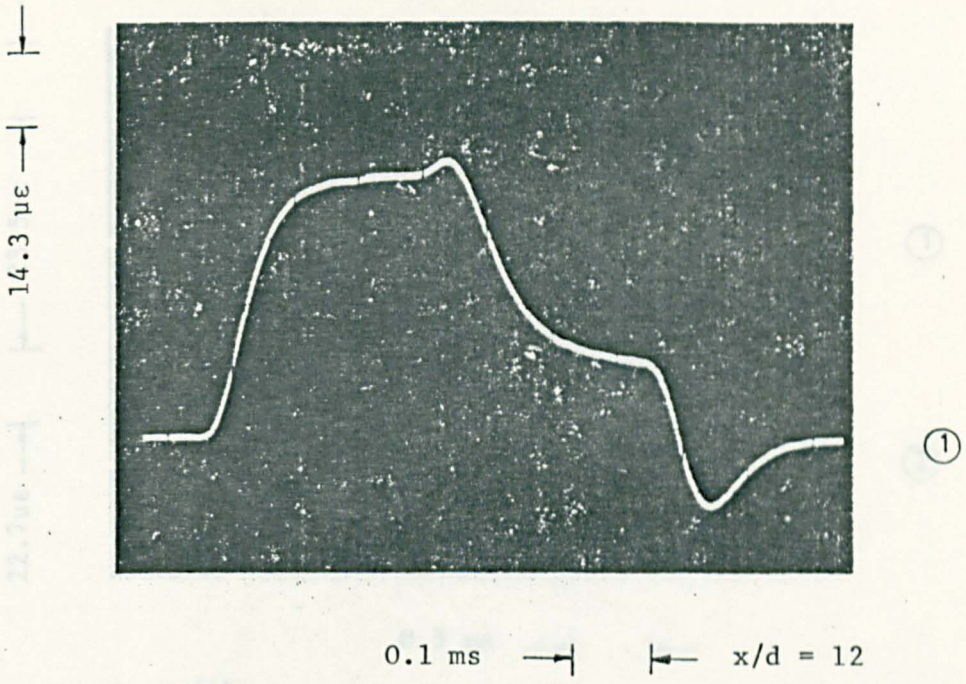

(a)

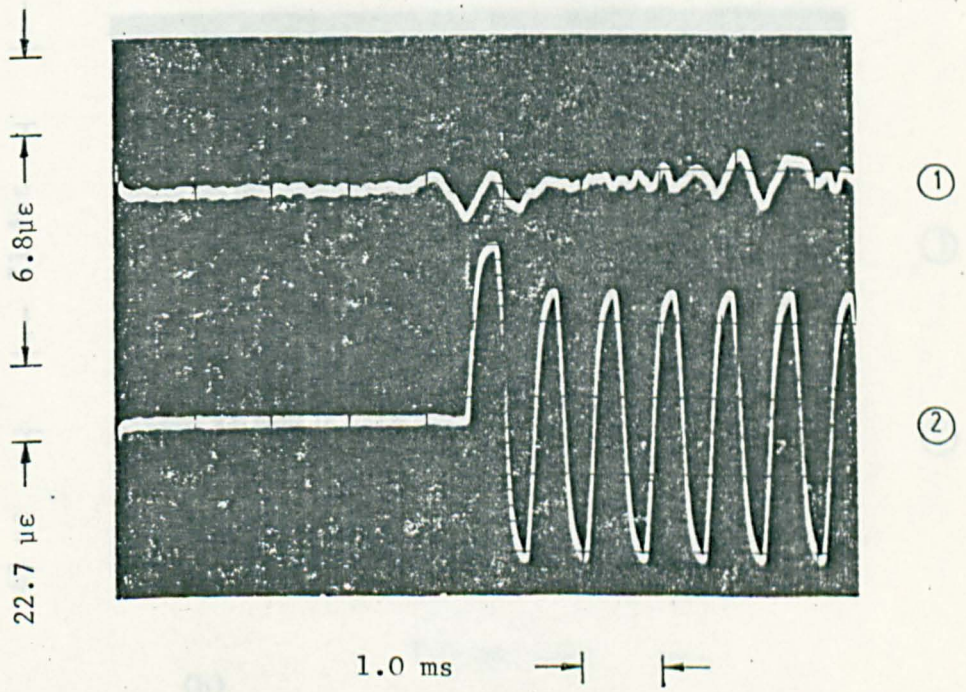

(b)

FIG. 7.11 EFFECT OF ECCENTRICITY ON THE VARIATION OF BENDING (ANTISYMMETRIC) STRAIN HISTORY

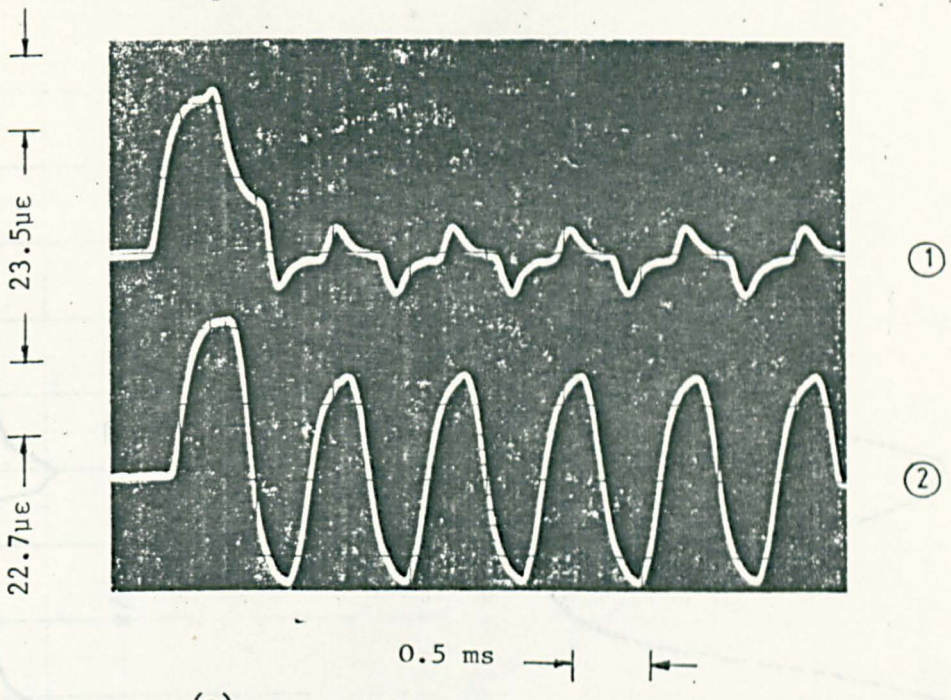

(a)

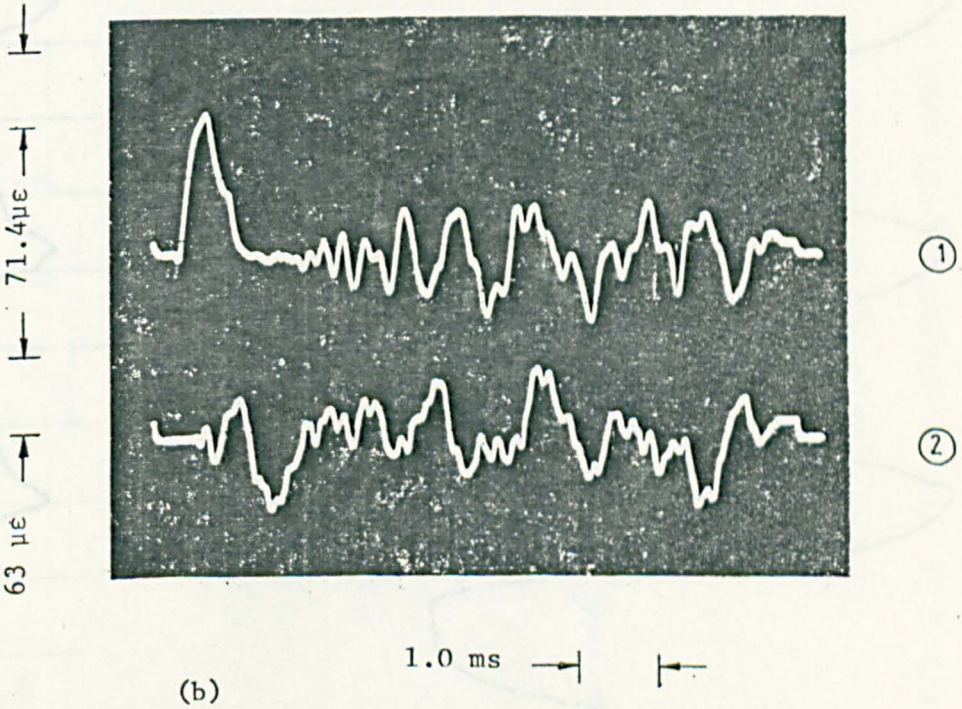

(b)

FIG. 7.12 LONGITUDINAL(a) AND BENDING(b) STRAIN-TIME RECORDS IN THE 2.0 m LONG STEPPED BEAM (TEST BEAM II) DUE TO ECCENTRIC IMPACT

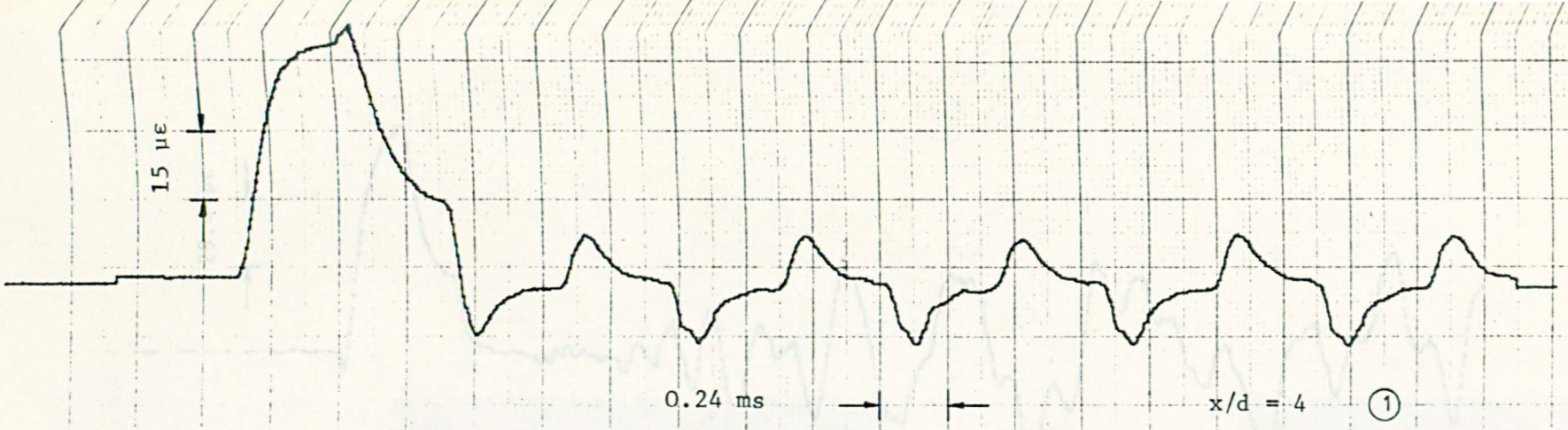

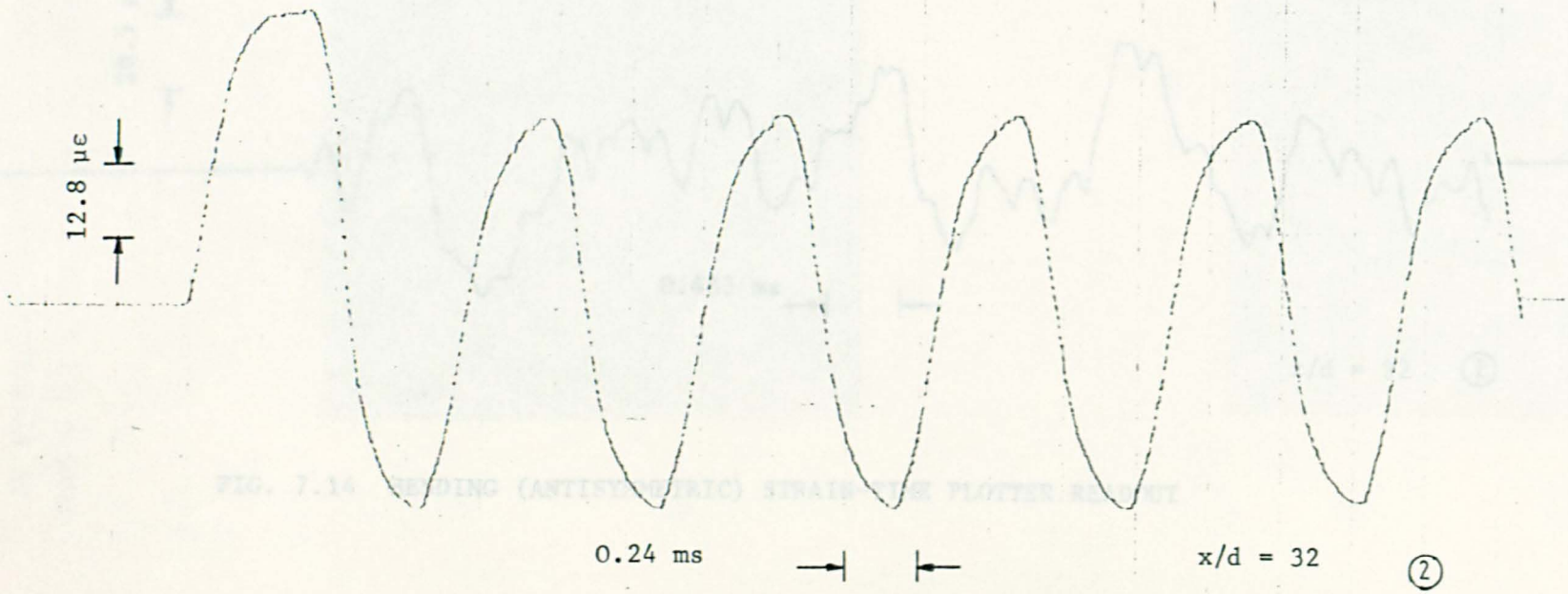

FIG. 7.13 LONGITUDINAL (AXISYMMETRIC) STRAIN-TIME PLOTTER READOUT

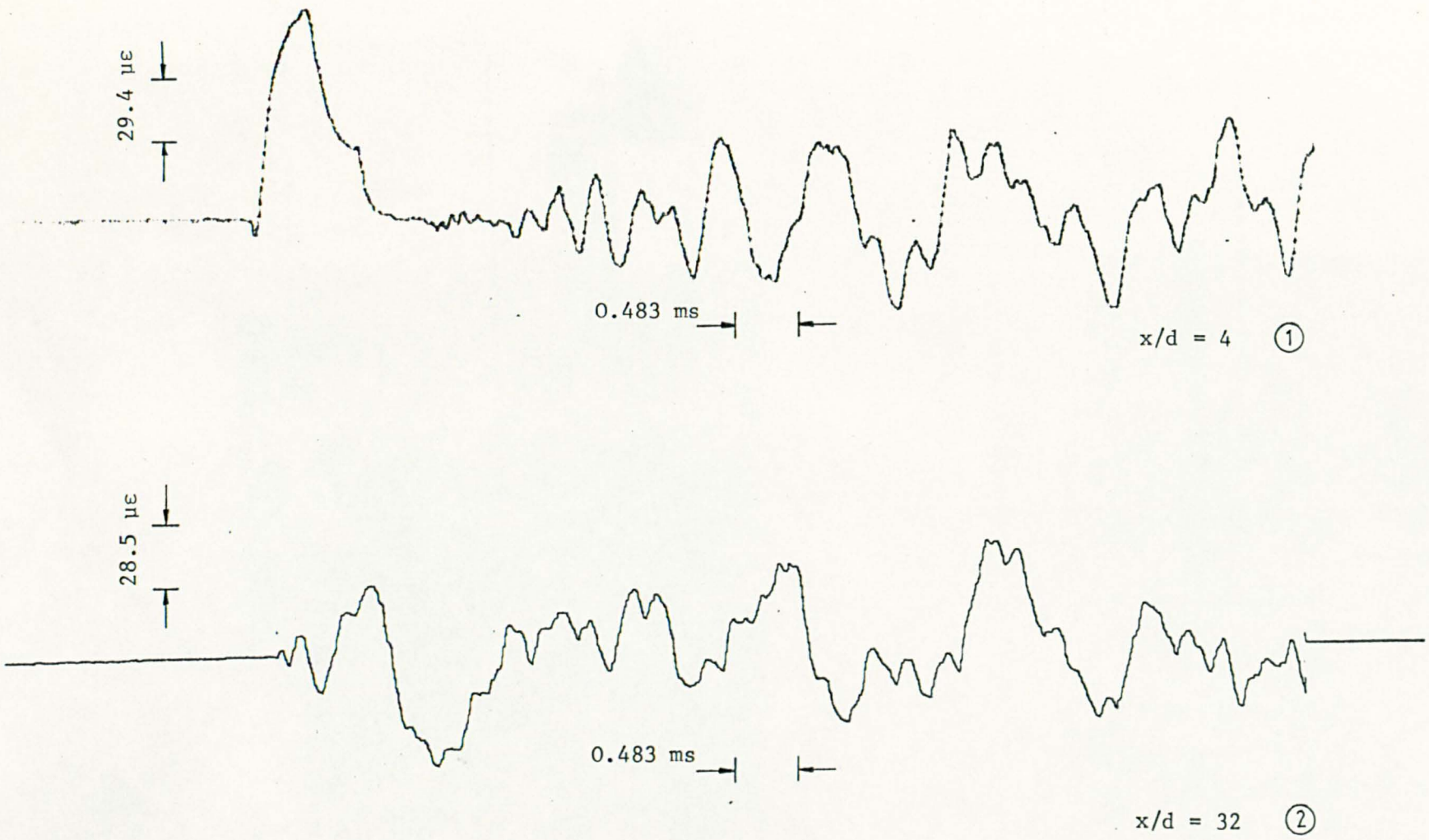

FIG. 7.14 BENDING (ANTISYMMETRIC) STRAIN-TIME PLOTTER READOUT

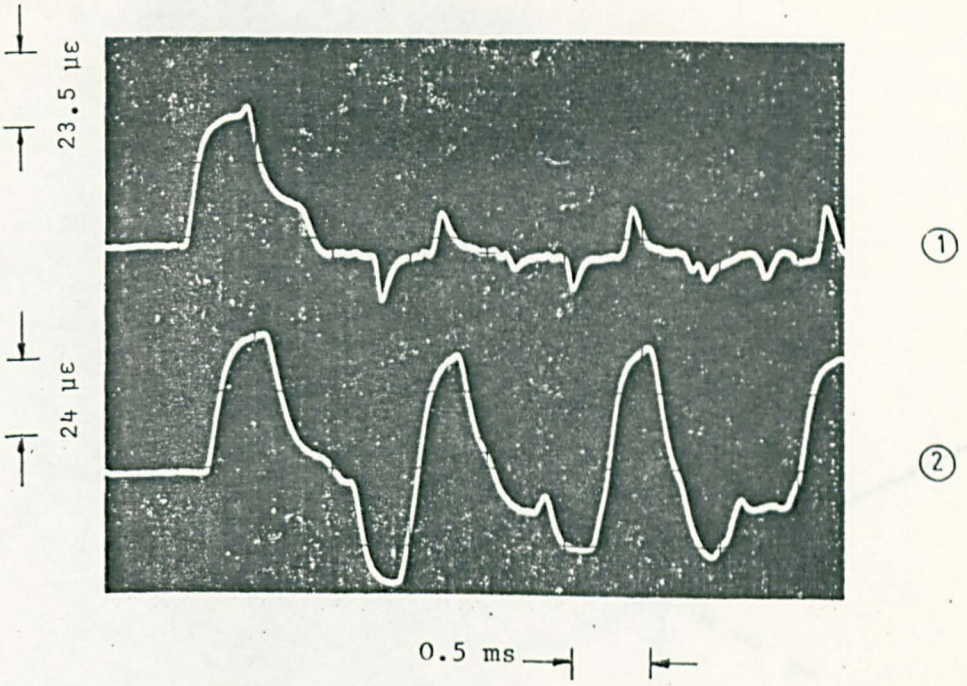

(a)

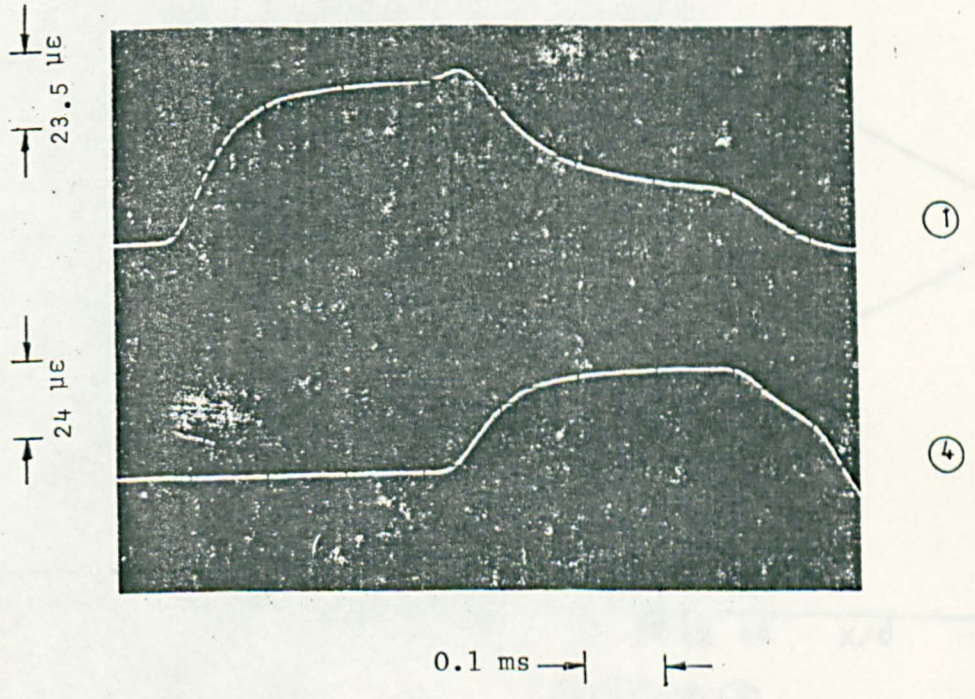

(b)

FIG. 7.15 LONGITUDINAL STRAIN-TIME RECORDS FOR THE 3.295 m LONG STEPPED BEAM (TEST BEAM III) STRUCK ECCENTRICALLY BY THE 1.0 m LONG CYLINDRICAL STRIKER

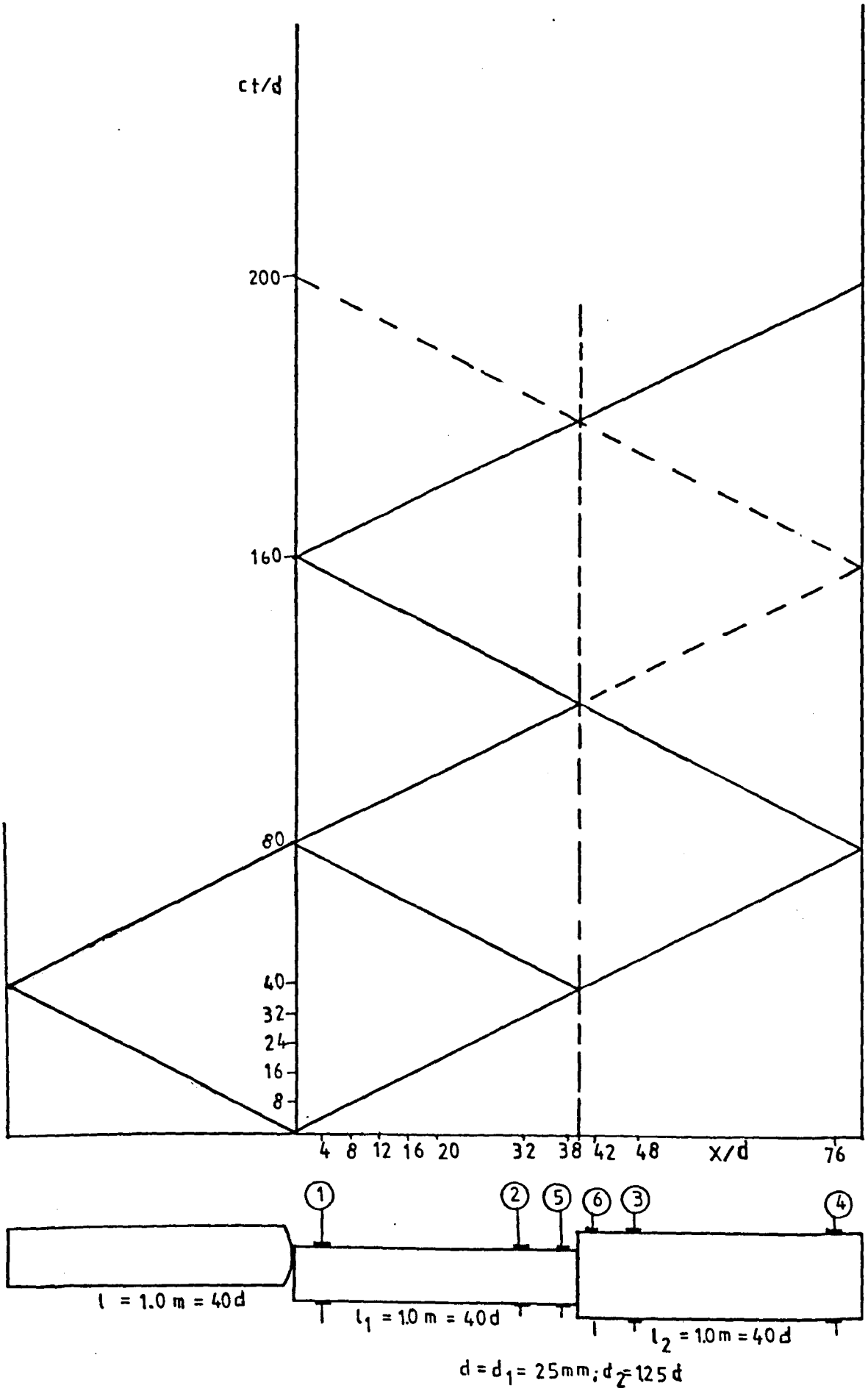

FIG. 7.16. SPACE-TIME DIAGRAM OF LONGITUDINAL WAVES

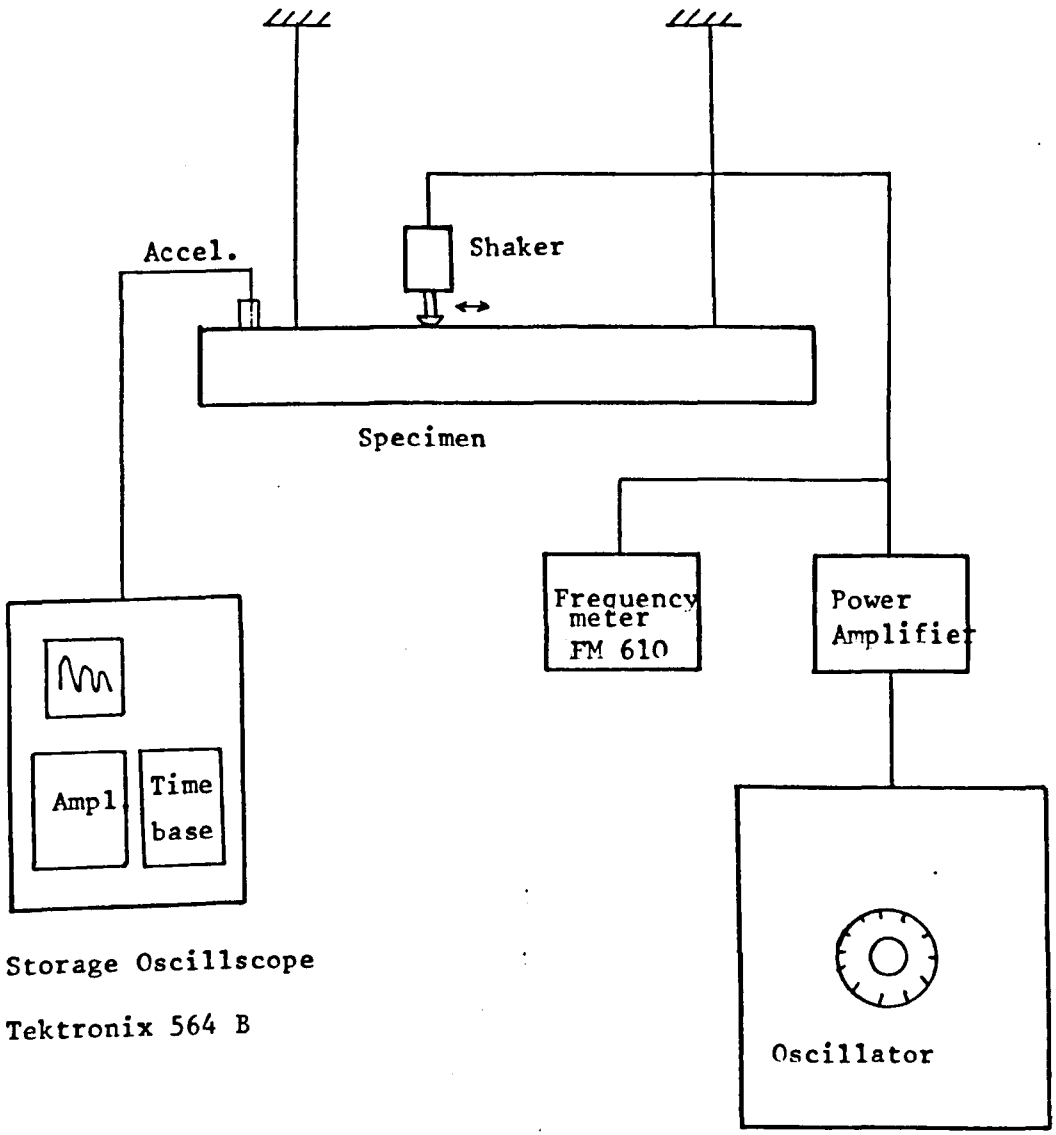

FIG. 7.17. BLOCKDIAGRAM OF RESONANCE TEST INSTRUMENTATION

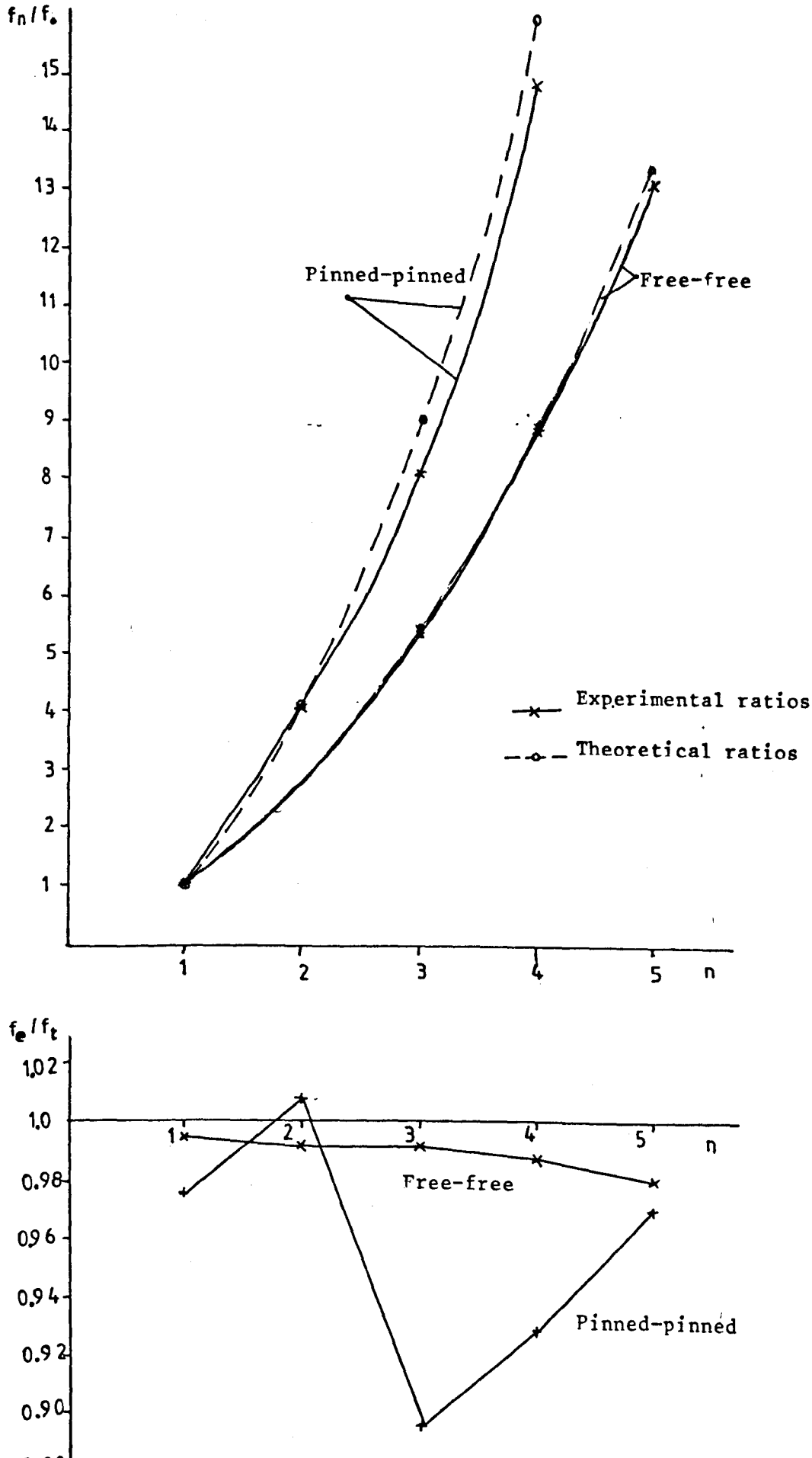

FIG. 7.18. COMPARISON OF EXP.& THEORETICAL FREQUENCIES

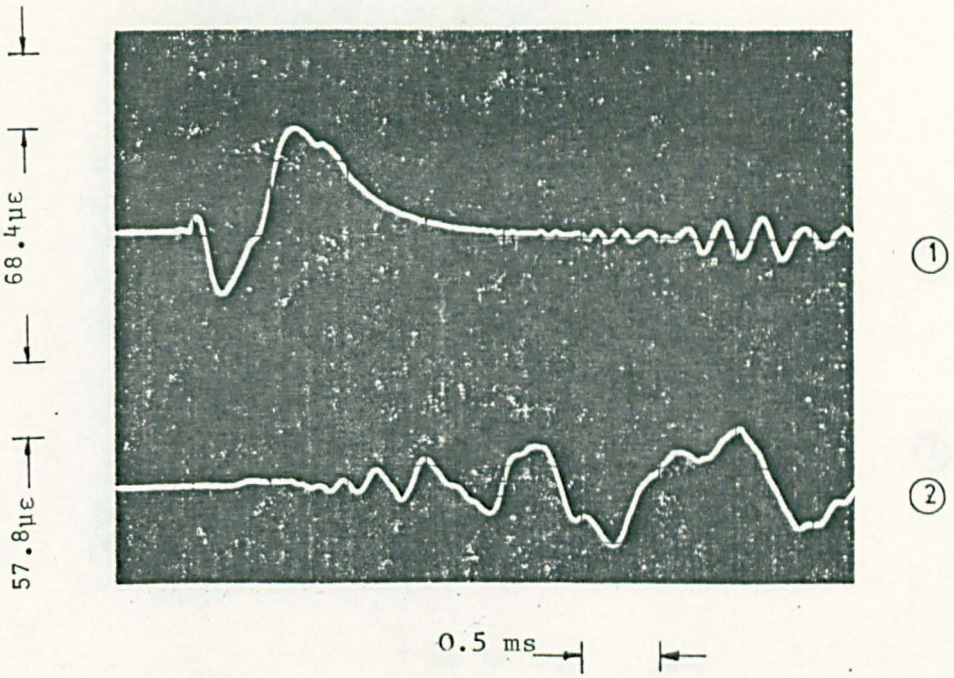

(a)

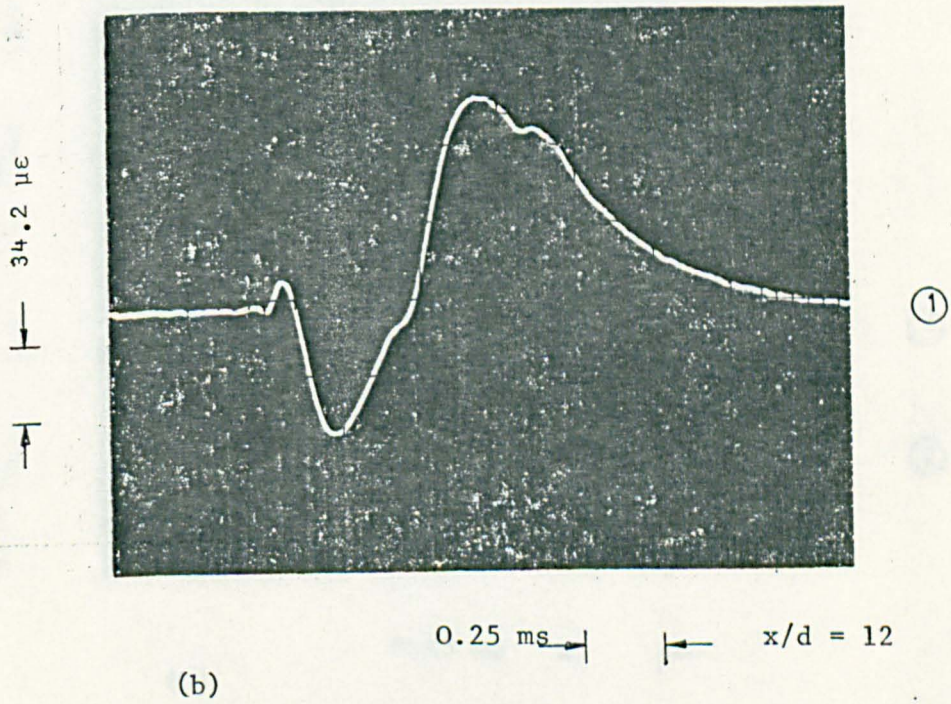

(b)

FIG. 7.19 BENDING STRAIN-TIME TRACES IN THE 3.0 m LONG UNIFORM BEAM (TEST BEAM I) OF CIRCULAR CROSS SECTION DUE TO ECCENTRIC IMPACT

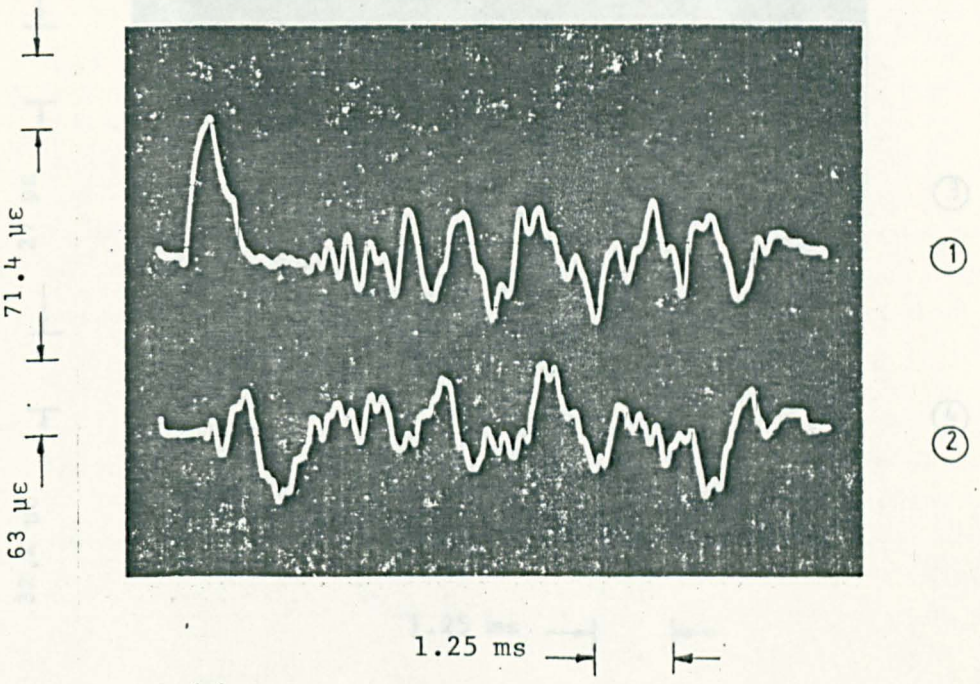

(a)

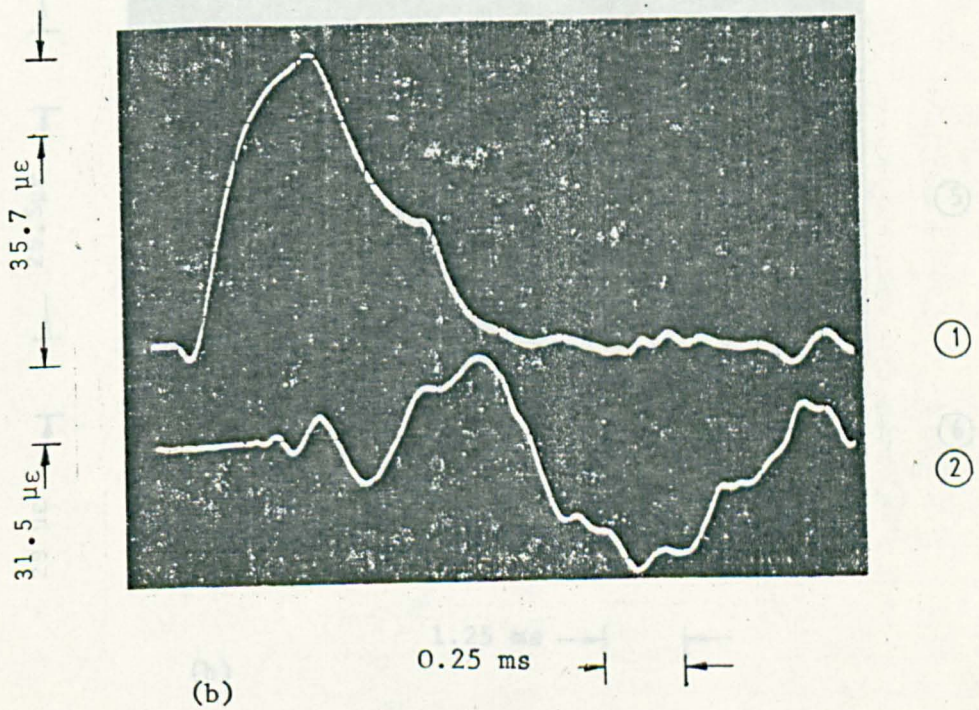

(b)

FIG. 7.20 BENDING STRAIN-TIME PROFILES IN THE 2.0 m LONG STEPPED BEAM (TEST BEAM II) DUE TO ECCENTRIC IMPACT

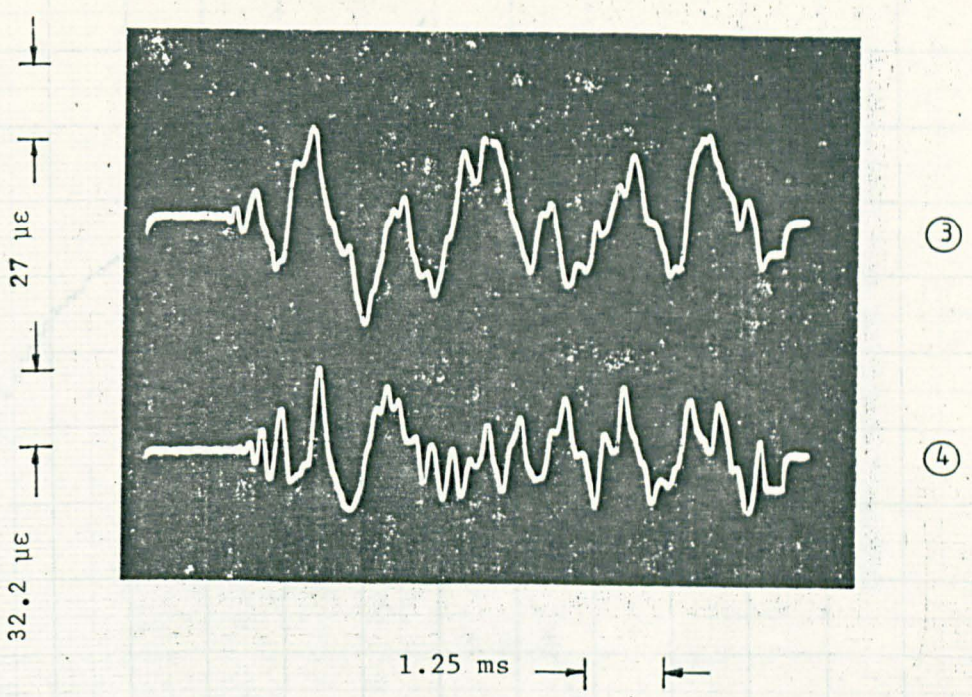

(a)

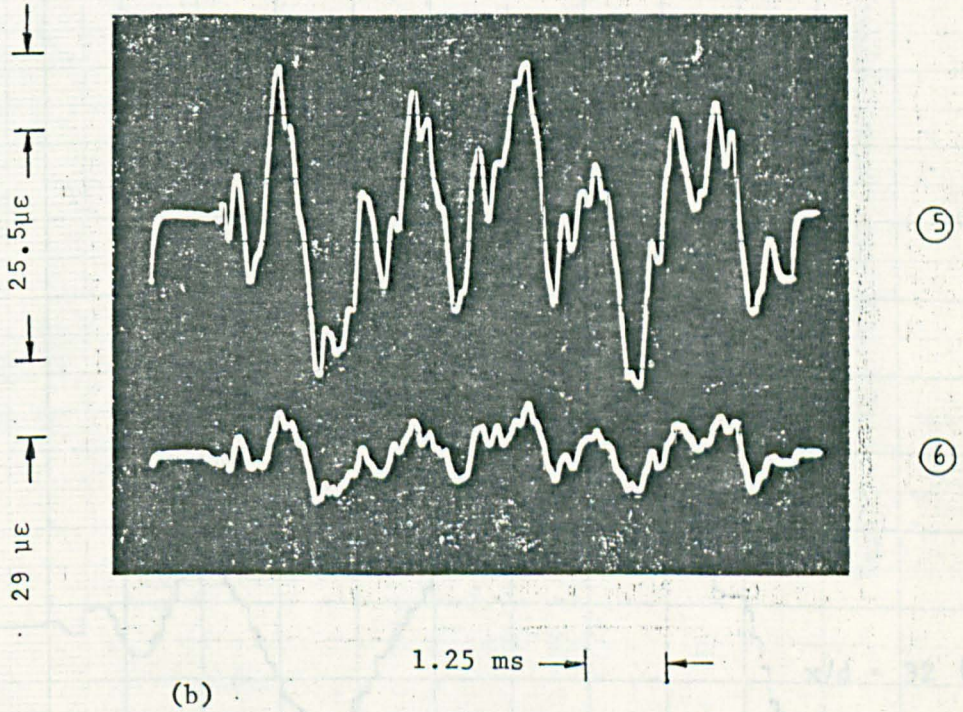

(b)

FIG. 7.21 BENDING STRAIN-TIME PROFILES AT VARIOUS POSITIONS ALONG THE 2.0 m LONG STEPPED BEAM DUE TO ECCENTRIC IMPACT

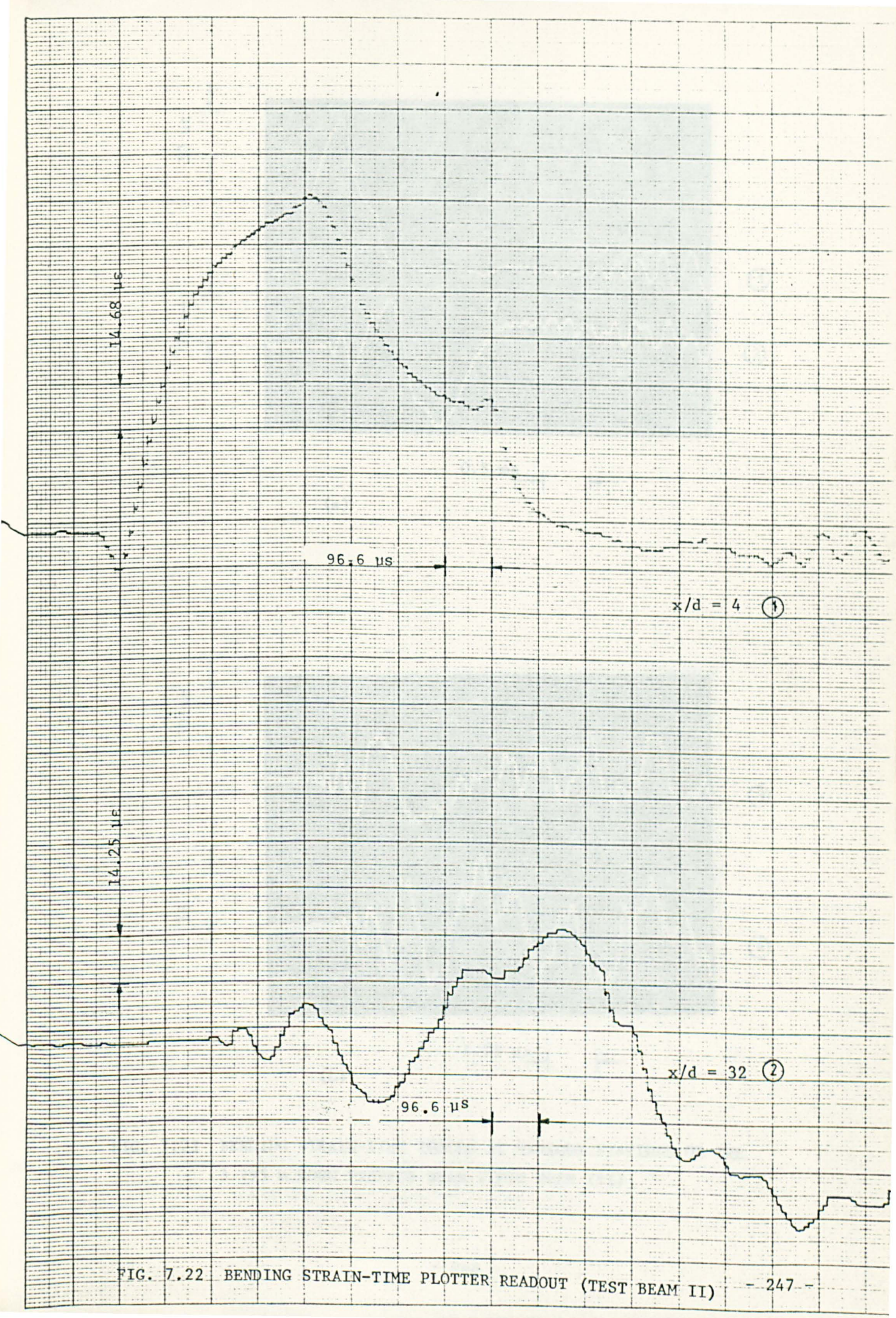

FIG. 7.22 BENDING STRAIN-TIME PLOTTER READOUT (TEST BEAM II)

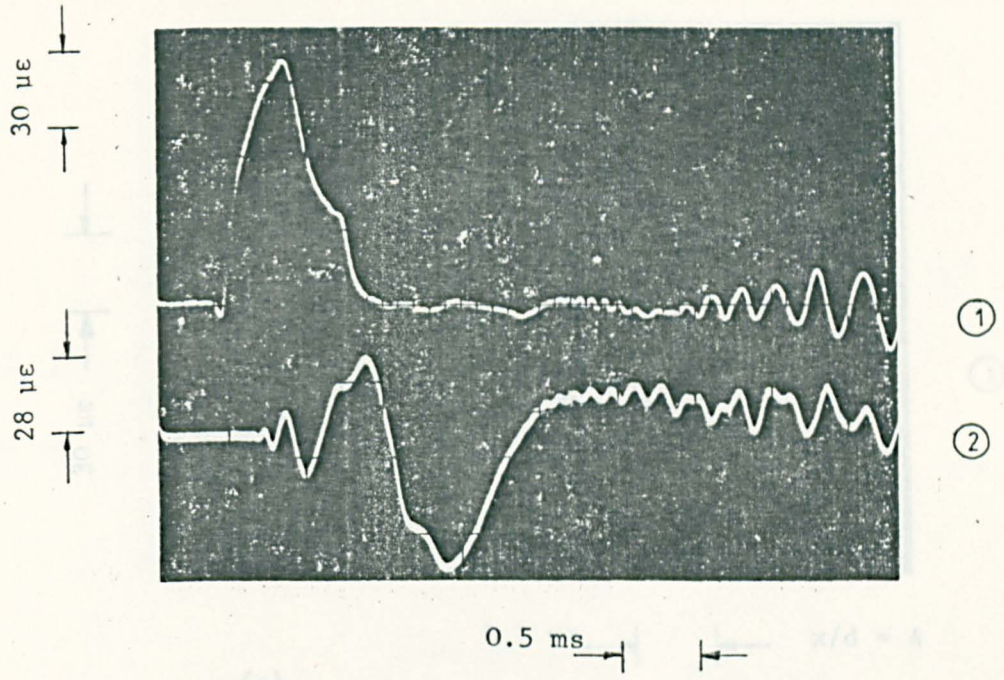

(a)

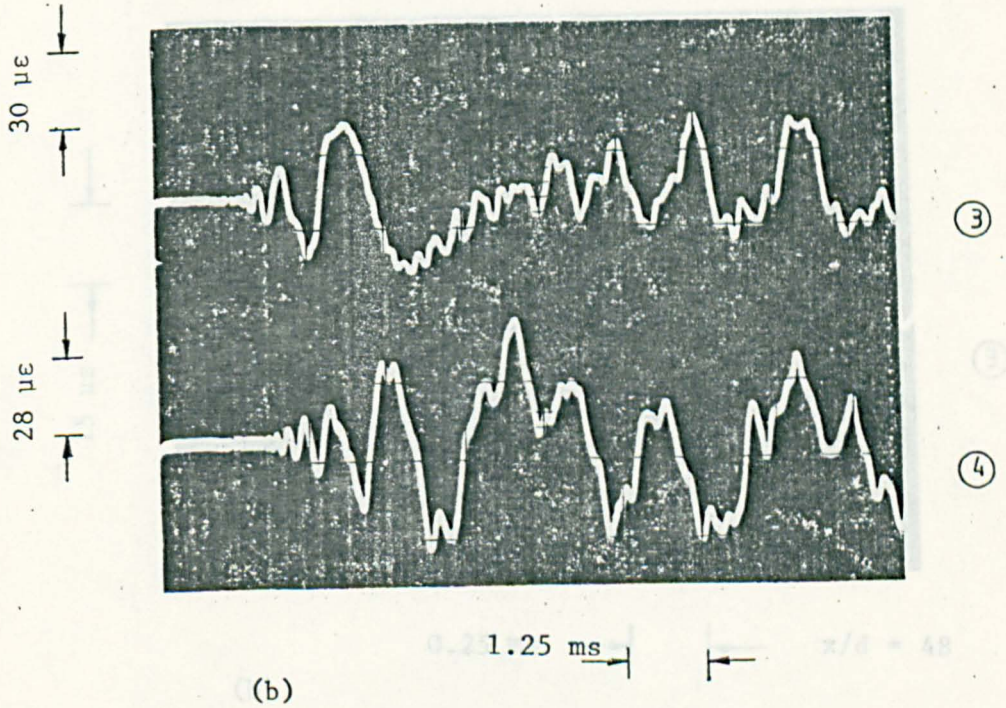

(b)

FIG. 7.23 BENDING STRAIN-TIME TRACES AT VARIOUS STATIONS OF THE 3.295 m LONG STEPPED BEAM (TEST BEAM III)

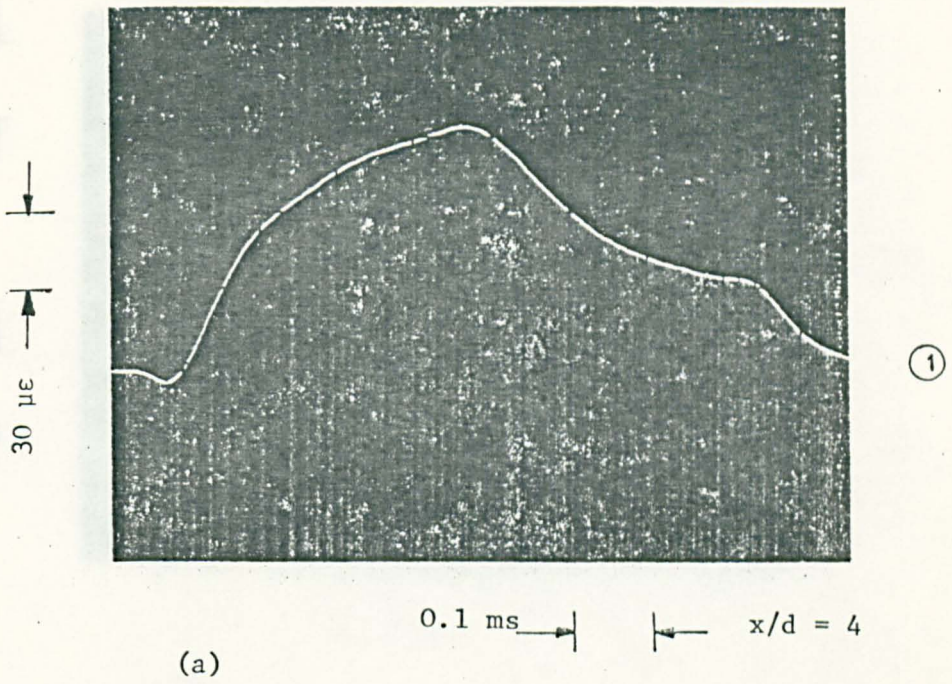

FIG. 7.24 BENDING STRAIN-TIME RECORDS AT 4 AND 48 BAR DIAMETERS FROM THE IMPACT END (TEST BEAM III)

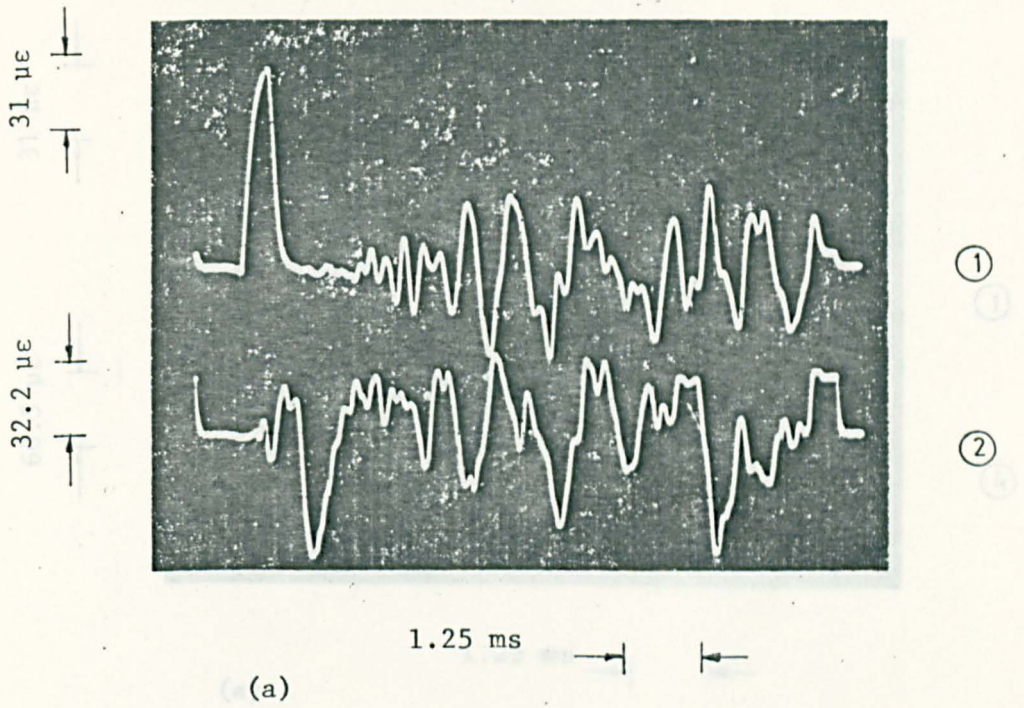

(a)

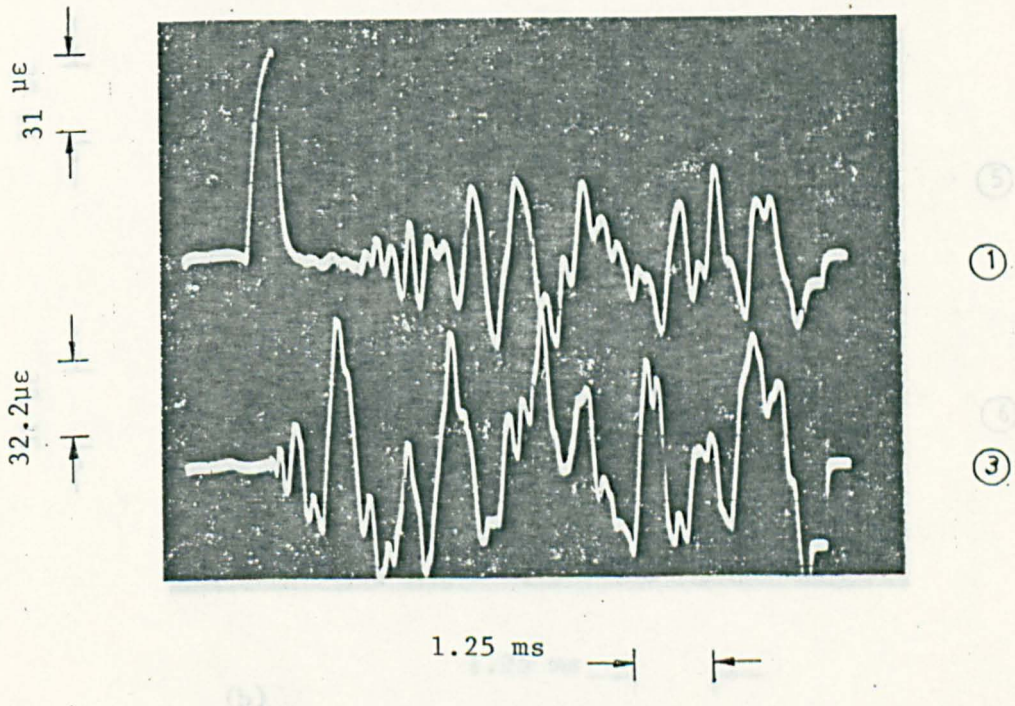

(b)

FIG. 7.25 BENDING STRAIN-TIME RECORDS FOR THE 2.0 m LONG STEPPED BEAM DUE TO ECCENTRIC IMPACT AT THE LARGE END

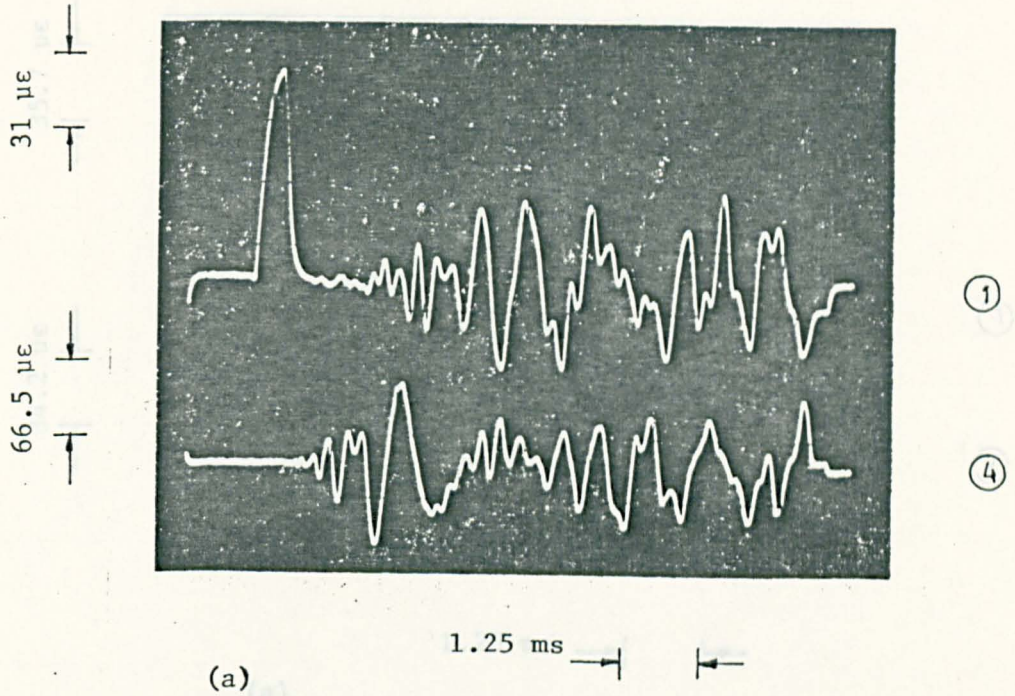

(a)

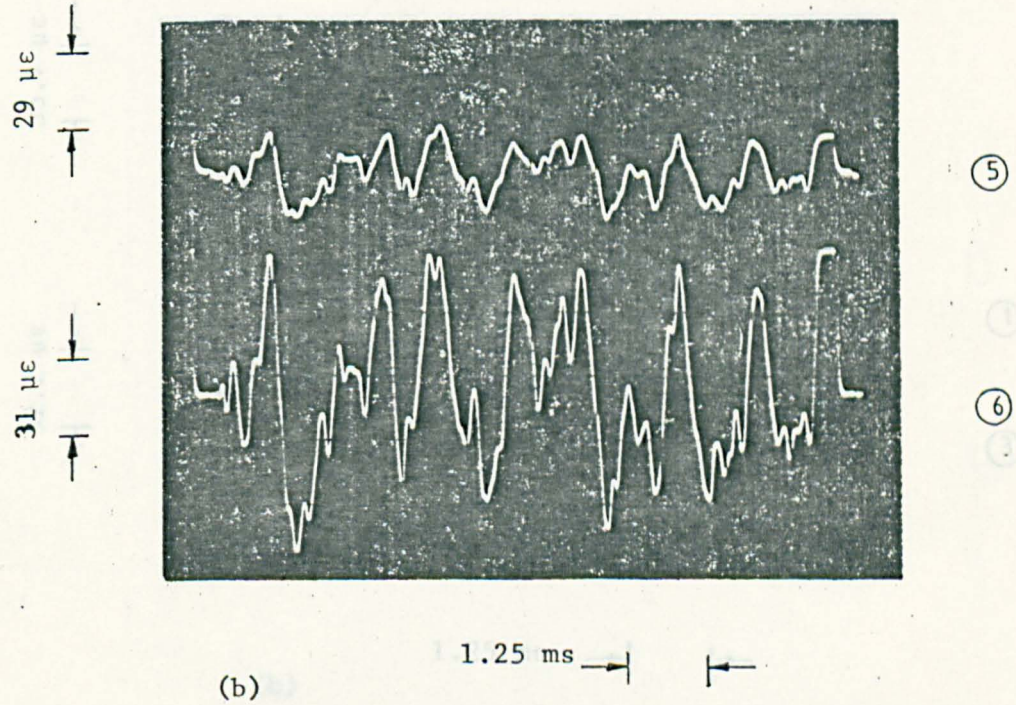

(b)

FIG. 7.26 BENDING STRAIN-TIME RECORDS AT VARIOUS STATIONS OF THE 2.0 m LONG STEPPED BEAM DUE TO ECCENTRIC IMPACT AT THE LARGE END

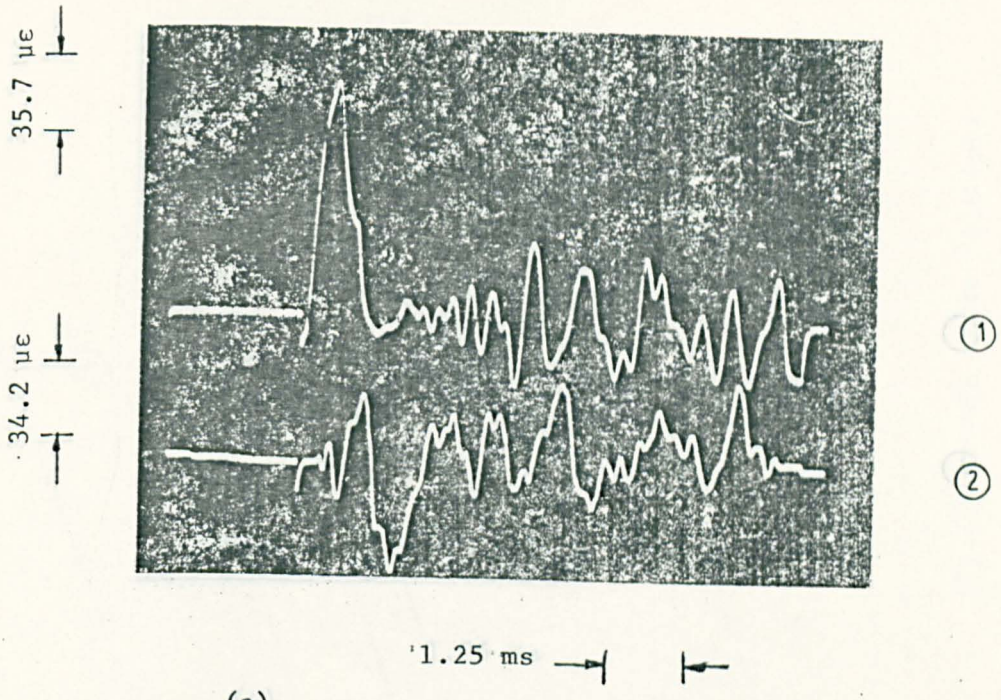

(a)

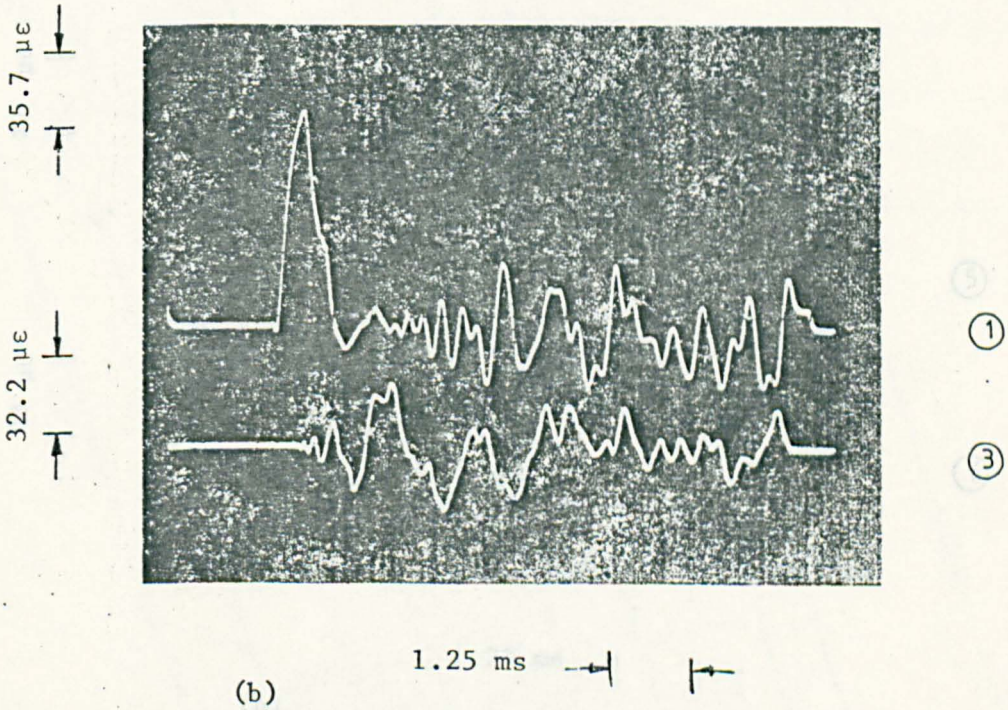

(b)

FIG. 7.27 BENDING STRAIN-TIME TRACES FOR THE 2.0 m LONG SIMPLY SUPPORTED STEPPED BEAM DUE TO ECCENTRIC IMPACT

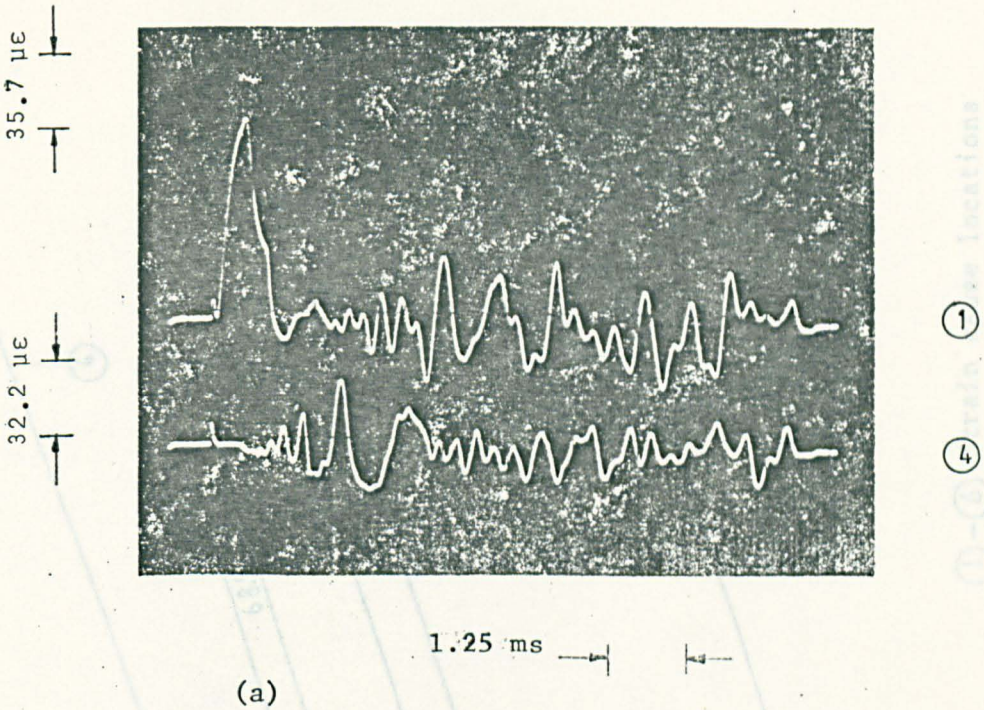

(a)

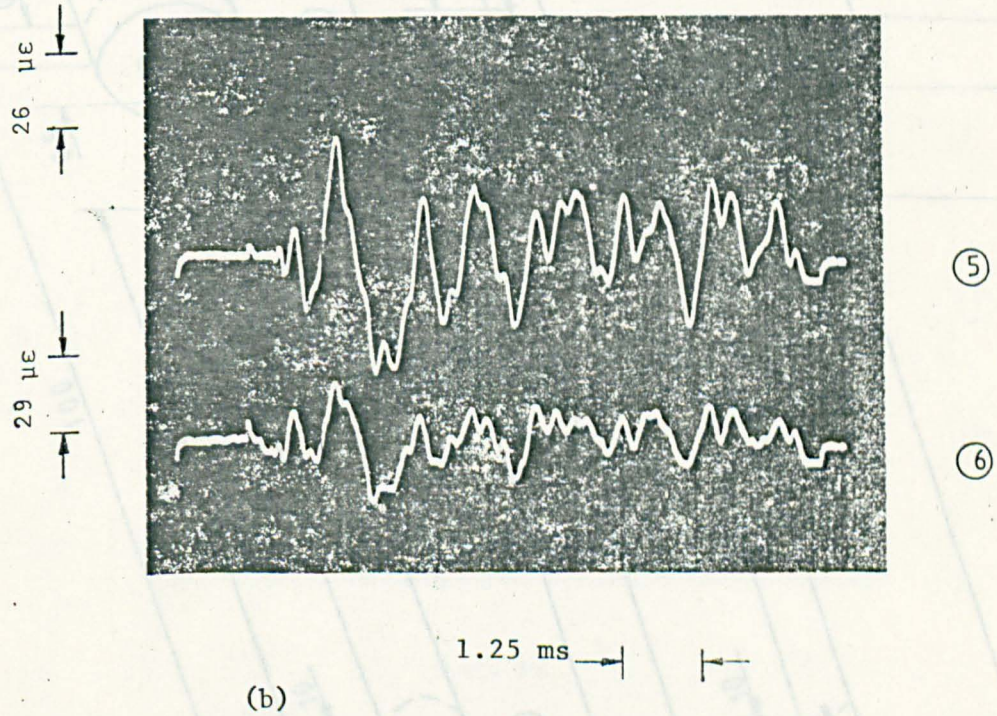

(b)

FIG. 7.28 BENDING STRAIN-TIME TRACES FOR THE 2.0 m LONG SIMPLY SUPPORTED STEPPED BEAM DUE TO ECCENTRIC IMPACT

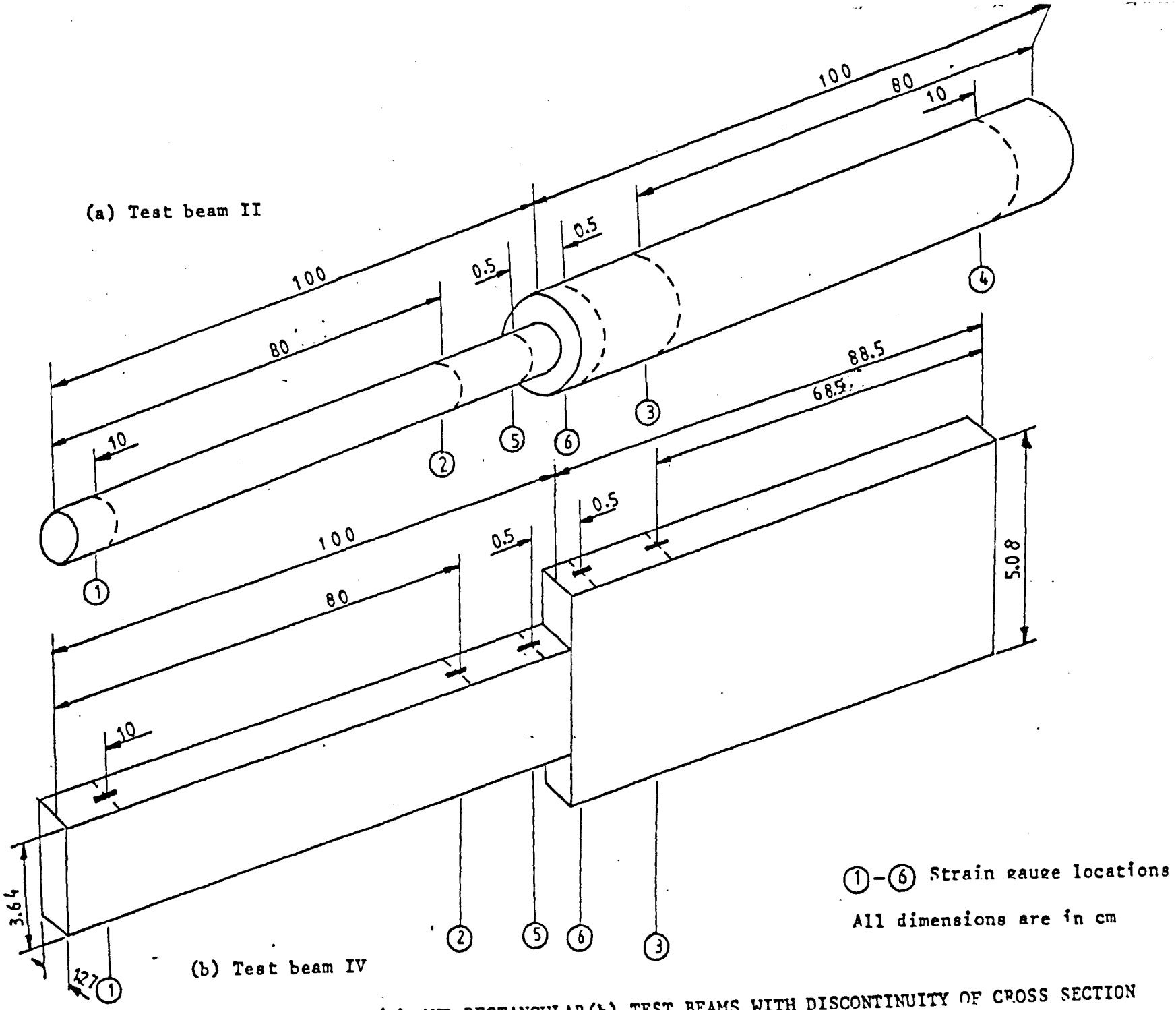

FIG. 7.29 CIRCULAR(a) AND RECTANGULAR(b) TEST BEAMS WITH DISCONTINUITY OF CROSS SECTION

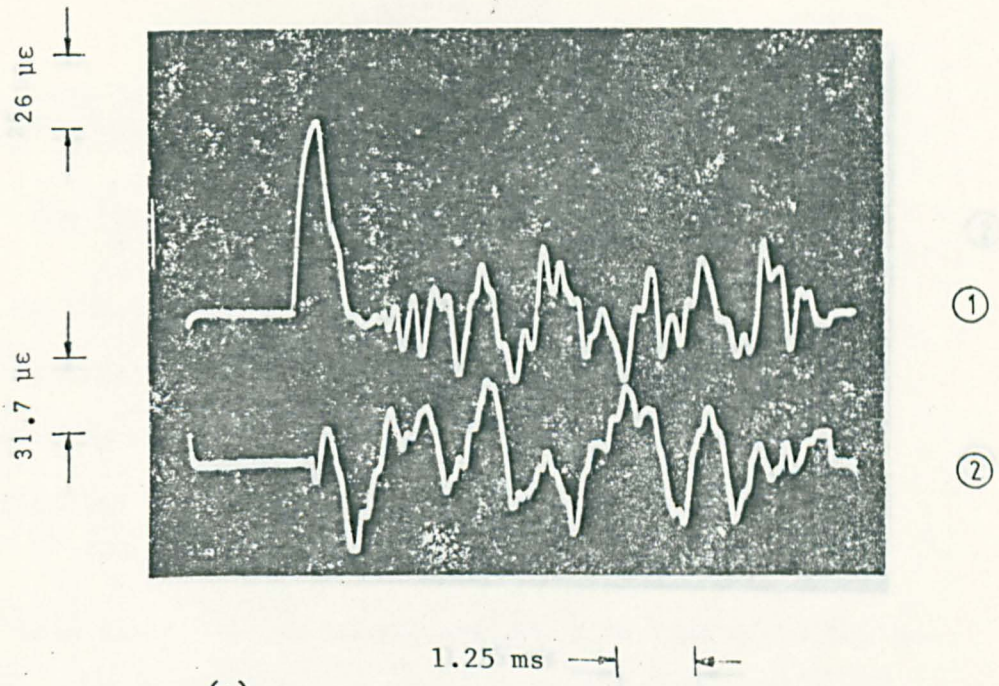

(a)

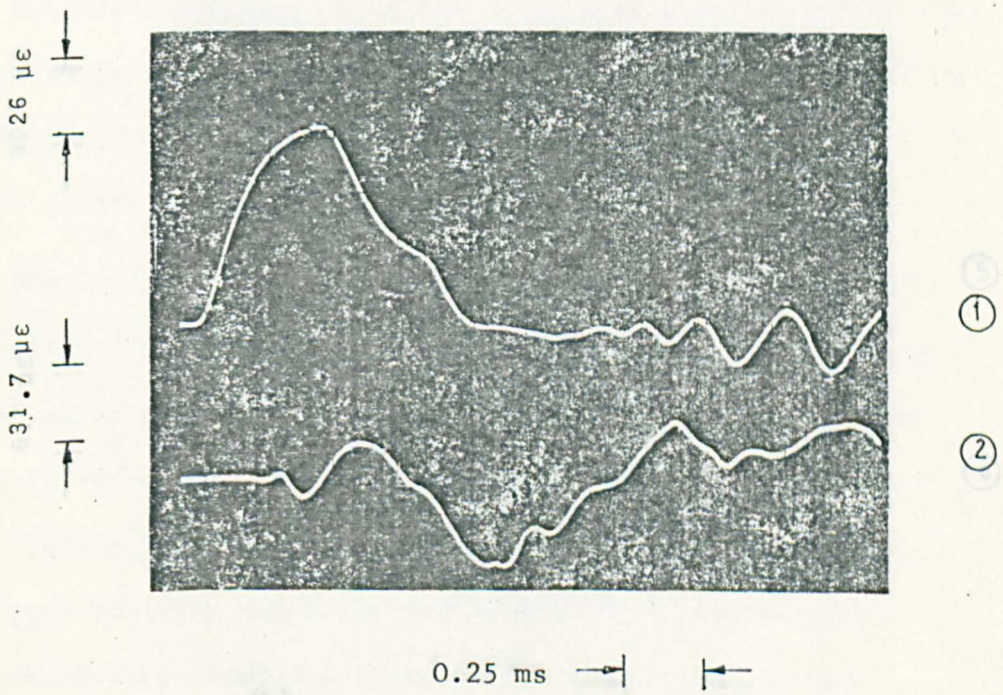

(b)

FIG. 7.30 BENDING STRAIN-TIME RESULTS FOR THE STEPPED BEAM OF RECTANGULAR CROSS SECTION DUE TO ECCENTRIC IMPACT WITH THE 1.0 m LONG CYLINDRICAL STRIKER

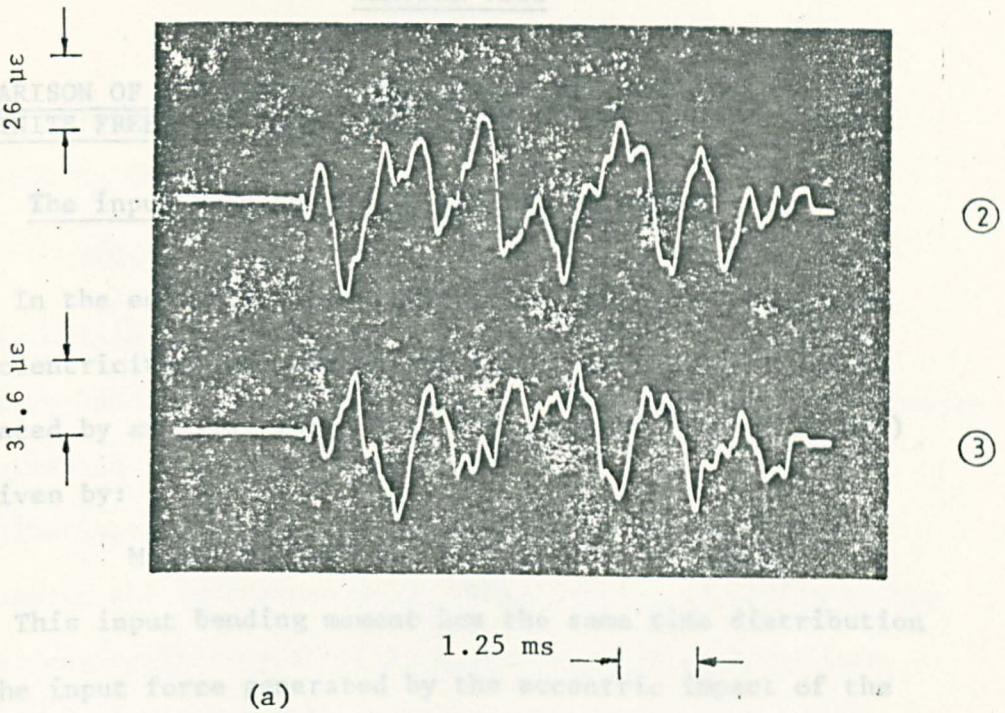

(a)

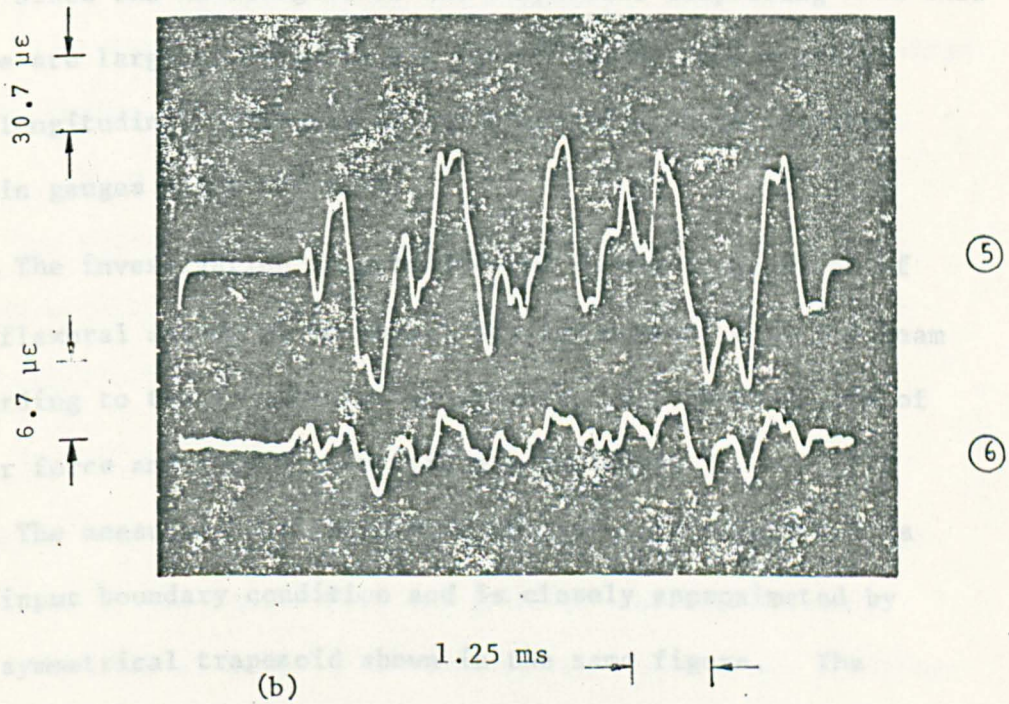

(b)

FIG. 7.31 BENDING STRAIN-TIME RESULTS FOR VARIOUS POSITIONS OF THE STEPPED BEAM OF RECTANGULAR CROSS SECTION DUE TO ECCENTRIC IMPACT WITH THE 1.0 m LONG CYLINDRICAL STRIKER

CHAPTER VIII

COMPARISON OF EXPERIMENTAL AND THEORETICAL RESULTS IN FINITE FREE-FREE TIMOSHENKO BEAMS

8.1. The input bending moment-time distribution

In the eccentric impact the force P(t) is applied with an eccentricity e and the eccentrically acting force can be replaced by an axial force P(t) and a couple M(t) where M(t) is given by:

$$M(t) = P(t).e \qquad (8.1)$$

This input bending moment has the same time distribution as the input force generated by the eccentric impact of the striker. The duration of this pulse is governed by the time necessary for the compressive wave front to move twice the length of the 1.0 m striker.

Since the wavelengths of the components comprising from this pulse are large compared to the beam diameter, the shape of the longitudinal pulse can be recorded quite accurately by strain gauges along the beam.

The investigation is concentrated on the propagation of the flexural strain waves (hence bending moment) down the beam according to the Timoshenko beam theory, where the effects of shear force and rotatory inertia are included.

The measured axial strain is presented in figure 8.1 as the input boundary condition and is closely approximated by the symmetrical trapezoid shown in the same figure. The trapezoidal form is used for the numerical computation where experimentally obtained loading conditions are used as input to the numerical solution.

The trapezoidal pulse shape is obtained as the difference

of two ramp platform input functions differing by the pulse duration t_d according to

$$M(0,t)_{TRP} = M(0,t)_{RP} - M(0,t-t_d)_{RP} \qquad (8.2)$$

where indices TRP and RP are for the trapezoidal and ramp platform bending moments respectively and their time distribution was given in table 4 (Chapter 5).

The input strain pulse presented in figure 8.1 is used to compute the equivalent axial force loading according to the one dimensional dispersionless elementary longitudinal wave theory. Unless otherwise stated, the maximum antisymmetric strain due to the eccentric impact was measured as $\varepsilon_m = 46.7\ \mu\varepsilon$ the maximum axial force

$$P_m = \varepsilon_m EA = 4831 \quad N \qquad (8.3)$$

Using the measured eccentricity of e = 7.85 mm, the maximum input bending moment is found to be

$$M_o = P_m.e = 38\ Nm \qquad (8.4)$$

The recorded maximum input axial strain is in very good agreement with the axial strain obtained from the elementary wave theory as

$$\varepsilon_m = \frac{\rho c_1 v}{2E} = \frac{v}{2c_1} = 47.8\ \mu\varepsilon \qquad (8.5)$$

where $c_1 = 5140$ m/s is the bar velocity, and v = 0.491 m/s is the value of the impact velocity used in most experiments.

The material properties used for the theoretical solutions throughout chapter 8 are those experimentally measured for the actual mild steel test beams and were listed in table 7 as

$$E = 205.6 \times 10^9 \quad N/m^2$$

$$\rho = 0.777 \times 10^4 \quad kg/m^3$$

$G = 79.69 \times 10^9 \ N/m^2$

$\nu = 0.29$

$c_1 = 5140$ m/s

$c_2 = 3011$ m/s

$k^2 = 0.8856$

The bending moment $M(0,t)$ is zero at $t = 0$ and reaches the maximum of $M_o = 38$ Nm after a short finite rise time of $t_o = 90$ μs during which a linear ramp increase is assumed. The pulse duration is obtained as

$$t_d = \frac{2\ell}{c_1} = 389 \ \mu s \qquad (8.6)$$

where ℓ is the length of the striker (1.0 m).

To generalize the discussion, the values of the bending moment and time are non-dimensionalized as

$$\bar{m} = \frac{M.d}{EI} \qquad (8.7)$$

$$\bar{T} = \frac{c_1.t}{d} \qquad (8.8)$$

where d = 25 mm (approximately equal to the diameter of the uniform beam and equal to the small diameters of the stepped beams).

The input bending moment was idealized as trapezoid and was obtained according to equation 8.2. which describes the input boundary condition for the antisymmetric strain components as long as the input pulse duration is less than $t_d + t_o$ and was set equal to zero outside this range. However, the experimentally observed axial strain decayed to zero at a later stage due to reflection from the far end of the test beam.

The maximum non-dimensional input bending moment is

calculated as

$$\bar{m} = \frac{M.d}{EI} = 0.225 \times 10^{-3} \qquad (8.9)$$

and the corresponding maximum bending strain on the outer surface of the test beam with radius r

$$\varepsilon = \frac{M.d}{2EI} = 115 \ \mu\varepsilon \qquad (8.10)$$

Unless otherwise stated the input boundary condition as pure bending moment loading was used for the uniform test beam of circular cross-section and for the two cylindrical beams with discontinuity of cross-section.

The time range of the bending strain investigation was very short (less than 2 ms) and therefore the influence of damping was expected to be very small and was not taken into consideration.

In comparing the experimental results and theoretical predictions, one should expect some degree of discrepancy due to one or more of the following reasons.

i) For the case of the numerical computation a relatively simple trapezoidal pulse was used to describe approximately the exact input pulse. This introduces a certain amount of error in the input boundary condition itself.

ii) The trapezoidal pulse is composed of a large spectrum of frequency components which are dispersed due to the different velocities at which each frequency is propagated. This dispersion is a characteristic of the bending wave.

iii) The Timoshenko theory gives an excellent prediction of the velocity for propagation in the first branch of the dispersion curve, but is less satisfactory in its predictions

for the next highest branch of the dispersion curve, particularly at high frequency where large deviations from the exact theory occur. A good agreement between theoretical and experimental results indicates that there are no waves generated in the second mode or there are only long wave transmissions.

iv) Although an excellent degree of reproducibility was achieved for the conducted sets of experiments, there are inherent errors in the experiments and in the reduction of experimental data.

Taking all these points into account, it will be shown in the next sections that the numerical solution by the method of characteristics according to the Timoshenko beam theory presents an accurate prediction of the observed flexural deformations in finite uniform beams and in beams with discontinuity of cross-section.

8.2. Uniform beam of circular cross-section subjected to eccentric impact

The eccentric impact of the beam by a striker of the same cross-section produced a system of strain waves which had both symmetrical and antisymmetrical components about the beam mid plane. However, the aim of the present work was to investigate the bending waves, i.e. to study the antisymmetrical strain-time distribution at each beam cross-section.

The comparison of the measured and predicted bending moment histories are shown in figure 8.2 for the position x/d = 12 and 84 of the 3.0 m long uniform beam of circular cross-section. The diameter of the test beam was 25.4 mm and the beam was subjected to eccentric impact by a 1.0 m striker of a diameter equal to the test beam.

The bending strain history shown in fig.8.2(a) for a position

12 diameters from the impact end indicates that the trapezoidal input bending moment of maximum positive magnitude $\bar{m} = 0.225 \times 10^{-3}$ has already built-up a negative peak of $\bar{m} = 0.9 \times 10^{-4}$ at $\bar{T} = 60$ and has a positive peak arriving at $\bar{T} = 140$ with a magnitude of $\bar{m} = 0.15 \times 10^{-3}$ which is only 60% of the input bending moment.

Comparison of results showed a good agreement between theoretical predictions and experimental observations both in magnitude and shape up to $\bar{T} = 150$. After that, the theoretical prediction approaches zero faster than the measured bending moment. This can be explained by the difference between the trapezoidal input function which is assumed to become zero at about $\bar{T} = 100$ and the actual pulse which still has a finite value at $\bar{T} = 100$ and approaches zero at a later time.

The comparison in figure 8.2(b) for the theoretical prediction of the bending moment history and its recorded history at position $x/d = 84$ indicate a good agreement and theory results in a slightly smaller magnitude than the experiment.

The results presented for the case of the uniform test beam are brief and are intended to give only an example before proceeding to the results of the finite free free beams with discontinuity of cross-section which is the main purpose of the present work.

A more detailed comparison of several cases of semi-infinite and finite uniform beams was conducted in chapter 5.

According to the wave theory, the fastest waves in beams are travelling with the bar velocity c_1 and therefore reflections in the present example are expected to arrive at position $x/d =$

12 after $\bar{T}$ = 228 and at position x/d = 84 after $\bar{T}$ = 156. However, there was little evidence of any reflections arriving within the considered non-dimensional time of $\bar{T}$ = 316 and 244 for x/d = 12 and 84 respectively. It is expected that the main components of the transient input bending moment are travelling at a slower velocity.

The dispersion of the flexural wave and the adequacy of the Timoshenko beam theory in predicting the main features of the beam response to eccentric impact are clearly demonstrated.

8.3 Cylindrical beam with discontinuity of cross-section at the middle

The comparison of bending moment history at various positions on both cross-sections of the stepped beam are presented in figures 8.3 - 8.5. The numerical results were obtained using the TMOTCU 3 computer program and the experimental data were based on the measured antisymmetric outer surface strains.

The experimental results and the numerical results are in extremely good agreement. In all cases the major features of the experimental results are reproduced by the numerical solution obtained by the method of characteristics.

Fig.8.3 shows the comparison of bending moment-time distribution at positions x/d = 4 and 32 corresponding to 0.1 m and 0.8 m from the eccentrically impacted end of the 2.0 m long test beam with the discontinuity of cross-section at the middle.

The maximum velocity of propagation of any wave component in the beam is c_1 and therefore the fastest possible arrival of the bending wave is at $\bar{T}$ = 4 and 32 for positions x/d = 4 and 32 respectively. However, the trapezoidal input bending moment becomes more and more widespread as it is propagated

along the beam.

For position x/d = 4 the agreement between experimental results and theoretical prediction is very good up to $\bar{T} = 96$ and even at this early location only 4 diameters from impact end, the dispersive character of the flexural wave is clearly visible in the production of a small initial negative peak and some reduction in the maximum peak of the input bending moment.

After $\bar{T} = 96$, the theoretical prediction reaches zero faster than the experimentally observed data due to the basic disagreement between the theoretically assumed trapezoidal input bending moment and the bending moment magnitude evaluated from the observed longitudinal strain, as demonstrated in figure 8.1.

The agreement at position x/d = 32 until $\bar{T} = 148$ is excellent in both amplitude and time. After $\bar{T} = 148$ there is some difference although the theoretical prediction still gives the general form of the experimentally observed bending moment history.

The experimental and theoretical bending moment-time distributions immediately before and after the position of discontinuity are compared in figure 8.4. The experimental records were obtained from strain gauge locations at x/d = 39.8 and 40.2 whereas the theoretical predictions are both for position x/d = 40 where the diameter of the test beam increased from $d_1 = 25.4$ mm to $d_2 = 31.75$ mm.

The time wise agreement between the two sets of results is excellent but the theoretical solution predicts slightly

smaller peaks at the initial stages and larger magnitudes from $\bar{T} = 200$ onwards. A peak value of $\bar{m} = 0.7 \times 10^{-4}$ at $\bar{T} = 152$ has decreased to $\bar{m} = 0.25 \times 10^{-4}$ due to an increase in the diameter of the test beam by 25%.

The comparison of experimental and theoretical bending moment history at position x/d = 48 and 76 is presented in figure 8.5.

The numerical results based on the method of characteristics produced good pulse magnitude and shape agreement with experiment.

The bending moment pulse at position x/d = 76 showed a more oscillatory form than the pulse at any position before and the main components arrived after $\bar{T} = 140$ indicating clearly that bending waves are travelling with velocities smaller than the bar velocity c_1.

Although the theoretical predictions of peaks were mostly lower than those observed experimentally, the experimental data showed the presence of a definite peak at the location predicted numerically.

The extremely good agreement of the numerical predictions using the TMOTCU3 computer program with experimental observations of the bending wave propagation indicated clearly the adequacy of the Timoshenko beam theory for flexural wave propagation in beams with discontinuity of cross-section.

8.4. Longer Cylindrical beam with discontinuity of cross-section subjected to eccentric impact

Comparisons of measured and predicted bending moment history are shown in figures 8.6 and 8.7 for a longer test beam of 3.295 m with the discontinuity of cross-section at the same distance from

the impact end as in the previous example. In this case, the reflected bending wave from the far end of the beam is expected to arrive at a later time.

The results shown in figure 8.6 for positions x/d = 4 and 32 are identical with the results shown in figure 8.3 for the same positions of the shorter beam except a small difference for x/d = 32 at $\bar{T}$ = 216. This indicates that within the considered time of $\bar{T}$ = 240 there were no reflections from the far end arriving at the monitoring positions and the significant change in the shape and magnitude of the input bending moment is due to dispersion and reflections from the position of discontinuity. Good agreement is noted for pulse magnitude and shape.

Figure 8.7 shows a comparison of experimental observations and theoretical predictions for positions x/d = 48 and 80. The agreement is extremely good, although the numerical solution predicts a slightly lower amplitude for the travelling bending wave.

8.5. Cylindrical stepped beam subjected to eccentric impact at the larger end

The 2.0 m long test beam with discontinuity of cross-section at the middle was subjected to eccentric impact at its large end of 31.75 mm diameter where the axial force was applied with an eccentricity of e = 9.5 mm.

The longitudinal surface strain was measured as ε_m = 34.5 με and the maximum axial force was obtained according to equation (8.3) as

$$P_m = \varepsilon_m EA = 5610 \text{ N} \qquad (8.11)$$

The maximum input bending moment is as in equation (8.1)

$$M_o = P_m.e = 53.3 \text{ Nm} \qquad (8.12)$$

The non-dimensional time is defined as in equation (8.8) as $\bar{T} = c_1.t/d$ with d still taken as 25 mm.

The bending moment was non-dimensionalized according to equation (8.7) as

$$\bar{m} = \frac{M.d}{EI} = 0.13 \times 10^{-3} \qquad (8.13)$$

where I is cross sectional moment of inertia of the larger cross section.

The maximum bending strain corresponding to the maximum input bending moment can be obtained as

$$\varepsilon = \frac{M.d}{2EI} = 82.5 \quad \mu\varepsilon \qquad (8.14)$$

The input bending moment for the numerical computation was assumed as before to be in the form of trapezoid with a finite rise time of $t_o = 90$ μs ($\bar{T}_o = 18.5$) as shown in figure 8.1.

Comparison of measurements and TMOTCU3 calculations are shown in figures 8.8. to 8.10 for the bending moment-time distribution at x/d = 4, 32, 40 and 48.

In figure 8.8. the experimental results and theoretical results are presented for strain gauge locations x/d = 4 and 32. The agreement for position x/d = 4 is seen to be excellent and the bending moment approaches the maximum of $\bar{m} = 0.125 \times 10^{-3}$ as from $\bar{T} = 68$.

At position x/d = 32, the theory predicts a larger peak for the bending moment at $\bar{T} = 100$ and at $\bar{T} = 144$ which are the same positions of the experimentally predicted peaks. The agreement in time variation between theory and experiment is extremely good.

The bending moment history at the position of discontinuity immediately before and after the reduction of cross-section at x/d = 40 is presented in figure 8.9 where theoretical solutions are obtained for x/d = 40, and experimental results were observed at strain gauge locations x/d = 39.8 and 40.2.

The theoretical solution was obtained for a shorter period of $\bar{T} = 160$ than in the case of increased cross-section, since the present case required a finer mesh size of $\Delta x = 0.625$ mm in contrast to the larger mesh size of $\Delta x = 1.25$ mm used in previous cases.

The bending moment at $\bar{T} = 116$ increased from 0.1×10^{-4} to 0.3×10^{-4} due to a reduction in the diameter from 31.75 mm to 25.4 mm and a larger peak was observed at $\bar{T} = 238$.

Figure 8.10 shows the comparison between experimental and theoretical bending moment- time results at position x/d = 48 where there is an extremely good agreement in magnitude and shape.

The level of the bending moment dropped to $\bar{m} = 0.15 \times 10^{-4}$ at $\bar{T} = 120$ and to a negative magnitude of $\bar{m} = -0.24 \times 10^{-4}$ at $\bar{T} = 140$, and the alternating sign of the antisymmetric dispersion bending wave is clearly visible.

8.6. Finite stepped beam of rectangular cross section subjected to eccentric impact

The last studied case of stepped beams consisted of a test-beam of rectangular cross-section with increased height from $h_1 = 36.4$ mm to $h_2 = 50.8$ mm at 1.0 m from the impact end and with a constant width of 12.7 mm over the whole length of 1.885 m (Test beam IV of figure 7.29).

The input axial force due to eccentric impact with the 1.0 m striker of circular cross-section was applied at an eccentricity of e = 9.8 mm.

The maximum longitudinal surface strain due to eccentric impact was measured as $\varepsilon_m = 48.4$ με.

The axial force is obtained according to equation (8.3) as

$$P_m = \varepsilon_m EA = 4600 \text{ N} \qquad (8.15)$$

This in turn results in an input bending moment of the following maximum magnitude.

$$M_o = P_m.e = 45 \text{ Nm} \qquad (8.16)$$

The non-dimensional input bending moment is defined as

$$\bar{m} = \frac{M.h_2}{EI} = 0.217 \times 10^{-3} \qquad (8.17)$$

The rise time of the trapezoidal input bending moment is taken as $t_o = 90$ μs and the non-dimensional time is defined as before.

$$\bar{T} = \frac{c_1 t}{d} \quad \text{where } d = 25 \text{ mm.}$$

The maximum bending strain due to the maximum input bending moment can be obtained as

$$\varepsilon = \frac{M_o.h_1/2}{EI} = 78 \ \mu\varepsilon \qquad (8.18)$$

The value of the shear correction factor for the rectangular cross section was taken as $k^2 = 0.849$ and then c_2 can be determined as

$$c_2 = \sqrt{k^2 G/\rho} = 2949 \text{ m/s} \qquad (8.19)$$

The non-dimensional bending moment-time distribution for positions x/d = 4, 32 40, and 48 are shown in figures 8.11 to 8.13.

The agreement between theoretical predictions and experimental results is good in magnitude and shape with the theoretical solution predicting higher peaks at the same positions of the measured peaks.

Fig.8.11 presents the bending moment history at positions x/d = 4 and 32. The change in the shape of the bending moment as it has travelled from x/d = 4 to x/d = 32 is clearly observed where the initial positive bending moment of $\bar{m} = 0.205 \times 10^{-3}$ at x/d = 4 builds up to a negative peak of $\bar{m} = 0.125 \times 10^{-3}$ at $\bar{T} = 204$ as monitored in position x/d = 32. This peak is followed by smaller oscillations.

More severe bending moment changes are noted in figure 8.12 representing the comparison of experimental and theoretical data at x/d = 40 where the bending moment-time distribution is plotted before and after the discontinuity of cross section.

A better agreement between theoretical and experimental results is noted at the initial period of $\bar{T} = 160$ with the theoretical predictions becoming higher than experimental results as time progressed.

Fig.8.13 demonstrates the comparison of experimental observations and theoretical predictions for the bending moment history at x/d = 48.

The theoretical solution predicts the shape of the propagating bending wave but with a shift of about $\bar{T} = 8$ where the experimental peaks trail behind the analytical peaks.

It can be concluded that the propagation of flexural waves in beams of circular and rectangular cross-section with discontinuity of cross-section are adequately predicted by the numerical solution according to the Timoshenko beam theory. The differences between theoretical results and experimental results were reasonably small.

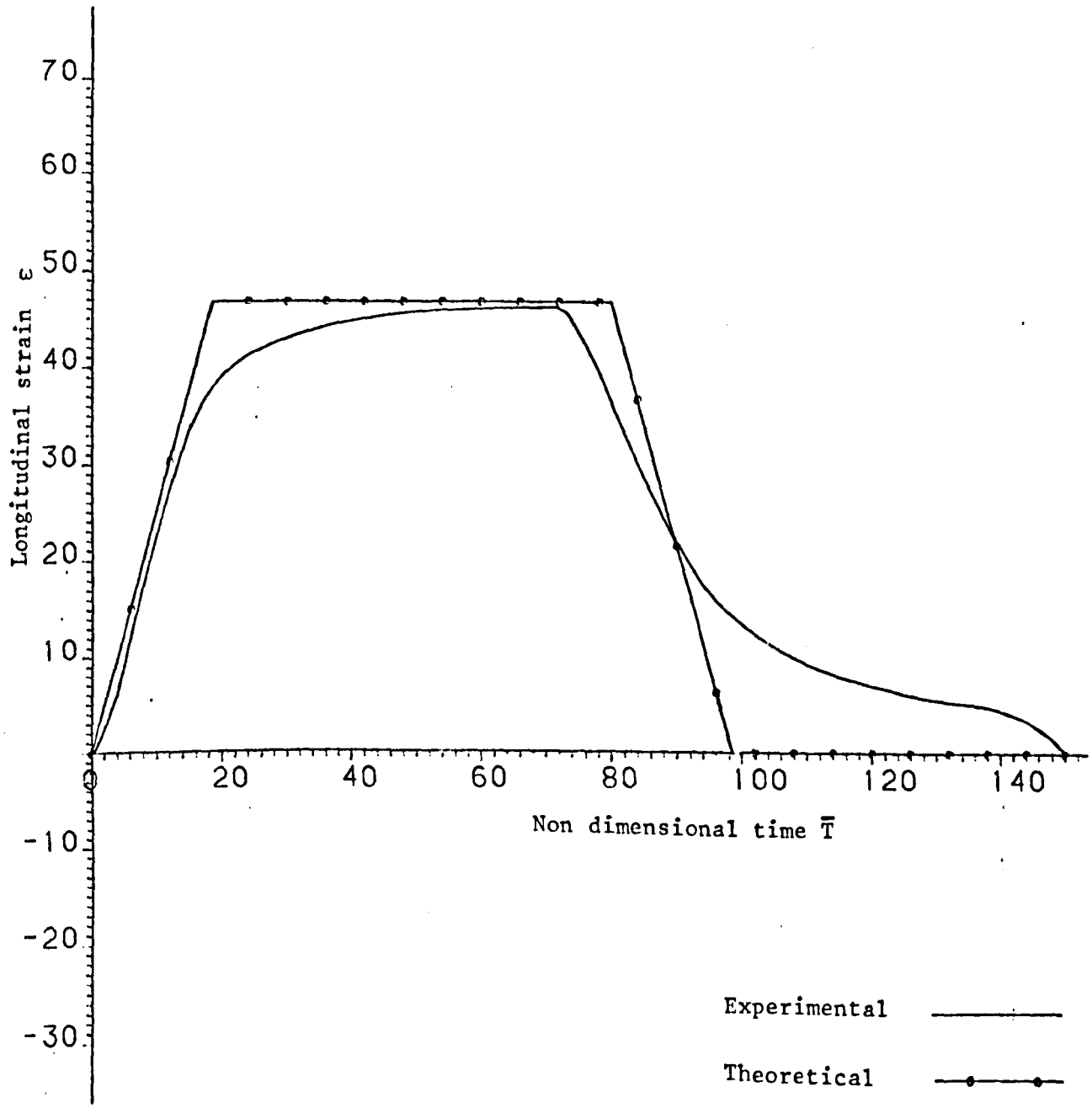

FIG. 8.1 RECORDED INCIDENT LONGITUDINAL PULSE AND TRAPEZOIDAL APPROXIMATION USED FOR NUMERICAL COMPUTATION

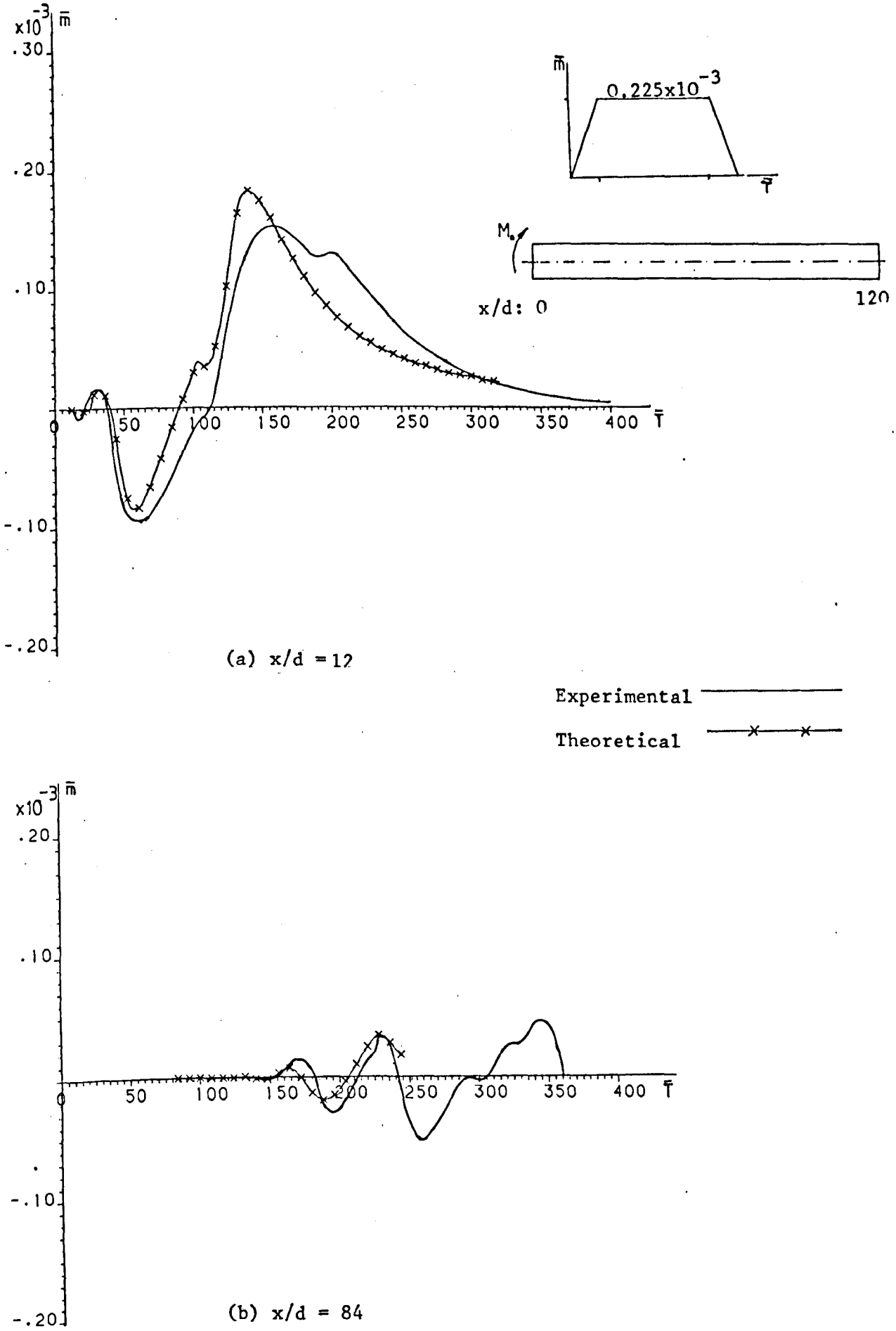

FIG. 8.2 COMPARISON OF RECORDED AND CALCULATED NON-DIMENSIONAL BENDING MOMENT HISTORY FOR THE 3.0 m LONG CYLINDRICAL UNIFORM BEAM

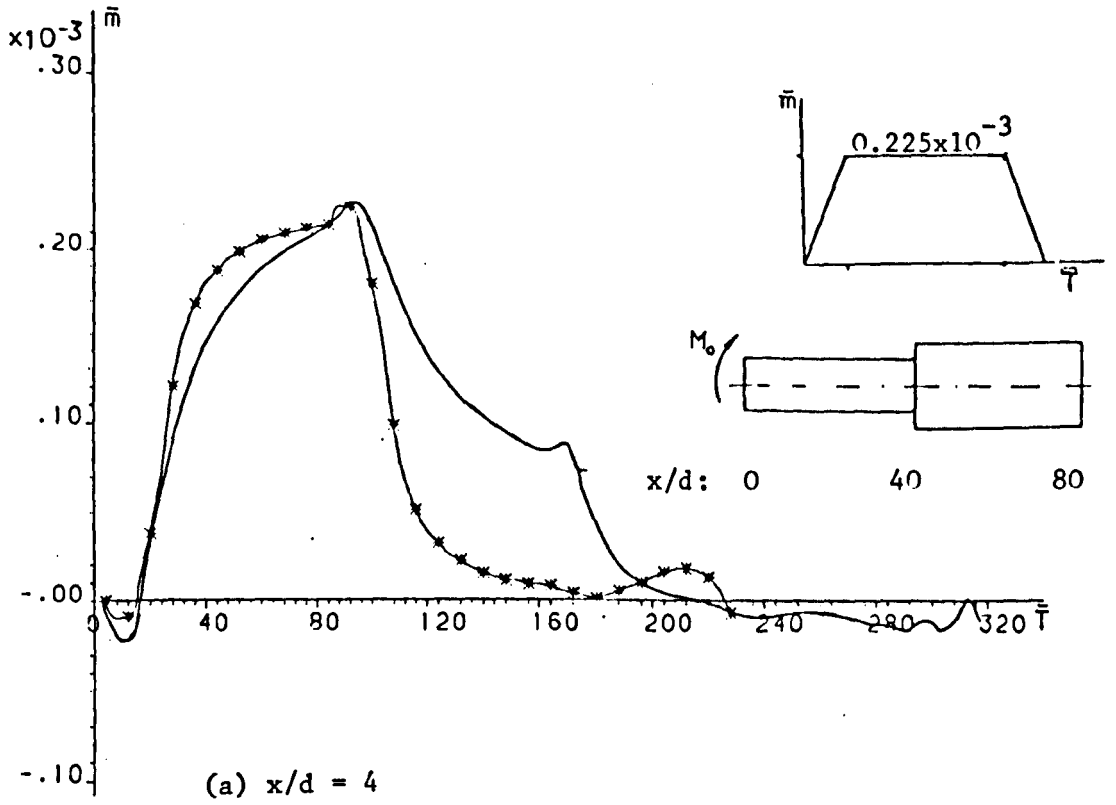

FIG. 8.3 COMPARISON OF EXPERIMENTAL AND THEORETICAL NON-DIMENSIONAL BENDING MOMENT HISTORY FOR THE 2.0 m LONG CYLINDRICAL BEAM WITH DISCONTINUITY

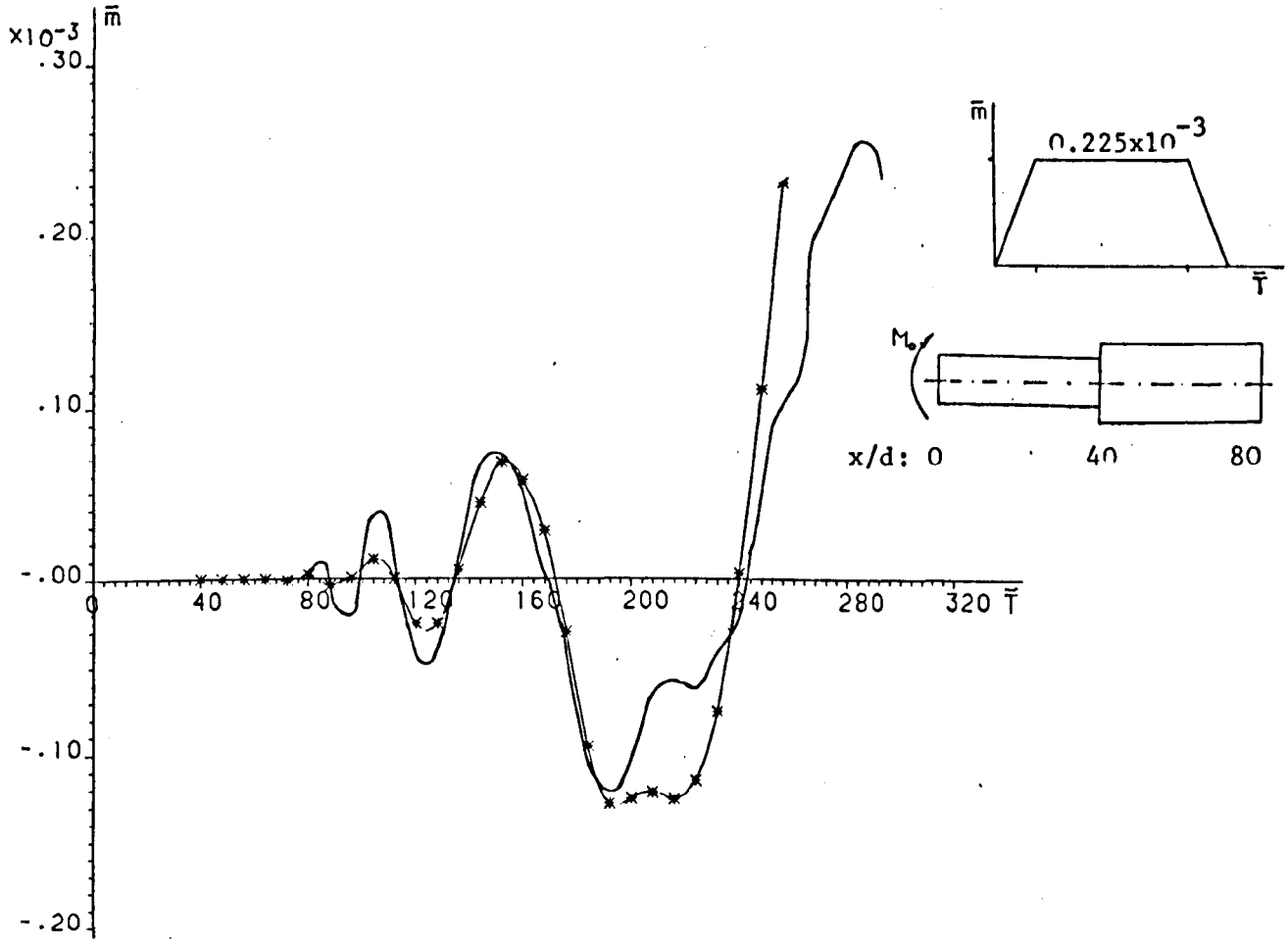

(a) x/d = 40

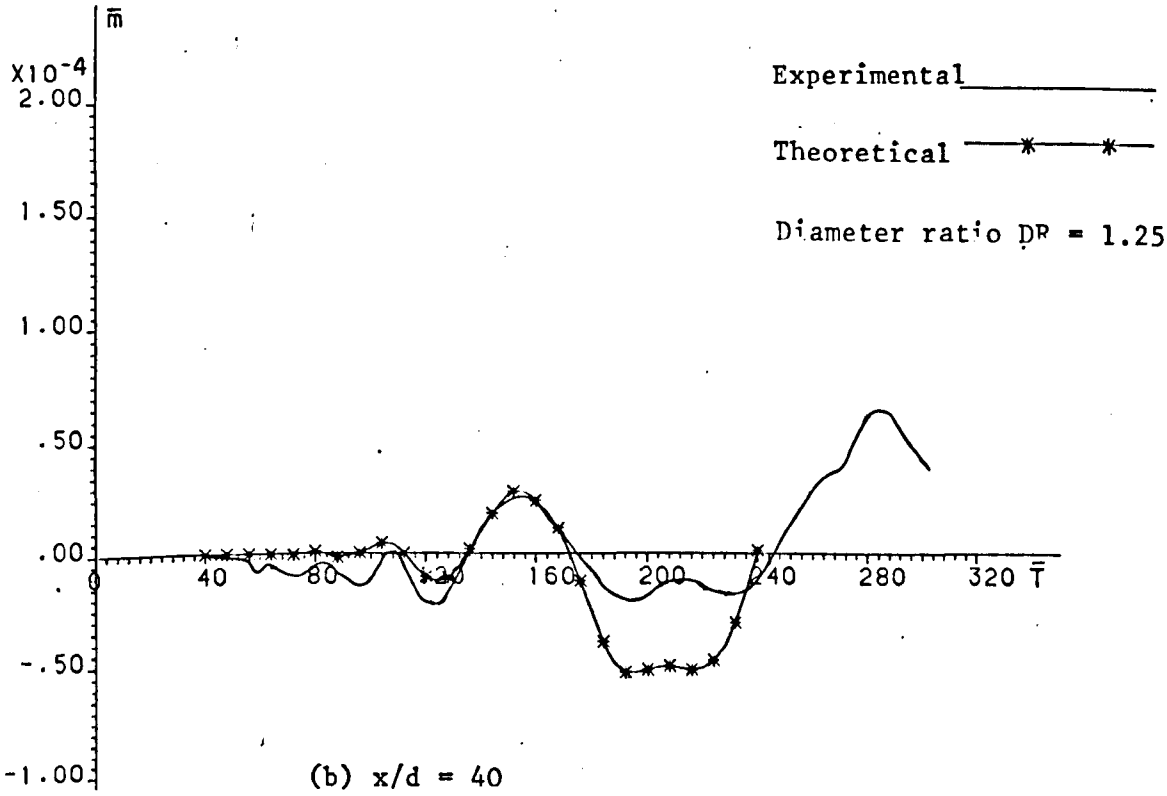

(b) x/d = 40

FIG. 8.4 COMPARISON OF EXPERIMENTAL AND THEORETICAL NONDIMENSIONAL BENDING MOMENT HISTORY FOR POSITIONS IMMEDIATLY BEFORE AND AFTER DISCONTINUITY

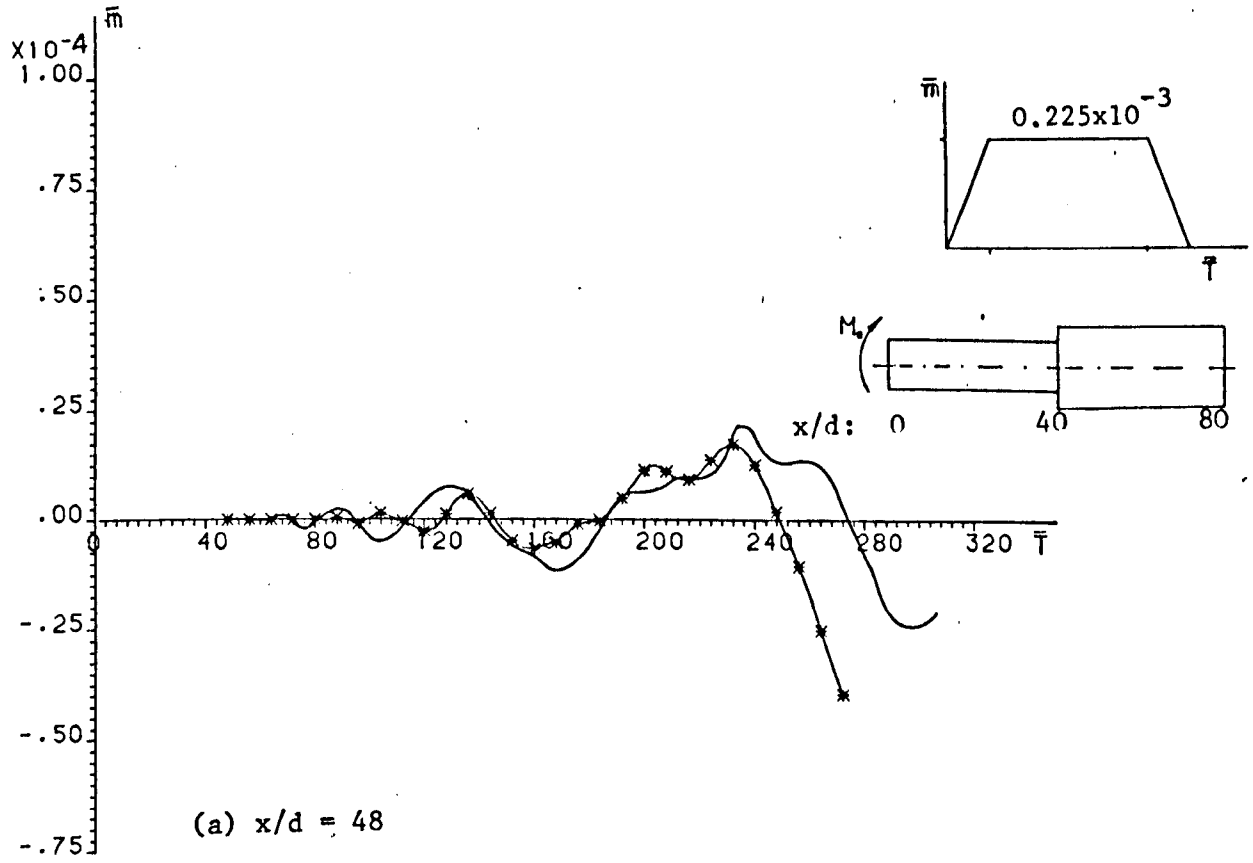

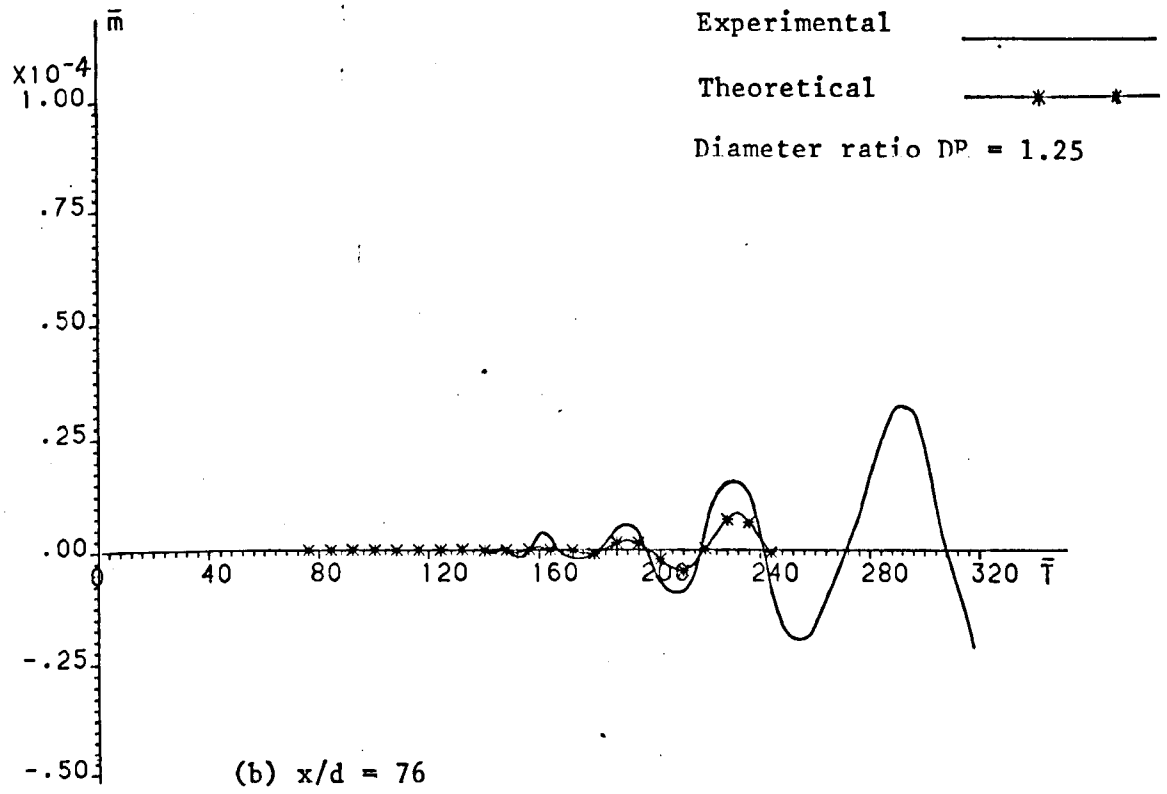

FIG. 8.5 COMPARISON OF EXPERIMENTAL AND THEORETICAL NON-DIMENSIONAL BENDING MOMENT HISTORY FOR THE 2.0 m LONG CYLINDRICAL BEAM WITH DISCONTINUITY

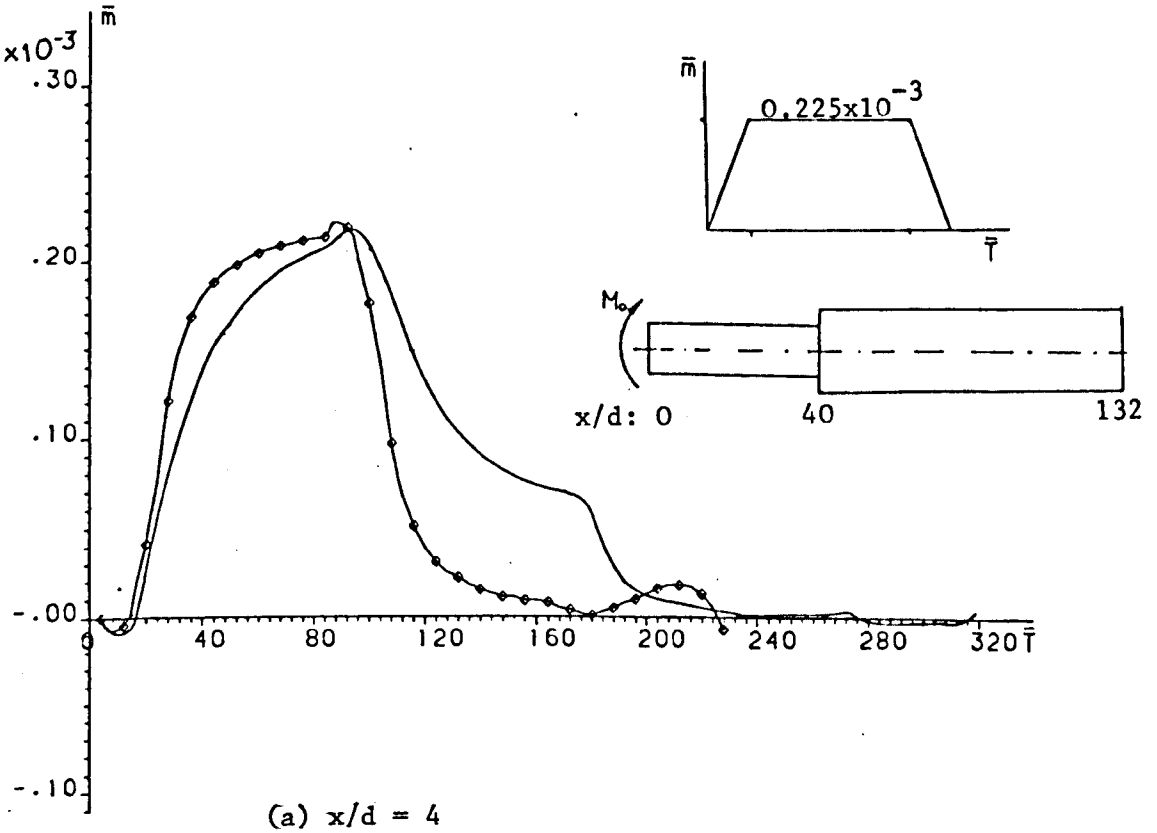

(a) x/d = 4

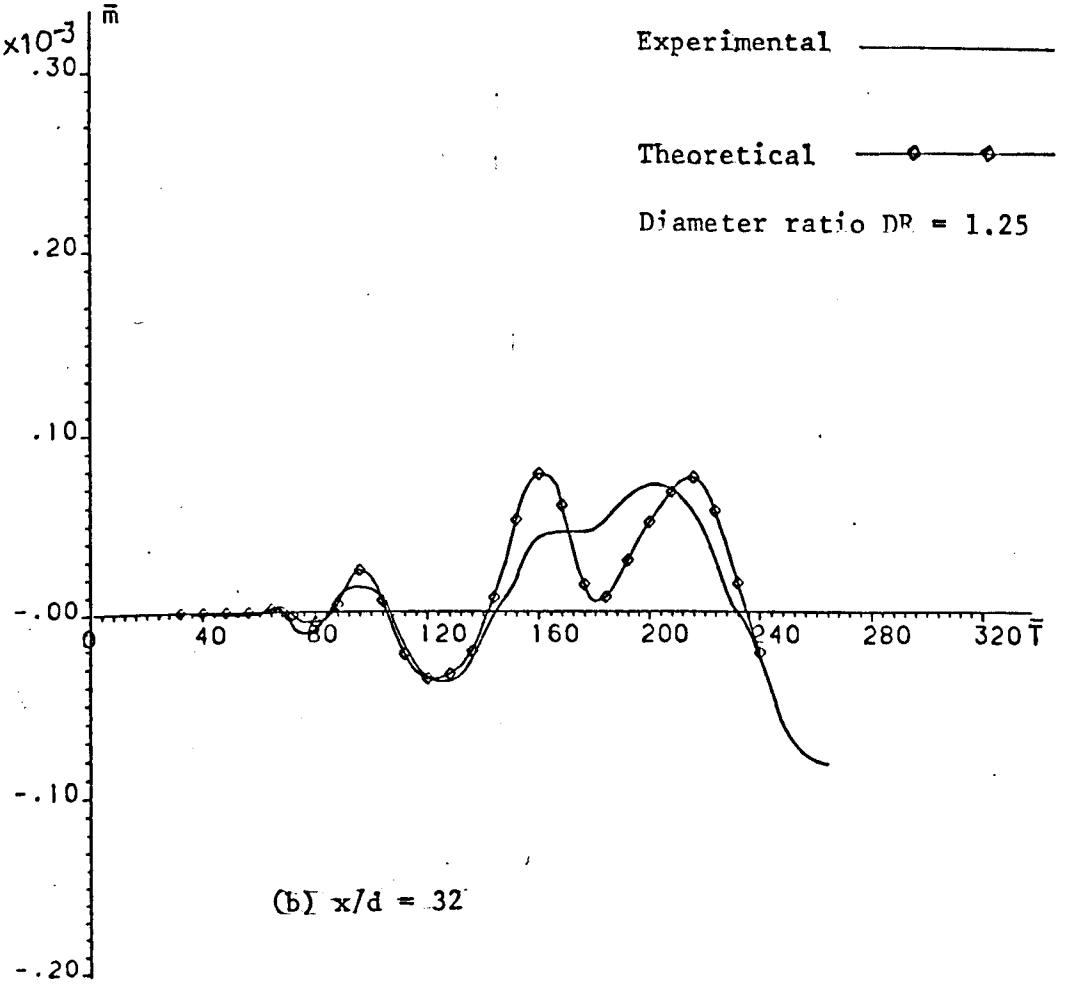

(b) x/d = 32

FIG. 8.6 COMPARISON OF EXPERIMENTAL AND THEORETICAL NON-DIMENSIONAL BENDING MOMENT HISTORY FOR THE 3.295 m LONG STEPPED BEAM

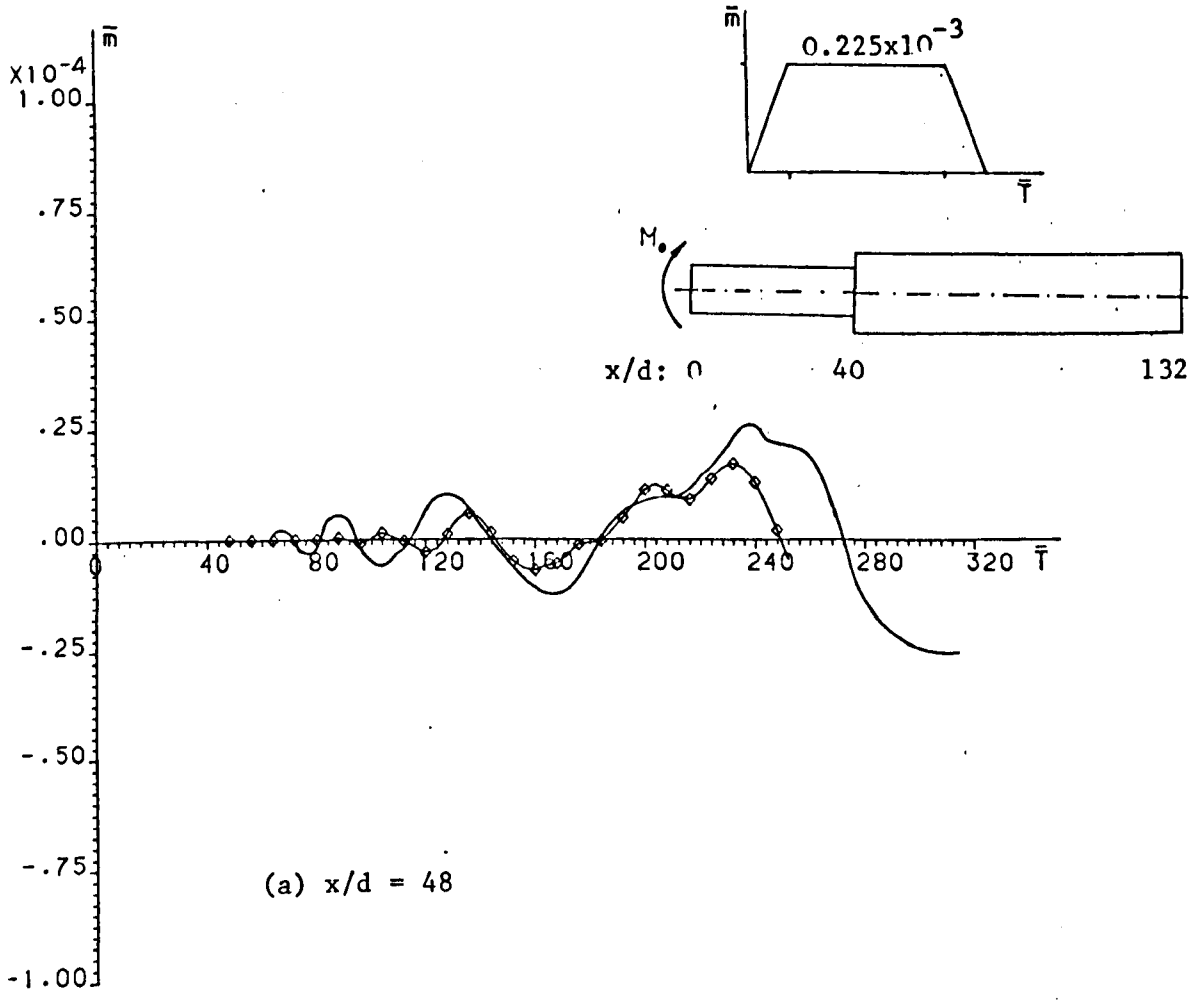

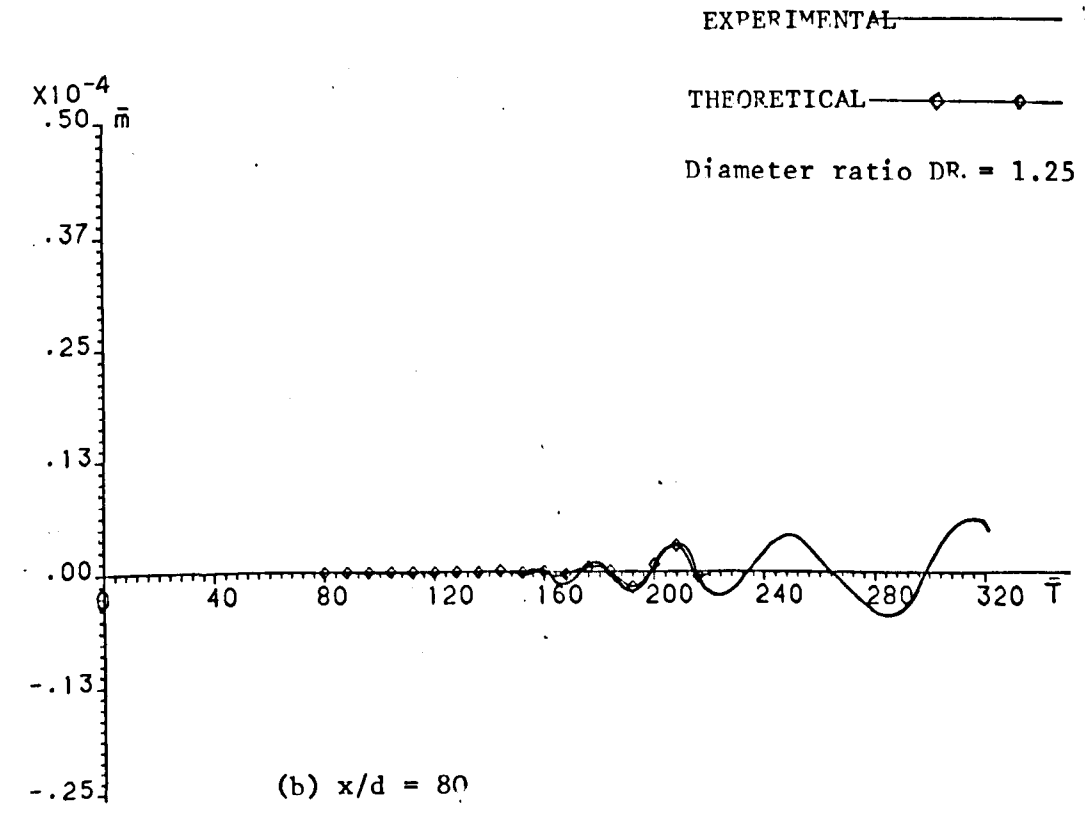

FIG. 8.7 COMPARISON OF EXPERIMENTAL AND THEORETICAL NON-DIMENSIONAL BENDING MOMENT HISTORY AT POSITIONS x/d = 48 AND x/d = 80 (L = 3.295 m)

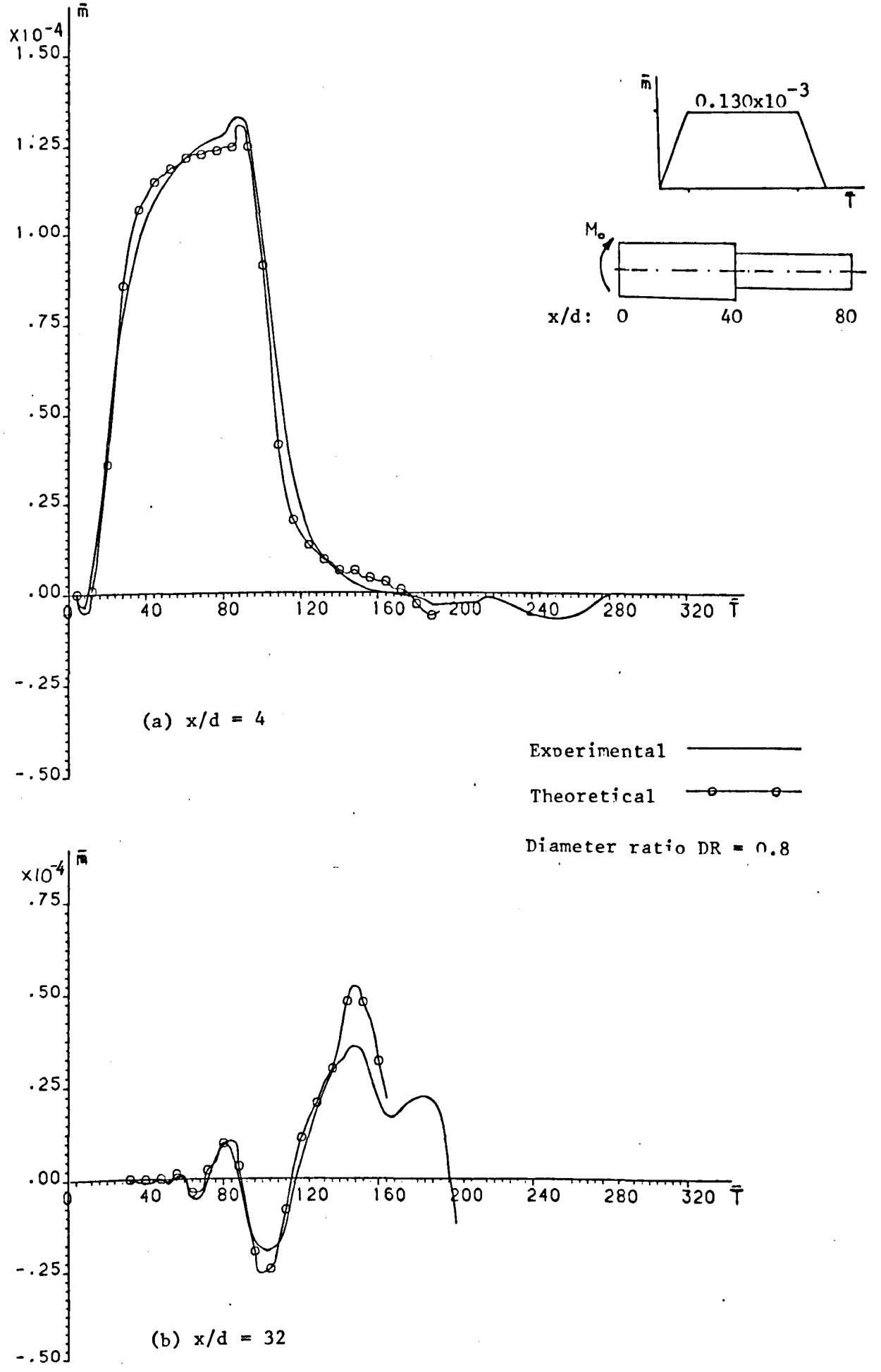

FIG. 8.8 MEASURED AND CALCULATED $\bar{m}$ - $\bar{T}$ CURVES FOR THE STEPPED BEAM SUBJECTED TO ECCENTRIC IMPACT AT ITS LARGE END (L = 2.0 m)

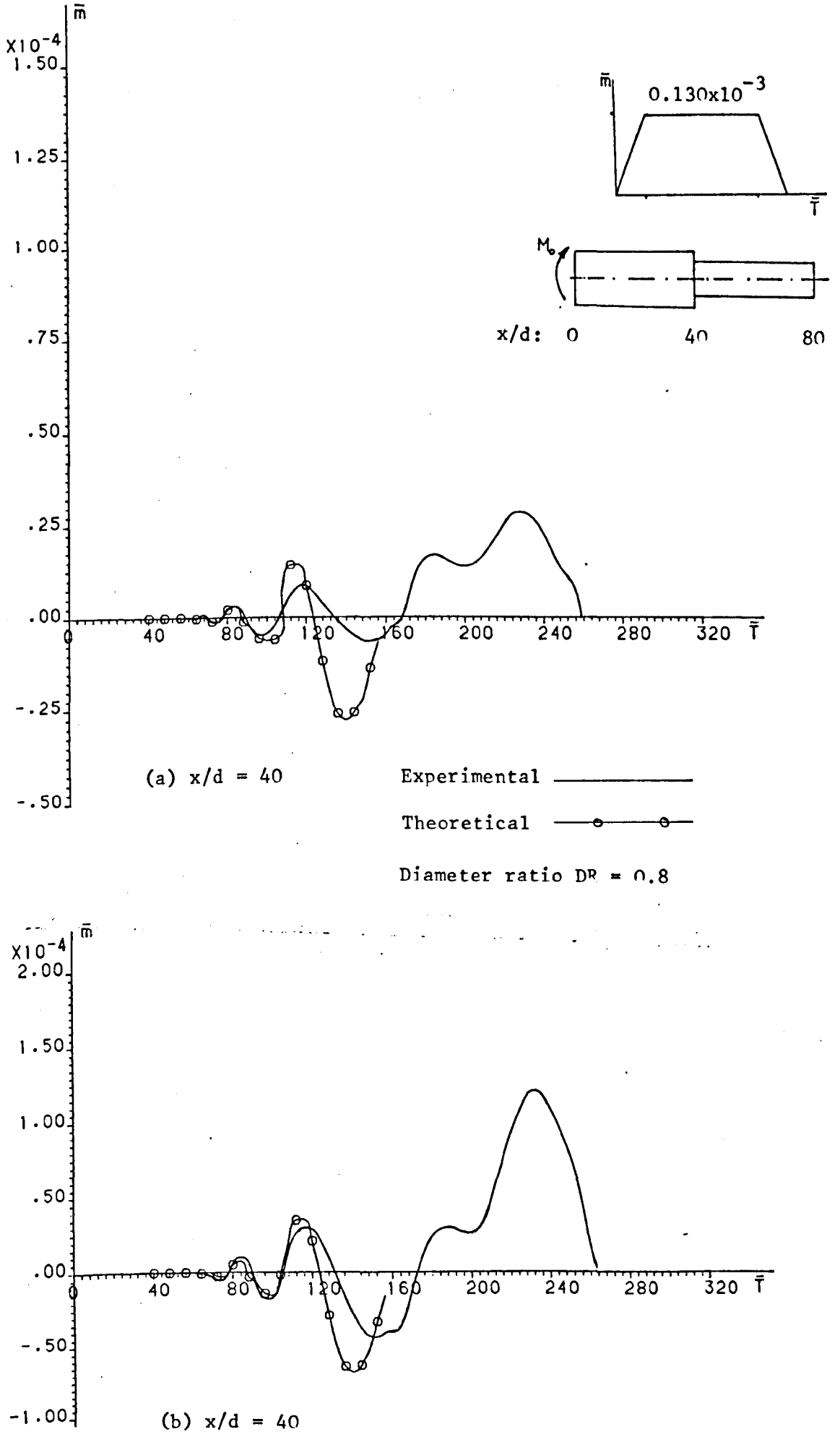

FIG. 8.9 MEASURED AND CALCULATED $\bar{m}$ - $\bar{T}$ CURVES AT POSITIONS IMMEDIATELY BEFORE AND AFTER THE POSITION OF DISCONTINUITY (L = 2.0 m)

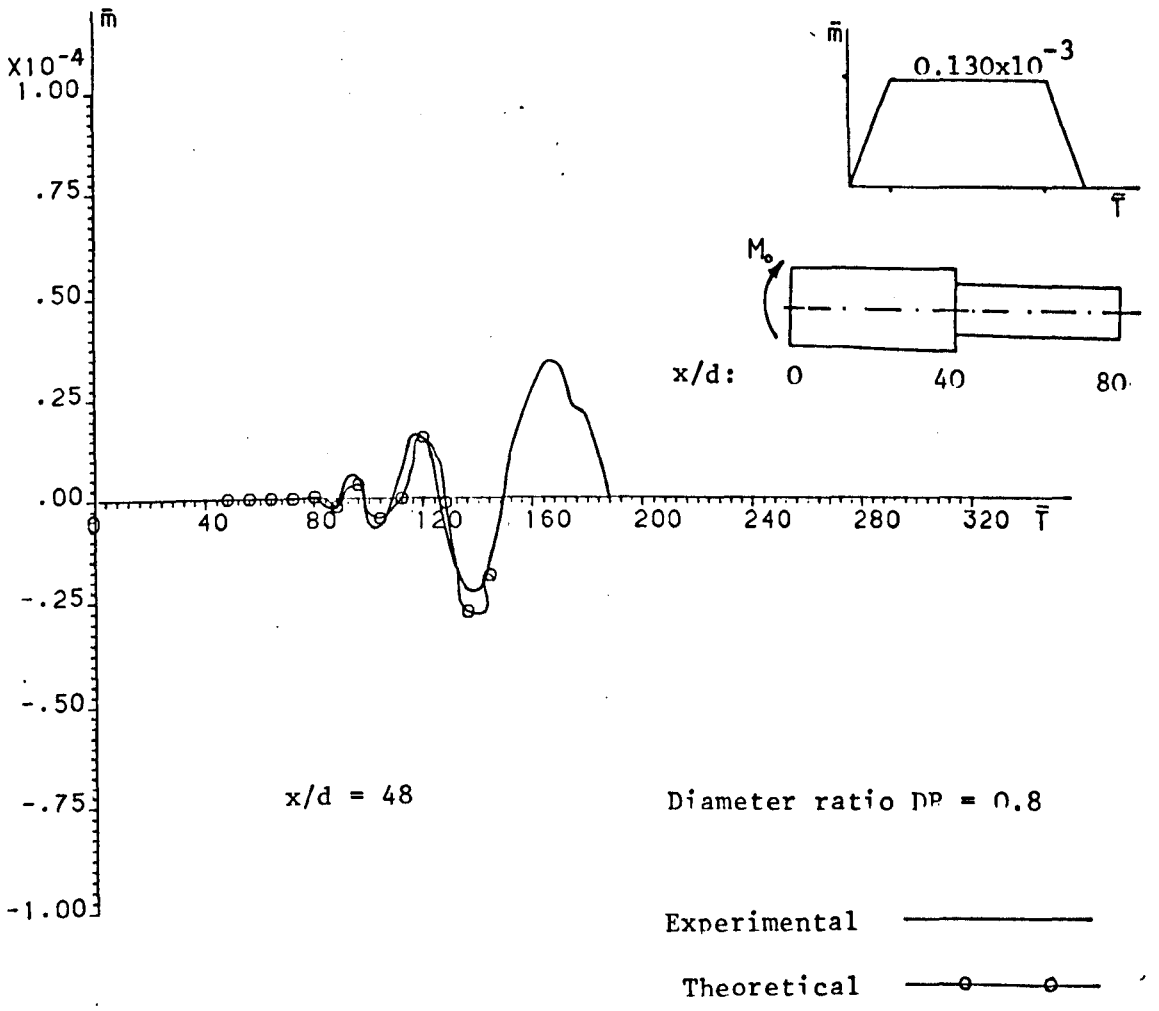

FIG. 8.10 MEASURED AND CALCULATED $\bar{m}$ - $\bar{T}$ CURVES FOR THE 2.0 m LONG STEPPED BEAM SUBJECTED TO ECCENTRIC IMPACT AT ITS LARGE END

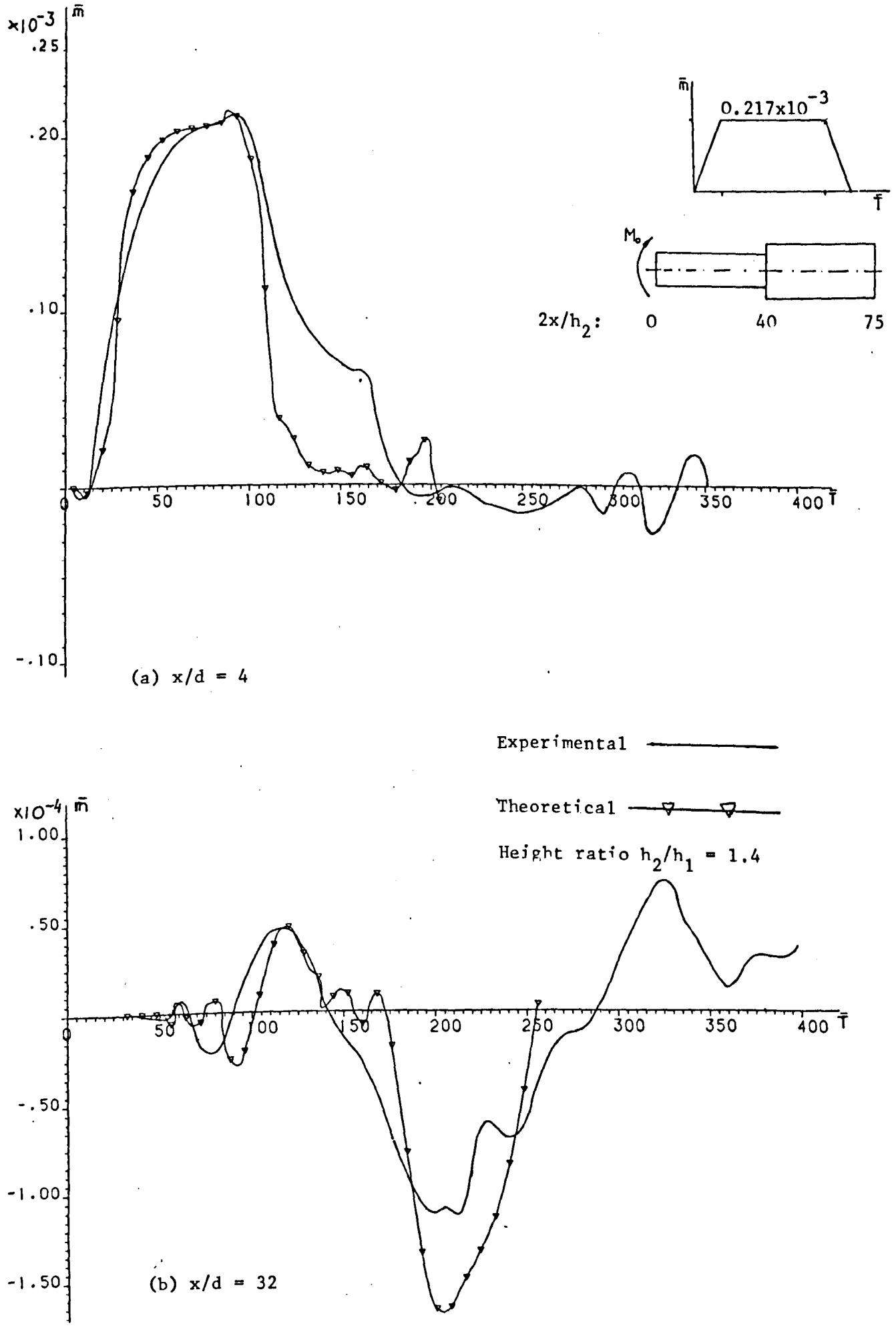

FIG. 8.11 COMPARISON OF RECORDED AND CALCULATED $\bar{m}$ - $\bar{T}$ RESULTS FOR THE 1.885 m STEPPED BEAM OF RECTANGULAR CROSS SECTION

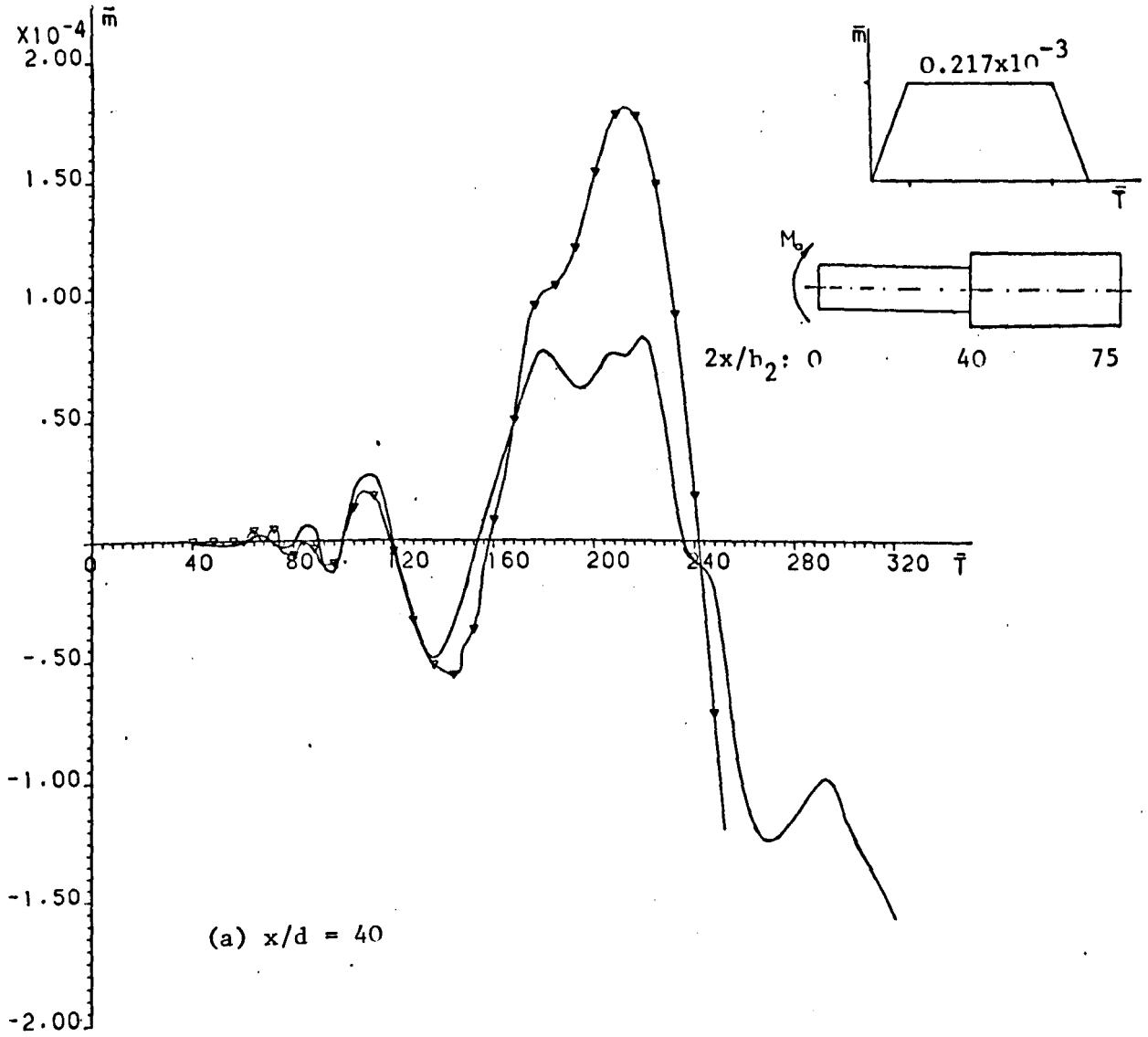

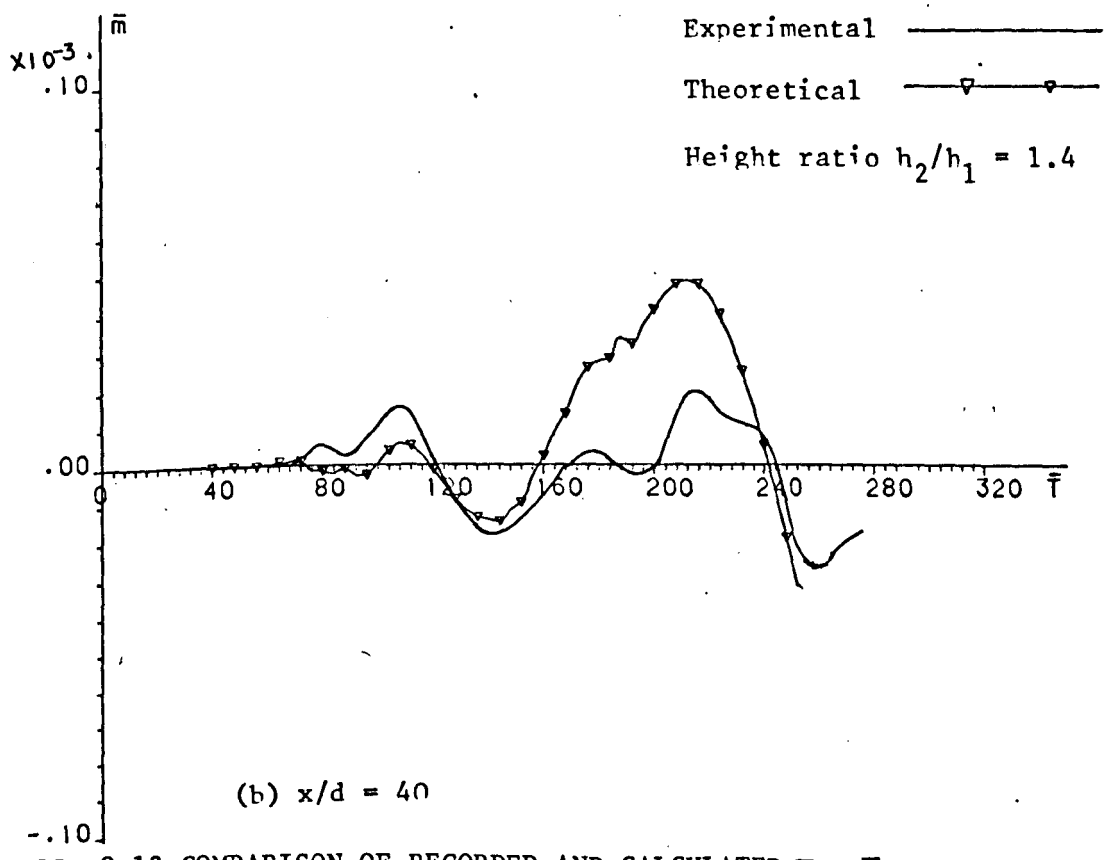

FIG. 8.12 COMPARISON OF RECORDED AND CALCULATED $\bar{m}$ - $\bar{T}$ RESULTS AT THE DISCONTINUITY

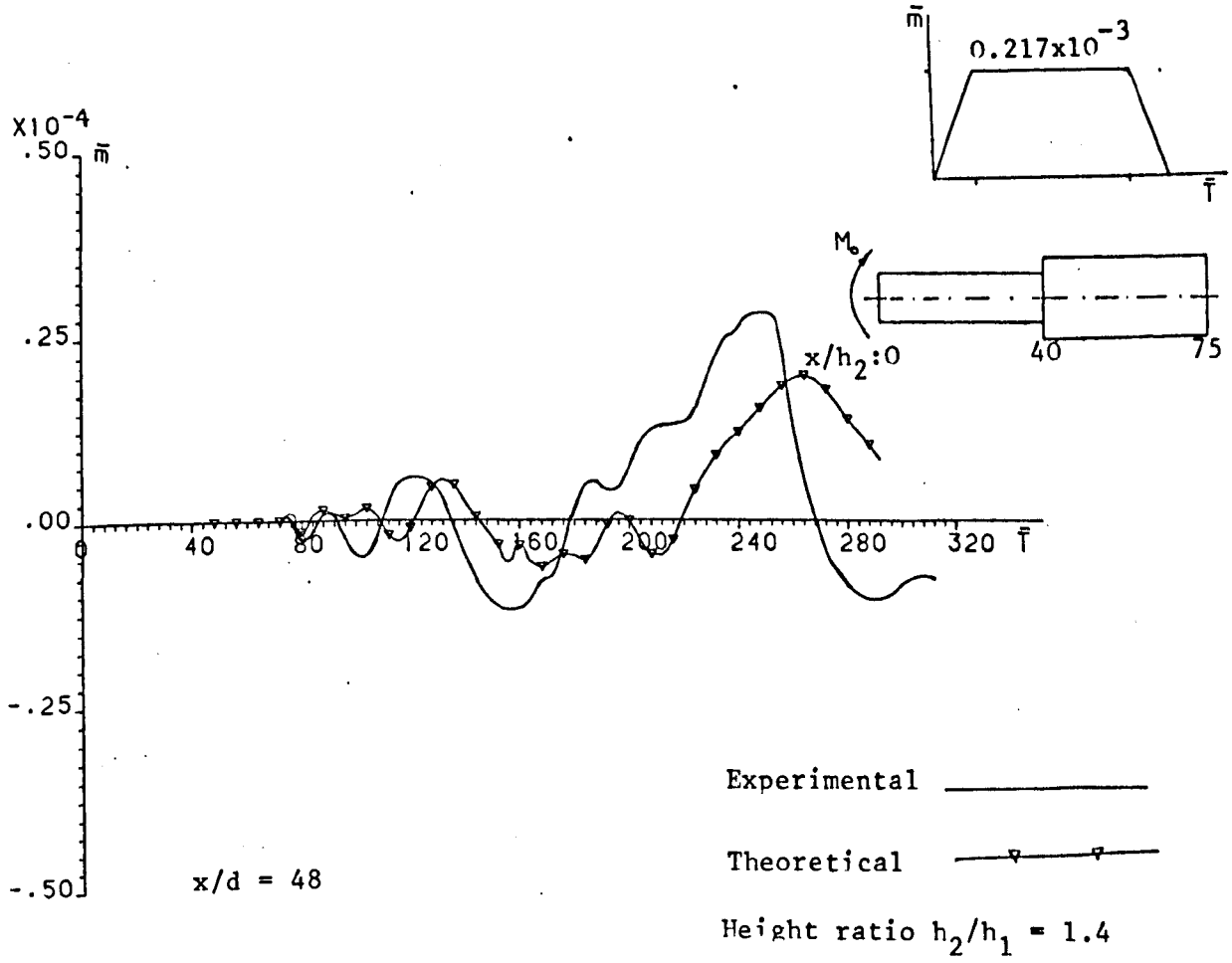

FIG. 8.13 COMPARISON OF RECORDED AND CALCULATED $\bar{m}$ - $\bar{T}$ RESULTS AT POSITION x/d = 48 OF THE STEPPED BEAM WITH RECTANGULAR CROSS SECTION (L=1.885m)

CHAPTER IX

DISCUSSION

The Euler-Bernoulli theory is known to be inadequate for the treatment of transient bending wave propagation problems, since it assumes an infinite velocity of propagation for disturbances with infinitely short wavelengths associated with the high frequency branches.

The transient response is associated with the impact where the duration of impact is much smaller than the period of the first flexural mode of vibration of the structure.

This period for the 2.0 m stepped beam is 10.3 ms and the pulse duration of the trapezoidal input bending moment was 0.48 ms, more than 21 times smaller than the fundamental period.

The Timoshenko beam theory, which takes into account the effects of rotatory inertia and shear, is practically the best approximate theory for solving transient flexural wave propagation problems.

From the literature survey no previous attempt to solve the problem of flexural wave propagation in beams with discontinuity of cross section according to the Timoshenko beam theory has been found.

The investigation concentrated on the study of antisymmetrical strain component-time distribution at various locations along test beams due to the considerable importance of beams in bending for engineering applications.

Several solution methods were discussed. The transform techniques require numerical inversion and numerical integration becomes more complicated with the incorporation of boundary

conditions.The Laplace transform method yields solutions in closed form only when a certain power distribution can be assumed for the variables.

Finite element methods are mostly used for frequency analysis of Timoshenko beams. However, computed stresses show severe oscillations making the method less attractive for transient wave propagation problems.

Although finite element methods are very useful in the treatment of geometrically complex structures and although they have been used successfully for the solution of elliptic and parabolic governing equations, they have yet to prove themselves for solving transient flexural wave propagation problems governed by hyperbolic partial differential equations.

Finite difference methods have been used widely in solving one dimensional and two dimensional longitudinal wave propagation problems. The main disadvantage of the finite difference techniques is the difficulties encountered in handling discontinuities in geometry and material.

The method of characteristics was shown to be most accurate and most effective in solving mixed initial boundary value problems governed by hyperbolic partial differential equations such as the problem of flexural wave propagation in beams when described by the Timoshenko beam equations.

The method of characteristics has the advantage that discontinuities in the initial values propagates along the characteristics and a unique solution is ensured in the region between the characteristic lines.

The method of characteristics has a wide range of applications

in the fields of elastic, viscoelastic and plastic wave propagation problems as well as other fields such as fluid mechanics and gas dynamics.

The method of characteristics was applied successfully in solving the present problem of flexural wave propagation in finite beams with discontinuity of cross-section, where reflections from the far end and the position of discontinuity are automatically absorbed into the solution by the presence of backward running characteristic curves at each grid point.

The adherence of the characteristic method to the stability criterion of $\frac{\Delta x}{c_1 \Delta t} \geq 1$ ensures convergence to the true solution as Δx and Δt approach zero.

The choice of the correct mesh size is affected by the type of loading, the rise time of the input load, boundary condition and the type and position of discontinuity. In order to select the largest mesh size with a minimal acceptable error, the mesh size was chosen in such a manner that any further reduction in its value did not alter the solution significantly (Fig.5.11 and 5.12)

The importance of the shear coefficient k^2 was discussed in chapter 5 (section 1) and after careful considerations the values of 0.8856 and 0.849 were chosen for beams of circular cross-section and rectangular cross-section respectively.

Numerical results based on the developed TMOTCU computer programs were compared with theoretical and experimental results of several other authors to establish the accuracy of the present numerical solution. The comparisons were carried out for the case of a semi-infinite beam subjected to eccentric impact by a

long rod (Fig.5.1) and the eccentric impact by a steel ball (Fig.5.4 and 5.5.). The numerical results of this work were also compared with previous results for a cantilever beam subjected to a ramp platform bending moment (Fig.5.6 and 5.7) and for the case of lateral impact of a simply supported beam (Fig.5.8).

The comparisons in all cases showed very good agreement and indicated the advantages of the current numerical solution in predicting recorded high frequency components of the transient responses.

Several cases with various end conditions were considered and theoretical solutions were obtained by the use of the 3 versions of the TMOTCU computer program. The bending moment time curves were presented for finite uniform beams and finite beams with discontinuity of cross-sections subjected to ramp platform end moment impacts.

The effect of the change of mesh size was demonstrated in figures 5.11 and 5.12 for three different mesh sizes obtained by successfully halving the original mesh size of $\Delta\bar{x} = 0.005$ and the results indicated small differences between 1% and 5% with the maximum differences concentrated at the peak values.

The bending moment time distribution in a free free beam, a simply supported beam and in a cantilever beam were presented in figures 5.13 and 5.14 for three beam positions of finite uniform beams.

The results indicated the importance of taking the reflections into account for the estimation of the level of stresses and strains in structures.

The problem of flexural waves in finite beams with discontinuity of cross section required a finer mesh size than in the case of a finite uniform beam.

For stepped beams, the effect of change of diameter ratio on propagated bending waves for diameter ratios 0.9, 1.0, 1.1, 1.5 and 2.0 was presented in figures 5.15 to 5.17. An increased diameter ratio resulted in an increased reflected bending wave arriving at the considered positions.

The effect of discontinuity of cross section on the shear force distribution in finite stepped beams subjected to ramp platform end bending moment was presented in figures 5.22, 5.23 and 5.25. The curves showed increased reflected shear force with increased diameter ratio and the effect of abrupt change in cross section was strongly manifested in the history of reflected and transmitted shear force.

In the experimental part of this work, experimental data were obtained for various test beams subjected to eccentric impact by a striker 1.0 m long. Results were presented for several positions along uniform beams and finite beams with discontinuity of cross section and of circular and rectangular cross section.

The eccentricity of the longitudinal impact was measured by a direct method of tracing the off-centre position for each impact and the results showed an excellent degree of reproducibility (Fig.7.10a).

The eccentric impact was considered to be perfectly elastic due to the low velocity of impact and any possible local plastic flow was neglected.

The pulse length was shown for these tests to be directly proportional to the striker length (Fig.7.7b) and the 1.0 m long striker provided an input pulse of approximately trapezoidal shape.

The bending wave indicated considerable dispersion as it travelled down the beam showing alternating sign and no definite constant velocity of propagation for the frequency components of the bending wave could be obtained. Fig.7.12b showed the bending strain records at positions x/d = 4 and 32. The original trapezoidal shape was still recognisable at 4 diameters from the impact end but was more widespread at 32 diameters distance and showed negative and positive peaks.

The bending strain-time distribution was recorded for six positions along the 2.0 m long stepped beam subjected to eccentric impact at the smaller end (Figs.7.20 and 7.21) and at the larger end (Figs.7.25 and 7.26) with particular emphasis on the bending strain-time distribution in the immediate vicinity of the abrupt change of the cross section.

An increased cross section had the effect of a sharp decrease in the level of the bending strains. A decreased cross section resulted in a considerable increase in the monitored strains.

Fig.7.26b showed a sharp increase in the bending strain where peak strains were more than doubled due to a 25% reduction in the diameter of the cross section. The effect of change in rectangular cross section on the propagated bending wave was investigated and the results presented in Fig.7.31b indicated a more drastic reduction in the level of bending strain than in the case of a stepped beam of circular cross section.

In order to check the validity of numerical solutions obtained by the TMOTCU computer programs, theoretical predictions were compared with experimental observations for several cases of finite beams with discontinuity of cross section.

Based on the ramp platform bending moment input, a trapezoidal bending moment shape was derived and closely approximated the value of the actual applied bending moment as obtained by multiplying the axial force-time curve with the measured eccentricity of the impact (Fig.8.1).

Comparisons of experimental and theoretical results showed extremely good agreement in magnitude and shape. A certain degree of discrepancy was expected due to some error introduced in the input data itself, and the inherent errors in experimental data reduction. Furthermore, the Timoshenko theory agrees with the Pochhammer Chree theory excellently only for the first branch of the dispersion curve and the agreement is less satisfactory for the next highest branch of the dispersion curve.

The comparison was carried out for non-dimensional bending moment versus non-dimensional time and the theoretical results predicted accurately the dispersive character of the bending wave, The agreement was better in the initial build up of the bending moment and at later stages theoretical predictions were somewhat higher than experimental records.

The pulse length of the input bending moment was many times greater than the cross sectional dimension of the test beams and the one dimensional Timoshenko beam theory adequately described the flexural wave propagation in the stepped beams.

The numerical solution by the method of characteristics

was successful since the agreement between theoretical solution and experimental observation was especially good for uniform beams and for beams with discontinuity of cross section.

The importance of the effect of abrupt changes in cross section was demonstrated in comparison between results obtained at stations immediately before and after the position of discontinuity in a 2.0 m long cylindrical stepped beam subjected to eccentric impact at its small end (Fig.8.4) and at its larger end (Fig.8.9) as well as for a stepped beam of rectangular cross section (Fig.8.12).

The level of change of stresses in the structure due to a sudden change in the cross section is of practical importance in engineering applications. The magnitude of stress variation can be derived directly from the bending moment-time curves.

In the small cross section with an area 64% of the larger cross section, the level of stresses at $\bar{T} = 160$ was 2.25 times the level of stresses recorded after the cross section was increased. This is derived from Fig.8.4.

A reduction of 36% in the cross sectional area resulted in an increase in the level of stresses to 2.4 times the original stress peak at $\bar{T} = 116$ on the larger cross sectional area. This is derived from Fig.8.9.

A similar drastic change in the level of stresses was noted for the case of cross section increase in a beam of rectangular cross section with increased depth (Fig.8.12).

The results of the present work indicated clearly the importance of the effect of discontinuity of cross section on antisymmetric strain and stress components in finite structures under transient dynamic loading.

CHAPTER X

CONCLUSIONS

The transient response of beams with discontinuity of cross section was established experimentally and accurate predictions were provided by the numerical method of characteristics using the Timoshenko beam theory.

Several other solution methods were discussed and although the method of characteristics is most suitable for one dimensional flexural wave propagation problems governed by the system of hyperbolic partial differential equations, other finite element techniques can be more efficient in solving two dimensional wave propagation problems.

The most satisfactory approximation in one case is not necessarily the most appropriate in another case. The choice of the solution method must depend on the required accuracy, the nature of the structure and its complexities, and the importance of the shear deformation and rotatory inertia effects.

One of the problems in the use of the method of characteristics was the choice of the correct mesh size which had to be decided for each problem depending on the type of loading, the rise time of the input function, the end conditions and the size and position of discontinuity.

For bending moment input impact problems of finite beams where reflections were taken into consideration the use of very small mesh size was inevitable. This may be regarded a limitation to the application of the method of characteristics. However, this disadvantage becomes less and less significant with the

development of ever faster computers.

The maximum values for peaks of bending moment, stresses and strains in finite stepped beams with increased cross section were found to be in the initial build up and at positions nearer to the impact end. However, the peaks of the same quantities in finite stepped beams with reduced cross section occured at positions on the second reduced cross section. Therefore reflections have to be considered in order to provide realistic design data for structures under transient dynamic loading.

The very good agreement between theory and experiment showed the success of the method of characteristics and makes it suitable for providing solutions for a wide range of flexural wave propagation problems in beams with discontinuity of cross section and for various loading configurations where the same solution equations can be used and only the appropriate initial and boundary conditions need to be specified.

The numerical results of the method of characteristics can be used to check the validity of other numerical methods and their usefulness in obtaining the dynamic transient response of more complicated structures.

Most of the experimental and theoretical work was concentrated on cases of free-free finite beams with discontinuity of cross section subjected to end bending moment due to eccentric longitudinal impact. However, other types of end conditions and lateral impact problems can be handled easily by the present TMOTCU computer programs where the time variation of quantities such as M, Q,W and v are all included.

The study of the discontinuity in material property combined with the discontinuity of cross section can be the subject of future works.

Furthermore, the developed TMOTCU computer programs can be used to solve flexural impact loading problems without assuming the form of the impact load, but merely using the impact velocity to formulate the input boundary condition. This is particularly useful for practical impact problems where the impact load is not known.

Another possible extension of the present work is to use the experimental results to obtain the velocity of propagation of pulse peaks and,based on that,to construct dispersion relationship curves .

REFERENCES

Aalami, B. and Atzori, B. (1974)
Flexural vibrations and Timoshenko's beam theory.
A I A A Journal 12: 679-685

Abbott, M.B. (1966)
An introduction to the method of characteristics-
(London: Thames and Hudson).

Abramson, H.N. and Norman, H. (1957)
Flexural waves in elastic beams of circular cross section.
The Journal of the Acoustical Society of America 29 (1): 42-46

Abramson ., H. N.; Plass, H.J. and Ripperger, E.A. (1958)
Stress wave propagation in rods and beams. In: Advances in applied mechanics 5: 111-194, ed. by H.L. Dryden.
(New York: Academic Press Inc.)

Allison, I.M. (1961)
The elastic stress concentration factors in shouldered shafts.
Part II: Shafts subjected to bending.
The Aeronautical Quarterly 12: 219-227

Alterman, Z. and Karal, F.C. (1970)
Propagation of elastic waves in a semi-infinite cylindrical rod using finite difference methods.
Journal of Sound and Vibration 13: 115-145

Alterman, Z. and Loewenthal, D. (1972)
Computer generated seismograms. In: Methods in Computational Physics 12: 35-164, ed. by B. Bolt.
(New York: Academic Press)

Ames, W.F. (1977)
Numerical methods for partial differential equations.
Second edition (London: Thomas Nelson & Sons).

Anderson, R.A. (1953)
Flexural vibrations in uniform beams according to the Timoshenko theory.
Journal of Applied Mechanics, Trans. ASME 20: 504-510

Angus, R.W. (1943)
Graphical analysis of impact of elastic bars (Discussion)
J. Appl. Mech. 10: A-112-A114.

Aprahamian, R.; Evensen, D.A. and others. (1971)
Application of pulsed holographic interferometry to the measurement of propagating transverse waves in beams
Experimental Mechanics 11: 309-314

Archer, J.S. (1965)
Consistent matrix formulations for structural analysis using finite-element techniques
AIAA Journal 3 (10): 1910-1918

Arnold, R. N. (1937)
Impact stresses in a freely supported beam.
Proceedings of the Institution of Mechanical Engineers
137: 217-281

Atkins, K. J. (1971)
Measurement of stress waves in impacted frames.
Strain 1: 142-146

Atkins, K. J. and Hunter, S.C. (1975)
The propagation of longitudinal elastic waves around right-angled corners in rods of square cross-section.
Quarterly Journal of Mechanics and applied Mathematics.
28: 245-260.

Ayre, R.S. and Jacobson, L.S. (1950)
Natural frequencies of continuous beams of uniform span length.
J. Appl. Mech. 17: 391-395

Bancroft, D. (1941)
The velocity of longitudinal waves in cylindrical bars.
Physical Review 59: 588-593

Barez, F.; Goldsmith, W. and Sackman, J.L. (1980)
Longitudinal wave propagation in axisymmetric structures with material and/or aereal discontinuity.
Exp. Mech. 20: 325-333

Barnhart, K. E. and Goldsmith, W. (1957)
Stresses in bending during transverse impact.
J. Appl. Mech. 24: 440-446

Baumeister, T. and Marks, L.S. (1967)
Standard Handbook for Mechanical Engineers.
Seventh edition (New York: McGraw Hill Co.).

Becker, E.C. (1962)
Transient loading technique for mechanical impedance measurement.
In: Experimental Techniques in Shock and Vibration, New York 1962.
Colloquium Proceedings. (New York: The American Society of Mechanical Engineering).

Becker, E. C. and Conway, H.D. (1964)
Generation and use of mechanical step transients in dynamic measurement.
British Journal of Applied Physics 15: 1225-1231

Beddoe, B. (1965)
Propagation of elastic stress waves in a necked rod.
J. Sound Vib. 2: 150-166.

Bejda, J. (1967)
A solution of the wave problem for elastic visco-plastic beams.
Journal de Mecanique 6 (2): 263-282.

Bell, J.F. (1960)
Propagation of large amplitude waves in annealed aluminum
Journal of Applied Physics 31: 277-282.

Bell, J.F. (1973)
The experimental foundations of solid mechanics. In:
Encyclopedia of Physics 6a/1-Mechanics of Solids ed. by
C. Truesdell (Berlin: Springer Verlag).

Belytschko, T. and Mullen, R. (1978)
On dispersive properties of finite element solutions.
In: Modern Problems in Elastic Wave Propagations.
ed. by J. Miklowitz & J.D. Achenbach. (New York: Interscience Publ. Inc.)

Bergeron, L. (1939)
Methode de Graphique de Resolutions des Problemes
de Propagation d'Ondes Planes. In: International Congress for
Applied Mechanics, 5th Cambridge, Mass. 1939. Proceedings, p p. 694-699

Bertholf, L.D. (1967)
Numerical solution for two-dimensional elastic wave propagation in
finite bars.
J. Appl. Mech. 34: 725-734

Bertholf, L. D. (1974)
Feasibility of two-dimensional numerical analysis of the split-Hopkinson
pressure bar system.
J. Appl. Mech. 41: 137-144

Bickle, L.W. (1970)
The response of strain gages to longitudinally sweeping strain pulses.
Exp. Mech. 10: 333-337

Bishop, R.E.D. and Price, W.G. (1976)
Allowance for shear distribution and rotatory inertia of ship hulls .
J. Sound Vib. 47: 303-311

Bodner, S.R. (1973)
Stress waves due to fracture of glass in bending.
Journal of the Mechanics and Physics of Solids 21: 1-9

Boley, B. A. and Chao, C.C. (1955)
Some solutions of the Timoshenko beam equations.
J. Appl. Mech. 22: 579-586

Boley, B.A. and Chao, C.C. (1958)
An approximate analysis of Timoshenko beams under dynamic loads.
J. Appl. Mech. 25: 31-36

Bond, L.J. (1978)
Surface cracks in metals and their characterisation using Rayleigh waves.
PhD thesis: The City University, Department of Physics.

Boore, DM. (1972)
Finite difference methods of Seismic wave propagation inheterogeneous
materials. In: Methods in Computational Physics, Vol. 11 ed. by
B.A. Bolt (New York: Academic Press)

Bresse, P.M. (1866)
Cours de Mecanique appliquee.
(Paris: Successeur de Mallet - Bachelier)

Bruner, J.D. and Muster, D. (1967)
Filtering characteristics of a long cylindrical steel bar with discontinuities in its cross sectional area. Technical Reprot No.8, University of Houston, Dept. of Mechanical Engineering.

Burton, R. (1958)
Vibration and Impact. Chapter 11, pp. 219-241.
(New York: Dover Publication).

Butler, D.S. (1960)
The numerical solution of hyperbolic systems of partial differential equations in three independent variables.
Proc. Roy. Soc. London, Ser. A 255: 232-252

Buturla, E.A. and Mclay, R.W. (1974)
On sparse matrices in finite element wave propagation.
J. Appl. Mech. 41: 1048-1053

Carnegie, W. and Thomas, J. (1972)
The effects of shear deformation and rotatory inertia on the lateral frequencies of cantilever beams in bending.
Journal of Engineering for Industry 94: 267-278

Carnes, W.R. (1964)
The propagation of flexural waves in beams according to the Timoshenko theory.
PhD thesis: University of Illinois (USA)

Chang, H.L. (1972)
Propagation of two-dimensional stress waves in cylindrical bars.
PhD thesis: North Carolina State University at Raleigh (USA)

Chiu, S.S. (1970)
Difference method for multiple reflection of elastic stress waves.
Journal of Computational Physics 6: 17-28

Chiu, S.S. and Neubert, V.H. (1967)
Difference method for wave analysis of the split Hopkinson pressure bar with a viscoelastic specimen.
Journal of the Mechanics and Physics of Solids 15: 177-195

Chou, P,C. (1965)
Flexural waves in elastic circular plates by the method of characteristics.
NASA CR - 69703. August 1965.

Chou, P.C. and Flis, W.J. (1975)
Comparison of solution methods for composite material beam response due to impact.
Report No. NADC - 76093 - 30. Naval Air Development Centre.

Chou, S.C. and Greif, R. (1968)
Numerical solution of stress waves in layered media.
AIAA Journal 6: 1067-1074

Chou, P.C.; Karpp, R.R. and Huang, S. (1967)
Numerical Calculation of blast waves by the method of characteristics.
AIAA Journal 5 (4): 618-623.

Chou, P.C. and Koenig, H.A. (1966)
A unified approach to cylindrical and spherical waves by method of characteristics.
J. Appl, Mech. 33: 159-167.

Chou, P.C. and Mortimer, R.W. (1966)
A unified approach to one-dimensional elastic waves by the method of characteristics.
NACA CR - 78493, September 1966.

Chou, P.C. and Mortimer, R.W. (1967)
Solution of one dimensional elastic wave problem by the method of characteristics.
J. Appl. Mech. 34: 745-750

Chree, C. (1889)
The equations of an isotropic elastic solid in polar and cylinder coordinates, their solution and application.
Trans. Camb. Phil. Soc. 14: 250-369

Christopherson, D.G. (1951)
Effect of shear in transverse impact on beams.
Proc. Inst. Mech. Eng. 165: 176-188

Clifton, R.J. (1967)
A difference method for plane problems in dynamic elasticity.
Quarterly Journal of Applied Mathematics 25: 97-116

Colton, J.D. (1973)
Multiple fracture of beams and plates under localized impulsive loading.
PhD thesis: Stanford University, Dpt. of Applied Mechanics.

Colton, J.D. (1975)
Dynamic fracture process in beams.
J. Appl, Mech. 42: 435-439

Colton, J.D. (1977)
Multiple fracture of beams under localized impulsive loading.
J. Appl. Mech. 44: 259-263.

Cone, S.A. (1963)
Wave propagation past a change in cross section
MSc. thesis The University of New Mexico (USA)

Conway, H.D. and Dubil, J.F. (1965)
Vibration frequencies of truncated cone and wedge beams.
J. Appl. Mech. 32: 932-934

Conway, H.D. and Jakubowski, M. (1969)
Axial impact of short cylindrical bars.
J. Appl. Mech. 36: 809-813

Cooper, J. L. B. (1947)
The propagation of elastic waves in a rod.
The Philosophical Magazine 38 Ser. 7: 1-22

Costantino, C. (1967)
Finite element approach to stress wave problems.
Journal of the Engineering Mechanics Division, Proceedings ASCE 93 EM2: 153-174

Courant, R.; Friedrichs, K. and Lewy, H. (1928)
Uber die partiellen Differenzengleichungen der mathematischen Physik.
Mathematische Annalen 100: 32-74

Courant, R. and Hilbert, D. (1937)
Methoden der Mathematischen Physik, Band II.
2te Auflage (Berlin: Springer Verlag).

Courant, R.; Isaqcson, E. and Rees, M. (1952)
On the solution of nonlinear hyperbolic differential equations by finite differences.
Communications on Pure and Applied Mathematics 5: 243-255.

Cowper, G.R. (1966)
The shear coefficient in Timoshenko's beam theory.
J. Appl. Mech. 33: 335-340

Cowper, G.R. (1968a)
On the accuracy of Timoshenko's beam theory.
J. Eng. Mech. Div., Proc. ASCE 94EM6: 1447-1453.

Cowper, G.R. (1968b)
A study of errors due to shear and rotatory inertia in the determination of Young's modulus by flexural vibration (Discussion).
British Journal of Applied Physics 1: 1766-1767

Cox, H. (1849)
On impact on elastic beams
Cambridge Philosophical Transactions 9 (1): 73-78

Cranch, E.T. and Adler, A. (1956)
Bending vibrations of variable section beams.
J. Appl. Mech. 23: 103-108

Crandall, S. H.; Karnop, D.C. and others (1968)
Dynamics of mechanical and electro-mechancial system
(New York: McGraw Hill Book Co.)

Cremer, L. (1943)
Bemerkungen zur Ausbreitung von "Biegewellen" in Stäben und Platten.
Zeitschrift fur angewandte Mathematik und Mechanik 23: 291-294

Cristescu, N. (1967)
Dynamic Plasticity. (Amsterdam: North Holland)

Crook, A.W. (1952)
A study of some impacts between metal bodies by a piezo-electric method.
Proc. Roy, Soc. London 212 Ser. A: 377-390

Crowley, F.B; Phillips, J.W. and Taylor, C.E. (1974)
Pulse propagation in straight and curved beams - Theory and experiment.
J. Appl. Mech. 41: 71-76

Cunningham, D.M.; Brown, G.W. and Griffith, J.C. (1970)
Photoelastometric recording of stress waves.
Exp. Mech. 10: 114-119

Cunningham, D.M. and Goldsmith, W. (1956)
An experimental investigation of beam stresses produced by oblique impact of a steel sphere.
J. Appl. Mech. 23: 606-611

Cunningham, D.M. and Goldsmith, W. (1959)
Short impulses produced by longitudinal impact.
Proc. Soc. Exp. Str. Anal. 16(2): 153-165

Curtis, C.W. (1960)
Propagation of an elastic strain pulse in a semi infinite bar. In: International Symposium on Stress wave propagation in materials. ed. by H. Kolsky and W. Prager. New York. pp. 15-43.

Cushman, J.H. (1979)
Difference schemes or element schemes.
International Journal for Numerical Methods in Engineering 14: 1643-1651.

Dally, J.W. and Riley, W.F. (1965)
Experimental stress analysis, Chapters 14-18
(New York: McGraw Hill Co.)

Datwyler G. and Clark, D.S. (1938)
Stress strain relations under tension impact loading.
Proceedings of the American Society for Testing of Materials, Part 2. Technical paper. pp. 98-106

Davids, N. and Kesti, N.E. (1965)
Stress-wave effects in the design of long bars and stepped shafts.
International Journal of Mechanical Sciences 7: 759-769

Davids, N. and Koenig, H.A. (1967)
Double stress-wave discontinuities in finite shear corrected beams and plates. In: Proceedings of the 10th Midwestern Conference on Mechanics. pp. 763-779

Davidson, T. and Meier, J.H. (1946)
Impact on prismatical bars.
Proc. Soc. Exp. Str. Anal. 4(1): 88-111

Davies, E.D.H. and Hunter, S.C. (1963)
The dynamic compression testing of solids by the method of the split Hopkinson pressure bar.
J. Mech. Phys. Solids 11: 155-181

Davies, R.M. (1937)
The frequency of transverse vibration of loaded fixed-free bars .
Philosophical Magazine 23 Ser 7: 562-573

Davies, R. M. (1948)
A critical study of the Hopkinson pressure bar.
Phil. Trans. Roy. Soc. London 240 SerA: 375-457

Davies, R.M. (1956)
Stress waves in solids. In: Survey in Mechanics. ed. by G.K. Batchelor and R. M. Davies.

Davies, R.; Henshell, R.D. and Warburton, G.B. (1972)
A Timoshenko beam element.
J. Sound Vib. 22: 475-487

Dengler, M.A. and Goland, M. (1951)
Transverse impact of long beams including rotatory inertia and shear effects. In: First U.S. National Congress of Applied Mechanics. Proceedings. New York: The Americal Society of Mechanical Engineering. pp. 179-186.

Dengler, M.; Goland, M. and Wickersham, P. (1952)
Propagation of elastic impact stresses.
Technical Reprot, Progress Report No. 3. 30 October 1952.
Cansas City: Midwest Research Inst., Eng. Mech. Div.

Dolph, C.L. (1954)
On the Timoshenko theory of transverse beam vibrations.
Quar. J. Appl. Math. 12(2): 175-187

Dong, S.B. and Wolf, J.A. (1973)
Effect of transverse shear deformation on vibrations of planar structures composed of beam type element.
J. Acoust. Soc. Am. 53: 120-127

Dohrenwend, C. O.; Drucker, D.C. and Moore, P. (1943)
Transverse impact transients.
Proc. Soc. Exp. Str. Anal. 1: 1-10

Dohrenwend, C.O. and Mehaffey, W.R. (1943)
Measurement of dynamic strain.
J. Appl. Mech. 10: A-85-A-92

Donnell, L. H. (1930)
Longitudinal wave transmission and impact.
Trans. Am. Soc. Mech. Eng. 52: 153-167

Dove, R.C. and Adams, P.H. (1964)
Experimental stress analysis and motion measurement.
(Columbus, OH: Merrill Books Inc.)

Downs, B. (1976)
Transverse vibration of a uniform simply supported Timoshenko beam without transverse deflection.
J. Appl. Mech. 43: 671-673

Downs, B. (1977)
Transverse vibrations of cantilever beams having unequal breadth and depth tapers.
J. Appl. Mech. 44: 737-742.

Durelli, A. J. and Riley, W. F. (1957)
Experiments for the determination of transient stress strain distributions in two-dimensional problems.
J. Appl. Mech. 24: 69-76

Dym, C.L. and Shames, I.H. (1973)
Solid mechanics, a variational approach (New York:
Mc Graw Hill Co.).

Duwes, P.E.; Clark, D.S. and Bohnenblust, H.F. (1950)
The behaviour of long beams under impact loading.
J. Appl. Mech. 17: 27-34

Edge, E.C. (1970)
A study of aircraft arresting hook unit dynamics using numerical wave propagation method. In: Symposium on Structural Dynamics.
Loughborough University of Technology. Paper No. D6.1 - 6.18.

Egle, D.M. (1969)
An approximate theory for transverse shear deformation and rotatory inertia effects in vibrating beams.
NASA - CR - 1317

Emschermann, H.H. und Rühl, K. (1954)
Beansprechungen eines Biegeträgers bei Schlagartiger Querbelastung.
VDI - Forschungsheft 443 (Düsseldorf: Deutscher Ingenieur Verlag GmbH)

Eringen, A.C. (1953)
Transverse impact on beams and plates.
J. Appl. Mech. 20: 461-468

Fanning, R. and Bassett, W.V. (1940)
Measurement of impact strains by a carbon strip extensometer.
Trans. ASME 62: A 24-A 28.

Fehr, Ro.O.; Parker, E.R. and De Micheal, D.J. (1944)
Measurement of dynamic stress and strain in tensile test specimens.
J. Appl. Mech. 11: A65-A71

Filippov. I.G. (1977)
Propagation of compression waves in elastic rods of variable cross-section.
Prikladnaya Mekhanika 13(11): 1149-1156.

Fink, K. (1950)
Eine dynamische Eichung von Dehnungsmeßstreifen.
Archiv fur das Eisenhuttenwesen 21(3/4): 137-142

Fischer, H.C. (1954)
Stress pulse in bar with neck or swell.
Applied Scientific Research A4: 317-328

Fischer, H.C. (1959)
On longitudinal impact. Part I & II.
Appl. Sci. Res. A8: 105-139; 278-308

Flügge, W. (1942)
Die Ausbreitung von Beigungswellen in Stäben.
Zeit. Angew. Math. Mech. 22(6): 312-318

Flügge, W. and Zajac, E.E. (1959)
Bending impact waves in beams.
Ingenieur Archiv 28: 59-70.

Flynn, P.D. and Frocht, M.M. (1961)
On Saint Venant's principle under dynamic conditions.
Exp. Mech. 1: 16-20

Föppl, A. (1897)
Vorlesungen uber technischen Mechanik III.
(Leipzig:

DeForest, A.V. (1941)
Some complexities of impact strength.
J. Iron and Steel Devision, Trans. Am. Inst. Min. Met. Eng. 145: 13-29.

Forrestal, M.J.; Bertholf, L.D. and Sagarty (1975)
An experiment and analysis on elastic waves in beams from lateral impact.
Int. J. Solid Struc. 11: 1161-1165.

Forrestal, M.J. and Sagartz, M.J. (1975)
Transient vibration experiments for determination of properties for viscoelastic structures.
J. Appl. Mech. 42: 205-208

Forsythe, G. and Wasow, W.R. (1960)
Finite difference methods for partial differential equations.
(London: John Wibey & Sons Inc.)

Fox, P. (1960)
The solution of hyperbolic partial differential equations by difference method. In: Mathematical methods for digital computers.
ed. by A. Ralston (London: Wiley).

Fu, C.C. (1970)
A method for the numerical integration of the equations of motion arising from a finite element analysis.
J. Appl. Mech. 37: 599-605.

Gaines, J. H. and Voltera, E. (1966)
Upper and lower bounds of frequencies for cantilever bars of variable cross-sections.
J. Appl. Mech. 33: 948-950.

Garrelick, J. M. (1969)
Analytical investigation of wave propagation and reflections in Timoshenko beams.
PhD thesis: The City University of New York. Mech. Eng.

Ghosh, N.G. (1974)
The effect of variation of shear stress factor on vibrating beams (Research Note).
Journal of the Mechanical Engineering Sciences 16(5): 346-348.

Gladwell, I. and Wait, R.; editors (1979)
A survey of numerical methods for partial differential equation.
(Oxford: Clarenden Press).

Goens, E. (1931)
Über die Bestimmung der Elastizitätsmodulus von Stäben mit Hilfe von Biegungsschwingungen.
Annalen der Physik 5(11): 649-679

Goland, M.; Wickersham, P.D. and Dengler, M.A. (1955)
Propagation of elastic impact in beams in bending.
J. Appl. Mech. 22: 1.7

Goldsmith, W. (1960)
Impact, the theory and physical behaviour of colliding system.
(London: Edward Arnold Publ.)

Goldsmith, W. and Cunningham, D.M. (1956)
Kinematic Phenomena observed during the oblique impact of a sphere on a beam.
J. Appl. Mech. 23: 612-616.

Goldsmith, W. and Katsamaris, F. (1979)
Fracture of notched and perforated polymeric bars produced by longitudinal impact.
Int. J. Mech. Sci. 21: 85-108

Goldsmith, W.; Lee, P.Y. and Sackman, J.L. (1972)
Pulse propagation in straight circular elastic tubes.
J. Appl. Mech. 39: 1011-1018.

Goldsmith, W. and Lyman, P.T. (1960)
The penetration of hard-steel spheres into plane metal surfaces.
J. Appl. Mech. 27: 717-72

Goel, R.P. (1976)
Transverse vibration of tapered beams.
J. Sound Vibr. 47(1): 1-7

Gordon, P. (1977)
Elastic waves in heterogeneous bars of varying cross-section.
Journal of Franklin Institute 303: 129-145

Gorman, D.J. (1975)
Free vibration analysis of beams and shafts.
(New York: John Wiley & Sons).

Graff, K.F. (1975)
Wave motion in elastic solids.
(Oxford: Claren den Press).

Le van Griffis (1944)
Measurement of dynamic strain (Discussion)
J. Appl. Mech. 11: A57-A62

Gupta, R.B. and Nilsson, L. (1978)
Elastic impact between a finite conical rod and a long cylindrical rod.
J. Sound Vibr. 60(4): 555-563

Gustafsson, B.; Kreiss, H.O. and Sundstrom, A. (1972)
Stability theory of difference approximations for mixed initial boundary value problems. Part II.
Mathematics of Computation 26: 649-686

Habberstad, J.L.; Hoge, K.G. and Foster, J.E. (1972)
An experimental and numerical study of elastic strain waves on the center line of a 6061 - T6 aluminum bar.
J. Appl. Mech. 39: 367-371.

Haddow, J.B. and Mioduchowski, A. (1979)
Waves from suddenly punched hole in plate subjected to uniaxial tension field.
J. Appl. Mech. 46: 873-877.

Hahn, S.G.
Stability criteria for difference schemes
Communications on Pure and Applied Mathematics 11: 243-255

Handelman, G.H. and Rubenfeld, L.A. (1972)
Wave propagation in a finite-length bar with variable cross-section (Brief Notes) .
J. Appl. Mechanics 39: 278-280

Hardie, D. and Parkins, R.N. (1968)
A study of the errors due to shear and rotatory inertia in the determination of Young's modulus by flexural vibrations.
Brit. J. Appl. Phy. 1 Ser. 2D: 77-85

Harris, C.M. and Crede, C.E. (Editors) 1961
Shock and vibration handbook Vol. 2
(New York: McGraw Hill Co.)

Harrison, H.R. (1977)
Impact, Transient vibration and Wave propagation.
Lecture notes, The City University (London)

Hashemi, S. H. (1979)
Transverse vibration of a stepped width beam.
MSc. thesis. The City University (London)

Hertz, H. (1882)
Über die Berührung fester elastischer Körper.
Journal fur die reine und angewändte Mathematik (Crelle) 22: 156-171

Haybey, O. and Karasz, F.E. (1976)
Experimental study of flexural vibration in thick beams.
Journal of Applied Physics 47: 3252-3260

Hoffman, J. D. (1973)
Accuracy studies of the numerical method of characteristics for axisymmetric, steady supersonic flows.
J. Comput. Phys. 11: 210-239

Holmes, N. and Belytschko, T. (1976)
Postprocessing of finite element transient response calculations by digital filters.
Computer and Structures 6: 211-216

Hopkinson, B. (1913)
A method for measuring the pressure produced in the detonation of high explosive or by the impact of bullets.
Phil. Trans. Roy. Soc. 213 Ser A: 437-456.

Hoppmann II, W.H. (1952)
Experimental study of the transverse impact of a mass on a column.
Proc. SESA. 9(2): 21-30

Hoppmann II, W.H. (1952)
Impulsive loads on beams.
Proc. SESA. 10(1): 157-164

Howe, C.E. and Howe, R.M. (1955)
Application of the electronic differential analyzer to the oscillation of beams, including shear and rotatory inertia.
J. Appl. Mech. 22: 13-19

Hsu, Y.W. (1975)
The shear coefficient of beams of circular cross-section (Brief Notes).
J. Appl. Mech. 42: 226-228

Huang, T.C. (1955)
Tables of eigenfunctions representing normal modes of vibration of Timoshenko beams.

Huang, T.C. (1958)
Effect of rotatory inertia and shear on the vibration of beams treated by the approximate methods of Ritz and Galerkin. In: Third National Congress of Applied Mechanics Proceedings. pp. 189-194.

Huang, T.C. (1961)
The effect of rotatory inertia and of shear deformation on the frequency and normal mode of uniform beams with simple end conditions.
J. Appl. Mech. 28: 579-584.

Hudson, G.E. (1943)
Dispersion of elastic waves in solid circular cylinders.
Physical Review 63: 46-51.

Hughes, D.S.; Pondrom, W.L. and Mims, R.L. (1949)
Transmission of elastic pulses in metal rods.
Physical Review 75: 1552-1556

Hurty, W.C. and Rubinstein, M.F. (1964)
On the effect of rotatory inertia and shear in beam vibration.
J. Franklin Inst. 278: 124-131.

Ilan, A.; Bond, L.J. and Spivack, M. (1979)
Interaction of a compressional impulse with a slot normal to the surface of an elastic half space.
Geophys. J. Roy. Soc. 57: 463-477

Iseman, J.M. (1967)
Transient analysis for velocity at branch outlet of pipe. In: Proceedings of 10th Midwestern Mechanics Conference at Colorado State University. ed. J.E. Cermak. pp. 1295-1315.

Jahsman, W.E. (1958)
Propagation of abrupt circular wave fronts in elastic sheets and plates. In: Proc. 3rd National Congress of Applied Mechanics. pp. 195-202.

Jahsman, W.E. (1971)
Reexamination of the Kolsky technique for measuring dynamic material behaviour.
J. Appl. Mech. 38: 75-82

Johnson, W. (1972)
Impact strength of materials.
(London: Edward Arnold).

Johnson, W. (1977)
Longitudinal elastic stress waves due to impact
Engineering 217: 106-108

Johnson, W. and Mamalis, A.G. (1977)
The fracture in some explosively end-loaded bars of plaster of Paris perspex containing transverse holes or changes in section.
Int. J. Mech. Sci. 19: 169-176.

Jones, R.P.N. (1955)
Transient flexural stresses in an infinite beam.
Quart. J. Mech. Appl. Math. 8(3): 373-384

Jones, R.P.N. (1964)
Transverse impact waves in a bar under conditions of plane-strain elasticity.
Quart. J. Mech. Appl. Math. 27: 401-421

De Juhasz, K.J. (1942)
Graphical analysis of impact of elastic bars.
J. Appl. Mech. 9: 122-128.

De Juhasz, K.J. (1949)
Graphical analysis of impact of bars stressed above the elastic range. Part I and II.
J. Franklin Inst. 248: 15-49; 113-142

Kaneko, T. (1975)
On Timoshenko correction for shear in vibrating beams.
J. Phys. D (Appl. Phys.) 8: 1927-1936

Kapur, K. K. (1966)
Vibration of a Timoshenkobeam using finite element approach.
J. Acoust. Soc. Amer. 40(5): 1058-1063

Karal, F.C. (1953)
The analogous acoustical impedance for discontinuities and constrictions of circular cross-section.
J. Acoust. Soc. Amer. 25: 327-334.

Karnes, C.H. and Bertholf, L.D. (1970)
Numerical investigation of two-dimensional axisymmetric elastic-plastic wave propagation near the impact end of idential 1100-0 aluminum bars. In: Inelastic Behaviour of solids. ed. by M.F. Kanninen and W.F. Adler.
(New York: McGraw Hill Co.)

Kawata, K. and Hashimoto, S. (1965)
On some differences between dynamic and static stress distribution.
In: 2nd SESA Int. Congress on Exp. Mech. Washington D.C. (Sept. 1965) ed. by B.E. Rossi.

Lord Kelvin (W. Thomson) 1856
On the electrodynamic qualities of metals.
Phil. Trans. Roy. Soc. London 146: 649-751.

Kenner, H. and Goldsmith, W. (1969)
One dimensional wave propagation through a short discontinuity.
J. Acoust. Soc. Amer. 45(1): 115-118

Kida, S. and Oda, J. (1982)
On fracture behaviour of brittle cantilever beam subjected to lateral impact load.
Exp. Mech. 22: 69-74

Klein, L. (1974)
Transverse vibrations of non-uniform beams.
J. Sound Vibr. 37(4): 491-505

Koenig, H.A. and Berry, G.F. (1973)
The transient response of non-uniform, non-homogeneous beams.
Int. J. Mech. Sci. 15: 399-413

Koenig, H.A. and Davids, N. (1968)
Dynamical finite element analysis for elastic waves in beams and plates.
Int. J. Solid Struc. 4: 643-660.

Kolsky, H. (1949)
An investigation of the mechanical properties of materials at very high rates of loading.
Proc. Phys. Soc. B62: 676-700

Kolsky, H. (1953)
Stress waves in solids
(Oxford: Clarenden Press)

Kolsky, H. (1954)
The propagation of longitudinal elastic waves along cylindrical bars.
Phil. Mag. 45: 712-726

Kolsky, H. (1970)
Recent experimental studies of the mechanical response of inelastic solids to rapidly changing stresses. In: Inelastic Behaviour of solids. ed. by: M.G. Kanninen and W.F. Adler. pp. 19-43.

Kolsky, H. (1971)
Some recent experimental investigations in stress wave propagation and fracture. In: Symposium on dynamic response of structures, Proc. ed. by Hermann and N. Perrone (London: Pergamon Press).

Kolsky, H. (1976)
The role of experiment in the development of solid mechanics - some examples. In: Advances in Applied Mechanics 16. ed. by: C.S. Yih (New York: Academic Press).

Krafft, J. M. (1955)
Elimination of the transient strain fluctuations which result from longitudinal impact of bars.
Proc. SESA 12(2): 173-180

Kreiss, H.O. (1971)
Difference approximations for initial boundary - value problems.
Proc. Roy. Soc. London A323: 255-261

Krieg, R.D. (1973)
On the behaviour of a numerical approximation to the rotatory inertia and transverse shear plate.
J. Appl. Mech. 40: 977-982.

Kruszewski, E.T. (1949)
Effect of transverse shear and rotatory inertia on the frequency of a uniform beam.
NACA Technical Note 1909 (July 1949).

Kuo, S.S. (1958)
Beam subjected to eccentric longitudinal impact and some related problems in the propagation of stress waves.
PhD thesis: Yale school of Engineering.

Kuo, S.S. (1959)
Bending waves in free-free beams. In: 4th Midwestern Conference of Solid Mechanics, Proc. pp.457-467.

Kuo, S.S. (1961)
Beam subjected to eccentric longitudinal impact.
Exp. Mech. 1: 102-108

Kuske, A. (1966)
Photoelastic Research on dynamic stresses.
Exp. Mech. 23: 105-112.

Lamb, (1917)
On waves in an elastic plate.
Proc. Roy. Soc. London 93 Ser. A 114-128.

Landon, J. and Quinney, H. (1923)
Experiments with the Hopkinson pressure bar.
Proc. Roy. Soc. London A-103: 622-643.

Langer, B.F. and Lamberger, E.H. (1943)
Calculation of load and stroke in oil-well pump rods.
J. Appl. Mech. 10: A1-A11.

Lax, P.D. (1958)
Differential equations, difference equations and matrix theory.
Comm. Pure Appl. Math. 11: 175-194

Lax, P.D. and Richtmyer, R.D. (1956)
Survey of the stability of linear finite difference equations.
Comm. Pure Appl. Math. 9: 267-293.

Lax, P.D. and Wendroff, B. (1964)
Difference schemes for hyperbolic equations with high order of accuracy.
Comm. Pure Appl. Math. 17: 381-398.

Lee, E.H. (1940)
The impact of a mass striking a beam.
J. Appl. Mech. 7: A129-A138.

Lee, E.H. (1953)
A boundary value problem in the theory of plastic wave propagation.
Quart. Appl. Math. 10(4): 335-346.

Lee, J.P. and Kolsky, H. (1972)
The generation of stress pulses at the junction of two noncollinear rods.
J. Appl. Mech. 39: 809-813.

Lee, T.C. (1974)
Note on wave propagation in a finite non homogeneous rod.
J. Appl. Mech. 41: 291-292.

Lee, T.M. and Sechler, E.E. (1975)
Longitudinal waves in wedges.
Exp. Mech. 15: 41-48.

Lee, P.C.Y. and Wang, Y.S. (1973)
Axially symmetric transient wave propagation in elastic rods with nonuniform section.
Int. J. Solids Struc. 9: 461-480.

Lennertz, J. (1937)
Beitrag zur Frage nach der Wirkung eines Querstoßes auf einen Stab.
Ingenieur Archiv 8: 37-46.

Leonard, R.W. and Budiansky, B. (1953)
On traveling waves in beams.
NACA-Report 1173. (April 1953).

Levinson, M. (1976)
Vibrations of stepped strings and beams.
J. Sound Vibr. 49: 287-291.

Lindholm, U.S. (1964)
Some experiments with the split Hopkinson pressure bar.
J. Mech. Phys. Solids 12: 317-335

Lindholm, U.S. and Doshi, K.D. (1965)
Wave propagation in an elastic nonhomogeneous bar of finite length.
J. Appl. Mech. 32: 135-142.

Lister, M. (1960)
The numerical solution of hyperbolic partial differential equations by the method of characteristics. In: Mathematical methods for digital computers. ed. by A. Ralston and H.F. Wilf.

Love, A.E.H. (1892)
A treatise on the mathematical theory of elasticity.
(Cambridge: University Press) 4th edt. 1927.

Lundberg, B. and Henchoz, A. (1977)
Analysis of elastic waves from two-point strain measurement
Exp. Mech. 17: 213-218

Mabie, H.H. and Rogers, C.B. (1972)
Transverse vibrations of double-tapered cantilever beams.
J. Acoust. Soc. Amer. 51(5): 1771-1774.

McMaster, R.C. (1963)
Resistance strain-gage tests. In: Non destructive testing Handbook, Vol. II. (New York: Ronald Press Co.)

Markham, M.F. (1957)
Measurement of elastic constants by the ultrasonic pulse method.
Brit. J. Appl. Phys. 8 Supplement No.6: 556-563

Mason, H.L. (1936)
Impact on beams.
J. Appl. Mech. 3: A55-A61.

Massau, J. (1889)
Mémoire surl' integration graphique des équations aux dérinees partielles. (Mons: Delporte)

Matsumoto, G.Y. and Simpson, W.J. (1977)
Accustodynamics of the longitudinal collinear impact of finite elastic cylinders.
J. Eng. Industry 99: 144-150

Mengi Y. and McNiven, H.D. (1970)
Analysis of the transient excitation of an elastic rod by the method of characteristics.
Int. J. Solid Struc. 6: 871-892.

Mengi, Y. and McNiven, H.D. (1971)
Axially symmetric waves in transversly isotropic rods.
J. Acoust. Soc. Amer. 50: 248-257

Miklowitz, J. (1953a)
Flexural wave solutions of coupled equations representing the more exact theory of bending.
J. Appl. Mech. 20: 511-514

Miklowitz, J. (1953b)
Elastic waves created during tensile fracture, the phenomenon of a second fracture.
J. Appl. Mech. 20: 122-130.

Miklowitz, J. (1960)
Elastic wave propagation
Applied Mechanics Review 13: 865-878.

Miklowitz, J. (1978)
The theory of elastic waves and waveguides.
(Amsterdam: North Holland Publ. Co.)

Miles, J.W. (1946)
The analysis of plane discontinuities in cylindrical tubes.
Part I.
J. Acoust. Soc. Amer. 17(3): 259-271.

Mindlin, R.D. (1951)
Influence of rotatory inertia and shear on flexural motions of isotropic plates.
J. Appl. Mech. 18: 31-38.

Mindlin, R.D. and Deresiewiez, H. (1954)
Timoshenko's shear coefficient for flexural vibrations of beams. In: 2nd. U.S. National Congress of Applied Mechanics, Proceedings. pp.175-178.

Mindlin, R.D. & Herrmann, G. (1951)
A one-dimensional theory of compressional waves in an elastic rod.
In: 1st. U.S. National Congress of Applied Mechanics, Proceedings.
pp. 187-191.

Mindlin, R.D. and McNiven, H.D. (1960)
Axially symmetric waves in elastic rods.
J. Appl. Mech. 27: 145-151.

Mitchell, A.R. (1969)
Computational methods in partial differential equations.
(London: John Wiley & Sons)

Moodie, T.B. and Barclay, D.W. (1976)
Transient solutions for longitudinally impacted inhomogeneous conical shells.
Journal of Elasticity 6(2): 209-219.

Mori, D. (1957)
Lateral impact on bars and plates.
Proc. SESA 15: 171-178.

Morley, L. S. D. (1961)
Elastic waves in a naturally curved rod .
Quart. J. Mech. and Appl. Math. 14(2): 155-172

Mortimer, R.; Chou, P.C. and Rose, J.L. (1968)
Annual report for wave propagation in stepped and joined shells.
NASA-N71-20701 (Sept. 1968)

Mortimer, R.W. and Hoburg, J. (1969)
A computer code for one dimensional elastic wave problems, MCDIT 21.
NASA CR - 1306. April 1969.

Mortimer, R.W.; Rose, J.L. and Blum, A. (1972)
Longitudinal impact of cylindrical shells with discontinuous cross-sectional area.
J. Appl. Mech. 39: 1005-1010.

Morton, K.W. (1976)
Finite difference and finite element methods.
Computer Physics Communications. 12: 99-108.

Mugiono, D. (1955)
Messungen der Reflexion von Biegewellen an Querschnittssprüngen auf stäben.
Acustica 5: 182-186.

Mukunoki, T.C. and Ting T.C.T. (1980)
Transient wave propagation normal to the layering of a finite layered medium.
Int. J. Solid Struc. 16: 239-251.

Nagaya, K. (1979)
Approximate dynamic analysis of Timoshenko beams and its application to tapered beams.
J. Acoust. Soc. Amer. 66: 794-800.

Nasim, M.;Al-Hassani, S.T.S. and Johnson, W. (1971)
Stress wave propagation and fracture in thin curved bars.
Int. J. Mech. Sci. 13: 599-603

Nederveen, C.J. and Schwarzl, F.R. (1964)
Correction for shear and rotatory inertia on flexural vibration of beams.
Brit. J. Appl. Phys. 15: 323-325.

Neubert, H.K. (1967)
Strain Gauges. (London: Macmillan)

Von Neuman, J. and Richtmyer, R.D. (1950)
A method for the numerical calculation of hydrodynamic shocks.
J. Appl. Phys. 21: 232-237.

Nevill, G.E.; Sierakowski, R.L. a.o. (1972)
One-dimensional wave pulses in steel epoxy composites.
Exp. Mech. 12: 278-282.

Newman, M.K. (1955)
Effect of rotatory inertia and shear on maximum strain in cantilever impact excitation.
Journal of the Aeronautical Sciences 22: 313-320

Nicholas, T. (1971)
An analytical study of the split Hopkinson bar technique for strain-rate dependent materials behaviour.
Technical Report AFML - TR - 155. Airforce Materials Lab. Ohio.

Nicholson, J.W. and Simmonds, J.G. (1977)
Timoshenko beam theory is not always more accurate than elementary beam theory and Discussions to the paper.
J. Appl. Mech. 44: 337-338 and 357-360.

Nickel, R.E. and Secor, G.A. (1972)
Convergence of consistently derived Timoshenko beam finite elements.
Int. J. Num. Meth. Eng. 5: 243-253.

Nowacki, W.K. (1978)
Stress waves in non-elastic solids.
(London: Pergamon Press)

O'Brien, G.; Hyman, M.A. and Kaplan, S. (1951)
A study of the numerical solution of partial differential equations.
J. Math. Phys. 29: 223-251.

Odaka, T. and Nakahara, I. (1967)
Stresses in an infinite beam impacted by an elastic bar.
Bulletin of Japanese Society Mech. Eng. 10: 863-872.

Oi, K. (1966)
Transient response of bonded strain gages.
Exp. Mech. 6: 463-469.

Olsson, R.G. (1934)
Die tatsächliche Durchbiegung des gebogenen Balkens.
Stahlbau 7: 13.

Osher, S. (1969)
Systems of difference equations with general homogeneous boundary conditions.
Trans. Amer. Math. Soc. 137: 177-201.

Osher, S. (1972)
Stability of parabolic difference approximations to certain mixed initial boundary value problems.
Math. Comput. 26: 13-39.

Parker, R.P. (1973)
High frequency response of bars and beams.
PhD thesis: Pennsylvania State University. Dpt. Eng. Mech.

Parker, R.P. and Neubert, V.H. (1975)
High frequency response of beams
J. Appl. Mech. 42: 805-808.

Perry, C.C. and Lissner, H.R. (1962)
The strain gage primer. 2nd ed.
(New York: McGraw Hill Co.).

Pfeiffer, F. (1947)
Über die Differentialgleichung der transversalen Stabschwingunguen.
Zeits. Angew. Math. Mech. 25127(3): 83-91.

Phillips, J.W. (1970)
Stress pulses produced during the fracture of brittle tensile specimens.
Int. J. Solids Struc. 6: 1403-1412.

Phillips, J.W. and Crowley III, F.B. (1972)
On the theory of pulse propagation in curved beams.
J. Sound Vibr. 24: 247-258.

Phillips, J.W.; Mak, A.F. and Ashbaugh, N.E. (1978)
Stress wave detection of an edge crack in an elastic rod.
Int. J. Solids Struc. 14: 141-152.

Pickett, G. (1945
Flexural vibration of unrestrained cylinders and disks.
J. Appl. Phys. 16: 820-831.

Plass, H.J. (1955)
Theory of plastic bending waves in a bar of strain rate material.
In: 2nd Midwestern Conference on Solid Mechanic, Proc. Purdue University (Sept. 1955) pp. 103-135.

Plass, H.J. (1958)
Some solutions of the Timoshenko beam equations for short pulse type loading.
J. Appl. Mech. 25: 379-385.

Pochhammer, L. (1876)
Über die Fontpflanzungsgeschwindigkeiten kleiner Schwingungen in einem unbegrenzten isotropen Kreiscylinder.
Zeitschrift für Mathematik 81: 33-61.

Pople, J. (1976)
Increasing the voltage output of a Wheatstone bridge having one or two active strain gauge arms.
Strain 12(1): 31-34

Pople, J. (1980)
D I Y Strain gauge transducers. Part 1 and 2.
Strain 16 (1):

Prandtl, L. (1920)
über die Härte plastischer Körper
Nachr. Ak. Wiss. Gaettingen, Math.-Phys. Kl. 74.

Prescott, J. (1942)
Elastic waves and vibration of thin rods.
Phil. Magaz. 33 Ser. 7: 703-754.

Rader, D. and Mao, M. (1972)
Amplification of longitudinal stress pulses in elastic bars with an intermediate tapered region.
Exp. Mech. 12: 90-94.

Ramamurti, V. and Mahrenholtz, O. (1974)
The application of the simultaneous iteration method to flexural vibration problems.
Int. J. Mech. Sci. 16: 269-283.

Ramamurti, V. and Ramanamurti, P.V. (1975)
Elastic wave propagation in finite bars with round ends. In: 4th World Congress on the Theory of Machines and Mechanisms. University of New Castle (London: Inst. Mech. Eng.).

Ramamurti, V. and Ramanamurti, P.V. (1977)
Impact on short length bars.
J. Sound Vibr. 53(4): 529-543.

Ramsauer, C. (1909)
Experimentelle und theoretische Grundlagen des elastischen und mechanischen Stoßes.
Annalen der Physik 30 Ser. 4: 417-495.

Raney, J. P. and Howlett, J.T. (1971)
A model solution for wave propagation in finite shells of revolution.
Journal of Spacecraft 8(6): 650-656.

Ranganath, S. (1971)
Normal impact of infinite elastic and elastic-plastic beams by a semi-infinite elastic rod.
PhD thesis: Brown University. Division of Engineering.

Ranganath, S. and Clifton, R.J. (1972)
A second-order accurate difference method for system of hyperbolic partial differential equations.
Comp. Meth. Appl. Mech. Eng. 1: 173-188.

Rao, V. and Kanaka, R.I. (1976)
Nonlinear vibrations of beams considering shear deformation and rotatory inertia.
A I A A Journal 14: 685-687.

Rawlings, B. (1963)
The present state of knowledge of the behaviour of steel structures under the action of impulsive loads.
Civil Engineering Transactions 5: 89-103.

Rayleigh, J.W.S. (1894)
The theory of sound. Volume I.
(New York: Dover Publ., 1943 reprint).

Reed, R.P. (1962)
Stress pulse trains from multiple reflection at a zone of many discontinuities. SC - 4642(RR)

Reismann, H. and Tsai, L.W. (1972)
Wave propagation in discretely inhomogeneous elastic cylindrical rods - a comparison of two theories.
Zeits. Angew. Math. Mech. 52: 1-10.

Reissner, E. (1945)
The effect of transverse shear deformation on the bending of elastic plates.
J. Appl. Mech. 12 A-69-A77.

Richardson, L.F. (1911)
The approximate arithmetical solution by finite differences of physical problems involving differential equations with an application in a Masonry Dam.
Phil. Trans. Roy. Soc. London 210 Ser. A: 307-357.

Richtmyer, R.D. and Morton, K.W. (1967)
Difference methods for initial value problems. 2nd ed.
(London: Interscience Publ., Wiley).

Riemann, B. (1860)
Über die Fortpflanzung ebener Luftwellen von endlicher Schwingungsweite.
Goettinger Abhandlungen 8,43.

Rinehart, J.S. and Pearson, J. (1954)
Behaviour of metals under impulsive loads
(Cleveland: Amer. Soc. Metals).

Ripperger, E.A. (1952)
Longitudinal impact of cylindrical bars.
Proc. SESA 10(1): 209-226.

Ripperger, E.A. (1953)
The propagation of pulses in cylindrical bars an experimental study. In: First Midwestern Conference on Solid Mechanics, Proc. Urbana, Illinois. pp.29-39.

Ripperger, E.A. (1955)
Measurement of short bending wave pulse in steel bars.
DRL - 367, CM - 8, July 1955. pp.1-37.

Ripperger, E.A. (1967)
The relationship between the constitutive equation and one-dimensional wave propagation. In: Mechanical behaviour of materials under dynamic loads. ed. by:
U.S. Lindlholm.

Ripperger, E.A. and Abramson, H. N. (1957a)
A study of the propagation of flexural waves in elastic beams.
J. Appl. Mech. 24: 431-434.

Ripperger, E. A. and Abramson, H.N. (1957b)
Reflection and transmission of elastic pulses in a bar at discontinuity in cross section. In: Third Midwestern Conference on Solid Mechanics, Proc. pp.135-145.

Ritchie, I.G. (1973)
Improved resonant bar techniques for the measurement of dynamic elastic moduli and test of the Timoshenko beam theory.
J. Sound Vibr. 31: 456-468.

Roberts, L. (1959)
On the numerical solution of the equations for spherical waves of finite amplitude II.
J. Math. Phys. 36: 329-337.

Robertson, E.R. and King, W. (1974)
The technique of holographic interferometry applied to the study of transient stresses.
Journal of Strain Analysis 9(1): 44-49.

Robinson, A. (1950)
Shock transmission in beams.
A.R.C. Technical Report R. & M. No. 2265. London.

Rose, J.L., Chou, S.C. and Chou, P.C. (1973)
Vibration analysis of thick walled spheres and cylinders.
J. Acoust. Soc. Amer. 53: 771-776.

Rose, J. L. and Mortimer, R.W. (1973)
Elastic wave analysis in non destructive testing.
Materials Evaluation 31(3): 33-38.

Rose, J.L.; Mortimer, R.W. and Blum, A. (1973)
Elastic wave propagation in a joined cylindrical-conical-cylindrical shell.
Exp. Mech. 13: 150-156.

Rosenfeld, R.L. and Miklowitz, J. (1965)
Elastic wave propagation in rods of arbitrary cross section
J. Appl. Mech. 32: 290-294.

Rosinger, H.E. and Ritchie I.G. (1974)
Acritical assessment of the cantilever beam method for the determination of dynamic Young's modulus.
J. Test. Eval. 2: 131-138.

Rosinger, H.E. and Ritchie, I.G. (1977)
On Timoshenko's correction for shear in vibrating isotropic beams.
J. Phy. D Appl. Phys. 10: 1461-1466.

Sagartz, M.J. and Forrestal, M.J. (1972)
Bending stresses propagating from the clamped support of an impulsively loaded beam.
A I A A J. 10: 1373-1374.

Sauer, R. (1954)
Anfangswertprobleme bei partiellen Differential gleichungen.
(Berlin: Springer Verlag).

Sauer, R. (1964)
Einfache Wellen inder charackteristiken Theorie von Systemen quasilinearer partieller Differential gleichungen.
Zeits. Angew. Math. Mech. 44: 203-209.

Sauerwein, H. (1967)
Numerical calculations of multidimensional and unsteady flows by the method of characteristics.
J. Comput. Phys. 1: 406-432.

Schirmer, H. (1952)
Über Biegewellen in Stäben.
Ingen. Arch. 20: 247-257.

Schulze, R. (1953)
Experimentelle Untersuchungen über den Babkenquerstoß
Zeits. Angew. Phys. 5(7): 252-260.

Schwieger, H. (1965)
A simple calculation of the transverse impact on beams and its experimental verification.
Exp. Mech. 5: 244-250.

Scott, R.A. (1978)
Linear elastic wave propagation. an annotated bibliography. I and II.
The Shock and Vibration Digest 10(2;3): 25-41; 11-41.

Sears, J. E. (1908)
On longitudinal impact of metal rods with rounded ends.
Proc. Cambr. Phil. Soc. 14: 257.

Sears, J. E. (1912)
On longitudinal impact of metal rods II.
Trans. Cambr. Phil Soc. 21: 49-106.

Sedney, R. (1969)
A survey of the method of characteristics for non equilibrium, internal flows. In: 7th Aerospace Sciences Meeting.
A I A A Paper No. 69-6. New York.

Sedney, R. (1970)
The method of characteristics. In: Gasdynamics. Volume I, Part II: Nonequilibrium flows. ed. by:
P. P. Wegener. (New York: Marcel Dekker Inc.) pp.160-233.

Seelig, J.M. and Hoppmann II, W.H. (1964)
Impact on an elastically connected double beam system.
J. Appl. Mech. 31: 621-626.

S E S A 's Manual on experimental stress analysis. (1949)
Chapters 1, 2, 3 and 8. Proc. SESA.

Shipley, S.A.; Leistner, H.G. and Jones R.E. (1967)
Elastic wave propagation - A comparison between finite element predictions and exact solutions. In: Int. Symp. of wave propagation and dynamic properties of earth materials.
University of New Mexico. pp. 509-519.

Sobel, L.H. and Geers, T.L. (1973)
Convergence of finite difference transient response computers and Structures 3: 1001-1035.

Spence, G.B. and Seldin, E.J. (1970)
Sonic resonances of a bar and compound torsion oscillator.
J. Appl. Phys. 41(8): 3383-3389.

Spinner, S.; Reichard, T.W. and Tefft, W.E. (1960)
A comparison of experimental and theoretical relations between Young's modulus and the flexural and longitudinal resonance frequencies of uniform bars.
Journal of Research of the National Bureau of Standards 64A(2): 147-155.

Spinner, S. and Tefft, W.E. (1961)
A method for determining resonance frequency and for calculating elastic moduli from these frequencies.
Proc. Amer. Soc. Test. Mat. 61: 1221-1238.

Stepanenko, M.V. (1976)
A method of analyzing transient impulsive deformations in elastic structures.
Soviet Mining Sciences 2: 53-57.

Stephen, N.G. (1978)
On the variation of Timoshenko shear coefficient with frequency.
J. Appl. Mech. 45(4): 695-697.

Stephen, N.G. (1980)
Timoshenko's shear coefficient from a beam subjected to gravity loading.
J. Appl. Mech. 2: 121-127.

Stephenson, G. and Wilhoit, J.C. (1965)
An experimental study of bending impact waves in beams.
Exp. Mech. 5: 16-21.

Stetter, H. J. (1961)
On the convergence of characteristic finite difference methods of high accuracy for quasi - linear hyperbolic equations.
Numerische Mathematik 3: 321-344.

Streeter, V.L.; Wylie, E.B. and Richart, F.E. (1974)
Soil motion computation by characteristics method.
Proc. Amer. Soc. Cevil Eng. 100(GT3): 247-263.

Suh, N.P. (1967)
Stress wave propagation in truncated cones against "rigid" wall.
Exp. Mech. 7: 541-544.

Sun, C.T. and Huang, S.N. (1975)
Transverse impact problems by higher order beam finite element.
Comput. Struc. 5: 297-303.

Sutherland, J.G. and Goodman, L.E. (1951)
Vibrations of prismatic bars including rotatory inertia and shear corrections.
Technical Report. University of Illinois. Dpt. Civil Eng.

Swartz, B. and Wendroff, B. (1974)
The relative efficiency of finite difference and finite element methods, I: Hyperbolic problems and splines.
SIAM J. Num. Anal. 11: 979-993.

Taleb, N.J. and Suppiger, E.W. (1961)
Vibration of stepped beams.
Journal of the Aerospace Sciences. 28: 295-298.

Tanaka, K. and Iwahashi, Y. (1977)
Dispersion relation of elastic waves in bars of rectangular cross section.
Bull, Japan. Soc. Mech. Eng. 20(146): 9-2-929.

Tanaka, K. and Motoyama, C. (1976)
The behaviour of an infinite circular bar subjected to impulsive bending load.
Bull. Japan. Soc. Mech. Eng. 19: 248-259.

Taylor, D.A.W. (1966)
Time and amplitude errors in the measurement of dynamic strain pulses by resistance strain gauges.
Int. J. Mech. Sci. 8: 193-212.

Tefft, W.E. (1960)
Numerical solution of the frequency equations for the flexural vibration of cylindrical rods.
J. Res. Nat. Bur. Stand. 64B(4): 237-242.

Tien, Y.T. (1968)
Wave propagation in a finite length bar with a variable cross section.
J. Appl. Mech. 35: 824-825.

Timoshenko, S.P. (1913)
Zur Frage nach der Wirkung eines Stoßes auf einen Balken.
Zeits. Math. Phys. 62: 198-209.

Timoshenko, S.P. (1921)
On the correction for shear of the differential equation for transverse vibrations of prismatic bars.
Phil Magaz. 41 Ser 6: 744-746.

Timoshenko, S.P. (1922)
On the transverse vibrations of bars of uniform cross section
Phil. Magaz. 43 Ser 6: 125-131.

Timoshenko, S.P. (1953)
History of strength of materials.
(New York: McGraw Hill Co.)

Timoshenko, S. P. (1928)
Vibration Problems in Engineering; Van Nostrand Co. Inc.

Todhunter, I. and Pearson, K. (1893)
A history of the theory of elasticity. Vol.II, Part I and II.
(New York: Dover Publ. Inc.)

Thomas, D.L.; Wilson, J.M. and Wilson, R.R. (1973)
Timoshenko beam finite elements.
J. Sound Vibr. 31(3): 315-330.

Thomas, J. and Abbas, B.A. (1975)
Finite element model for dynamic analysis of Timoshenko beam.
J. Sound Vibr. 41: 291-299.

Thomas, D.L. (1976)
Comments on "Finite element model for dynamic analysis of Timoshenko beam".
J. Sound Vibr. 46(2): 285-290.

Thornhill, C.K. (1952)
The numerical method of characteristics for hyperbolic problems in three independent variables.
ARC Technical Report. R & M. 2615.

Traill-Nash, R.W. and Collar, A.R. (1953)
The effects of shear flexibility and rotatory inertia on the bending vibrations of beams.
Quart. J. Mech. Appl. Math. 6: 186-222.

Troke, R.W. (1976)
Improving strain-measurement accuracy when using shunt calibrations.
Exp. Mech. 16: 397-400.

Tsai, Y. N. and Kolsky, H. (1966)
Surface wave propagation for linear viscoelastic solids.
J. Mech. Phys. Solids 16: 99-109.

Tschudi, E.W. (1921)
Duration of impact of bars.
Physical Review 18 Ser. 2: 423-430.

Tuzi, Z. and Nisida, M. (1936)
Photoelastic studies of stresses due to impact
Philosophical Magazine 21 Ser 7: 448-473.

Uckan, Y. and Ang, A.H. (1971)
Numerical stability in wave propagation problems.
Computers and Structures 1: 495-510-

Uflyand, Y.S. (1948)
The propagation of waves in the transverse vibration of bars and plates (in Russian)
Prikl. Mat. Mekh. (PMM) 12: 287-300.

Vasudeva, R.Y. and Bhaskara, R.K. (1978)
Propagation of a pulse in a nonhomogeneous elastic rod with varying cross section.
J. Appl. Mech. 45: 942-944.

Vigness, I. (1951)
Transverse waves in beams.
Proc. SESA 8: 69-82

Voltera, E. (1948)
Alcuni risultati di prove dinamichesui materiali
Nuovo Cimento 4.

Voltera, E. (1958)
A study of the propagation of flexural waves in elastic beams (Discussion).
J. Appl. Mech. 25: 153-154.

Wagstaff, J. E. P. (1924)
Experiments on the duration of impacts,mainly of bars with rounded ends, in elucidation of the elastic theory .
Proc. Roy. Soc. London, Ser.A-105: 544-570

Watson, H. (1972)
Gage-length errors in the resolution of dispersive stress waves.
Exp. Mech. 29(2): 352-358.

Weinberger, H.F. (1965)
A first course in partial differential equations
University of Minnesota: Xerox College Publ.

Whittier, J.S. (1965)
A note on wave propagation in a nonhomogeneous bar.
J. Appl. Mech. 32: 947-949.

Wylie, E.B. and Streeter, V.L. (1976)
One-dimensional soil transients by characteristics.
In: Engineering Foundation Conference.
Numerical Methods in Geomechanics. Virginia Polytechnic.

Yang, C.Y. (1966)
Propagation of discontinuous waves in nonuniform Timoshenko beam.
J. Appl. Mech. 33: 706-708.

Yang, J.C. and Hassett, R.J. (1972)
Transient stresses in axisymmetric bodies of varying area.
Exp. Mech. 12: 304-310.

Yew, E. H. and Chen, C.S. (1978)
Experimental study of dispersive waves in beam and rod using Fast Fourier Transform.
J. Appl. Mech. 45: 940-942.

Zemanek, J. and Rudnick, I. (1961)
Attenuation and dispersion of elastic waves in a cylindrical bar.
J. Acoust. Soc. Amer. 33(10): 1283-1288.

Zienkiewicz, O.C. (1970)
The finite element method in engineering sciences.
(New York: McGraw Hill Co.).

Ziv, M. (1969)
Two spatial dimensional elastic wave propagation by the theory of characteristics.
J. Solid Struc. 5: 1135-1151.

Ziv., M. (1975)
Finite longitudinally multilayered membrane shells subjected to impact loads.
AIAA J. 13: 717-718.

A P P E D I C E S

APPENDIX A

TMOTCU-3 CMPUTER PROGRAM FOR TRANSIENT FLEXURAL WAVE PROPAGATION IN BEAMS WITH DISCONTINUITIES OF CROSS SECTION

```
C MCDIT 21 COMPUTER CODE FOR 1-DIMEN. ELASTIC WAVE PROBLEMS
      COMMONU(9,8001),Y(12,12),W(9,9),F(6,3),G(6,3),H(6,3),Z(12),UU(12),
     1DU(9),V(9),UP(9),A(7),B(7),C(7),D(7),E(7),P(7),PINC,XLI,EM,C1,C2,X
     2ZERO,I,M,S1,DS(9),R1,R2
    1 FORMAT(I5,4E15.8)
    2 FORMAT(2E15.8)
    3 FORMAT(5E15.8)
    4 FORMAT (1H ,38HNUMBER OF POINTS ALONG LEADING WAVE = ,I4)
    5 FORMAT (1H ,8HXZERO = ,E15.8,5X,9HDELTAX = ,E15.8)
    6 FORMAT(1H ,5HC1 = ,E15.8,5X,5HC2 = ,E15.8)
    7 FORMAT(1H ,1H(,E15.8,7H)*U1X+(,E15.8,6H)*U1+(,E15.8,7H)*U2X+(,E15.
     18,6H)*U2+(,E15.8,7H)*U3X+(,E15.8,4H)*U3)
    8 FORMAT(1H ,4H  +(,E15.8,37H)*U1T = BOUNDARY CONDITION FUNCTION 1)
    9 FORMAT(1H ,4H  +(,E15.8,37H)*U2T = BOUNDARY CONDITION FUNCTION 2)
   10 FORMAT(1H ,4H  +(,E15.8,37H)*U3T = BOUNDARY CONDITION FUNCTION 3)
   11 FORMAT(1H ,9HELBEAM = ,E12.4,5HS1 = ,E12.4)
   12 FORMAT(4E12.4)
   13 FORMAT(1H ,5HR1 = ,E12.4,5HR2 = ,E12.4)
C  THE SHEAR CORRECTION FACTOR IS GIVEN AS C2
C  DR IS DIAMETER RATIO
   24 FORMAT(1H ,43HSLOPE OF II+ LINE EXCEEDS OR EQUALS MAXIMUM)
   25 FORMAT(1H ,41HVALUE OF 3.0 COMPATIBLE WITH THIS PROGRAM)
   37 FORMAT(1H ,14HERROR IN LOGIC)
   38 FORMAT(1H ,36HENDBEAM BOUNDARY CONDITION FUNCTION,/)
   69 FORMAT(1H ,////)
      READ(5,1)MZERO,XZERO,PINC,C1,C2
      READ(5,12)ELBEAM,S1,R1,DR
      READ(5,3)A(1),A(2),A(3),A(4),A(5)
      READ(5,2)A(6),A(7)
      READ(5,3)B(1),B(2),B(3),B(4),B(5)
      READ(5,2)B(6),B(7)
      READ(5,3)C(1),C(2),C(3),C(4),C(5)
      READ(5,2)C(6),C(7)
      READ(5,3)D(1),D(2),D(3),D(4),D(5)
      READ(5,2)D(6),D(7)
      READ(5,3)E(1),E(2),E(3),E(4),E(5)
      READ(5,2)E(6),E(7)
      READ(5,3)P(1),P(2),P(3),P(4),P(5)
      READ(5,2)P(6),P(7)
      C2 = C1*SQRT(C2/2.58)
      WRITE(6,4)MZERO
      WRITE(6,5)XZERO,PINC
      WRITE(6,6)C1,C2
      WRITE(6,11)ELBEAM,S1
      R2 = DR*R1
      WRITE(6,13)R1,R2
      WRITE(6,7)A(1),A(2),A(3),A(4),A(5),A(6)
      WRITE(6,8)A(7)
      WRITE(6,7)B(1),B(2),B(3),B(4),B(5),B(6)
      WRITE(6,9)B(7)
      WRITE(6,7)C(1),C(2),C(3),C(4),C(5),C(6)
      WRITE(6,10)C(7)
      WRITE(6,38)
```

```
      WRITE(6,7)D(1),D(2),D(3),D(4),D(5),D(6)
      WRITE(6,8)D(7)
      WRITE(6,7)E(1),E(2),E(3),E(4),E(5),E(6)
      WRITE(6,9)E(7)
      WRITE(6,7)P(1),P(2),P(3),P(4),P(5),P(6)
      WRITE(6,10)P(7)
      CONST1 = 1.373/R1**2
      CONST2 = 1.373/R2**2
      CON1 = (R2/R1)**2
      CON2 = CON1**2
      WRITE(6,12)CONST1,CONST2,CON1,CON2
      EM = C1/C2
      IF(EM-3.)22,23,23
   23 WRITE(6,24)
      WRITE(6,25)
      GOTO9999
   22 WRITE(6,69)
      XLI=1.
      CALLFIRSTP
   91 LI=2
      IYZ=1.-2./(EM+1.)
      GOTO26
   27 XLI=LI
      I=1
      IYZZ=IYZ
      IYZ=XLI-(2.*XLI)/(EM+1.)
      MESH = ELBEAM/PINC + .5
   40 IF(LI-MESH)41,41,42
   41 CALL INPUTP
      GOTO35
   42 CALL ENDP(ELBEAM)
   35 IF(I-LI)28,29,29
   28 IF(I-1-IYZZ)30,31,32
   31 IF(IYZZ-IYZ)33,34,34
   32 IF(I-1-IYZ)36,30,30
   36 WRITE(6,37)
      GOTO9999
   29 CALLBOUNDP
   92 LI=LI+1
   26 IF(LI-MZERO)27,9999,9999
   30 IF((LI-I)*PINC.NE.S1)GOTO 39
      CALL DISCONT
      GOTO35
   39 CALL ORDINP
      GOTO 35
   33 IF((LI-I)*PINC.NE.(S1+PINC))GOTO 43
      CALL DISCON3
      GOTO35
   43 CALL CASE32
      GOTO35
   34 IF((LI-I)*PINC.NE.S1)GOTO 44
      CALL DISCON1
      GOTO35
   44 CALL CASE1P
      GOTO35
 9999 CALLEXIT
      END
```

```
C SIMOLTANEOUS SOLUTION SUBROUTINE
      SUBROUTINEMASUB
      COMMONU(9,8001),Y(12,12),W(9,9),F(6,3),G(6,3),H(6,3),Z(12),UU(12),
     1DU(9),V(9),UP(9),A(7),B(7),C(7),D(7),E(7),P(7),PINC,XLI,EM,C1,C2,X
     2ZERO,I,M,S1,DS(9),R1,R2
      N=M-1
      DO 5200 NN=1,N,1
      NNN=NN+1
      DO 5100 JJ=NNN,M,1
      FRAC =-Y(JJ,NN)/Y(NN,NN)
      DO 5050 KK=NN,M,1
 5050 Y(JJ,KK)=FRAC*Y(NN,KK)+Y(JJ,KK)
 5100 Z(JJ)=FRAC*Z(NN)+Z(JJ)
 5200 CONTINUE
      DO 5500 NN=1,N,1
      NNN=M-NN
      JJ=NNN+1
      DO 5400 KK=1,NNN,1
 5400 Z(KK)=-Z(JJ)*(Y(KK,JJ)/Y(JJ,JJ))+Z(KK)
 5500 CONTINUE
      DO 5600 KKK=1,M,1
 5600 UU(KKK)=Z(KKK)/Y(KKK,KKK)
 9999 RETURN
      END
C FIRST POINT SUBROUTINE
      SUBROUTINEFIRSTP
      COMMONU(9,8001),Y(12,12),W(9,9),F(6,3),G(6,3),H(6,3),Z(12),UU(12),
     1DU(9),V(9),UP(9),A(7),B(7),C(7),D(7),E(7),P(7),PINC,XLI,EM,C1,C2,X
     2ZERO,I,M,S1,DS(9),RR1,RR2
      DIMENSIONHOLD(12)
      ZERO = 0.
      PHI=(EM-1.)/(EM+1.)
      ALPH=1.-((4.*EM)/((1.+EM)**2))
      SLOP=PHI
      X5=XZERO
      T5 = 0.
      X1=XZERO
      T1=2.*PINC/C1
      X3=XZERO+PINC
      T3=T1/2.
      X2=XZERO+(2.*PINC)/(1.+EM)
      X4=ALPH*(X5-X3)+X3
      X6=XZERO
      X7=SLOP*(X6-X2)+X2
      CALLJUMPI(X5,UX5,UT5,VX5,VT5)
      CALLJUMPII(XZERO,WX5,WT5)
      CALLJUMPI(X3,UX3,UT3,VX3,VT3)
      CALLJUMPI(X4,UX4,UT4,VX4,VT4)
      CONST = 1.373/RR1**2
      CALLGECOFF(1,X2,X3,CONST)
      CALLGECOFF(2,X2,X6,CONST)
      CALLGECOFF(3,X1,X2,CONST)
      CALLGECOFG(1,X2,X3)
      CALLGECOFG(2,X2,X6)
      CALLGECOFG(3,X1,X2)
      CALLGECOFH(1,X2,X4)
      CALLGECOFH(2,X2,X5)
      CALLGECOFH(3,X1,X7)
      CALLBCTF1(T1,R1)
```

```
      CALLBCTF2(T1,R2)
      CALLBCTF3(T1,R3)
      CALLJUMPII(X2,DU(8),DU(9))
      DX23=X2-X3
      DX24=X2-X4
      DX26=X2-X6
      DT15=T1-T5
      DX25=X2-X5
      DX12=X1-X2
      DX17=X1-X7
      Y(1,1)=A(1)
      Y(1,2)=A(2)*DT15/2.+A(7)
      Y(1,3)=A(3)
      Y(1,4)=A(4)*DT15/2.
      Y(1,5)=A(5)
      Y(1,6)=A(6)*DT15/2.
      Y(1,7)=0.
      Y(1,8)=0.
      Y(1,9)=0.
      Y(1,10)=0.
      Y(1,11)=0.
      Y(1,12)=0.
      Z(1)=R1-A(2)*DT15*UT5/2.-A(4)*DT15*VT5/2.-A(6)*DT15*WT5/2.
      Y(2,1)=C1*(1.-F(1,3)*DX12/2.)
      Y(2,2)=1.-C1*DX12*DT15*F(2,3)/4.
      Y(2,3)=-C1*DX12*F(3,3)/2.
      Y(2,4)=-C1*DX12*DT15*F(4,3)/4.
      Y(2,5)=-C1*DX12*F(5,3)/2.
      Y(2,6)=-C1*DX12*DT15*F(6,3)/4.
      Y(2,7)=C1*(-1.-F(1,3)*DX12/2.-F(2,3)*DX12*DX23/4.)
      Y(2,8)=-1.+F(2,3)*DX12*DX23/4.
      Y(2,9)=(-C1*DX12/2.)*(F(3,3)+F(4,3)*DX23/2.)
      Y(2,10)=F(4,3)*DX12*DX23/4.
      Y(2,11)=(-C1*DX12/2.)*(F(5,3)+F(6,3)*DX24/2.)
      Y(2,12)=C1*F(6,3)*DX12*DX24/(4.*C2)
      Z(2)=(C1*DX12/2.)*(F(2,3)*DT15*UT5/2.+F(2,3)*DX23*(UX3-UT3/C1)/2.+
     1F(4,3)*DT15*VT5/2.+F(4,3)*DX23*(VX3-VT3/C1)/2.+F(6,3)*DT15*WT5/2.+
     2F(6,3)*DX24*(-DU(8)+DU(9)/C2)/2.)
      Y(3,1)=B(1)
      Y(3,2)=B(2)*DT15/2.
      Y(3,3)=B(3)
      Y(3,4)=B(4)*DT15/2.+B(7)
      Y(3,5)=B(5)
      Y(3,6)=B(6)*DT15/2.
      Y(3,7)=0.
      Y(3,8)=0.
      Y(3,9)=0.
      Y(3,10)=0.
      Y(3,11)=0.
      Y(3,12)=0.
      Z(3)=R2-B(2)*DT15*UT5/2.-B(4)*DT15*VT5/2.-B(6)*DT15*WT5/2.
      Y(4,1)=-C1*DX12*G(1,3)/2.
      Y(4,2)=-C1*DX12*DT15*G(2,3)/4.
      Y(4,3)=C1*(1.-G(3,3)*DX12/2.)
      Y(4,4)=1.-C1*DX12*DT15*G(4,3)/4.
      Y(4,5)=-C1*DX12*G(5,3)/2.
      Y(4,6)=-C1*DX12*DT15*G(6,3)/4.
      Y(4,7)=(-C1*DX12/2.)*(G(1,3)+G(2,3)*DX23/2.)
      Y(4,8)=G(2,3)*DX12*DX23/4.
```

```
 Y(4,9)=C1*(-1.-G(3,3)*DX12/2.-G(4,3)*DX12*DX23/4.)
 Y(4,10)=-1.+G(4,3)*DX12*DX23/4.
 Y(4,11)=(-C1*DX12/2.)*(G(5,3)+G(6,3)*DX24/2.)
 Y(4,12)=C1*DX12*DX24*G(6,3)/(4.*C2)
 Z(4)=(C1*DX12/2.)*(G(2,3)*DT15*UT5/2.+G(2,3)*DX23*(UX3-UT3/C1)/2.+
1G(4,3)*DT15*VT5/2.+G(4,3)*DX23*(VX3-VT3/C1)/2.+G(6,3)*DT15*WT5/2.+
2G(6,3)*DX24*(-DU(8)+DU(9)/C2)/2.)
 Y(5,1)=(-C2*DX17/2.)*H(1,3)*(1.+SLOP*PHI)
 Y(5,2)=(-C2*DX17*DT15/4.)*H(2,3)*(1.+SLOP*PHI)
 Y(5,3)=(-C2*DX17/2.)*H(3,3)*(1.+SLOP*PHI)
 Y(5,4)=(-C2*DX17*DT15/4.)*H(4,3)*(1.+SLOP*PHI)
 Y(5,5)=C2*(1.-SLOP*PHI-(H(5,3)*DX17/2.)*(1.+SLOP*PHI))
 Y(5,6)=1.-SLOP*PHI-(C2*DX17*DT15*H(6,3)/4.)*(1.+SLOP*PHI)
 Y(5,7)=(-C2*DX17/2.)*(H(1,3)*(1.-SLOP)+(H(2,3)*DX23/2.)*(1.-SLOP))
 Y(5,8)=(C2*DX17*DX23*H(2,3)/(4.*C1))*(1.-SLOP)
 Y(5,9)=(-C2*DX17/2.)*(H(3,3)*(1.-SLOP)+(H(4,3)*DX23/2.)*(1.-SLOP))
 Y(5,10)=(C2*DX17*DX23*H(4,3)/(4.*C1))*(1.-SLOP)
 Y(5,11)=C2*(SLOP-1.-(H(5,3)*DX17/2.)*(1.-SLOP)-(H(6,3)*DX17*DX24/4
1.)*(1.-SLOP))
 Y(5,12)=SLOP-1.+(H(6,3)*DX17*DX24/4.)*(1.-SLOP)
 Z(5)=SLOP*(WT5*(1.-PHI))+C2*SLOP*WX5*(1.-PHI)+(C2*DX17/2.)*(H(1,3)
1*SLOP*UX5*(1.-PHI)+(H(2,3)*DT15*UT5/2.)*(1.+SLOP*PHI)+(H(2,3)*DX23
2*(UX3-UT3/C1)/2.)*(1.-SLOP)+H(3,3)*SLOP*VX5*(1.-PHI)+(H(4,3)*DT15*
3VT5/2.)*(1.+SLOP*PHI)+(H(4,3)*DX23*(VX3-VT3/C1)/2.)*(1.-SLOP)+H(5,
43)*SLOP*WX5*(1.-PHI)+(H(6,3)*DT15*WT5/2.)*(1.+SLOP*PHI)+(H(6,3)*DX
524*(-DU(8)+DU(9)/C2)/2.)*(1.-SLOP))
 Y(6,1)=C(1)
 Y(6,2)=C(2)*DT15/2.
 Y(6,3)=C(3)
 Y(6,4)=C(4)*DT15/2.
 Y(6,5)=C(5)
 Y(6,6)=C(6)*DT15/2.+C(7)
 Y(6,7)=0.
 Y(6,8)=0.
 Y(6,9)=0.
 Y(6,10)=0.
 Y(6,11)=0.
 Y(6,12)=0.
 Z(6)=R3-C(2)*DT15*UT5/2.-C(4)*DT15*VT5/2.-C(6)*DT15*WT5/2.
 Y(7,1)=0.
 Y(7,2)=0.
 Y(7,3)=0.
 Y(7,4)=0.
 Y(7,5)=0.
 Y(7,6)=0.
 Y(7,7)=C1*(1.-F(1,1)*DX23/2.-F(2,1)*DX23**2/4.)
 Y(7,8)=1.+F(2,1)*DX23**2/4.
 Y(7,9)=(-C1*DX23/2.)*(F(3,1)+F(4,1)*DX23/2.)
 Y(7,10)=F(4,1)*DX23**2/4.
 Y(7,11)=(-C1*DX23/2.)*(F(5,1)+F(6,1)*DX24/2.)
 Y(7,12)=C1*DX23*DX24*F(6,1)/(4.*C2)
 Z(7)=UT3+C1*UX3+C1*DX23*(F(1,1)*UX3/2.+F(2,1)*DX23*(UX3-UT3/C1)/4.
1+F(3,1)*VX3/2.+F(4,1)*DX23*(VX3-VT3/C1)/4.+F(5,1)*(-DU(8))/2.+F(6,
21)*DX24*(-DU(8)+DU(9)/C2)/4.)
 Y(8,1)=C1*PHI*(1.+F(1,2)*DX26/2.)
 Y(8,2)=PHI*(-1.+C1*DX26*DT15*F(2,2)/4.)
 Y(8,3)=C1*DX26*F(3,2)*PHI/2.
 Y(8,4)=C1*DX26*DT15*F(4,2)*PHI/4.
 Y(8,5)=C1*DX26*F(5,2)*PHI/2.
 Y(8,6)=C1*DX26*DT15*F(6,2)*PHI/4.
```

```
 Y(8,7)=C1*(-1.+F(1,2)*DX26/2.+F(2,2)*DX26*DX23/4.)
 Y(8,8)=1.-F(2,2)*DX26*DX23/4.
 Y(8,9)=(C1*DX26/2.)*(F(3,2)+F(4,2)*DX23/2.)
 Y(8,10)=-F(4,2)*DX26*DX23/4.
 Y(8,11)=(C1*DX26/2.)*(F(5,2)+F(6,2)*DX24/2.)
 Y(8,12)=-C1*DX26*DX24*F(6,2)/(4.*C2)
 Z(8)=UT5*(1.-PHI)+C1*UX5*(PHI-1.)-(C1*DX26/2.)*(F(1,2)*UX5*(1.-PHI
1)+F(2,2)*DX23*(UX3-UT3/C1)/2.+F(2,2)*DT15*PHI*UT5/2.+F(3,2)*VX5*(1
2.-PHI)+F(4,2)*DX23*(VX3-VT3/C1)/2.+F(4,2)*DT15*PHI*VT5/2.+F(5,2)*W
3X5*(1.-PHI)+F(6,2)*DX24*(-DU(8)+DU(9)/C2)/2.+F(6,2)*DT15*PHI*WT
45/2.)
 Y(9,1)=C1*PHI*G(1,2)*DX26/2.
 Y(9,2)=C1*DX26*DT15*G(2,2)*PHI/4.
 Y(9,3)=C1*PHI*(1.+G(3,2)*DX26/2.)
 Y(9,4)=PHI*(-1.+C1*DX26*DT15*G(4,2)/4.)
 Y(9,5)=C1*G(5,2)*DX26*PHI/2.
 Y(9,6)=C1*DX26*DT15*G(6,2)*PHI/4.
 Y(9,7)=(C1*DX26/2.)*(G(1,2)+G(2,2)*DX23/2.)
 Y(9,8)=-G(2,2)*DX26*DX23/4.
 Y(9,9)=C1*(-1.+G(3,2)*DX26/2.+G(4,2)*DX26*DX23/4.)
 Y(9,10)=1.-G(4,2)*DX26*DX23/4.
 Y(9,11)=(C1*DX26/2.)*(G(5,2)+G(6,2)*DX24/2.)
 Y(9,12)=-C1*DX26*DX24*G(6,2)/(4.*C2)
 Z(9)=VT5*(1.-PHI)+C1*VX5*(PHI-1.)-(C1*DX26/2.)*(G(1,2)*UX5*(1.-PHI
1)+G(2,2)*DX23*(UX3-UT3/C1)/2.+G(2,2)*DT15*PHI*UT5/2.+G(3,2)*VX5*(1
2.-PHI)+G(4,2)*DX23*(VX3-VT3/C1)/2.+G(4,2)*DT15*PHI*VT5/2.+G(5,2)*W
3X5*(1.-PHI)+G(6,2)*DX24*(-DU(8)+DU(9)/C2)/2.+G(6,2)*DT15*PHI*WT5/
42.)
 Y(10,1)=0.
 Y(10,2)=0.
 Y(10,3)=0.
 Y(10,4)=0.
 Y(10,5)=0.
 Y(10,6)=0.
 Y(10,7)=(-C1*DX23/2.)*(G(1,1)+G(2,1)*DX23/2.)
 Y(10,8)=G(2,1)*DX23**2/4.
 Y(10,9)=C1*(1.-G(3,1)*DX23/2.-G(4,1)*DX23**2/4.)
 Y(10,10)=1.+G(4,1)*DX23**2/4.
 Y(10,11)=(-C1*DX23/2.)*(G(5,1)+G(6,1)*DX24/2.)
 Y(10,12)=C1*DX23*DX24*G(6,1)/(4.*C2)
 Z(10)=VT3+C1*VX3+C1*DX23*(G(1,1)*UX3/2.+G(2,1)*DX23*(UX3-UT3/C1)/4
1.+G(3,1)*VX3/2.+G(4,1)*DX23*(VX3-VT3/C1)/4.+G(5,1)*(-DU(8))/2.+G(6
2,1)*DX24*(-DU(8)+DU(9)/C2)/4.)
 Y(11,1)=0.
 Y(11,2)=0.
 Y(11,3)=0.
 Y(11,4)=0.
 Y(11,5)=0.
 Y(11,6)=0.
 Y(11,7)=(-C2*DX24/2.)*(H(1,1)+H(2,1)*DX23/2.)
 Y(11,8)=C2*DX24*DX23*H(2,1)/(4.*C1)
 Y(11,9)=(-C2*DX24/2.)*(H(3,1)+H(4,1)*DX23/2.)
 Y(11,10)=C2*DX24*DX23*H(4,1)/(4.*C1)
 Y(11,11)=C2*(1.-H(5,1)*DX24/2.-H(6,1)*DX24**2/4.)
 Y(11,12)=1.+H(6,1)*DX24**2/4.
 Z(11)=DU(9)+C2*DU(8)+C2*DX24*(H(1,1)*UX4/2.+H(2,1)*DX23*(UX3-UT3/C
11)/4.+H(3,1)*VX4/2.+H(4,1)*DX23*(VX3-VT3/C1)/4.+H(5,1)*(-DU(8))/2.
2+H(6,1)*DX24*(-DU(8)+DU(9)/C2)/4.)
 Y(12,1)=0.
```

```
   Y(12,2)=0.
   Y(12,3)=0.
   Y(12,4)=0.
   Y(12,5)=0.
   Y(12,6)=0.
   Y(12,7)=(C2*DX25/2.)*(H(1,2)+H(2,2)*DX23/2.)
   Y(12,8)=-C2*DX25*DX23*H(2,2)/(4.*C1)
   Y(12,9)=(C2*DX25/2.)*(H(3,2)+H(4,2)*DX23/2.)
   Y(12,10)=-C2*DX25*DX23*H(4,2)/(4.*C1)
   Y(12,11)=C2*(-1.+H(5,2)*DX25/2.+H(6,2)*DX25*DX24/4.)
   Y(12,12)=1.-H(6,2)*DX25*DX24/4.
   Z(12)=WT5-C2*WX5-(C2*DX25/2.)*(H(1,2)*UX5+H(2,2)*DX23*(UX3-UT3/C1)
  1/2.+H(3,2)*VX5+H(4,2)*DX23*(VX3-VT3/C1)/2.+H(5,2)*WX5+H(6,2)*DX24*
  2(-DU(8)+DU(9)/C2)/2.)
   M=12
   IF(Y(1,1))1,2,1
 2 DO3J=1,12
   HOLD(J)=Y(1,J)
   Y(1,J)=Y(2,J)
 3 Y(2,J)=HOLD(J)
   CEEP=Z(1)
   Z(1)=Z(2)
   Z(2)=CEEP
 1 IF(Y(3,3))4,5,4
 5 DO6J=1,12
   HOLD(J)=Y(3,J)
   Y(3,J)=Y(4,J)
 6 Y(4,J)=HOLD(J)
   CEEP=Z(3)
   Z(3)=Z(4)
   Z(4)=CEEP
 4 IF(Y(6,6))98,8,98
 8 DO9J=1,12
   HOLD(J)=Y(6,J)
   Y(6,J)=Y(5,J)
 9 Y(5,J)=HOLD(J)
   CEEP=Z(6)
   Z(6)=Z(5)
   Z(5)=CEEP
98 CALLMASUB
99 UP(2)=UU(7)
   UP(3)=UU(8)
   UP(5)=UU(9)
   UP(6)=UU(10)
   UP(8)=UU(11)
   UP(9)=UU(12)
   U(2,2)=UU(1)
   U(3,2)=UU(2)
   U(5,2)=UU(3)
   U(6,2)=UU(4)
   U(8,2)=UU(5)
   U(9,2)=UU(6)
   U(1,2)=(U(3,2)+UT5)*DT15/2.
   U(4,2)=(U(6,2)+VT5)*DT15/2.
   U(7,2)=(U(9,2)+WT5)*DT15/2.
   UP(1)=((UP(2)+UX3)/2.-(UP(3)+UT3)/(2.*C1))*DX23
   UP(4)=((UP(5)+VX3)/2.-(UP(6)+VT3)/(2.*C1))*DX23
   UP(7)=((UP(8)-DU(8))/2.-(UP(9)-DU(9))/(2.*C2))*DX24
   U(1,1)=0.
   U(2,1)=UX3
```

```
      U(3,1)=UT3
      U(4,1)=0.
      U(5,1)=VX3
      U(6,1)=VT3
      U(7,1)=0.
      U(8,1)=0.
      U(9,1)=0.
      CALLPRINTO(X5,T5,ZERO,UX5,UT5,ZERO,VX5,VT5,ZERO,WX5,WT5,XLI)
      CALLPRINTO(X3,T3,U(1,1),U(2,1),U(3,1),U(4,1),U(5,1),U(6,1),U(7,1),
     1U(8,1),U(9,1),XLI)
      CALLPRINTO(X1,T1,U(1,2),U(2,2),U(3,2),U(4,2),U(5,2),U(6,2),U(7,2),
     1U(8,2),U(9,2),XLI)
 9999 RETURN
      END
C     INPUT POINT SUBROUTINE
      SUBROUTINEINPUTP
      COMMONU(9,8001),Y(12,12),W(9,9),F(6,3),G(6,3),H(6,3),Z(12),UU(12),
     1DU(9),V(9),UP(9),A(7),B(7),C(7),D(7),E(7),P(7),PINC,XLI,EM,C1,C2,X
     2ZERO,I,M,S1,DS(9),R1,R2
      X=XZERO+XLI*PINC
      T=XLI*PINC/C1
      V(1)=0.
      V(4)=0.
      V(7)=0.
      V(8)=0.
      V(9)=0.
      CALLJUMPI(X,V(2),V(3),V(5),V(6))
      CALLPRINTO(X,T,V(1),V(2),V(3),V(4),V(5),V(6),V(7),V(8),V(9),XLI)
  290 RETURN
      END
C BOUNDARY POINT SUBROUTINE
      SUBROUTINEBOUNDP
      COMMONU(9,8001),Y(12,12),W(9,9),F(6,3),G(6,3),H(6,3),Z(12),UU(12),
     1DU(9),V(9),UP(9),A(7),B(7),C(7),D(7),E(7),P(7),PINC,XLI,EM,C1,C2,X
     2ZERO,I,M,S1,DS(9),RR1,RR2
      DIMENSIONHOLD(12)
      XI=I
      X1=XZERO
      T=(XLI+XI)*PINC/C1
      SMUK=2./(EM+1.)
      X3=X1+PINC
      X4=X1+SMUK*PINC
      DO10J=1,9
      W(J,3)=V(J)
   10 W(J,4)=U(J,I)+SMUK*(V(J)-U(J,I))
      WX4A=W(8,4)
      WT4A=W(9,4)
      CONST = 1.373/RR1**2
      CALL GECOFF(1,X1,X3,CONST)
      CALLGECOFG(1,X1,X3)
      CALLGECOFH(1,X1,X4)
      CALLBCTF1(T,R1)
      CALLBCTF2(T,R2)
      CALLBCTF3(T,R3)
      DX13=X1-X3
      DX14=X1-X4
      Y(2,1)=C1*(1.-F(1,1)*DX13/2.)
      Y(2,2)=1.+F(2,1)*DX13**2/2.
      Y(2,3)=-C1*F(3,1)*DX13/2.
      Y(2,4)=F(4,1)*DX13**2/2.
```

```
      Y(2,5)=-C1*F(5,1)*DX13/2.
      Y(2,6)=F(6,1)*DX13**2/2.
      Z(2)=W(3,3)+C1*W(2,3)+C1*DX13*(F(1,1)*W(2,3)+F(2,1)*(W(1,3)+U(1,I)
     1-U(3,I)*DX13/C1)+F(3,1)*W(5,3)+F(4,1)*(W(4,3)+U(4,I)-U(6,I)*DX13/C
     21)+F(5,1)*W(8,3)+F(6,1)*(W(7,3)+U(7,I)-U(9,I)*DX13/C1))/2.
      Y(4,1)=-C1*G(1,1)*DX13/2.
      Y(4,2)=G(2,1)*DX13**2/2.
      Y(4,3)=C1*(1.-G(3,1)*DX13/2.)
      Y(4,4)=1.+G(4,1)*DX13**2/2.
      Y(4,5)=-C1*G(5,1)*DX13/2.
      Y(4,6)=G(6,1)*DX13**2/2.
      Z(4)=W(6,3)+C1*W(5,3)+C1*DX13*(G(1,1)*W(2,3)+G(2,1)*(W(1,3)+U(1,I)
     1-U(3,I)*DX13/C1)+G(3,1)*W(5,3)+G(4,1)*(W(4,3)+U(4,I)-U(6,I)*DX13/C
     21)+G(5,1)*W(8,3)+G(6,1)*(W(7,3)+U(7,I)-U(9,I)*DX13/C1))/2.
      DT=-2.*DX13/C1
      Y(5,1)=-C2*H(1,1)*DX14/2.
      Y(5,2)=-C2*H(2,1)*DT*DX14/4.
      Y(5,3)=-C2*H(3,1)*DX14/2.
      Y(5,4)=-C2*H(4,1)*DT*DX14/4.
      Y(5,5)=C2*(1.-H(5,1)*DX14/2.)
      Y(5,6)=1.-C2*H(6,1)*DT*DX 14/4.
      Z(5)=W(9,4)+C2*W(8,4)+C2*DX14*(H(1,1)*W(2,4)+H(2,1)*(W(1,4)+U(1,I)
     1+U(3,I)*DT/2.)+H(3,1)*W(5,4)+H(4,1)*(W(4,4)+U(4,I)+U(6,I)*DT/2.)+H
     2(5,1)*W(8,4)+H(6,1)*(W(7,4)+U(7,I)+U(9,I)*DT/2.))/2.
      Y(1,1)=A(1)
      Y(1,2)=A(7)+A(2)*DT/2.
      Y(1,3)=A(3)
      Y(1,4)=A(4)*DT/2.
      Y(1,5)=A(5)
      Y(1,6)=A(6)*DT/2.
      Z(1)=R1-A(2)*(U(1,I)+U(3,I)*DT/2.)-A(4)*(U(4,I)+U(6,I)*DT/2.)-A(6)
     1*(U(7,I)+U(9,I)*DT/2.)
      Y(3,1)=B(1)
      Y(3,2)=B(2)*DT/2.
      Y(3,3)=B(3)
      Y(3,4)=B(7)+B(4)*DT/2.
      Y(3,5) = B(5)
      Y(3,6)=B(6)*DT/2.
      Z(3)=R2-B(2)*(U(1,I)+U(3,I)*DT/2.)-B(4)*(U(4,I)+U(6,I)*DT/2.)-B(6)
     1*(U(7,I)+U(9,I)*DT/2.)
      Y(6,1)=C(1)
      Y(6,2)=C(2)*DT/2.
      Y(6,3)=C(3)
      Y(6,4)=C(4)*DT/2.
      Y(6,5)=C(5)
      Y(6,6)=C(7)+C(6)*DT/2.
      Z(6)=R3-C(2)*(U(1,I)+U(3,I)*DT/2.)-C(4)*(U(4,I)+U(6,I)*DT/2.)-C(6)
     1*(U(7,I)+U(9,I)*DT/2.)
      IF(Y(1,1))1,2,1
    2 DO3J=1,6
      HOLD(J)=Y(1,J)
      Y(1,J)=Y(2,J)
    3 Y(2,J)=HOLD(J)
      CEEP=Z(1)
      Z(1)=Z(2)
      Z(2)=CEEP
    1 IF(Y(3,3))4,5,4
    5 DO6J=1,6
      HOLD(J)=Y(3,J)
```

```
      Y(3,J)=Y(4,J)
    6 Y(4,J)=HOLD(J)
      CEEP=Z(3)
      Z(3)=Z(4)
      Z(4)=CEEP
    4 IF(Y(6,6))99,8,99
    8 DO9J=1,6
      HOLD(J)=Y(6,J)
      Y(6,J)=Y(5,J)
    9 Y(5,J)=HOLD(J)
      CEEP=Z(6)
      Z(6)=Z(5)
      Z(5)=CEEP
   99 CALLMASUB
      DO11J=1,3
      V(3*J-1)=UU(2*J-1)
   11 V(3*J)=UU(2*J)
      V(1)=U(1,I)+(U(3,I)+V(3))*DT/2.
      V(4)=U(4,I)+(U(6,I)+V(6))*DT/2.
      V(7)=U(7,I)+(U(9,I)+V(9))*DT/2.
      DO12J=1,9
      U(J,I)=W(J,3)
   12 U(J,I+1)=V(J)
      CALLPRINTO(X1,T,V(1),V(2),V(3),V(4),V(5),V(6),V(7),V(8),V(9),XLI,
 9999 RETURN
      END
 ORDINARY POINT SUBROUTINE
      SUBROUTINEORDINP
      COMMONU(9,8001),Y(12,12),W(9,9),F(6,3),G(6,3),H(6,3),Z(12),UU(12),
     1DU(9),V(9),UP(9),A(7),B(7),C(7),D(7),E(7),P(7),PINC,XLI,EM,C1,C2,X
     2ZERO,I,M,S1,DS(9),R1,R2
      XI=I
      X1=XZERO+(XLI-XI)*PINC
      T=(XLI+XI)*PINC/C1
      SMUK=2./(EM+1.)
      X3=X1+PINC
      X9=X1-PINC
      X4=X1+SMUK*PINC
      X6=X1-SMUK*PINC
      DO1J=1,9
      W(J,3)=V(J)
      IF(ABS(X9-S1)-0.1E-04)27,27,26
   26 W(J,9)=U(J,I+1)
      W(J,6)=U(J,I)+SMUK*(U(J,I+1)-U(J,I))
      GOTO 28
   27 W(J,9)=DS(J)
      W(J,6) = U(J,I)+SMUK*(DS(J)-U(J,I))
   28 W(J,4)=U(J,I)+SMUK*(V(J)-U(J,I))
    1 U(J,I)=V(J)
      WX4A=W(8,4)
      WT4A=W(9,4)
      CONST = 1.373/R1**2
      IF(X1.GT.S1)CONST = 1.373/R2**2
      CALLGECOFF(1,X1,X3,CONST)
      CALLGECOFF(2,X1,X9,CONST)
      CALLGECOFG(1,X1,X3)
      CALLGECOFG(2,X1,X9)
      CALLGECOFH(1,X1,X4)
      CALLGECOFH(2,X1,X6)
```

```
      DX13=X1-X3
      DX14=X1-X4
      DX19=X1-X9
      DX16=X1-X6
      CALLSOLMAT(WX4A,WT4A,DX13,DX14,DX19,DX16)
      CALLMASUB
   99 DO2J=1,3
      V(3*J-1)=UU(2*J-1)
    2 V(3*J)=UU(2*J)
      V(1)=W(1,3)+(W(2,3)+V(2)-(W(3,3)+V(3))/C1)*DX13/2.
      V(4)=W(4,3)+(W(5,3)+V(5)-(W(6,3)+V(6))/C1)*DX13/2.
      V(7)=W(7,4)+(W(8,4)+V(8)-(W(9,4)+V(9))/C2)*DX14/2.
      CALLPRINTO(X1,T,V(1),V(2),V(3),V(4),V(5),V(6),V(7),V(8),V(9),XLI)
  290 I=I+1
 9999 RETURN
      END
C BEAM END POINT SUBROUTINTE
      SUBROUTINE ENDP(ELBEAM)
      COMMONU(9,8001),Y(12,12),W(9,9),F(6,3),G(6,3),H(6,3),Z(12),UU(12),
     1DU(9),V(9),UP(9),A(7),B(7),C(7),D(7),E(7),P(7),PINC,XLI,EM,C1,C2,X
     2ZERO,I,M,S1,DS(9),RR1,RR2
      DIMENSIONHOLD(12)
      I = XLI - (ELBEAM/PINC)
      XI = I
      X1 = ELBEAM
      T = (2*XLI-(ELBEAM/PINC))*PINC/C1
      SMUK=2./(EM+1.)
      X3 = X1-PINC
      X4 = X1-SMUK*PINC
      DO 10 J = 1,9
      W(J,3)=U(J,I+1)
   10 W(J,4)=U(J,I)+SMUK*(U(J,I+1)-U(J,I))
      WX4A = W(8,4)
      WT4A = W(9,4)
      CONST = 1.373/RR2**2
      CALL GECOFF(1,X1,X3,CONST)
      CALL GECOFG(1,X1,X3)
      CALL GECOFH(1,X1,X4)
      CALL BCTN1(T,R1)
      CALL BCTN2(T,R2)
      CALL BCTN3(T,R3)
      DX13 = X1-X3
      DX14 = X1-X4
      Y(2,1) = C1*(-1.+F(1,1)*DX13/2.)
      Y(2,2) = 1.-F(2,1)*DX13**2/2.
      Y(2,3) = C1*F(3,1)*DX13/2.
      Y(2,4) = -F(4,1)*DX13**2/2.
      Y(2,5) = C1*F(5,1)*DX13/2.
      Y(2,6) = -F(6,1)*DX13**2/2.
      Z(2) = W(3,3)-C1*W(2,3)-(C1*DX13/2.)*(F(1,1)*W(2,3)+F(2,1)*(W(1,3)
     1+U(1,I)-U(3,I)*DX13/C1)+F(3,1)*W(5,3)+F(4,1)*(W(4,3)+U(4,I)-U(6,I)
     2*DX13/C1)+F(5,1)*W(8,3)+F(6,1)*(W(7,3)+U(7,I)-U(9,I)*DX13/C1))
      Y(4,1) = C1*G(1,1)*DX13/2.
      Y(4,2) = -G(2,1)*DX13**2/2.
      Y(4,3) = C1*(-1.+G(3,1)*DX13/2.)
      Y(4,4) = 1.-G(4,1)*DX13/2.
      Y(4,5) = C1*G(5,1)*DX13/2.
      Y(4,6) = -G(6,1)*DX13**2/2.
```

```
      Z(4) = W(6,3)-C1*W(5,3)-(C1*DX13/2.)*(G(1,1)*W(2,3)+G(2,1)*(W(1,3)
     1+U(1,I)-U(3,I)*DX13/C1)+G(3,1)*W(5,3)+G(4,1)*(W(4,3)+U(4,I)-U(6,I)
     2*DX13/C1)+G(5,1)*W(8,3)+G(6,1)*(W(7,3)+U(7,I)-U(9,I)*DX13/C1))
      DT = 2.*DX13/C1
      Y(5,1) = C2*H(1,1)*DX14/2.
      Y(5,2) = C2*H(2,1)*DT*DX14/4.
      Y(5,3) = C2*H(3,1)*DX14/2.
      Y(5,4) = C2*H(4,1)*DT*DX14/4.
      Y(5,5) = C2*(-1.+H(5,1)*DX14/2.)
      Y(5,6) = 1.+C2*H(6,1)*DT*DX14/4.
      Z(5) = W(9,4)-C2*W(8,4)-(C2*DX14/2.)*(H(1,1)*W(2,4)+H(2,1)*(W(1,4)
     1+U(1,I)+U(3,I)*DT/2.)+H(3,1)*W(5,4)+H(4,1)*(W(4,4)+U(4,I)+U(6,I)*D
     2T/2.)+H(5,1)*W(8,4)+H(6,1)*(W(7,4)+U(7,I)+U(9,I)*DT/2.))
      Y(1,1) = D(1)
      Y(1,2) = D(7)+D(2)*DT/2.
      Y(1,3) = D(3)
      Y(1,4) = D(4)*DT/2.
      Y(1,5) = D(5)
      Y(1,6) = D(6)*DT/2.
      Z(1) = R1-D(2)*(U(1,I)+U(3,I)*DT/2.)-D(4)*(U(4,I)+U(6,I)*DT/2.)-D(
     16)*(U(7,I)+U(9,I)*DT/2.)
      Y(3,1) = E(1)
      Y(3,2) = E(2)*DT/2.
      Y(3,3) = E(3)
      Y(3,4) = E(7)+E(4)*DT/2.
      Y(3,5) = E(5)
      Y(3,6) = E(6)*DT/2.
      Z(3) = R2-E(2)*(U(1,I)+U(3,I)*DT/2.)-E(4)*(U(4,I)+U(6,I)*DT/2.)-E(
     16)*(U(7,I)+U(9,I)*DT/2.)
      Y(6,1) = P(1)
      Y(6,2) = P(2)*DT/2.
      Y(6,3) = P(3)
      Y(6,4) = P(4)*DT/2.
      Y(6,5) = P(5)
      Y(6,6) = P(7)+P(6)*DT/2.
      Z(6) = R3-P(2)*(U(1,I)+U(3,I)*DT/2.)-P(4)*(U(4,I)+U(6,I)*DT/2.)-P(
     16)*(U(7,I)+U(9,I)*DT/2.)
      IF(Y(1,1))1,2,1
    2 DO3 J = 1,6
      HOLD(J) = Y(1,J)
      Y(1,J) = Y(2,J)
    3 Y(2,J) = HOLD(J)
      CEEP = Z(1)
      Z(1) = Z(2)
      Z(2) = CEEP
    1 IF(Y(3,3))4,5,4
    5 DO6 J = 1,6
      HOLD(J) = Y(3,J)
      Y(3,J) = Y(4,J)
    6 Y(4,J) = HOLD(J)
      CEEP = Z(3)
      Z(3) = Z(4)
      Z(4) = CEEP
    4 IF(Y(6,6))99,8,99
    8 DO9 J = 1,6
      HOLD(J) = Y(6,J)
      Y(6,J) = Y(5,J)
    9 Y(5,J) = HOLD(J)
      CEEP = Z(6)
```

```
      Z(6) = Z(5)
      Z(5) = CEEP
   99 CALLMASUB
      DO11 J = 1,3
      V(3*J-1) = UU(2*J-1)
   11 V(3*J) = UU(2*J)
      V(1) = U(1,I)+(U(3,I)+V(3))*DT/2.
      V(4) = U(4,I)+(U(6,I)+V(6))*DT/2.
      V(7) = U(7,I)+(U(9,I)+V(9))*DT/2.
      CALLPRINTO(X1,T,V(1),V(2),V(3),V(4),V(5),V(6),V(7),V(8),V(9),XLI)
  295 I = I+1
 9999 RETURN
      END
      SUBROUTINECASE1P
      COMMONU(9,8001),Y(12,12),W(9,9),F(6,3),G(6,3),H(6,3),Z(12),UU(12),
     1DU(9),V(9),UP(9),A(7),B(7),C(7),D(7),E(7),P(7),PINC,XLI,EM,C1,C2,X
     2ZERO,I,M,S1,DS(9),R1,R2
      XI=I
      T=(XLI+XI)*PINC/C1
      X1=XZERO+(2.*PINC*XLI)/(EM+1.)
      X9=X1-PINC
      X3=XZERO+(XLI-XI+1.)*PINC
      X4=XZERO+(4.*PINC*EM*XLI)/(EM+1.)**2-(2.*PINC*(XI-1.))/(EM+1.)
      X6=X1-2.*PINC/(EM+1.)
      SMUK9=(1.-2./(EM+1.))/(2.*(XLI-1.)/(EM+1.)-(XLI-XI-1.))
      SMUK4=(XLI-XI+1.)-(4.*EM*XLI/(EM+1.)**2)+(2.*(XI-1.)/(EM+1.))
      DO1J=1,9
      W(J,3)=V(J)
      IF(ABS((XLI-XI)*PINC-(S1+PINC))-0.1E-04)37,37,36
   36 W(J,9) = UP(J)+SMUK9*(U(J,I+1)-UP(J))
      GOTO 38
   37 W(J,9) = UP(J)+SMUK9*(DS(J)-UP(J))
   38 W(J,4) = V(J)+SMUK4*(U(J,I)-V(J))
      W(J,6)=UP(J)
    1 U(J,I)=V(J)
      CALLJUMPII(X1,DU(8),DU(9))
      W(8,3)=W(8,3)-DU(8)
      WX4A=W(8,4)+DU(8)
      WT4A=W(9,4)+DU(9)
      W(8,4)=W(8,4)-DU(8)
      W(9,4)=W(9,4)-DU(9)
      CONST = 1.373/R1**2
      IF(X1.GT.S1)CONST = 1.373/R2**2
      CALL GECOFF(1,X1,X3,CONST)
      CALL GECOFF(2,X1,X9,CONST)
      CALLGECOFG(1,X1,X3)
      CALLGECOFG(2,X1,X9)
      CALLGECOFH(1,X1,X4)
      CALLGECOFH(2,X1,X6)
      DX13=X1-X3
      DX14=X1-X4
      DX19=X1-X9
      DX16=X1-X6
      CALLSOLMAT(WX4A,WT4A,DX13,DX14,DX19,DX16)
      CALLMASUB
   99 DO2J=1,3
      W(3*J-1,3)=UU(2*J-1)
    2 W(3*J,3)=UU(2*J)
      W(1,3)=V(1)+(V(2)+W(2,3)-(V(3)+W(3,3))/C1)*DX13/2.
```

```
      W(4,3)=V(4)+(V(5)+W(5,3)-(V(6)+W(6,3))/C1)*DX13/2.
      W(7,3)=W(7,4)+(W(8,4)+W(8,3)-(W(9,4)+W(9,3))/C2)*DX14/2.
      X3=X1
      X1=XZERO+(XLI-XI)*PINC
      X9=X1-PINC
      X4=XZERO+(PINC/(EM+1.))*(XLI+XI+EM*(XLI-XI)-2.*EM*XLI/(EM+1.)+2.*X
     1LI/(EM+1.))
      X6 = XZERO+(PINC*(XLI-XI-2.)+EM*PINC*(XLI-XI))/(EM+1.)
      SMUK4=(2.*XLI*(EM-1.)/(EM+1.)**2)-(XLI-XI)*(EM-1.)/(EM+1.)
      SMUK6 = ((XLI-XI-2.+EM*(XLI-XI))/(EM+1.)-(XLI-XI-1.))/(2.*(XLI-1.)
     1/(EM+1.)-(XLI-XI-1.))
      DO3J=1,9
      W(J,4)=W(J,3)+SMUK4*(W(J,9)-W(J,3))
      UP(J)=W(J,3)
      IF(ABS(X9-S1)-0.1E-04)27,27,26
   26 W(J,9)=U(J,I+1)
      GOTO 3
   27 W(J,9)=DS(J)
    3 W(J,6)=W(J,9)+SMUK6*(W(J,6)-W(J,9))
      WX4A=W(8,4)
      WT4A=W(9,4)
      CONST = 1.373/R1**2
      IF(X1.GT.S1)CONST = 1.373/R2**2
      CALLGECOFF(1,X1,X3,CONST)
      CALLGECOFF(2,X1,X9,CONST)
      CALLGECOFG(1,X1,X3)
      CALLGECOFG(2,X1,X9)
      CALLGECOFH(1,X1,X4)
      CALLGECOFH(2,X1,X6)
      DX13=X1-X3
      DX14=X1-X4
      DX19=X1-X9
      DX16=X1-X6
      CALLSOLMAT(WX4A,WT4A,DX13,DX14,DX19,DX16)
      CALLMASUB
   98 DO4J=1,3
      V(3*J-1)=UU(2*J-1)
    4 V(3*J)=UU(2*J)
      V(1)=W(1,3)+(W(2,3)+V(2)-(W(3,3)+V(3))/C1)*DX13/2.
      V(4)=W(4,3)+(W(5,3)+V(5)-(W(6,3)+V(6))/C1)*DX13/2.
      V(7)=W(7,4)+(W(8,4)+V(8)-(W(9,4)+V(9))/C2)*DX14/2.
      CALLPRINTO(X1,T,V(1),V(2),V(3),V(4),V(5),V(6),V(7),V(8),V(9),XLI)
  290 I=I+1
 9999 RETURN
      END
C CASE II POINT SUBROUTINE
      SUBROUTINECASE32
      COMMONU(9,8001),Y(12,12),W(9,9),F(6,3),G(6,3),H(6,3),Z(12),UU(12),
     1DU(9),V(9),UP(9),A(7),B(7),C(7),D(7),E(7),P(7),PINC,XLI,EM,C1,C2,X
     2ZERO,I,M,S1,DS(9),R1,R2
      XI=I
      T=(XLI+XI)*PINC/C1
      X1=XZERO+(2.*PINC*XI)/(EM-1.)
      X3=X1+PINC
      X9=XZERO+(XLI-XI-1.)*PINC
      X6=XZERO+2.*PINC*(XLI-1.)/(EM+1.)
      DO1J=1,7
    1 W(J,6)=UP(J)
      W(8,6)=UP(8)-DU(8)
```

```
    W(9,6)=UP(9)-DU(9)
    SMUK4=XLI-XI+1.-(4.*EM*XI)/((EM+1.)*(EM-1.))+(2.*(XI-1.)/(EM+1.))
    IF(SMUK4-1.)302,302,306
302 X4=XZERO+(4.*EM*PINC*XI)/((EM+1.)*(EM-1.))-2.*PINC*(XI-1.)/(EM+1.)
    DO2J=1,9
  2 W(J,4)=V(J)+SMUK4*(U(J,I)-V(J))
    GOTO 308
306 X4=XZERO+(4.*EM*PINC*XI/(EM-1.)**2)-(2.*PINC*(XLI-1.)/(EM-1.))
    SMUK4=(XLI-XI-4.*EM*XI/(EM-1.)**2+2.*(XLI-1.)/(EM-1.))/(XLI-XI-2.*
   1(XLI-1.)/(EM+1.))
    DO3J=1,9
  3 W(J,4)=U(J,I)+SMUK4*(W(J,6)-U(J,I))
308 SMUK3=XLI-(XI*(EM+1.)/(EM-1.))
    DO4J=1,9
    IF(ABS(X9-S1)-0.1E-04)27,27,26
 26 W(J,9) = U(J,I+1)
    GOTO 4
 27 W(J,9) = DS(J)
  4 W(J,3) = V(J)+SMUK3*(U(J,I)-V(J))
    CALLJUMPII(X1,DU(8),DU(9))
    W(8,9)=W(8,9)+DU(8)
    WX4A=W(8,4)
    WT4A=W(9,4)
    CONST = 1.373/R1**2
    IF(X1.GT.S1)CONST = 1.373/R2**2
    CALL GECOFF(1,X1,X3,CONST)
    CALL GECOFF(2,X1,X9,CONST)
    CALLGECOFG(1,X1,X3)
    CALLGECOFG(2,X1,X9)
    CALLGECOFH(1,X1,X4)
    CALLGECOFH(2,X1,X6)
    DX13=X1-X3
    DX14=X1-X4
    DX19=X1-X9
    DX16=X1-X6
    CALLSOLMAT(WX4A,WT4A,DX13,DX14,DX19,DX16)
    CALLMASUB
 99 DO5J=1,3
    W(3*J-1,9)=UU(2*J-1)
  5 W(3*J,9)=UU(2*J)
    W(1,9)=W(1,3)+(W(2,3)+W(2,9)-(W(3,3)+W(3,9))/C1)*DX13/2.
    W(4,9)=W(4,3)+(W(5,3)+W(5,9)-(W(6,3)+W(6,9))/C1)*DX13/2.
    W(7,9)=W(7,4)+(W(8,4)+W(8,9)-(W(9,4)+W(9,9))/C2)*DX14/2.
    X9=X1
    X1=XZERO+(XLI-XI)*PINC
    X3=X1+PINC
    X4=X1+2.*PINC/(EM+1.)
    X6=X1-2.*PINC/(EM+1.)
    SMUK6=(XLI-XI-(XLI-XI-2.+EM*(XLI-XI))/(EM+1.))/(XLI-XI-2.*(XLI-1.)
   1/(EM+1.))
    SMUK4=(EM-1.)/(EM+1.)
    DO7J=1,9
    W(J,3)=V(J)
    W(J,6)=U(J,I)+SMUK6*(W(J,6)-U(J,I))
    W(J,4)=V(J)+SMUK4*(U(J,I)-V(J))
  7 U(J,I)=V(J)
    WX4A=W(8,4)
    WT4A=W(9,4)
    CONST = 1.373/R1**2
```

```
      IF(X1.GT.S1)CONST = 1.373/R2**2
      CALL GECOFF(1,X1,X3,CONST)
      CALL GECOFF(2,X1,X9,CONST)
      CALLGECOFG(1,X1,X3)
      CALLGECOFG(2,X1,X9)
      CALLGECOFH(1,X1,X4)
      CALLGECOFH(2,X1,X6)
      DX13=X1-X3
      DX14=X1-X4
      DX19=X1-X9
      DX16=X1-X6
      CALLSOLMAT(WX4A,WT4A,DX13,DX14,DX19,DX16)
      CALLMASUB
   98 DO8J=1,3
      V(3*J-1)=UU(2*J-1)
    8 V(3*J)=UU(2*J)
      V(1)=W(1,3)+(W(2,3)+V(2)-(W(3,3)+V(3))/C1)*DX13/2.
      V(4)=W(4,3)+(W(5,3)+V(5)-(W(6,3)+V(6))/C1)*DX13/2.
      V(7)=W(7,4)+(W(8,4)+V(8)-(W(9,4)+V(9))/C2)*DX14/2.
      CALLPRINTO(X1,T,V(1),V(2),V(3),V(4),V(5),V(6),V(7),V(8),V(9),XLI)
  290 I=I+1
      XI=I
      T=(XLI+XI)*PINC/C1
      X1=XZERO+(2.*PINC*XLI)/(EM+1.)
      X9=X1-PINC
      X3=XZERO+(XLI-XI+1.)*PINC
      X4=XZERO+(4.*PINC*EM*XLI)/(EM+1.)**2-(2.*PINC*(XI-1.))/(EM+1.)
      X6=XZERO+(2.*PINC*(XI-1.))/(EM-1.)
      DO9J=1,7
    9 W(J,6)=W(J,9)
      W(8,6)=W(8,9)+DU(8)
      W(9,6)=W(9,9)+DU(9)
      SMUK9=XLI-XI+1.-2.*XLI/(EM+1.)
      SMUK4=((XLI-XI+1.)-(4.*EM*XLI/(EM+1.)**2)+(2.*(XI-1.)/(EM+1.)))/(X
     1LI-XI+1.-(2.*(XI-1.)/(EM-1.)))
      DO10J=1,9
      W(J,4)=V(J)+SMUK4*(W(J,9)-V(J))
      IF(ABS((XLI-XI)*PINC-(S1+PINC))-0.1E-04)37,37,36
   36 W(J,9) = U(J,I)+SMUK9*(U(J,I+1)-U(J,I))
      GOTO 10
   37 W(J,9) = U(J,I)+SMUK9*(DS(J)-U(J,I))
   10 W(J,3) = V(J)
      CALLJUMPII(X1,DU(8),DU(9))
      W(8,3)=W(8,3)-DU(8)
      WX4A=W(8,4)+DU(8)
      WT4A=W(9,4)+DU(9)
      W(8,4)=W(8,4)-DU(8)
      W(9,4)=W(9,4)-DU(9)
      CONST = 1.373/R1**2
      IF(X1.GT.S1)CONST = 1.373/R2**2
      CALL GECOFF(1,X1,X3,CONST)
      CALL GECOFF(2,X1,X9,CONST)
      CALLGECOFG(1,X1,X3)
      CALLGECOFG(2,X1,X9)
      CALLGECOFH(1,X1,X4)
      CALLGECOFH(2,X1,X6)
      DX13=X1-X3
      DX14=X1-X4
      DX19=X1-X9
```

```
      DX16=X1-X6
      CALLSOLMAT(WX4A,WT4A,DX13,DX14,DX19,DX16)
      CALLMASUB
   97 DO11J=1,3
      W(3*J-1,3)=UU(2*J-1)
   11 W(3*J,3)=UU(2*J)
      W(1,3)=V(1)+(V(2)+W(2,3)-(V(3)+W(3,3))/C1)*DX13/2.
      W(4,3)=V(4)+(V(5)+W(5,3)-(V(6)+W(6,3))/C1)*DX13/2.
      W(7,3)=W(7,4)+(W(8,4)+W(8,3)-(W(9,4)+W(9,3))/C2)*DX14/2.
      X3=X1
      X1=XZERO+(XLI-XI)*PINC
      X9=X1-PINC
      X6=X1-2.*PINC/(EM+1.)
      X4=XZERO+(PINC/(EM+1.))*(XLI+XI+EM*(XLI-XI)-2.*EM*XLI/(EM+1.)+2.*X
     1LI/(EM+1.))
      SMUK4=(2.*XLI*(EM-1.)/(EM+1.)**2)-(XLI-XI)*(EM-1.)/(EM+1.)
      SMUK6=(EM-1.)/(EM+1.)
      DO12J=1,9
      UP(J)=W(J,3)
      W(J,4)=W(J,3)+SMUK4*(W(J,9)-W(J,3))
      IF(ABS(X9-S1)-0.1E-04)30,30,29
   29 W(J,9) = U(J,I+1)
      GOTO 31
   30 W(J,9) = DS(J)
   31 W(J,6) = W(J,9)+SMUK6*(U(J,I)-W(J,9))
   12 U(J,I) = V(J)
      WX4A=W(8,4)
      WT4A=W(9,4)
      CONST = 1.373/R1**2
      IF(X1.GT.S1)CONST = 1.373/R2**2
      CALL GECOFF(1,X1,X3,CONST)
      CALL GECOFF(2,X1,X9,CONST)
      CALLGECOFG(1,X1,X3)
      CALLGECOFG(2,X1,X9)
      CALLGECOFH(1,X1,X4)
      CALLGECOFH(2,X1,X6)
      DX13=X1-X3
      DX14=X1-X4
      DX19=X1-X9
      DX16=X1-X6
      CALLSOLMAT(WX4A,WT4A,DX13,DX14,DX19,DX16)
      CALLMASUB
   96 DO13J=1,3
      V(3*J-1)=UU(2*J-1)
   13 V(3*J)=UU(2*J)
      V(1)=W(1,3)+(W(2,3)+V(2)-(W(3,3)+V(3))/C1)*DX13/2.
      V(4)=W(4,3)+(W(5,3)+V(5)-(W(6,3)+V(6))/C1)*DX13/2.
      V(7)=W(7,4)+(W(8,4)+V(8)-(W(9,4)+V(9))/C2)*DX14/2.
      CALLPRINTO(X1,T,V(1),V(2),V(3),V(4),V(5),V(6),V(7),V(8),V(9),XLI)
  293 I=I+1
 9999 RETURN
      END
      SUBROUTINE DISCONT
      COMMONU(9,8001),Y(12,12),W(9,9),F(6,3),G(6,3),H(6,3),Z(12),UU(12),
     1DU(9),V(9),UP(9),A(7),B(7),C(7),D(7),E(7),P(7),PINC,XLI,EM,C1,C2,X
     2ZERO,I,M,S1,DS(9),R1,R2
      XI=I
      X1=XZERO+(XLI-XI)*PINC
      T=(XLI+XI)*PINC/C1
```

```
      SMUK=2./(EM+1.)
      X2 = X1
      X3=X1+PINC
      X9=X1-PINC
      X4=X1+SMUK*PINC
      X6=X1-SMUK*PINC
      DO 17 J = 1,9
      W(J,3) = V(J)
      W(J,9) = U(J,I+1)
      IF(ABS(T-((S1+2.*PINC)/C1)).GT.0.1E-09)GOTO15
      W(J,4)=U(J,I)+SMUK*(V(J)-U(J,I))
      GOTO 16
   15 W(J,4) = DS(J)+SMUK*(V(J)-DS(J))
   16 W(J,6) = U(J,I)+SMUK*(U(J,I+1)-U(J,I))
   17 U(J,I) = V(J)
      WX4A=W(8,4)
      WT4A=W(9,4)
      CONST = 1.373/R2**2
      CALLGECOF F(1,X2,X3,CONST)
      CONST = 1.373/R1**2
      CALL GECOFF(2,X1,X9,CONST)
      CALLGECOF G(1,X2,X3)
      CALLGECOFG(2,X1,X9)
      CALLGECOF H(1,X2,X4)
      CALLGECOFH(2,X1,X6)
      DX13=X1-X3
      DX14=X1-X4
      DX19=X1-X9
      DX16=X1-X6
      CON1 = (R2/R1)**2
      CON2 = CON1**2
      CALL SCONMAT(WX4A,WT4A,DX13,DX14,DX19,DX16)
      CALLMASUB
      DO20 J = 1,3
      V(3*J-1)=UU(2*J-1)
   20 V(3*J) = UU(2*J)
      V(1)=W(1,9)+(W(2,9)+V(2)+(W(3,9)+V(3))/C1)*DX19/2.
      V(4)=W(4,9)+(W(5,9)+V(5)+(W(6,9)+V(6))/C1)*DX19/2.
      V(7)=W(7,6)+(W(8,6)+V(8)+(W(9,6)+V(9))/C2)*DX16/2.
      DS(2) = V(2)/CON2
      DS(3) = V(3)
      DS(5) = V(5)
      DS(6) = V(6)
      DS(9) = V(9)
      DS(1) = W(1,3)+(W(2,3)+DS(2)-(W(3,3)+DS(3))/C1)*DX13/2.
      DS(4) = W(4,3)+(W(5,3)+DS(5)-(W(6,3)+DS(6))/C1)*DX13/2.
      DS(8) = DS(1)+(V(8)-V(1))/CON1
      DS(7) = W(7,4)+(W(8,4)+DS(8)-(W(9,4)+DS(9))/C2)*DX14/2.
      CALLPRINTO(X1,T,V(1),V(2),V(3),V(4),V(5),V(6),V(7),V(8),V(9),XLI)
      CALL PRINTO(X1,T,DS(1),DS(2),DS(3),DS(4),DS(5),DS(6),DS(7),DS(8),D
     1S(9),XLI)
      I = I+1
      RETURN
      END
      SUBROUTINE DISCON1
      COMMONU(9,8001),Y(12,12),W(9,9),F(6,3),G(6,3),H(6,3),Z(12),UU(12),
     1DU(9),V(9),UP(9),A(7),B(7),C(7),D(7),E(7),P(7),PINC,XLI,EM,C1,C2,X
     2ZERO,I,M,S1,DS(9),R1,R2
      XI=I
```

```
      T=(XLI+XI)*PINC/C1
      X1=XZERO+(2.*PINC*XLI)/(EM+1.)
      X9=X1-PINC
      X3=XZERO+(XLI-XI+1.)*PINC
      X4=XZERO+(4.*PINC*EM*XLI)/(EM+1.)**2-(2.*PINC*(XI-1.))/(EM+1.)
      X6=X1-2.*PINC/(EM+1.)
      SMUK9=(1.-2./(EM+1.))/(2.*(XLI-1.)/(EM+1.)-(XLI-XI-1.))
      SMUK4=(XLI-XI+1.)-(4.*EM*XLI/(EM+1.)**2)+(2.*(XI-1.)/(EM+1.))
      DO1J=1,9
      W(J,3)=V(J)
      W(J,9)=UP(J)+SMUK9*(U(J,I+1)-UP(J))
      W(J,4) = V(J)+SMUK4*(DS(J)-V(J))
      W(J,6)=UP(J)
    1 U(J,I)=V(J)
      CALLJUMPII(X1,DU(8),DU(9))
      W(8,3)=W(8,3)-DU(8)
      WX4A=W(8,4)+DU(8)
      WT4A=W(9,4)+DU(9)
      W(8,4)=W(8,4)-DU(8)
      W(9,4)=W(9,4)-DU(9)
      CONST = 1.373/R2**2
      CALL GECOFF(1,X1,X3,CONST)
      CONST = 1.373/R1**2
      CALL GECOFF(2,X1,X9,CONST)
      CALLGECOFG(1,X1,X3)
      CALLGECOFG(2,X1,X9)
      CALLGECOFH(1,X1,X4)
      CALLGECOFH(2,X1,X6)
      CON1 = (R2/R1)**2
      CON2 = CON1**2
      DX13=X1-X3
      DX14=X1-X4
      DX19=X1-X9
      DX16=X1-X6
      CALL SCONMAT(WX4A,WT4A,DX13,DX14,DX19,DX16)
      CALLMASUB
   99 DO2J=1,3
      W(3*J-1,3)=UU(2*J-1)
    2 W(3*J,3)=UU(2*J)
      W(1,3)=V(1)+(V(2)+W(2,3)-(V(3)+W(3,3))/C1)*DX13/2.
      W(4,3)=V(4)+(V(5)+W(5,3)-(V(6)+W(6,3))/C1)*DX13/2.
      W(7,3)=W(7,4)+(W(8,4)+W(8,3)-(W(9,4)+W(9,3))/C2)*DX14/2.
      X3=X1
      X1=XZERO+(XLI-XI)*PINC
      X9=X1-PINC
      X4=XZERO+(PINC/(EM+1.))*(XLI+XI+EM*(XLI-XI)-2.*EM*XLI/(EM+1.)+2.*X
     1LI/(EM+1.))
      X6 = XZERO+(PINC*(XLI-XI-2.)+EM*PINC*(XLI-XI))/(EM+1.)
      SMUK4=(2.*XLI*(EM-1.)/(EM+1.)**2)-(XLI-XI)*(EM-1.)/(EM+1.)
      SMUK6 = ((XLI-XI-2.+EM*(XLI-XI))/(EM+1.)-(XLI-XI-1.))/(2.*(XLI-1.)
     1/(EM+1.)-(XLI-XI-1.))
      DO3J=1,9
      W(J,4)=W(J,3)+SMUK4*(W(J,9)-W(J,3))
      UP(J)=W(J,3)
      W(J,9)=U(J,I+1)
    3 W(J,6)=W(J,9)+SMUK6*(W(J,6)-W(J,9))
      WX4A=W(8,4)
      WT4A=W(9,4)
      CONST = 1.373/R2**2
```

```
      CALL GECOFF(1,X1,X3,CONST)
      CONST = 1.373/R1**2
      CALL GECOFF(2,X1,X9,CONST)
      CALLGECOFG(1,X1,X3)
      CALLGECOFG(2,X1,X9)
      CALLGECOFH(1,X1,X4)
      CALLGECOFH(2,X1,X6)
      DX13=X1-X3
      DX14=X1-X4
      DX19=X1-X9
      DX16=X1-X6
      CALL SCONMAT(WX4A,WT4A,DX13,DX14,DX19,DX16)
      CALLMASUB
   98 DO4J=1,3
      V(3*J-1)=UU(2*J-1)
    4 V(3*J)=UU(2*J)
      V(1)=W(1,9)+(W(2,9)+V(2)+(W(3,9)+V(3))/C1)*DX19/2.
      V(4)=W(4,9)+(W(5,9)+V(5)+(W(6,9)+V(6))/C1)*DX19/2.
      V(7)=W(7,6)+(W(8,6)+V(8)+(W(9,6)+V(9))/C2)*DX16/2.
      DS(2) = V(2)/CON2
      DS(3) = V(3)
      DS(5) = V(5)
      DS(6) = V(6)
      DS(9) = V(9)
      DS(1) = W(1,3)+(W(2,3)+DS(2)-(W(3,3)+DS(3))/C1)*DX13/2.
      DS(4) = W(4,3)+(W(5,3)+DS(5)-(W(6,3)+DS(6))/C1)*DX13/2.
      DS(8) = DS(1)+(V(8)-V(1))/CON1
      DS(7) = W(7,4)+(W(8,4)+DS(8)-(W(9,4)+DS(9))/C2)*DX14/2.
      CALLPRINTO(X1,T,V(1),V(2),V(3),V(4),V(5),V(6),V(7),V(8),V(9),XLI)
      CALL PRINTO(X1,T,DS(1),DS(2),DS(3),DS(4),DS(5),DS(6),DS(7),DS(8),D
     1S(9),XLI)
  290 I=I+1
 9999 RETURN
      END
      SUBROUTINE DISCON3
      COMMONU(9,8001),Y(12,12),W(9,9),F(6,3),G(6,3),H(6,3),Z(12),UU(12),
     1DU(9),V(9),UP(9),A(7),B(7),C(7),D(7),E(7),P(7),PINC,XLI,EM,C1,C2,X
     2ZERO,I,M,S1,DS(9),R1,R2
      XI=I
      T=(XLI+XI)*PINC/C1
      X1=XZERO+(2.*PINC*XI)/(EM-1.)
      X3=X1+PINC
      X9=XZERO+(XLI-XI-1.)*PINC
      X6=XZERO+2.*PINC*(XLI-1.)/(EM+1.)
      DO1J=1,7
    1 W(J,6)=UP(J)
      W(8,6)=UP(8)-DU(8)
      W(9,6)=UP(9)-DU(9)
      SMUK4=XLI-XI+1.-(4.*EM*XI)/((EM+1.)*(EM-1.))+(2.*(XI-1.)/(EM+1.))
      IF(SMUK4-1.)302,302,306
  302 X4=XZERO+(4.*EM*PINC*XI)/((EM+1.)*(EM-1.))-2 *PINC*(XI-1.)/(EM+1.)
      DO2J=1,9
    2 W(J,4) = V(J)+SMUK4*(U(J,I)-V(J))
      GOTO 308
  306 X4=XZERO+(4.*EM*PINC*XI/(EM-1.)**2)-(2.*PINC*(XLI-1.)/(EM-1.))
      SMUK4=(XLI-XI-4.*EM*XI/(EM-1.)**2+2.*(XLI-1.)/(EM-1.))/(XLI-XI-2.*
     1(XLI-1.)/(EM+1.))
      DO3J=1,9
    3 W(J,4)=U(J,I)+SMUK4*(W(J,6)-U(J,I))
```

```
308 SMUK3=XLI-(XI*(EM+1.)/(EM-1.))
    DO4J=1,9
    W(J,3)=V(J)+SMUK3*(U(J,I)-V(J))
  4 W(J,9) = DS(J)
    CALLJUMPII(X1,DU(8),DU(9))
    W(8,9)=W(8,9)+DU(8)
    WX4A=W(8,4)
    WT4A=W(9,4)
    CONST = 1.373/R2**2
    CALL GECOFF(1,X1,X3,CONST)
    CALL GECOFF(2,X1,X9,CONST)
    CALLGECOFG(1,X1,X3)
    CALLGECOFG(2,X1,X9)
    CALLGECOFH(1,X1,X4)
    CALLGECOFH(2,X1,X6)
    DX13=X1-X3
    DX14=X1-X4
    DX19=X1-X9
    DX16=X1-X6
    CALLSOLMAT(WX4A,WT4A,DX13,DX14,DX19,DX16)
    CALLMASUB
 99 DO 5J = 1,3
    W(3*J-1,9)=UU(2*J-1)
  5 W(3*J,9)=UU(2*J)
    W(1,9)=W(1,3)+(W(2,3)+W(2,9)-(W(3,3)+W(3,9))/C1)*DX13/2.
    W(4,9)=W(4,3)+(W(5,3)+W(5,9)-(W(6,3)+W(6,9))/C1)*DX13/2.
    W(7,9)=W(7,4)+(W(8,4)+W(8,9)-(W(9,4)+W(9,9))/C2)*DX14/2.
    X9=X1
    X1=XZERO+(XLI-XI)*PINC
    X3=X1+PINC
    X4=X1+2.*PINC/(EM+1.)
    X6=X1-2.*PINC/(EM+1.)
    SMUK6=(XLI-XI-(XLI-XI-2.+EM*(XLI-XI))/(EM+1.))/(XLI-XI-2.*(XLI-1.)
   1/(EM+1.))
    SMUK4=(EM-1.)/(EM+1.)
    DO7J=1,9
    W(J,3)=V(J)
    W(J,6)=U(J,I)+SMUK6*(W(J,6)-U(J,I))
    W(J,4) = V(J)+SMUK4*(U(J,I)-V(J))
  7 U(J,I)=V(J)
    WX4A=W(8,4)
    WT4A=W(9,4)
    CONST = 1.373/R2**2
    CALL GECOFF(1,X1,X3,CONST)
    CALL GECOFF(2,X1,X9,CONST)
    CALLGECOFG(1,X1,X3)
    CALLGECOFG(2,X1,X9)
    CALLGECOFH(1,X1,X4)
    CALLGECOFH(2,X1,X6)
    DX13=X1-X3
    DX14=X1-X4
    DX19=X1-X9
    DX16=X1-X6
    CALLSOLMAT(WX4A,WT4A,DX13,DX14,DX19,DX16)
    CALLMASUB
 98 DO8J=1,3
    V(3*J-1)=UU(2*J-1)
  8 V(3*J)=UU(2*J)
    V(1)=W(1,9)+(W(2,9)+V(2)+(W(3,9)+V(3))/C1)*DX19/2.
```

```
      V(4)=W(4,9)+(W(5,9)+V(5)+(W(6,9)+V(6))/C1)*DX19/2.
      V(7)=W(7,6)+(W(8,6)+V(8)+(W(9,6)+V(9))/C2)*DX16/2.
      CALLPRINTO(X1,T,V(1),V(2),V(3),V(4),V(5),V(6),V(7),V(8),V(9),XLI)
  290 I=I+1
      XI=I
      T=(XLI+XI)*PINC/C1
      X1=XZERO+(2.*PINC*XLI)/(EM+1.)
      X9=X1-PINC
      X3=XZERO+(XLI-XI+1.)*PINC
      X4=XZERO+(4.*PINC*EM*XLI)/(EM+1.)**2-(2.*PINC*(XI-1.))/(EM+1.)
      X6=XZERO+(2.*PINC*(XI-1.))/(EM-1.)
      DO9J=1,7
    9 W(J,6)=W(J,9)
      W(8,6)=W(8,9)+DU(8)
      W(9,6)=W(9,9)+DU(9)
      SMUK9=XLI-XI+1.-2.*XLI/(EM+1.)
      SMUK4=((XLI-XI+1.)-(4.*EM*XLI/(EM+1.)**2)+(2.*(XI-1.)/(EM+1.)))/(X
     1LI-XI+1.-(2.*(XI-1.)/(EM-1.)))
      DO10J=1,9
      W(J,3)=V(J)
      W(J,4)=V(J)+SMUK4*(W(J,9)-V(J))
   10 W(J,9)=U(J,I)+SMUK9*(U(J,I+1)-U(J,I))
      CALLJUMPII(X1,DU(8),DU(9))
      W(8,3)=W(8,3)-DU(8)
      WX4A=W(8,4)+DU(8)
      WT4A=W(9,4)+DU(9)
      W(8,4)=W(8,4)-DU(8)
      W(9,4)=W(9,4)-DU(9)
      CONST = 1.373/R2**2
      CALL GECOFF(1,X1,X3,CONST)
      CONST = 1.373/R1**2
      CALL GECOFF(2,X1,X9,CONST)
      CALLGECOFG(1,X1,X3)
      CALLGECOFG(2,X1,X9)
      CALLGECOFH(1,X1,X4)
      CALLGECOFH(2,X1,X6)
      DX13=X1-X3
      DX14=X1-X4
      DX19=X1-X9
      DX16=X1-X6
      CON1 = (R2/R1)**2
      CON2 = CON1**2
      CALL SCONMAT(WX4A,WT4A,DX13,DX14,DX19,DX16)
      CALLMASUB
   97 DO11J=1,3
      W(3*J-1,3)=UU(2*J-1)
   11 W(3*J,3)=UU(2*J)
      W(1,3)=V(1)+(V(2)+W(2,3)-(V(3)+W(3,3))/C1)*DX13/2.
      W(4,3)=V(4)+(V(5)+W(5,3)-(V(6)+W(6,3))/C1)*DX13/2.
      W(7,3)=W(7,4)+(W(8,4)+W(8,3)-(W(9,4)+W(9,3))/C2)*DX14/2.
      X3=X1
      X1=XZERO+(XLI-XI)*PINC
      X9=X1-PINC
      X6=X1-2.*PINC/(EM+1.)
      X4=XZERO+(PINC/(EM+1.))*(XLI+XI+EM*(XLI-XI)-2.*EM*XLI/(EM+1.)+2.*X
     1LI/(EM+1.))
      SMUK4=(2.*XLI*(EM-1.)/(EM+1.)**2)-(XLI-XI)*(EM-1.)/(EM+1.)
      SMUK6=(EM-1.)/(EM+1.)
      DO12J=1,9
```

```
      UP(J)=W(J,3)
      W(J,4)=W(J,3)+SMUK4*(W(J,9)-W(J,3))
      W(J,9)=U(J,I+1)
      W(J,6)=W(J,9)+SMUK6*(U(J,I)-W(J,9))
   12 U(J,I)=V(J)
      WX4A=W(8,4)
      WT4A=W(9,4)
      CONST = 1.373/R2**2
      CALL GECOFF(1,X1,X3,CONST)
      CONST = 1.373/R1**2
      CALL GECOFF(2,X1,X9,CONST)
      CALLGECOFG(1,X1,X3)
      CALLGECOFG(2,X1,X9)
      CALLGECOFH(1,X1,X4)
      CALLGECOFH(2,X1,X6)
      DX13=X1-X3
      DX14=X1-X4
      DX19=X1-X9
      DX16=X1-X6
      CALL SCONMAT(WX4A,WT4A,DX13,DX14,DX19,DX16)
      CALLMASUB
   96 DO13J=1,3
      V(3*J-1)=UU(2*J-1)
   13 V(3*J)=UU(2*J)
      V(1)=W(1,3)+(W(2,3)+V(2)-(W(3,3)+V(3))/C1)*DX13/2.
      V(4)=W(4,3)+(W(5,3)+V(5)-(W(6,3)+V(6))/C1)*DX13/2.
      V(7)=W(7,4)+(W(8,4)+V(8)-(W(9,4)+V(9))/C2)*DX14/2.
      DS(2) = V(2)/CON2
      DS(3) = V(3)
      DS(5) = V(5)
      DS(6) = V(6)
      DS(9) = V(9)
      DS(1) = W(1,3)+(W(2,3)+DS(2)-(W(3,3)+DS(3))/C1)*DX13/2.
      DS(4) = W(4,3)+(W(5,3)+DS(5)-(W(6,3)+DS(6))/C1)*DX13/2.
      DS(8) = DS(1)+(V(8)-V(1))/CON1
      DS(7) = W(7,4)+(W(8,4)+DS(8)-(W(9,4)+DS(9))/C2)*DX14/2.
      CALLPRINTO(X1,T,V(1),V(2),V(3),V(4),V(5),V(6),V(7),V(8),V(9),XLI)
      CALL PRINTO(X1,T,DS(1),DS(2),DS(3),DS(4),DS(5),DS(6),DS(7),DS(8),D
     1S(9),XLI)
  293 I=I+1
 9999 RETURN
      END
C DISCONTINUITY SOLUTION MATRIX SUBROUTINE
      SUBROUTINE SCONMAT(WX4A,WT4A,DX13,DX14,DX19,DX16)
      COMMONU(9,8001),Y(12,12),W(9,9),F(6,3),G(6,3),H(6,3),Z(12),UU(12),
     1DU(9),V(9),UP(9),A(7),B(7),C(7),D(7),E(7),P(7),PINC,XLI,EM,C1,C2,X
     2ZERO,I,M,S1,DS(9),R1,R2
      CON1 = (R2/R1)**2
      CON2 = CON1**2
      Y(1,1)=C1*(-1.+F(1,2)*DX19/2.+F(2,2)*DX19*DX13/4.)
      Y(1,2)=1.-F(2,2)*DX19*DX13/4.
      Y(1,3)=C1*(F(3,2)*DX19/2.+F(4,2)*DX19*DX13/4.)
      Y(1,4)=-F(4,2)*DX19*DX13/4.
      Y(1,5)=C1*(F(5,2)*DX19/2.+F(6,2)*DX19*DX14/4.)
      Y(1,6)=-C1*F(6,2)*DX19*DX14/(4.*C2)
      Z(1)=W(3,9)-C1*W(2,9)-(C1*DX19/2.)*(F(1,2)*W(2,9)+F(2,2)*DX13*(W(2
     1,3)-W(3,3)/C1)/2.+F(2,2)*(W(1,3)+W(1,9))+F(3,2)*W(5,9)+F(4,2)*DX13
     2*(W(5,3)-W(6,3)/C1)/2.+F(4,2)*(W(4,3)+W(4,9))+F(5,2)*W(8,9)+F(6,2)
     3*DX14*(W(8,4)-W(9,4)/C2)/2.+F(6,2)*(W(7,4)+W(7,9)))
```

```
      Y(3,1)=C1*(G(1,2)*DX19/2.+G(2,2)*DX19*DX13/4.)
      Y(3,2)=-G(2,2)*DX19*DX13/4.
      Y(3,3)=C1*(-1.+G(3,2)*DX19/2.+G(4,2)*DX19*DX13/4.)
      Y(3,4)=1.-G(4,2)*DX19*DX13/4.
      Y(3,5)=C1*(G(5,2)*DX19/2.+G(6,2)*DX19*DX14/4.)
      Y(3,6)=-C1*DX19*DX14*G(6,2)/(4.*C2)
      Z(3)=W(6,9)-C1*W(5,9)-(C1*DX19/2.)*(G(1,2)*W(2,9)+G(2,2)*DX13*(W(2
     1,3)-W(3,3)/C1)/2.+G(2,2)*(W(1,3)+W(1,9))+G(3,2)*W(5,9)+G(4,2)*DX13
     2*(W(5,3)-W(6,3)/C1)/2.+G(4,2)*(W(4,3)+W(4,9))+G(5,2)*W(8,9)+G(6,2)
     3*DX14*(W(8,4)-W(9,4)/C2)/2.+G(6,2)*(W(7,4)+W(7,9)))
      Y(6,1)=C2*(H(1,2)*DX16/2.+H(2,2)*DX16*DX13/4.)
      Y(6,2)=-C2*DX16*DX13*H(2,2)/(4.*C1)
      Y(6,3)=C2*(H(3,2)*DX16/2.+H(4,2)*DX16*DX13/4.)
      Y(6,4)=-C2*DX16*DX13*H(4,2)/(4.*C1)
      Y(6,5)=C2*(-1.+H(5,2)*DX16/2.+H(6,2)*DX16*DX14/4.)
      Y(6,6)=1.-H(6,2)*DX16*DX14/4.
      Z(6)=W(9,6)-C2*W(8,6)-(C2*DX16/2.)*(H(1,2)*W(2,6)+H(2,2)*DX13*(W(2
     1,3)-W(3,3)/C1)/2.+H(2,2)*(W(1,3)+W(1,6))+H(3,2)*W(5,6)+H(4,2)*DX13
     2*(W(5,3)-W(6,3)/C1)/2.+H(4,2)*(W(4,3)+W(4,6))+H(5,2)*W(8,6)+H(6,2)
     3*DX14*(W(8,4)-W(9,4)/C2)/2.+H(6,2)*(W(7,4)+W(7,6)))
      Y(2,1) = (C1/CON2)*(1.-F(1,1)*DX13/2.-F(2,1)*DX13**2/(4.*CON1))
      Y(2,2) = 1.+F(2,1)*DX13**2/(4.*CON1)
      Y(2,3)=C1*(-F(3,1)*DX13/2.-F(4,1)*DX13**2/4.)
      Y(2,4)=F(4,1)*DX13**2/4.
      Y(2,5) = (C1/CON1)*(-F(5,1)*DX13/2.-F(6,1)*DX13*DX14/4.)
      Y(2,6)=C1*DX13*DX14*F(6,1)/(4.*C2)
      Z(2)=W(3,3)+C1*W(2,3)+C1*DX13*(F(1,1)*W(2,3)/2.+F(2,1)*DX13*(W(2,3
     1)-W(3,3)/C1)/4.+F(2,1)*W(1,3)/CON1+F(3,1)*W(5,3)/2.+F(4,1)*DX13*(W
     2(5,3)-W(6,3)/C1)/4.+F(4,1)*W(4,3)+F(5,1)*W(8,3)/2.+F(6,1)*DX14*(W(
     38,4)-W(9,4)/C2)/4.+F(6,1)*(W(7,4)+W(7,3))/2.)
      Y(4,1) = (C1/CON2)*(-G(1,1)*DX13/2.-G(2,1)*DX13**2/(4.*CON1))
      Y(4,2) = G(2,1)*DX13**2/(4.*CON1)
      Y(4,3)=C1*(1.-G(3,1)*DX13/2.-G(4,1)*DX13**2/4.)
      Y(4,4)=1.+G(4,1)*DX13**2/4.
      Y(4,5)=C1*(-G(5,1)*DX13/2.-G(6,1)*DX13*DX14/4.)/CON1
      Y(4,6)=C1*DX13*DX14*G(6,1)/(4.*C2)
      Z(4)=W(6,3)+C1*W(5,3)+C1*DX13*(G(1,1)*W(2,3)/2.+G(2,1)*DX13*(W(2,3
     1)-W(3,3)/C1)/4.+G(4,1)*W(1,3)/CON1+G(3,1)*W(5,3)/2.+G(4,1)*DX13*(W
     2(5,3)-W(6,3)/C1)/4.+G(4,1)*W(4,3)+G(5,1)*W(8,3)/2.+G(6,1)*DX14*(W(
     38,4)-W(9,4)/C2)/4.+G(6,1)*(W(7,4)+W(7,3))/2.)
      Y(5,1) = (C2/CON2)*(-H(1,1)*DX14/2.-H(2,1)*DX14*DX13/(4.*CON1))
      Y(5,2) = C2*DX14*DX13*H(2,1)/(4.*C1*CON1)
      Y(5,3)=C2*(-H(3,1)*DX14/2.-H(4,1)*DX14*DX13/4.)
      Y(5,4)=C2*DX14*DX13*H(4,1)/(4.*C1)
      Y(5,5)=C2*(1.-H(5,1)*DX14/2.-H(6,1)*DX14**2/4.)/CON1
      Y(5,6)=1.+H(6,1)*DX14**2/4.
      Z(5)=WT4A+C2*WX4A+C2*DX14*(H(1,1)*W(2,4)/2.+H(2,1)*DX13*(W(2,3)-W(
     13,3)/C1)/4.+H(2,1)*(W(1,3)/CON1+W(1,4))/2.+H(3,1)*W(5,4)/2.+H(4,1)
     2*DX13*(W(5,3)-W(6,3)/C1)/4.+H(4,1)*(W(4,3)+W(4,4))/2.+H(5,1)*W(8,4
     3)/2.+H(6,1)*DX14*(W(8,4)-W(9,4)/C2)/4.+H(6,1)*W(7,4))
      M=6
      RETURN
      END
C SOLUTION MATRIX SUBROUTINE
      SUBROUTINESOLMAT(WX4A,WT4A,DX13,DX14,DX19,DX16)
      COMMONU(9,8001),Y(12,12),W(9,9),F(6,3),G(6,3),H(6,3),Z(12),UU(12),
     1DU(9),V(9),UP(9),A(7),B(7),C(7),D(7),E(7),P(7),PINC,XLI,EM,C1,C2,X
     2ZERO,I,M,S1,DS(9),R1,R2
      Y(1,1)=C1*(-1.+F(1,2)*DX19/2.+F(2,2)*DX19*DX13/4.)
```

```
 Y(1,2)=1.-F(2,2)*DX19*DX13/4.
 Y(1,3)=C1*(F(3,2)*DX19/2.+F(4,2)*DX19*DX13/4.)
 Y(1,4)=-F(4,2)*DX19*DX13/4.
 Y(1,5)=C1*(F(5,2)*DX19/2.+F(6,2)*DX19*DX14/4.)
 Y(1,6)=-C1*F(6,2)*DX19*DX14/(4.*C2)
 Z(1)=W(3,9)-C1*W(2,9)-(C1*DX19/2.)*(F(1,2)*W(2,9)+F(2,2)*DX13*(W(2
1,3)-W(3,3)/C1)/2.+F(2,2)*(W(1,3)+W(1,9))+F(3,2)*W(5,9)+F(4,2)*DX13
2*(W(5,3)-W(6,3)/C1)/2.+F(4,2)*(W(4,3)+W(4,9))+F(5,2)*W(8,9)+F(6,2)
3*DX14*(W(8,4)-W(9,4)/C2)/2.+F(6,2)*(W(7,4)+W(7,9)))
 Y(3,1)=C1*(G(1,2)*DX19/2.+G(2,2)*DX19*DX13/4.)
 Y(3,2)=-G(2,2)*DX19*DX13/4.
 Y(3,3)=C1*(-1.+G(3,2)*DX19/2.+G(4,2)*DX19*DX13/4.)
 Y(3,4)=1.-G(4,2)*DX19*DX13/4.
 Y(3,5)=C1*(G(5,2)*DX19/2.+G(6,2)*DX19*DX14/4.)
 Y(3,6)=-C1*DX19*DX14*G(6,2)/(4.*C2)
 Z(3)=W(6,9)-C1*W(5,9)-(C1*DX19/2.)*(G(1,2)*W(2,9)+G(2,2)*DX13*(W(2
1,3)-W(3,3)/C1)/2.+G(2,2)*(W(1,3)+W(1,9))+G(3,2)*W(5,9)+G(4,2)*DX13
2*(W(5,3)-W(6,3)/C1)/2.+G(4,2)*(W(4,3)+W(4,9))+G(5,2)*W(8,9)+G(6,2)
3*DX14*(W(8,4)-W(9,4)/C2)/2.+G(6,2)*(W(7,4)+W(7,9)))
 Y(6,1)=C2*(H(1,2)*DX16/2.+H(2,2)*DX16*DX13/4.)
 Y(6,2)=-C2*DX16*DX13*H(2,2)/(4.*C1)
 Y(6,3)=C2*(H(3,2)*DX16/2.+H(4,2)*DX16*DX13/4.)
 Y(6,4)=-C2*DX16*DX13*H(4,2)/(4.*C1)
 Y(6,5)=C2*(-1.+H(5,2)*DX16/2.+H(6,2)*DX16*DX14/4.)
 Y(6,6)=1.-H(6,2)*DX16*DX14/4.
 Z(6)=W(9,6)-C2*W(8,6)-(C2*DX16/2.)*(H(1,2)*W(2,6)+H(2,2)*DX13*(W(2
1,3)-W(3,3)/C1)/2.+H(2,2)*(W(1,3)+W(1,6))+H(3,2)*W(5,6)+H(4,2)*DX13
2*(W(5,3)-W(6,3)/C1)/2.+H(4,2)*(W(4,3)+W(4,6))+H(5,2)*W(8,6)+H(6,2)
3*DX14*(W(8,4)-W(9,4)/C2)/2.+H(6,2)*(W(7,4)+W(7,6)))
 Y(2,1)=C1*(1.-F(1,1)*DX13/2.-F(2,1)*DX13**2/4.)
 Y(2,2)=1.+F(2,1)*DX13**2/4.
 Y(2,3)=C1*(-F(3,1)*DX13/2.-F(4,1)*DX13**2/4.)
 Y(2,4)=F(4,1)*DX13**2/4.
 Y(2,5)=C1*(-F(5,1)*DX13/2.-F(6,1)*DX13*DX14/4.)
 Y(2,6)=C1*DX13*DX14*F(6,1)/(4.*C2)
 Z(2)=W(3,3)+C1*W(2,3)+C1*DX13*(F(1,1)*W(2,3)/2.+F(2,1)*DX13*(W(2,3
1)-W(3,3)/C1)/4.+F(2,1)*W(1,3)+F(3,1)*W(5,3)/2.+F(4,1)*DX13*(W(5,3)
2-W(6,3)/C1)/4.+F(4,1)*W(4,3)+F(5,1)*W(8,3)/2.+F(6,1)*DX14*(W(8,4)-
3W(9,4)/C2)/4.+F(6,1)*(W(7,4)+W(7,3))/2.)
 Y(4,1)=C1*(-G(1,1)*DX13/2.-G(2,1)*DX13**2/4.)
 Y(4,2)=G(2,1)*DX13**2/4.
 Y(4,3)=C1*(1.-G(3,1)*DX13/2.-G(4,1)*DX13**2/4.)
 Y(4,4)=1.+G(4,1)*DX13**2/4.
 Y(4,5)=C1*(-G(5,1)*DX13/2.-G(6,1)*DX13*DX14/4.)
 Y(4,6)=C1*DX13*DX14*G(6,1)/(4.*C2)
 Z(4)=W(6,3)+C1*W(5,3)+C1*DX13*(G(1,1)*W(2,3)/2.+G(2,1)*DX13*(W(2,3
1)-W(3,3)/C1)/4.+G(2,1)*W(1,3)+G(3,1)*W(5,3)/2.+G(4,1)*DX13*(W(5,3)
2-W(6,3)/C1)/4.+G(4,1)*W(4,3)+G(5,1)*W(8,3)/2.+G(6,1)*DX14*(W(8,4)-
3W(9,4)/C2)/4.+G(6,1)*(W(7,4)+W(7,3))/2.)
 Y(5,1)=C2*(-H(1,1)*DX14/2.-H(2,1)*DX14*DX13/4.)
 Y(5,2)=C2*DX14*DX13*H(2,1)/(4.*C1)
 Y(5,3)=C2*(-H(3,1)*DX14/2.-H(4,1)*DX14*DX13/4.)
 Y(5,4)=C2*DX14*DX13*H(4,1)/(4.*C1)
 Y(5,5)=C2*(1.-H(5,1)*DX14/2.-H(6,1)*DX14**2/4.)
 Y(5,6)=1.+H(6,1)*DX14**2/4.
 Z(5)=WT4A+C2*WX4A+C2*DX14*(H(1,1)*W(2,4)/2.+H(2,1)*DX13*(W(2,3)-W(
13,3)/C1)/4.+H(2,1)*(W(1,3)+W(1,4))/2.+H(3,1)*W(5,4)/2.+H(4,1)*DX13
2*(W(5,3)-W(6,3)/C1)/4.+H(4,1)*(W(4,3)+W(4,4))/2.+H(5,1)*W(8,4)/2.+
3H(6,1)*DX14*(W(8,4)-W(9,4)/C2)/4.+H(6,1)*W(7,4))
```

```
      M=6
      RETURN
      END
      SUBROUTINE JUMPI(X,DU1X,DU1T,DU2X,DU2T)
      DU1X = 0.
      DU1T = -DU1X*0.5140E+04
      DU2X=0.
      DU2T=0.
      RETURN
      END
      SUBROUTINEJUMPII(X,DU3X,DU3T)
      DU3X = 0.
      DU3T = 0.
      RETURN
      END
      SUBROUTINE GECOF F(ID,XA,XB,CONST)
      COMMON U(9,8001),Y(12,12),W(9,9),F(6,3)
      X = (XA+XB)/2.
      F(1,ID) = 0.
      F(2,ID) = CONST
      F(3,ID) = 0.
      F(4,ID) = 0.
      F(5,ID) = -CONST
      F(6,ID) = 0.
      RETURN
      END
      SUBROUTINE GECOFG(ID,XA,XB)
      COMMON U(9,8001),Y(12,12),W(9,9),F(6,3),G(6,3)
      DO 1 J = 1,6
    1 G(J,ID) = 0.
      RETURN
      END
      SUBROUTINE GECOFH(ID,XA,XB)
      COMMON U(9,8001),Y(12,12),W(9,9),F(6,3),G(6,3),H(6,3)
      X = (XA+XB)/2.
      H(1,ID) = 1.
      DO 1 J = 2,6
    1 H(J,ID) = 0.
      RETURN
      END
      SUBROUTINE BCTF1(T,F1)
      IF(T-0.90E-04)1,1,2
    1 F1 = T*0.1E+03
      GOTO 3
    2 F1 = 0.90E-02
    3 RETURN
      END
      SUBROUTINE BCTF2(T,F2)
      F2 = 0.
      RETURN
      END
      SUBROUTINE BCTF3(T,F3)
      F3 = 0.
      RETURN
      END
      SUBROUTINE BCTN1(T,F1)
      F1 = 0.
      RETURN
      END
```

```
      SUBROUTINE BCTN2(T,F2)
      F2 = 0.
      RETURN
      END
      SUBROUTINE BCTN3(T,F3)
      F3 = 0.
      RETURN
      END
      SUBROUTINEPRINTO(X,T,U1,U1X,U1T,U2,U2X,U2T,U3,U3X,U3T,XLI)
    1 FORMAT(1H ,4HX = ,E15.8,2X,4HT = ,E15.8)
   10 FORMAT(1H ,5HU1 = ,E15.8,2X,6HU1X = ,E15.8,2X,6HU1T = ,E15.8)
   11 FORMAT(1H ,5HU2 = ,E15.8,2X,6HU2X = ,E15.8,2X,6HU2T = ,E15.8)
   12 FORMAT(1H ,5HU3 = ,E15.8,2X,6HU3X = ,E15.8,2X,6HU3T = ,E15.8)
   13 FORMAT(1H ,4HQ = ,E15.8,2X,4HY = ,E15.8)
    2 FORMAT(1H ,4HV = ,E15.8,2X,4HW = ,E15.8,2X,4HS = ,E15.8,/)
      TOL = 0.100E-03
      TTOL = 0.40E-06
      IF(ABS(X-0.)-TOL)8,8,3
    3 IF(ABS(X-0.1)-TOL)8,8,4
    4 IF(ABS(X-0.3)-TOL)8,8,5
    5 IF(ABS(X-0.8)-TOL)8,8,6
    6 IF(ABS(X-1.0)-TOL)8,8,7
    7 IF(ABS(X-1.2)-TOL)8,8,9
    9 IF(ABS(X-1.9)-TOL)8,8,14
    8 TLIM = 0.0
      DO 16 IDO = 1,900
      IF(ABS(T-TLIM)-TTOL)17,17,16
   16 TLIM = TLIM+0.194552E-04
      GOTO 14
   17 WRITE(6,1)X,T
      WRITE(6,10)U1,U1X,U1T
      WRITE(6,11)U2,U2X,U2T
      WRITE(6,12)U3,U3X,U3T
      Q = 5.45*(U3X-U1)
      Y = U3/0.025
      V = X/0.025
      W = 0.5140E+04*T/0.025
      S = -0.025*U1X
   21 FORMAT(1H ,5HVA = ,E15.8,2X,5HWB = ,E15.8)
      VA = U3T/0.5140E+04
      WB = 0.025*U1T/0.5140E+04
      WRITE(6,13)Q,Y
      WRITE(6,21)VA,WB
      WRITE(6,2)V,W,S
      WRITE(8,92)X,T,S
   92 FORMAT(3E12.4)
   14 RETURN
      END
```

INPUT DATA CARDS FOR TMOTCU-3 COMPUTER PROGRAM

card no.	
1	+4000+0.00000000E+00+0.12500000E-02+5.14000000E+03+0.88558000E+00
2	+ 2.0000E+00+ 1.0000E+00+12.7000E-03+ 1.2500E+00
3	-0.10000000E+01+0.00000000E+00+0.00000000E+00+0.00000000E+00+0.00000000E+00
4	+0.00000000E+00+0.00000000E+00
5	+0.00000000E+00+0.00000000E+00+0.00000000E+00+0.10000000E+01+0.00000000E+00
6	+0.00000000E+00+0.00000000E+00
7	+0.00000000E+00-0.10000000E+01+0.00000000E+00+0.00000000E+00+0.10000000E+01
8	+0.00000000E+00+0.00000000E+00
9	-0.10000000E+01+0.00000000E+00+0.00000000E+00+0.00000000E+00+0.00000000E+00
10	+0.00000000E+00+0.00000000E+00
11	+0.00000000E+00+0.00000000E+00+0.00000000E+00+0.10000000E+01+0.00000000E+00
12	+0.00000000E+00+0.00000000E+00
13	+0.00000000E+00-0.10000000E+01+0.00000000E+00+0.00000000E+00+0.10000000E+01
14	+0.00000000E+00+0.00000000E+00

APPENDIX B

Flexural vibration of beams with discontinuity of cross section

The simplest governing differential equation for the lateral vibration of beams that have step changes in the properties of their cross section is based on the Euler-Bernoulli theory and consists of disassembling the structure into sub-beam components of uniform bending stiffness.

$$\frac{\partial^4 y_1}{\partial x_1^4} + \frac{\rho_1 A_1}{E_1 I_1} \frac{\partial^2 y_1}{\partial t^2} = 0$$

$$\frac{\partial^4 y_2}{\partial x_2^4} + \frac{\rho_2 A_2}{E_2 I_2} \frac{\partial^2 y_2}{\partial t^2} = 0 \qquad \text{(B.1)}$$

A solution can be obtained by formulating the displacements of the beam segments of constant cross-sectional properties by individual functions in the form of

$$X_1(x_1) = C_1 \sin\beta_1 x_1 + C_2 \cos \beta_1 x_1 + C_3 \sinh\beta_1 x_1 + C_4 \cosh\beta_1 x_1$$

$$\text{and } X_2(x_2) = C_5 \sin\beta_2 x_2 + C_6 \cos\beta_2 x_2 + C_7 \sinh\beta_2 x_2 + C_8 \cosh\beta_2 x_2 \qquad \text{(B.2)}$$

$$\text{where } y_1 = X_1(x_1).\ T(t) \text{ and } y_2 = X_2(x_2).\ T(t) \qquad \text{(B.3)}$$

$$\text{and } \beta_1^4 = \frac{\rho_1 A_1}{E_1 I_1} \omega^2 \text{ and } \beta_2^4 = \frac{\rho_2 A_2}{E_2 I_2} \omega^2 \qquad \text{(B.4)}$$

The subscripts 1 and 2 refer to the right-hand and left hand segments of the beam shown in figure 4.8.

The frequency equation is found using the proper boundary condition and expanding the determinant, and solutions are obtained numerically for the given values of material properties and dimensions.

To obtain the solution for a free-free beam, the corresponding boundary conditions are applied together with the continuity conditions of displacement, slope, momnet, and shear at the junction of the two parts of the beam, in a similar way to that described in chapter 4 (eqts. 4.6 and 4.7)

$$\partial^2 X_1(\ell_1)/\partial x_1^2 = \partial^3 X_1(\ell_1)/\partial x_1^3 = 0 \qquad (B.5)$$

$$\partial^2 X_2(\ell_2)/\partial x_2^2 = \partial^3 X_2(\ell_2)/\partial x_2^3 = 0 \qquad (B.6)$$

Equations (B.5) and (B.6) satisfy the requirements of zero bending moment and shearing force at both ends of the free-free beam and the continuity conditions at the junctions are formulated as

$$X_1(0) = X_2(0) \qquad (B.7)$$

$$\partial X_1(0)/\partial x_1 = -\partial X_2(0)/\partial x_2 \qquad (B.8)$$

$$E_1 I_1 \partial^2 X_1(0)/\partial x_1^2 = E_2 I_2 \partial^2 X_2(0)/\partial x_2^2 \qquad (B.9)$$

$$E_1 I_1 \partial^3 X_1(0)/\partial x_1^3 = -E_2 I_2 \partial^3 X_3(0)/\partial x_2^3 \qquad (B.10)$$

Substituting the derivatives of equations (B.2) in equations (B.5) and (B.6)

$$\begin{aligned}
&C_1 \sin\beta_1\ell_1 + C_2\cos\beta_1\ell_1 - C_3\sinh\beta_1\ell_1 - C_4\cosh\beta_1\ell_1 = 0\\
&C_1\cos\beta_1\ell_1 - C_2\sin\beta_1\ell_1 - C_3\cosh\beta_1\ell_1 - C_4\sinh\beta_1\ell_1 = 0\\
&C_5\sin\beta_2\ell_2 + C_6\cos\beta_2\ell_2 - C_7\sinh\beta_2\ell_2 - C_8\cosh\beta_2\ell_2 = 0\\
&C_5\cos\beta_2\ell_2 - C_6\sin\beta_2\ell_2 - C_7\cosh\beta_2\ell_2 - C_8\sinh\beta_2\ell_2 = 0
\end{aligned} \qquad (B.11)$$

Further 4 equations for the constants $C_1 \ldots\ldots C_8$ are obtained by substitution of equations (B.2) in equation (B.7) to (B.10).

The eigenvalues are now obtained from the coefficient matrix of the system of equation, as those values that make the determinant of the coefficient matrix vanish.

For the determination of the roots of the frequency equations, the values of E, I, ρ, A for both parts of the beam are to be specified and when the whole beam is made of the same material, one has $E_1 = E_2$ and $\rho_1 = \rho_2$.

The ratio of I/A is to be obtained from the geometry of the beam, and beams of rectangular cross section and rods of circular cross section are of interest.

The flexural vibration of a stepped beam of rectangular cross section is either flatwise or edgewise and the value of I/A is determined for each

section, and for a beam of the same thickness h and different widths b_1 and b_2

i) For flatwise vibration

$$I_1/A_1 = (b_1h^3/12)/b_1h = h^2/12$$

$$I_2/A_2 = (b_2h^3/12)/b_2h = h^2/12$$

and therefore $(I_1/A_1) = I_2/A_2)$

ii) For edgewise vibration

$$I_1/A_1 = (hb_1^3/12)/hb_1 = b_1^2/12$$

$$I_2/A_2 = (hb_2^3/12)/hb_2 = b_2^2/12$$

and therefore (I_1/A_1) is different from (I_2/A_2)

iii) For a stepped beam of circular cross section

$$I_1/A_1 = (\pi r_1^4/4)/\pi r_1^2 = r_1^2/4$$

$$I_2/A_2 = (\pi r_2^4/4)/\pi r_2^2 = r_2^2/4$$

The computer programme uses the so called "Bisection method" to solve the frequency equations for beams with discontinuitv of cross sections for various width ratios ($WR = R_2/R_1$) and length ratios ($LR = \ell_2/\ell_1$).

When the beam becomes uniform over its entire length, i.e. $\rho, A_1 = A_2$ and $I_1 = I_2$, the frequency is obtained from hte expression

$$f_n = \frac{1}{2\pi L^2}\sqrt{\frac{E_1 I_1}{\rho_1 A_1}}\,\beta_n^2$$

and for a beam of circular cross section

$$f_n = \frac{rc_1\,\beta n^2}{4\pi L^2}$$

The programme was used to obtain the fundamental frequency and its six higher modes for two unifrom beams for L = 2.0m and d = 25.4mm, d = 31.75mm and the frequencies of a beam of $L_1 = L_2 = 1.0$m and $d_1 = 31.75$mm and $d_2 = 25.4$mm where E = 2.056 x 10"N/m^2 and ρ=0.77743x10^4kg/m^3.

The following values were obtained for n = 1,2,3,4,5,6,7

i) For the unifrom beam of 25.4mm diameter, the frequencies in Hertz are f_n/Hz = 29.083; 80.166; 157.150; 259.733; 388.036; 541.954 and 722.333.

ii) For the uniform beam of 31.75mm diameter, the frequencies in Hz are f_n/Hz = 36.354; 100.212; 196.437; 324.668; 485.041; 677.556 and 900.976

iii) For the stepped beam, the frequencies in Hz are f_n/Hz = 34.353; 93.780; 175.662; 291.645: 436.880; 611.345 and 815.064

The lateral frequencies of stepped beams with various end conditions were obtained by Gorman (1975). A stepped beam of rectangular cross section in flatwise vibration was investigated by Hashemi (1979).

The vibration analysis can be carried out further to obtain impedance and mobility ,a concept particularly useful for the prediction of transient response of structures subjected to impact loading.

Point impedance measurement for the finite beam with discontinuity of cross section can be used to describe the dynamic system in the frequency domain in terms of input-output characteristics under sinusoidal conditions. The motion is described without the need for a complete analysis of the entire system. This impedance concept is widely used in electrical engineering and is adaptable to dynamical systems by electro-mechanical analogy .

COMPUTER PROGRAM FOR FLEXURAL VIBRATION OF FINITE STEPPED BEAMS

```
      MASTER
      REAL WR(5),LR(10),RFE(7),AA(7),RI(7),LI(10),BI(7),W(7)
      REAL K1,K2
      READ(1,80)N,M
   80 FORMAT(2I4)
   79 FORMAT(10F0.0)
      READ(1,79)(WR(I),I=1,N)
      READ(1,79)(LR(J),J=1,M)
      READ(1,95)(AA(II),II=1,7)
   95 FORMAT(10F0.0)
      READ(1,78)C1
   78 FORMAT(E15.8)
      READ(1,79)(RI(I),I=1,N)
      READ(1,79)(LI(J),J=1,M)
      DO 10 I=1,N
      K1=0.5+0.5/WR(I)
      K2=1.-K1
      WRITE(2,60)
   60 FORMAT(1H1,////,5X,2HWR,4X,2HLR,5X,8H1ST-ROOT,6X,8H2ND-ROOT,6X,8H3
     1RD-ROOT,6X,8H4TH-ROOT,6X,8H5TH-ROOT,6X,8H6TH-ROOT,6X,8H7TH-ROOT,//
     2)
      DO 10 J=1,M
      KK=0
      R=LR(J)
      Y2=0.
      BL1=0.
   30 A=BL1
      Y1=Y2
      BL1=BL1+0.1
      B=BL1
      BL2 = BL1*R*SQRT(1/WR(I))
      F1=0.5*(EXP(BL1)-EXP(-BL1))
      F2=0.5*(EXP(BL1)+EXP(-BL1))
      F3=0.5*(EXP(BL2)-EXP(-BL2))
      F4=0.5*(EXP(BL2)+EXP(-BL2))
      T1=F1*COS(BL1)-F2*SIN(BL1)
      T2=F2*COS(BL1)-F1*SIN(BL1)
      T3=F1*SIN(BL1)+F2*COS(BL1)
      T4=F2*SIN(BL1)+F1*COS(BL1)
      T5=F3*COS(BL2)-F4*SIN(BL2)
      T6=F4*COS(BL2)-F3*SIN(BL2)
      T7=F3*SIN(BL2)+F4*COS(BL2)
      T8=F4*SIN(BL2)+F3*COS(BL2)
      AL1=K1*T3-K2*T3*T7-K1*T7+K2*T1*T8+K2
      AL2=K1*T4-K2*T4*T7+K1*T8+K2*T2*T8
      AL3=K1*T1+K2*T3*T5+K1*T5-K2*T1*T6
      AL4=K1*T2+K2*T4*T5-K1*T6-K2*T2*T6+K2
      Y2=AL1*AL4-AL2*AL3
      IF(Y2)15,40,25
   15 IF(Y1)30,30,35
   25 IF(Y1)35,30,30
   35 CALL ROOTS (A,B,R,K1,K2,Y1,X)
      KK=KK+1
      BI(KK) = X
      BI(KK) = BI(KK)/LI(J)
      W(KK) = BI(KK)*BI(KK)*(RI(I)/2.)*C1
```

```
      RFE(KK)=(X**2./AA(KK)**2.)*((1.+LR(J))**2.)
      IF(KK-7)30,45,45
   40 KK=KK+1
      RFE(KK)=(BL1**2./AA(KK)**2.)*((1.+LR(J))**2.)
      IF(KK-7)30,45,45
   45 WRITE(2,50)WR(I),LR(J),(RFE(JJ),JJ=1,7)
      WRITE(2,50)WR(I),LR(J),(BI(KK),KK=1,7)
      WRITE(2,50)RI(I),LI(J),(W(KK),KK=1,7)
   50 FORMAT(1HO,2X,3F7.3,7E14.5)
   10 CONTINUE
      STOP
      END
      SUBROUTINE ROOTS (A,B,R,K1,K2,Y1,X)
      REAL K1,K2
   15 X=(A+B)/2.
      Z=X*R
      F1=0.5*(EXP(X)-EXP(-X))
      F2=0.5*(EXP(X)+EXP(-X))
      F3=0.5*(EXP(Z)-EXP(-Z))
      F4=0.5*(EXP(Z)+EXP(-Z))
      T1=F1*COS(X)-F2*SIN(X)
      T2=F2*COS(X)-F1*SIN(X)
      T3=F1*SIN(X)+F2*COS(X)
      T4=F2*SIN(X)+F1*COS(X)
      T5=F3*COS(Z)-F4*SIN(Z)
      T6=F4*COS(Z)-F3*SIN(Z)
      T7=F3*SIN(Z)+F4*COS(Z)
      T8=F4*SIN(Z)+F3*COS(Z)
      AL1=K1*T3-K2*T3*T7-K1*T7+K2*T1*T8+K2
      AL2=K1*T4-K2*T4*T7+K1*T8+K2*T2*T8
      AL3=K1*T1+K2*T3*T5+K1*T5-K2*T1*T6
      AL4=K1*T2+K2*T4*T5-K1*T6-K2*T2*T6+K2
      Y=AL1*AL4-AL2*AL3
      IF(ABS(B-X)-0.001)40,40,45
   45 IF(Y1)5,40,25
    5 IF(Y)10,40,20
   10 A=X
      GO TO 15
   20 B=X
      GO TO 15
   25 IF(Y)30,40,35
   30 B=X
      GO TO 15
   35 A=X
      GO TO 15
   40 RETURN
      END
      FINISH
****
DOC DATA
   3   3
1.0   0.8   1.0
1.0   0.0   0.0
4.7305  7.8539  10.996  14.137  17.279  20.42   23.575
+5.14400000E+03
0.0254   0.03175   0.0254
2.0   3.0   2.0
****
```

B585

370